Molecular characterisation of dominant repressors of the cytokinin deficiency syndrome

Dissertation

zur Erlangung des akademischen Grades des
Doktors der Naturwissenschaften (Dr. rer. nat.)

eingereicht im Fachbereich Biologie, Chemie, Pharmazie
der Freien Universität Berlin

vorgelegt von

Helen Jensen
aus Velbert

Februar 2013

Die Arbeit wurde von April 2006 bis Februar 2013 am Lehrstuhl ,,Molekulare Entwicklungsbiologie der Pflanzen‘‘ des Instituts für Biologie / Angewandte Genetik unter der Leitung von Prof. Dr. Thomas Schmülling angefertigt

1. Gutachter: Prof. Dr. Thomas Schmülling

2. Gutachter: Prof. Dr. Tomáš Werner

Disputation am 05.02.2014

Table of contents

List of Figures

List of Tables

Abbreviations

:	under the control of (in the context of promoter-gene constructs)
%	percentage
∞	infinity
#	number
°C	degrees Celsius
Ω	ohm
µ	micro
3'	three prime end of DNA fragment
5'	five prime end of DNA fragment
35S	promoter of the Cauliflower Mosaic Virus
BA	benzyl adenine
BAC	bacterial artificial chromosome
bp	base pair
A	adenine
ADP	adenosine 5-diphosphate
ATP	adenosine 5-triphosphate
C	cytosine
CAPS	cleaved amplified polymorphic sequences
cDNA	complementary DNA
CDS	cytokinin deficiency syndrome
CHASE	cyclases/histidine kinases associated sensor extracellular
cM	centimorgan
CK	cytokinin
Col	*Arabidopsis thaliana* ecotype Columbia-0
*c*Z	*cis*-zeatin
DAG	days after germination
DAE	days after emerging
DMAPP	dimethyl allyldiphosphate
DMSO	dimethyl sulfoxide
DNA	desoxyribonucleic acid
DTT	dithiothreitol
DZ	dihydrozeatin
E	Einstein
E. coli	*Escherichia coli*
EDTA	ethylendiamintetraacetate
e.g.	*exempli gratia* [Lat.] for example
EMS	ethyl methanesulfonate
et al.	*et alii* / *et aliae* [Lat.] and others
F	phenylalanine
F1, F2, F3...	first, second, third... filial generation after a cross
FW	fresh weight
FU	Freie Universität/free university
G	guanine
g	gram
h	hour
^{3}H	tritium
I	isoleucine
Ile	isoleucine
iP	N^{6}-(Δ^{2}-isopentenyl)adenine

iPR	N^6-(Δ^2-isopentenyl)adenine riboside
kb	kilobase pair
L	litre/leucine
LB	Luria-Broth
LD	long-day
L*er*	Landsberg *erecta*
Leu	leucine
M	molar (mol/l)
m	milli
min	minute
mRNA	messenger RNA
MS	Murashige-Skoog
n	nano
no	number
OD_{600}	optical density 600nm
PCR	polymerase chain reaction
pH	negative logarithm of proton concentration
Phe	phenylalanine
PPT	Phosphinothricin
RDP	riboside-5′-diphosphate
RMP	riboside-5′-monophosphate
RTP	riboside-5′-triphosphate
RNA	ribonucleic acid
RNase	ribonuclease
rpm	revolutions per minute
RT	room temperature
RT-PCR	reverse transcription PCR
SAM	shoot apical meristem
SD	short-day
SDS	sodium dodecyl sulfate
SE	standard error
SSLP	simple sequence length polymorphism
T	thymine/threonine
TAE	Tris-acetate-EDTA
Thr	threonine
Tris	Tris-(hydroxymethyl)-aminomethane
tRNA	transfer RNA
*t*Z	*trans*-zeatin
*t*ZR	*trans*-zeatin riboside
U	enzyme unit
UTR	untranslated region
v	volume
V	volt
w	weight
wt	wild type
x	crossed to (crosses are always indicated in the order: female x male)

1 Introduction

Plants are sessile organisms, and therefore the location and time at which a seed germinates determines where the plant will grow and reproduce. To ensure optimal development and reproductive success, plant form is influenced by environmental factors. Plants have a functionally differentiated organ system composed of different tissues, which in turn are composed of cells of different types. Thus, during plant development, distantly-located organs, such as photosynthetic and non-photosynthetic organs and vegetative and reproductive organs, must communicate in order to optimize morphological and physiological processes, which allow the organism to adapt to environmental inputs. For this communication, local and long-distance messengers, which are transported among cells and organs, are essential. Cytokinins, a class of phytohormones, regulate a variety of processes fundamental for growth and development and are one of the recognized signalling molecules, which function as both local and long-distance regulatory signals for the coordination and fine–tuning of organ growth and development.

Cytokinins were discovered in search for factors that stimulate plant cells division in cultured plant cells (Letham 1963; Miller et al. 1956; Miller et al. 1955). In 1955, the synthetic cytokinin analogue kinetin was discovered as a breakdown product of DNA. In the presence of auxin, kinetin would stimulate tobacco pith parenchyma tissue to proliferate in culture. Several years after the discovery of kinetin, Letham discovered the first natural cytokinin in extracts of immature maize endosperm, which was called zeatin (Letham 1963). Like kinetin, zeatin stimulated mature plant cells to divide when added to a culture medium along with an auxin. To date, a variety of natural cytokinin species, including *trans*-zeatin (*t*Z), N^6-(Δ^2-isopentenyl)adenine (iP), *cis*-zeatin (*c*Z), and their conjugates have been identified (Mok and Mok 2001) . The active cytokinin species are mainly the free base type (Mok and Mok 2001). However, cytokinin ribosides and ribotides have also been shown to have signalling functions, but only with specific receptors (Spichal et al. 2004; Yonekura-Sakakibara et al. 2004).

Since their discovery, cytokinins have been shown to have an effect on many other physiological and developmental processes, including the control of cell division in meristems, chloroplast development, photomorphogenesis, vascular differentiation, leaf senescence, the modulation of sink-source relationships, nutrient acquisition, nodulation, the response to biotic and abiotic stresses and fertility (Argueso et al. 2009; Mok and Mok 2001; Werner and Schmülling 2009). Thus, cytokinins are important regulators of plant growth and development in multiple tissues and under diverse environmental conditions.

To regulate such plant developmental processes, cytokinin activity must be finely controlled. Therefore, the cytokinin-dependent intrinsic genetic network demands a highly coordinated regulation of the metabolism, translocation, and signal transduction of this phytohormone class (Mok and Mok 2001; Sakakibara 2006; Werner and Schmülling 2009).

1.1 Cytokinin biosynthesis

Naturally occurring cytokinins are adenine derivatives that carry either an isoprene-derived side chain or an aromatic side chain at the N^6-terminus, called isoprenoid cytokinins or aromatic cytokinins, respectively. Isoprenoid cytokinins are classified into one of four basic molecules: N^6-(Δ^2-isopentenyl)adenine (iP), *trans*-zeatin (*t*Z), *cis*-zeatin (*c*Z) and dihydrozeatin (DZ). Each cytokinin molecule is distinguished by characteristics of the side chain, namely the presence or the absence of a hydroxyl group at the end of the prenyl chain and the stereoisomeric position (Kamada-Nobusada and Sakakibara 2009; Mok and Mok 2001; Sakakibara 2006). iP carries an unmodified isopentenyl side chain, whereas *t*Z and *c*Z carry hydroxylated side chains. Among the four species, *t*Z and iP are most common in plants, but the physiological meaning of the differences in side chain structure is unclear. Cytokinins exist in free-base, riboside, and ribotide forms and may be modified by glucosylation at the *N3*, *N7* or *N9* positions of the adenine ring to form N-glucosides or alternatively, the hydroxyl group of *t*Z and *c*Z may be glucosylated or xylosylated to form zeatin-*O*-glucosides or zeatin-*O*-xylosides (Kamada-Nobusada and Sakakibara 2009; Mok and Mok 2001; Sakakibara 2006).

The current model of the isoprenoid cytokinin biosynthetic pathway in higher plants suggests that the isoprenoid side chain of iP and *t*Z predominantly comes from the methylerythritol phosphate (MEP) pathway in plastids, whereas that of cZ mainly originates from the mevalonate (MVA) pathway in the cytosol (Kamada-Nobusada and Sakakibara 2009; Kasahara et al. 2004).

The rate-limiting step in cytokinin biosynthesis is catalyzed by isopentenyl transferases (IPTs), which exist as adenosine phosphate-IPTs and tRNA-IPTs, depending on their substrates. Work by Miyawaki et al. (Miyawaki et al. 2006) has clarified the long-standing question of the biosynthetic routes for iP-, *t*Z-, and *c*Z-type cytokinin production. Analysis of *Arabidopsis* mutants lacking IPTs has shown that *c*Z formation in *Arabidopsis* depends entirely on the activity of tRNA-IPTs, as plants mutated in the corresponding genes lacked *c*Z-type cytokinins, although the levels of iP- and *t*Z-type CKs were unaffected. Adenosine phosphate-IPTs preferably utilize adenosine 5-triphosphate (ATP) and adenosine 5-diphosphate (ADP) as isoprenoid acceptors and are entirely responsible for the synthesis of iP and *t*Z cytokinins (Miyawaki et al. 2006).

The *Arabidopsis* genome encodes seven genes belonging to the ATP/ADP group (*IPT1* and *IPT3-8*) and two genes (*IPT2* and *IPT9*) resemble tRNA IPTs in their amino acid sequences (Kakimoto 2003; Miyawaki et al. 2006; Sakakibara 2006). The *Arabidopsis ipt3;5;7* triple and *ipt1;3;5;7* quadruple mutants have severely decreased levels of iP-type and *t*Z-type cytokinins, and their overall growth is severely affected, revealing the importance of these cytokinins (Miyawaki et al. 2006). *c*Z-type cytokinins produced by tRNA-IPTs play only a minor role in the growth of *Arabidopsis* plants (Miyawaki et al. 2006). The biosynthesis and role of aromatic cytokinins are not well known.

Traditionally it was thought that cytokinins were synthesized in the root and transported to the shoots through the xylem (Beveridge et al. 1997; Letham and Palni 1983). However, analysis of expression patterns of *Arabidopsis IPT* genes have demonstrated that cytokinins are produced not only in roots, but also in various sites within the aerial parts of the plant, including roots, leaves, stems, flowers, and siliques (Miyawaki et al. 2004; Nordström et al. 2004; Takei et al. 2004a). *IPT1* is expressed in xylem precursor cell files in root, leaf axils, ovules, and immature seeds; *IPT3* is expressed in phloem tissues; *IPT4* and *IPT8* are expressed in immature seeds with higher expression in the chalazal endosperm; *IPT5* is expressed in lateral root primordia, columella root caps, and fruit abscission zones; and *IPT7* is expressed in phloem, the endodermis of the root elongation zones, trichomes on young leaves, and in pollen tubes (Miyawaki et al., 2004).

In *Arabidopsis*, three IPTs (IPT1, IPT5 and IPT8) are localized in plastids. In contrast, IPT4 and IPT7 localize in the cytosol and mitochondria, respectively (Kasahara et al. 2004). A special role was discovered for IPT3. *Arabidopsis* IPT3 is a substrate of the protein farnesyl transferase, and IPT3 farnesylation directs the localization of the protein in the nucleus/cytoplasm, whereas the nonfarnesylated protein is located in the plastids. Interestingly, *Arabidopsis* IPT3 gain-of-function mutant analysis indicated that the different subcellular localization of the farnesylated protein and the nonfarnesylated protein is closely correlated with either isopentenyl-type or zeatin-type cytokinin biosynthesis. In addition, the farnesyl acceptor side was also shown to be essential for catalytic activity (Galichet et al. 2008).

In the initial step of iP and *t*Z, adenosine phosphate-IPTs utilize ADP or ATP as isoprenoid acceptors and catalyze N-prenylation at the N^6-terminus using dimethylallyl diphosphate (DMAPP) as the side chain donor, to generate iP-ribotides iPRTP and iPRDP, respectively (Kakimoto 2001). The cytokinin-nucleotides can be converted into the corresponding *t*Z-nucleotides by monooxygenases CYP735A1 and CYP735A2, which catalyze hydroxylation of the prenyl side chain of iP ribotides (Takei et al. 2004b). Dephosphorylation by phosphatase may occur in those di- or tri-phosphorylated cytokinin-nucleosides (Kamada-Nobusada and Sakakibara 2009). The biosynthesis of *c*Z is initiated by tRNA-IPTs that catalyze the prenylation of some tRNA species using DMAPP, what leads to the production

of *c*ZRMP (Golovko et al. 2002; Sakakibara 2006). Prenylated-tRNA has a *cis*-hydroxyl group, thus further degradation of prenylated tRNA generates *c*Z (Sakakibara 2006).

To become biologically active, cytokinin-nucleotides produced by IPTs and CYP735As have to be converted to the free base forms. Two pathways have been proposed to be involved in producing active cytokinin species from nucleotides in plants: the two-step activation pathway and the direct activation pathway (Chen and Kristopeit 1981; Kurakawa et al. 2007). The two-step model supposes that iP- and tZ-nucleotides are converted to nucleobase forms by dephosphorylation and deribosylation, but genes encoding the nucleotidase and nucleosidase have not yet been identified (Chen and Kristopeit 1981).

Recently, a cytokinin-activating enzyme named LONELY GUY (LOG) that converts biologically inactive cytokinin-nucleotides precursor forms to their active nucleobases in a single step, was identified in rice (Kurakawa et al. 2007). The *LOG* gene encodes a phosphoribohydrolase that utilize all four cytokinin nucleoside 5-monophosphates, iPRMP, *t*ZRMP, DZRMP and *c*ZRMP, but the di- or triphosphates are not suitable substrates. In rice, the *LOG* messenger RNA is specifically localized in the shoot meristem tip, suggesting that bioactive cytokinins are restricted to defined developmental domains whose activities depend on the actions of cytokinin-activating enzymes. In rice *log* mutants, maintenance of the shoot meristem is defective and flowers often contain only one stamen but no pistil. This phenotype shows the importance of the LOG-dependent cytokinin activation pathway in maintenance of shoot apical meristem in rice.

In *Arabidopsis thaliana*, seven homologs of rice LOG with enzymatic activities equivalent to that of rice LOG have been identified (Kuroha et al. 2009). Histochemical analyses of expression patterns of *Arabidopsis* LOGs suggest that activation of cytokinin occurs in nearly all parts of the plant (Kuroha et al. 2009). In the *Arabidopsis log1log2log3log4log5log7log8* septuple mutant overall growth is severely affected, suggesting a dominant role of the single-step activation pathway mediated by LOGs for cytokinin production (Tokunaga et al. 2012).

1.2 Cytokinin modification and catabolism

The catabolism of cytokinins is a vital component of hormonal regulation, contributing to the control of active forms of cytokinins and their cellular distribution. Cytokinin activity *in planta* is thought to be controlled by a fine balance of biosynthesis, conjugation and degradation (Mok and Mok 2001).

The active cytokinin can be inactivated by degradation or conjugation. Inactivation by conjugation to sugars can be both irreversible and reversible. Glucose-conjugation to cytokinins occurs at the *N3*, *N7* and *N9* positions of the purine ring. These modifications are generally irreversible, and such

conjugated forms of cytokinin are inactive in bioassays, with the exception of N_3-glucosides (Kamada-Nobusada and Sakakibara 2009; Mok and Mok 2001; Sakakibara 2006). The hydroxyl group of the prenyl side chain of *t*Z, DZ and *c*Z can also be conjugated to glucose residues, yielding O-glucosides. Conjugations at the side chain can be removed by glucosidase enzymes to yield free cytokinins (Brzobohaty et al. 1993; Sakakibara 2006). Thus, cytokinin O-glucosides may be a storage form of cytokinins.

Cytokinin oxidase/dehydrogenases (CKX), which oxidatively remove the *N6*- side chain of cytokinins to produce a corresponding aldehyde, play a major role in regulating cytokinin levels in planta and are responsible for most metabolic cytokinin inactivation (Ashikari et al. 2005; Schmülling et al. 2003; Werner et al. 2001). Therefore, the degradation step is of high importance in regulating or limiting cytokinin effects and regulating cytokinin activity (Ashikari et al. 2005; Werner et al. 2003; Werner et al. 2001).

A gene encoding *CKX* was first identified in maize (Houba-Hérin et al. 1999; Morris et al. 1999). Analysis of the entire genome of *Arabidopsis thaliana* has revealed seven distinct CKX-encoding genes (*CKX1*-*CKX7*) (Werner et al. 2006; Werner et al. 2003). Cytokinin bases and nucleosides were identified as preferred substrates for CKX proteins. CKX enzymes cleave the side chains from *c*Z, *t*Z, zeatin riboside, iP, and their *N*-glucosides, but not their O-glucosides. However, DZ and its conjugates are resistant to cleavage (Bilyeu et al. 2001; Galuszka et al. 2007).

CKX enzymes differ in their biochemical properties, in regulation of their expression and in subcellular localization (Galuszka et al. 2007; Schmülling et al. 2003). In *Arabidopsis*, N-terminal sequences of CKX proteins and studies of GFP fusion proteins indicate that CKX proteins are targeted to the plant secretory pathway (endoplasmic reticulum/extracellular space) (CKX2, CKX4 and CKX6) or are present in vacuoles (CKX1, CKX3 and CKX5), whereas CKX7 is localized to the cytosol due to the lack of any recognized signal peptide (Köllmer 2009; Werner et al. 2003). New results indicate that the CKX1 protein is localized in the endoplasmic reticulum (personal communication, H. Weber, FU Berlin).

In *Arabidopsis*, the activity of the CKX enzymes is induced by high cytokinin concentrations and they are expressed tissue specifically in shoot and root (Brenner et al. 2005; Kiba et al. 2005; Rashotte et al. 2003; Werner et al. 2006). Their expression was mainly localized in proliferating tissues like the shoot meristem (*CKX1* and *CKX2*), auxiliary buds, the procambial region of the root meristem (*CKX5*), root primordia (*CKX5* and *CKX6*), young leaves (*CKX4* and *CKX5*), stomata cells (*CKX4* and *CKX6*), the root cap and trichomes (*CKX4*), in the gynoecium (*CKX6* and *CKX7)* and vascular tissue (*CKX6*) (Brenner et al. 2005; Werner et al. 2006; Werner et al. 2003). Generally, expression levels of *CKX* genes are quite low.

Expression domains of *CKX* genes partially overlap with cytokinin-synthesizing *IPT* genes in meristematic tissues and endo-reduplicating cells. Hence, cytokinin gets degraded in the same tissue where it is synthesized, indicating a locally restricted function of cytokinin (Werner et al. 2006). On the other hand, their expression in vascular tissue suggests a function in controlling transported cytokinin (Werner et al. 2006).

Constitutive expression of some *CKX* genes (*CKX1*, *CKX3* and *CKX5*) results in a drastic reduction of endogenous cytokinins in both root and shoot meristems and causes aberrant phenotypic traits which are collectively termed "cytokinin deficiency syndrome". The main features of this syndrome are the formation of stunted shoots with reduced meristems, reduced apical dominance, small rosette leaves, increased seed size, and an enhanced root system (Galuszka et al. 2004; Werner et al. 2003; Werner et al. 2001).

Studies on the loss-of-function of individual *CKX* gene family members indicate a high degree of functional redundancy (Bartrina et al. 2011). Nevertheless, specific functions were found for some CKX proteins. In rice, it was shown that a decreased expression of Os*CKX2* leads to an increased cytokinin content what causes the formation of more reproductive organs what leads to an increased grain yield (Ashikari et al. 2005). In *Arabidopsis*, CKX6 is functionally involved in the rapid arrest of leaf primordium growth caused by a low ratio of red and far-red light (Carabelli et al. 2007). Bartrina et al. (2011) showed that an increase of endogenous cytokinin in *Arabidopsis* inflorescences caused by the simultaneous mutation of the *CKX3* and *CKX5* gene, leads to the formation of a larger reproductive meristem. The enhanced cytokinin content increased the cell number and, as a consequence, the size of floral organs and particularly the ovule-bearing gynoecia increased, causing the formation of more seeds.

1.3 Cytokinin signal transduction

Characterization of two-component elements in *Arabidopsis* together with genetic experiments revealed that cytokinin signals through a complex two-component system that is similar to bacterial two component phosphorelays with which bacteria sense and respond to environmental stimuli (D'Agostino et al. 2000; Hwang and Sheen 2001; Inoue et al. 2001; Kakimoto 1996; Sakai et al. 2001; Yamada et al. 2001).

There are four major steps in the cytokinin phosphorelay: cytokinin sensing and initiation of signalling by autophosphorylation of cytokinin receptors; transfer of a phosphoryl group to phospho-transfer proteins and nuclear translocation of these proteins; phosphotransfer to nuclear B-type response regulator proteins that activate transcription of A-type response regulators; and negative

feedback and output through A-type response regulators. Perception of cytokinins by receptors is the first step in the cytokinin signalling pathway. In *Arabidopsis thaliana*, cytokinin is perceived by a class of membrane-bound receptor histidine kinases with three members, namely AHK2, AHK3, and AHK4 (also known as CRE1 or WOL) (Inoue et al. 2001; Suzuki et al. 2001; Yamada et al. 2001).

All three receptors are localized in the endoplasmic reticulum and contain in the N-terminal part a extracytosolic cyclases/histidine kinases associated sensor extracellular (CHASE) domain, which is responsible for hormone recognition, and a C-terminal His kinase domain that is thought to be orientated towards the cytoplasm and/or nuclear compartment (Anantharaman and Aravind 2001; Caesar et al. 2011; Wulfetange et al. 2011; Yamada et al. 2001).

An evolutionary tracing approach identified four conserved amino acids in the CHASE domain of *Arabidopsis* cytokinin receptors to be crucial for cytokinin binding (Heyl et al. 2007). Miwa et al. (2007) on the other hand identified several single amino acid substitution within the second membrane-spanning segment, or within the region around the phosphorylation His site, that cause a constitutive active version of AHK4 and AHK3 in *E. coli*. However, introduction of these constitutively active cytokinin receptors into *Arabidopsis* wild-type plants failed, perhaps due to a harmful effect of the constitutively active cytokinin receptors (Miwa et al. 2007).

A live cell-based direct binding assay revealed the different biochemical characteristics and ligand bonding preferences of the cytokinin receptors AHK4 and AHK3. Both receptors bind *trans*-zeatin with a high affinity, but AHK3 showed a significantly lower affinity for iP-type cytokinins. Furthermore, for AHK3, cytokinin ribosides (*t*ZR, iPR) and *cis*-zeatin had true binding activity, although lower than that of tZ (Romanov et al. 2006; Romanov et al. 2005; Spichal et al. 2004).

Endogenous expression of the three receptors seems to largely overlap and analysis of *Arabidopsis* single, double and triple receptor mutants as well as gain-of-function analysis revealed that although they mainly act redundantly, they also have specific roles in plant development. Knockout studies of single receptor genes did not show any obvious plant phenotype, whereas in the triple receptor knockout mutant plant growth is severely impaired (Higuchi *et al.,* 2004; Nishimura *et al.,* 2004; Riefler *et al.,* 2006). It was shown recently that AHK3 plays a specific role in leaf senescence and chlorophyll retention (Kim et al. 2006; Riefler et al. 2006). Furthermore, it was proposed that AHK3 plays a predominant role in different aspects of shoot development; including the regulation of leaf and shoot growth, chloroplast development, shoot de-etiolation and far-red light resistance. By contrast, the AHK4 receptor is of primary importance in root development and tissue culture (Higuchi et al. 2004; Inoue et al. 2001; Kim et al. 2006; Nishimura et al. 2004; Riefler et al. 2006).

In the current model, binding of the hormone to the extracellular CHASE domain of the receptor causes a conformational change, leading to the autophosphorylation of a highly conserved histidine

within the intracellular kinase domain. The phosphate is then passed to a conserved aspartic acid in the receiver domain of the cytokinin receptor and from there to a conserved histidine of one of five histidine phospho-transfer proteins (AHP1-AHP5) (Hutchison et al. 2006), which subsequently transfer the phosphoryl groups to ARABIDOPSIS RESPONSE REGULATOR (ARRs), most of which are predominantly localized in the nucleus (Kiba et al. 2002; Sweere et al. 2001).

Single *ahp* mutants are indistinguishable from wild-type seedlings in cytokinin response assays. However, higher-order mutants display reduce sensitivity to cytokinin and show various abnormalities in growth and development, which include reduced fertility, increased seed size, reduced vascular development, and a shortened primary root, indicating that most of the AHPs are redundant, positive regulators of cytokinin signalling and affect multiple aspects of plant development (Hutchison et al. 2006).

It was long thought that AHP proteins were transported to the nucleus only in response to cytokinin treatment (Hwang and Sheen 2001; Yamada et al. 2004), but in 2010 Punwani et al. showed that the AHP proteins are in constant flux between cytosol and nucleus independent of their phosphorylation status and independent of cytokinin signalling (Punwani et al. 2010).

AHPs act as positive regulators of cytokinin signalling with one exception: AHP6. AHP6 is considered to be a pseudo-AHP because an inert asparagine (Asn) residue is found where AHP1 to AHP5 have a conserved His residue that is required for phosphorylation. AHP6 has been shown to impair phosphotransfer from AHKs, most likely by directly competing with functional AHPs for interaction with AHKs (Mähönen et al. 2006; Suzuki et al. 2001). Furthermore, for AHK4 it was shown that in the absence of cytokinin, AHK4 acts as a phosphatase to remove phosphate from AHP proteins but AHK2 and AHK3 do not seem to possess this function (Mähönen et al. 2006).

Three different classes of effectors in the cytokinin signalling pathway have been identified: the type-A ARRs, type-B ARRs and the CRFs. Upon entering the nucleus, the phosphorylated AHPs can pass its phosphate on to members of a transcription factor family with 11 members, called the type-B response regulators (ARR1, ARR2, ARR10–ARR14, ARR18–ARR21). Type-B ARRs activate the expression of primary cytokinin-response genes, including ten type-A ARRs (ARR3–ARR9, ARR15–ARR17) (Hwang and Sheen 2001; Mason et al. 2004; Mason et al. 2005; Sakai et al. 2001). Phosphorylated type-A ARRs mediate downstream processes and generally function as negative regulators of cytokinin signalling. They establish a negative-feedback loop in the pathway that dampens the response to cytokinin (To et al., 2004, 2007). Transfer of phosphoryl groups from the AHKs to the AHPs and then to the ARRs has been demonstrated *in vitro* as well as in artificially constructed cytokinin response pathways in bacteria and yeast (Inoue et al. 2001; Suzuki et al. 2002; Suzuki et al. 2001; Yamada et al. 2001).

The CYTOKININ RESPONSE FACTORS (CRFs) belong to the *Arabidopsis* APETALA2 (*AP2*) gene family and are thought to mediate cytokinin-regulated gene expression in tandem with type-B ARRs (Rashotte et al. 2006). Interestingly, fusion proteins of CRFs and green fluorescent protein (GFP) enter the nucleus through a mechanism that is dependent on cytokinin, AHKs, and AHPs. The *Arabidopsis* genome encodes six *CRFs*, but only three *CRF* transcripts (*CRF2, CRF5* and *CRF6*) are rapidly induced by cytokinin in a type-B ARR dependent manner. Microarray experiments showed that the expression of approximately half of the cytokinin- regulated genes is altered in loss-of-function *crf* mutant backgrounds, but not A-type *ARR* genes, and the genes misregulated in the *crf* mutants overlap to a great extend with genes affected in the type-B *arr1,12* mutant (Rashotte et al. 2006).

However, type-B ARRs seem to regulate the majority of transcriptional changes that characterize the cytokinin response (Argyros et al. 2008; Heyl et al. 2008). Argyros et al. (2008) could show that triple loss-of-function mutants of the B-type *ARR* genes, *ARR1*, *ARR10* and *ARR12*, showed hallmarks of the cytokinin-deficiency syndrome, indicating that these genes are central regulators of cytokinin activity during vegetative development. Microarray analysis of a triple null mutant for *ARR1*, *ARR10*, and *ARR12* verified that these type B mutations affect the majority of the expression of cytokinin-regulated genes (Argyros et al. 2008).

A novel approach to explore function and importance of the type-B ARR proteins was chosen by Heyl et al. (Heyl et al. 2008). Here CRES-T was used as a tool to overcome the functional redundancy among B-type ARRs by adding a transcriptional silencer domain (SRDX domain) to the type-B ARR1 protein. The dominant negative ARR1-SRDX causes a strong cytokinin-deficiency phenotype similar to the one observed in plants with a lowered cytokinin content or signalling (Higuchi et al. 2004; Nishimura et al. 2004; Riefler et al. 2006; Werner et al. 2003; Yang et al. 2003), suggesting that the activity of B-type ARRs is involved in most, if not all, of the cytokinin-regulated processes.

1.4 Transport of cytokinins

Due to their immobile nature, plants require highly efficient mechanisms for acclimation to rapidly changing environmental conditions and for communication between their distal organs. For this communication, local and long-distance messengers, such as cytokinins, which are transported among cells and organs, are essential.

The previous widely accepted idea that cytokinin is synthesized only in root tips and shoot apices, has been overturned. The hormone has functions as long-distance messengers as well as a local

paracrine signal and is synthesized and acts at various sites in a plant body (Hirose et al. 2008; Miyawaki et al. 2004; Nordström et al. 2004; Takei et al. 2004b).

In higher plants, long-distance translocation of cytokinins is mediated by the xylem, a transport system that mediates transpiration flow, and the phloem, which translocates products of photosynthesis and regulatory signals from mature leaves to areas of growth and storage, including the roots. The presence of cytokinins in xylem sap and leaf exudates suggests the possibility of cytokinins being mobile regulators. In xylem sap, the major form of cytokinin is *trans*-zeatin riboside (*t*ZR) (Hirose et al. 2008; Takei et al. 2001), and in phloem sap, the major forms are iP-type cytokinins, such as iP-ribosides (iPR) and iP-ribotides (Corbesier et al. 2003; Hirose et al. 2008). This suggests that *t*Z-type cytokinins are mainly transported from the root to the shoot and iP-type cytokinins are mainly transported from source organs to sink organs.

This hypothesis is supported by a grafting experiment using an *Arabidopsis ipt1,3,5,7* quadruple mutant, in which the content of both iP-type and tZ-type cytokinins decreased in comparison with wild-type plants (Miyawaki et al. 2006). When an *ipt1,3,5,7* shoot scion was grafted onto WT root stock, both the root and shoot grew normally and *t*Z-type cytokinins in the shoot were restored to WT levels, but the level of iP-type cytokinins in the shoot remained unchanged. Conversely, wild-type shoot-scions recovered the iP-type cytokinins in the mutant root-stocks to normal levels, whereas the *t*Z-type cytokinins were only partially recovered and both the root and shoot grew normally (Matsumoto-Kitano et al. 2008). Reciprocal grafting experiments also restored visible mutant phenotypes, such as defects in the thickening growth of roots and inflorescence stems (Matsumoto-Kitano et al. 2008).

Cytokinin translocation via the xylem is controlled both by environmental and endogenous signals. It has been shown that in barley and maize the *t*ZR content of the xylem sap is significantly increased by nitrate supplement, suggesting that *t*ZR may act as a messenger for nitrate signalling (Takei et al. 2001). Furthermore, xylem cytokinins upregulated by nitrate supplement induced the accumulation of cytokinin-responsive gene transcripts in leaves (Takei et al. 2001; Taniguchi et al. 1998). In *Arabidopsis* roots, the accumulation of *IPT3* transcripts is induced by nitrate and it was shown that *IPT3* is a key gene for the nitrate-dependent *de novo* biosynthesis of cytokinins (Takei et al. 2002; Takei et al. 2004a). Promoter-reporter analyses of transgenic *Arabidopsis* plants showed that the *IPT3* promoter is active in phloem companion cells rather than xylem tissues (Takei et al. 2004a). Thus, there may well be a cytokinin translocation system operating between the phloem and xylem tissues.

As cytokinins are a mobile class of phytohormones, multiple cellular importers and exporters are required to allow efficient mobilization and targeted translocation (Cedzich et al. 2008; Hirose et al.

2008). However, little is known about the mechanisms of cytokinin transport. Characterization of cytokinin transport in *Arabidopsis* cell cultures suggest the presence of proton-coupled multiphasic cytokinin transport systems (Cedzich et al. 2008).

Recently, low-affinity transporters for adenine and cytokinin nucleobases belonging to the purine permease (PUP) family in Arabidopsis (Bürkle et al. 2003; Gillissen et al. 2000) and for cytokinin nucleosides belonging to the equilibrative nucleoside transporter (ENT) family in rice and *Arabidopsis* (Hirose et al. 2005; Hirose et al. 2008) have been identified. Among *Arabidopsis* PUP family proteins, the ability of PUP1 and PUP2 to transport the nucleobases *t*Z and iP was shown by direct uptake of radiolabeled *t*Z into yeast expressing this transporter (Bürkle et al. 2003). *PUP2* is expressed in the phloem of *Arabidopsis* leaves. This result, together with findings demonstrating the expression of *IPT3* (Miyawaki et al. 2004; Takei et al. 2004a) in companion cells of sieve elements, indicates that PUP2 may have a role in the loading and transport of adenine and possibly cytokinins in phloem.

For plant ENT proteins, competitive uptake studies in yeast cells suggested that *Arabidopsis* ENT3, ENT6, ENT7, and rice ENT2 can transport iPR and *t*ZR (Hirose et al. 2005; Hirose et al. 2008). *ENT* genes are mainly expressed in the vascular system of plants. ENT8 was identified in a screen for suppressors of *Arabidopsis gain-of –function IPT8* mutants providing genetic evidence for its relevance in cytokinin function (Sun et al. 2005). *ENT8* and *ENT3* loss-of-function and gain-of-function mutants are less sensitive or hypersensitive towards applied *t*ZR, respectively, suggesting a role in transport of cytokinin nucleosides *in planta* (Sun et al. 2005).

1.5 Cytokinin functions in meristems

Cytokinins were originally identified based on their ability to promote cell division in plant cells and the classic experiments of Skoog and Miller (1957) demonstrated that cytokinins could stimulate the formation of shoot meristems in plant tissue culture.

Consistent with these results, decreasing active cytokinin levels and cytokinin signalling in *Arabidopsis* and rice causes reduced shoot development (Kurakawa et al. 2007; Miyawaki et al. 2006; Shani et al. 2006; Werner et al. 2003; Werner et al. 2001). *ahk2 ahk3 ahk4* triple mutants display pleiotropic phenotypes including a dramatic reduction in meristem size and leaf-initiation rate, as well as impaired leaf development (Higuchi et al. 2004; Nishimura et al. 2004; Riefler et al. 2006). Similar defects were observed in *Arabidopsis* quadruple and quintuple *ipt* mutants and triple *log* mutants (Kuroha et al. 2009; Miyawaki et al. 2006). In rice, the cytokinin biosynthesis gene *LOG* is expressed in the apical region of the shoot meristem and is required for meristem maintenance (Kurakawa et al. 2007). A drastic reduction of endogenous cytokinins in shoot meristems caused by

constitutive expression of *CKX* genes also results in a strong decrease in meristem size and organ primordia formation, providing direct evidence for the requirement of cytokinin for proliferative shoot apical meristem activity (Werner et al. 2003; Werner et al. 2001). Furthermore, overexpression of a constitutively active type-A ARR ($ARR7^{D85E}$) causes meristem arrest, suggesting that type-A ARRs negatively regulate meristem function by phospho-dependent interactions (Leibfried et al. 2005).

Contrary effects were shown in plants with an enhanced cytokinin status. In maize, mutations in a type-A response regulator cause an enlarged meristem (Giulini et al. 2004) and gain-of-function type-B ARR display phenotypes consistent with a hyperactive meristems, like ectopic shoot formation and unusual proliferation of tissues (Imamura et al. 2003; Sakai et al. 2001; Tajima et al. 2004).

Shoot apical meristem maintenance is regulated by two main signalling pathways: the WUSCHEL (WUS) pathway and the SHOOTMERISTEMLESS (STM) pathway (Lenhard et al. 2002). An essential regulatory mechanism for meristem organization is a regulatory loop between WUS and CLAVATA (CLV) (Brand et al. 2000; Schoof et al. 2000). This intercellular signalling network coordinates the development of the organization centre, organ boundaries and distant organs. Central to the action of cytokinin at the shoot apical meristem is the WUS transcription factor, which acts to promote stem cell activity (Gordon et al. 2009; Leibfried et al. 2005). The cytokinin signal and WUS reinforce each other through multiple feedback loops. Cytokinin activates WUS directly and independently of the CLV pathway (Buechel et al. 2010; Gordon et al. 2009). At the same time, repression of CLV1 by cytokinin further facilitates WUS expression (Gordon et al. 2009). On the other hand, several type-A ARRs (ARR7/15) have been shown to be negatively regulated by WUS and positively regulated by CLV3 in *Arabidopsis* (Leibfried et al. 2005; Zhao et al. 2010). Furthermore, ARR7 and ARR15 are required for CLV3 expression (Zhao et al. 2010). ARR7 is expressed in the *Arabidopsis* meristem and WUS was shown to bind sequences in the ARR7 promoter directly to repress their expression (Leibfried et al. 2005). Since the type-A response regulators normally inhibit cytokinin signalling, this repressor activity of WUS should serve to make the cells more sensitive to cytokinin, resulting in a positive feedback loop that promotes meristem activity (Kieber and Schaller 2010).

Bartrina et al. (2011) postulated a possible function for cytokinin degrading CKX enzymes in the circuitry regulating the cytokinin status and, thus, the size of the WUS domain, as the CKX3 expression domain was similar to that of WUS in inflorescence and floral meristems and the mutation of the *CKX3* gene in combination with other *CKX* genes, leads to the formation of a larger reproductive meristem.

Cytokinin also interacts with KNOX transcription factors that specify SAM identity in a positive feedback loop. Ectopic activation of the KNOX protein STM results in a rapid increase in the expression of the cytokinin biosynthesis gene *IPT7* and accumulation of cytokinin (Jasinski et al. 2005;

Yanai et al. 2005). In turn, cytokinin upregulates the expression of the KNOX transcription factor genes *KNAT1* and *STM* (Rupp et al. 1999). In addition, application of exogenous cytokinin or the expression of a bacterial *IPT* gene through the *STM* promoter was able to partially rescue the meristem function of *stm* loss-of-function mutants (Yanai et al. 2005) whereas the cytokinin receptor mutant *wol* enhanced the phenotype of a weak *stm* allele (Jasinski et al. 2005).

In addition to the apical meristems, cytokinins play an essential role in cambium formation and activity (Hejatko et al. 2009; Matsumoto-Kitano et al. 2008; Nieminen et al. 2008). Cambium activity results in the production of xylem and phloem, in its self-maintenance, and in stem radial expansion (Savidge 2001). Nieminen et al. (2008) reported that in *Populus* and birch trees, orthologs of the AHK cytokinin receptors and a type-A response regulator (PtRR7) are expressed in the cambial zone of Populus stems. Expression of an *Arabidopsis* cytokinin degrading enzyme (AtCKX2) under the promoter for a birch cytokinin receptor gene caused a reduction of cytokinin concentration in the stems and reduced responsiveness to cytokinins. This led to fewer cell divisions in the vascular cambium and hence a reduction in radial growth, suggesting that the stimulatory effect of cytokinins on cell division is required for normal vascular cambium function.

Supporting this, Matsumoto-Kitano et al. (2008) showed that cytokinins are required for cambial activity in *Arabidopsis*. The *Arabidopsis ipt1,3,5,7* quadruple mutant, lacking four cytokinin biosynthetic ATP/ADP isopentenyl transferase enzymes, has a strongly reduced concentration of cytokinin (Miyawaki et al. 2006), which leads to severely reduced fascicular and interfascicular cambial activity and reduced thickening of root and stem (Matsumoto-Kitano et al. 2008). The only recognizable phenotype of the *Arabidopsis ipt3* mutant is the moderate decrease in secondary growth, revealing that cambium activity responds sensitively to a decrease in cytokinin levels (Matsumoto-Kitano et al. 2008). As mentioned previously (see chapter 1.4), the cambial activities in mutant *ipt1,3,5,7* roots and shoots were completely restored by grafting a wild-type scion or root stock, indicating that cytokinin functions as a mobile bidirectional signal in the control of cambial growth (Matsumoto-Kitano et al. 2008).

Consistent with a role for cytokinin as a positive regulator of vascular cambium, Hejatko et al. (Hejatko et al. 2009) could show that the cytokinin receptors AHK2 and AHK3 together with CYTOKININ-INDEPENDENT1 (CKI1), a cytokinin-independent histidine kinase implicated in cytokinin signalling, are important regulators of vascular tissue development in *Arabidopsis thaliana* shoots. *CKI1* expression is observed in vascular tissues of inflorescence stems and genetic modifications of CKI1 activity in *Arabidopsis* cause dysfunction of the two-component signalling pathway and defects in procambial cell maintenance. Loss-of-function *ahk2* and *ahk3* mutants also showed defects in procambium proliferation and the absence of secondary growth. *CKI1* overexpression partially

rescued *ahk2 ahk3* phenotypes in vascular tissue, while the negative mutation CKI1^{H405Q} further accentuated mutant phenotypes. These results indicate that the cytokinin-independent activity of CKI1 and cytokinin-induced *AHK2* and *AHK3* are involved in vascular bundle formation in *Arabidopsis* (Hejatko et al. 2009).

In contrast to its positive role on proliferation of meristematic cells in the shoot, cytokinins negatively regulate root growth. Cytokinin-deficient plants as well as plants with lowered cytokinin signal output, form an enhanced root system (Heyl et al. 2008; Mason et al. 2005; Miyawaki et al. 2006; Riefler et al. 2006; Werner et al. 2003; Werner et al. 2001). Lowering endogenous cytokinin levels by overexpressing cytokinin degrading CKX enzymes or disruption of *IPT* genes as well as reduced cytokinin responsiveness leads to an increase in apical root meristem size, while increased cytokinin levels or sensitivity causes a reduction in the size of the root apical meristem (Dello Ioio et al. 2007; Dello Ioio et al. 2008; Werner et al. 2003). Expression of *CKX* genes in different domains of the root apical meristem revealed that cytokinin acts primarily within the root transition zone, where it promotes cell differentiation and thus decreases the number of cells in the meristematic zone (Dello Ioio et al. 2007).

A more detailed analysis has shown that, in the root meristem of *Arabidopsis thaliana*, cytokinin promotes cell differentiation by repressing both auxin signalling and transport, whereas auxin sustains root meristem activity by promoting cell division (Moubayidin et al. 2009; Müller and Sheen 2008). The primary cytokinin-response transcription factors, ARR1 and ARR12, activate the gene *SHORT HYPOCOTYL 2* (*SHY2)*, a repressor of auxin signalling that negatively regulates the *PIN-FORMED* (*PIN)* auxin transport genes. Thereby, cytokinin causes auxin redistribution, which leads to an increase in cell differentiation rate and a decrease in the rate of cell division. Conversely, auxin mediates degradation of the SHY2 protein, sustaining PIN activities and cell division. Thus, the cell differentiation and division balance necessary for controlling root meristem size and root growth is the result of the interaction between cytokinin and auxin through a regulatory circuit converging on the *SHY2* gene (Ioio et al. 2008; Moubayidin et al. 2010).

Using a novel cytokinin response reporter that visualizes universal cytokinin output *in vivo*, Müller and Sheen showed that cytokinin and auxin play an antagonistic role in root stem cell specification during embryo development (Müller and Sheen 2008). The authors detected early cytokinin activity in the hypophysis, the founder cell of the root stem cell system. Its apical daughter cell, which is the precursor of the quiescent centre, maintained a cytokinin output signal, while it was repressed in the basal cell lineage. In these cells, auxin up-regulates the expression of *ARR7* and *ARR15*, suppressing cytokinin signalling in the basal daughter cell of the hypophysis, ultimately regulating the expression of transcription factor genes controlling stem cell specification, such as SCARECROW (SCR), WUS-

RELATED HOMEOBOX 5 (WOX5) and PLETHORA (PLT1). Loss of ARR7 and ARR15 function or ectopic cytokinin signalling in the basal cell during early embryogenesis resulted in a defective root stem-cell system (Müller and Sheen 2008).

Analyses of plants with an altered cytokinin status demonstrated that cytokinin is also a negative regulator of lateral root formation (Kuderová et al. 2008; Mason et al. 2005; Riefler et al. 2006; Werner et al. 2003; Werner et al. 2001). Plants with reduced cytokinin content or cytokinin signalling display a greater number lateral roots (Hutchison et al. 2006; Mason et al. 2005; Riefler et al. 2006; Werner et al. 2003), while exogenous cytokinin treatments inhibit lateral root initiation and development (Laplaze et al. 2007; Li et al. 2006). In *Arabidopsis*, lateral roots originate from pericycle founder cells at the periphery of the xylem poles (Fukaki and Tasaka 2009). The cytokinin receptor AHK4 was shown to mainly mediate the inhibition of lateral root initiation through blocking the division of pericycle founder cells at the G2 to M transition phase (Laplaze et al. 2007; Li et al. 2006). Lateral root initiation is regulated by auxin, and the establishment of a PIN-dependent auxin maximum in LR founder cells coordinates cell-cycle progression and cell fate specification (Benková et al. 2003). Exogenous application of cytokinin affects expression of *PIN* genes and affects their spatial expression in lateral root primordia. This perturbs the formation of an auxin gradient and leads to disorganized patterns of cell division during primordia organogenesis (Laplaze et al. 2007).

Taken together, cytokinin regulates cell division in the context of the root, shoot, and lateral meristems, albeit with sometimes differing roles.

1.6 Aim of the study

Cytokinins have been shown to have positive effects on many physiological and developmental processes. For example, cytokinins stimulate the formation and activity of shoot meristems, was shown to have positive effects on organ size and seed yield, delays leaf senescence, and plays a role in seed germination, nutrient acquisition, and stress responses (Bartrina et al. 2011; Mok and Mok 2001; Werner and Schmülling 2009). Constitutive expression of the *CKX1* gene causes a cytokinin deficiency syndrome, which mainly consists of a stunted shoot with a smaller apical meristem, reduced apical dominance, small rosette leaves, and an enhanced root system (Galuszka et al. 2004; Werner et al. 2003; Werner et al. 2001). Suppressor mutagenesis of *CKX1* overexpressing *Arabidopsis* plants led to the identification of the mutants *rock2 CKX1ox (#205), rock3 CKX1ox* (#608) and *rock4 CKX1ox* (#29) (Bartrina 2006), which show a partial reversion of the cytokinin-deficient phenotype. The aim of this approach was to identify factors which are necessary for the establishment of the cytokinin deficiency syndrome, and therefore might play a role in the cytokinin-

dependent regulation of the shoot apical meristem and organ growth (e.g. negative regulatory elements of cytokinin signalling or metabolism).

The first aim of this study was to identify the genes which cause the phenotypic changes in *rock3 CKX1ox* and *rock4 CKX1ox Arabidopsis* plants using map-based cloning, and to further describe the phenotypic changes of the *rock2 CKX1ox, rock3 CKX1ox,* and *rock4 CKX1ox* mutants in the cytokinin-deficient background.

The identification of the *rock2* and *rock3* alleles as gain-of-function mutations in the *AHK2* and *AHK3* cytokinin receptor genes, and *rock4* as a gain-of-function IPT3 variant, provided the opportunity to further characterise the mutant phenotypes in the wild-type background. As cytokinin has growth promoting effects, special attention was given to the investigation of phenotypes that might be of relevance in the potential use of these mutations in transgenic crop design, e.g. improved plant growth characteristics, seed productivity and the regulation of senescence.

An additional aim of this thesis was to unravel the functionality of the gain-of-function receptor mutants *rock2* and *rock3*, by testing if the mutations cause higher cytokinin binding or rather constitutively active receptors.

2 Material & Methods

2.1 Bacteria, yeast and plant culture media

The bacterial, yeast and plant media were prepared as described (Bertrani 1951; Estelle and Somerville 1987; Kramer et al. 1996; Murashige and Skoog 1962; Rose et al. 1990; Sambrook and Russel 2001).

Bacteria culture media:

LB medium
(Bertrani 1951)
25 g/L LB medium (Roth, Karlsruhe)
for solid media:
15 g/L Agar

M9 medium
(Sambrook and Russel 2001)
200 ml/L 5x M9 Minimal Salts (Sigma-Aldrich, Steinheim)
2 ml 1 M $MgSO_4$
20 ml 1 M Glucose

SOC medium
(Sambrook and Russel 2001)
20 g/L Bacto Tryptone
5 g/L Bacto yeast extract
0.5 g/L NaCL
pH adjusted to 7,0 with 5N NaOH
after autoclavation:
5 ml/L 2 M $MgCl_2$
20 ml/L 1 M Glucose

Yeast culture media:

YPD medium
(Rose et al. 1990)
10 g/L Bacto yeast extract
20 g/L Bacto Peptone
for solid media:
15 g/L Agar
pH adjusted to 6,5 with HCl
after autoclavation:
50 ml/L 40% Glucose or Galactose

YEP medium
(Rose et al. 1990)
10 g/L Yeast extract
10 g/L Peptone
5 g/L NaCl
pH adjusted to 7.0 with HCl

YNB medium
(Rose et al. 1990)
6.7 g/L Yeast nitrogen base without amino acids
for solid media:
15 g/L Agar
pH adjusted to 5,8 with HCl
after autoclavation:
50ml/L 40% Glucose or Galactose

Plant culture media:

¼ Hoagland medium
(Kramer et al. 1996)

1.5 ml/L	1 M Ca(NO3)2·6H20
0.28 ml/L	1 M KH2PO4·4H2O
0.75 ml/L	1 M MgSO4·7H2O
1.25 ml/L	1 M KNO3
10 ml/L	1 mM NaFeEDTA
1 ml/L	Micronutrients: 70 mM H_3BO_3, 14 mM $MnCl_2$, 0,5 mM $CuSO_4$, 1 mM $ZnSO_4$, 0,2 mM Na_2MoO_4, 10 mM NaCl, 0,01 mM $CoCl_2$
0.4 g/L	MES

pH adjusted to 5,7 with 1 N KOH
for solid media:
5.5 g/L Phytagel

ATS medium
(Estelle and Somerville 1987)

5 ml/L	1 M KNO_3
2.5 ml/L	1 M KPO_4
2 ml/L	1 M $MgSO_4$
2 ml/L	1 M $Ca(NO_3)_2$
2.5 ml/L	20 mM Fe-EDTA
1 ml/L	Micronutrients: 70 mM H_3BO_3, 14 mM $MnCl_2$, 0.5 mM $CuSO_4$, 1 mM $ZnSO_4$, 0.2 mM Na_2MoO_4, 10 mM NaCl, 0.01 mM $CoCl_2$
5 g/L	Sucrose

for solid media:
7 or 12 g/L Agar (horizontal or vertical plates)

MS medium
(Murashige and Skoog 1962)

4.6 g/L	MS-vitamin mix (Duchefa, Haarlem, Netherlands)
0.5 g/L	MES
5 g/L	Sucrose

for solid media:
7 or 12 g/L Agar (horizontal or vertical plates)
pH adjusted to 5.7 with 1 N KOH

Plant soil composition: 65% compost soil (Einheitserdewerk™, Uetersen)
10% Granulate (Knaufperlite™ GmbH, Dortmund)
25% Sand

Liquid and solid media were prepared and autoclaved (20 min at 120 °C) before use. Appropriate antibiotics, amino acids or hormones were added to media after autoclaving and cooling (for solid media), or immediately prior to use (liquid media). Stock solutions of all antibiotics were stored at -20 °C. The appropriate amino acids histidine and/or leucine were dissolved in water to prepare 0.2% stock solutions and added to YNB media in final concentrations of 20 mg/L and 100 mg/L, respectively.

The final concentrations of the different antibiotics and herbicides are listed in Table 1.

Table 1: Antibiotics and herbicides used in this study

Substance	Stock solution	Final concentration in media
Ampicillin	100 mg/ml in water	100 mg/L
Carbenicillin	100 mg/ml in water	100 mg/L
Chloramphenicol	25 mg/ml in 100% ethanol	25mg/L
Gentamycin	25 mg/ml in water	25 mg/L
Hygromycin	50 mg/ml	20 mg/L
Kanamycin	50 mg/ml in water	50 mg/L
Rifampicin	50 mg/ml in DMSO	10 mg/L
Spectinomycin	50 mg/ml in water	50 mg/L
PPT	30 mg/ml in water	30mg/L
BASTA	-	0,1%

2.2 Cloning vectors and plasmids

The following vectors were used in this study (Table 2).

Table 2: Vectors used in the present study.

Vector	Company/Source	Function/Cloning purpose
pDONR221	Invitrogen™	Gateway™ Entry-Vector
pDONRP4P1R	Invitrogen™	Gateway™ Entry-Vector
pDEST15	Invitrogen™	*E. coli* expression vector
pB2GW7	(Karimi et al. 2002)	Plant expression vector
pK7m24GW,3	(Karimi et al. 2005)	Plant expression vector
pDONR222-AHK3	(Wulfetange et al. 2011)	Gateway™ cloning
pDONR221-AHK3-Chase-TMD	(Wulfetange et al. 2011)	Gateway™ cloning
p4P1R-pAHK2	(Stolz et al. 2011)	Gateway™ promoter cloning
p4P1R-pAHK3	(Stolz et al. 2011)	Gateway™ promoter cloning
p4P1R-pAHK4	(Stolz et al. 2011)	Gateway™ promoter cloning
pDONR201-AHK4	(Wulfetange et al. 2011)	Gateway™ cloning
pDONR201-AHK4-CHASE	(Wulfetange et al. 2011)	Gateway™ cloning
p423TEF	(Mumberg et al. 1995)	Yeast expression vector
p423TEF-AHK2	Y. Higuchi, Tokyo, Japan	Protein expression in yeast
p423TEF-AHK3	Y. Higuchi, Tokyo, Japan	Protein expression in yeast
p423TEF-AHK4	Y. Higuchi, Tokyo, Japan	Protein expression in yeast

2.3 Bacteria, yeast and plant material

2.3.1 Bacteria and yeast strains

The bacteria and yeast strains used in this study are listed in Table 3.

Table 3: Bacteria and yeast strains used in this study.

Organism	Strain	Genetic marker, reference	Purpose
Escherichia coli	DH5α	F-ϕ80d *lacZ*ΔM15 *end*A1 *rec*A1 *hsd*R17 (r_k-,m_k+) *sup*E44 *thi*-1 λ-*gyr*A96 (Nal_r) *rel*A1 D(*lac*ZYA-*arg*F) U169. (Grant et al. 1990; Hanahan 1983)	Plasmid amplification
Escherichia coli	DH10B	F– *mcr*A Δ(*mrr-hsd*RMS-*mcr*BC) Φ80*lac*ZΔM15 Δ*lac*X74 *rec*A1 *end*A1 *ara*D139 Δ(*ara leu*) 7697 *gal*U *gal*K *rps*L *nup*G λ– (Calvin and Hanawalt 1988; Grant et al. 1990; Raleigh et al. 1988)	Plasmid amplification
Escherichia coli	DB3.1	F– *gyr*A462 *end*A1 Δ(sr1-*rec*A) *mcr*B *mrr* *hsd*S20(rB–, mB–) *sup*E44 *ara*-14 *gal*K2 *lac*Y1 *pro*A2 *rps*L20(SmR) *xyl*-5 λ– *leu* *mtl*1 (Invitrogen) (Hanahan, 1983; Bernard and Couturier, 1992)	Propagation of plasmids containing *ccdB* gene
Escherichia coli	BL21(DE3) pLysS	F– *omp*T *hsd*SB(rB–, mB–) *gal dcm* (DE3) pLysS (CamR) (Davanloo et al. 1984; Studier and Moffatt 1986)	Protein expression in *E. coli*
Agrobacterium tumefaciens	GV3101:: pMP90	Rif^R, $Gent^R$ (Koncz and Schell 1986)	Stable plant transformation
Saccharomyces cerevisiae	TM182 (Δsln1)	MATa leu2 ura3 his3 sln1::hisG [pSSP25] (Maeda et al. 1995)	cytokinin sensing system
Saccharomyces cerevisiae	TM101	MATa ura3 leu2 his3 (Maeda et al. 1995)	control strain

2.3.2 Plants

The *Arabidopsis thaliana* ecotype Columbia-0 (Col) was used as wild type in all experiments. The *Arabidopsis thaliana* ecotype Landsberg *erecta* (L*er*) was used for establishment of mapping populations.

2.3.3 Mutant plant lines

The T-DNA insertion line *ahk2-5* was obtained from M. Riefler (Riefler et al. 2006).

The promoter-GUS reporter line *pARR5:GUS* was obtained from Joe Kieber (University of North Carolina, Chapel Hill, USA) (D'Agostino et al. 2000).

The transgenic *35S:AtCKX1* overexpressing line AtCKX1-11 (named *CKX1ox*) was obtained from T. Werner (Werner et al. 2003).

The mutant line *ore12-1* was kindly obtained by I. Hwang (Kim et al. 2006).

The lines *rock2 CKX1ox*, *rock3 CKX1ox* and *rock4 CKX1ox* derive from an EMS mutagenesis of *CKX1ox* plants carried out by I. Bartrina (FU Berlin). The transgenic line *pAHK2:rock2 CKX1ox* was also created by I. Bartrina (FU Berlin).

2.4 Computer Programms

The databank of the National Center for Biotechnology Information (NCBI), Bethesda, USA or the Arabidopsis Information Resource (TAIR) (Huala et al. 2001) was used for sequence analysis. Oligonucleotides were designed using the program Primer3 (Rozen and Skaletsky 2000) (http://frodo.wi.mit.edu/primer3) or the Genoplante™ Specific Primers and Amplification Design Software (SPADS) (http://urgi.versailles.inra.fr/spads/). For restriction analysis the program Vector NTI or the internet program Webcutter 2.0 (www.firstmarket.com/cutter/cut2.html) were used. The program Scion Image (Scion Corporation, Frederick, Maryland, USA) was used for area and length measurements of photographed plant organs. For DNA Alignments, the PC-program BioEdit 7.0.4.1 (Hall 1999) was used.

2.5 Oligonucleotides

Oligonucleotides for PCR and sequencing were obtained from Invitrogen (Karlsruhe) or GATC Biotech AG (Konstanz). Oligonucleotides purified by high-performance liquid chromatography (HPLC) and used for site-directed mutagenesis were obtained from Invitrogen (Karlsruhe). Lyophilized oligonucleotides were resuspended in ddH_2O to a final concentration of 50 µmol/µL and were stored at -20 °C. If primers were used for real-time PCR (qRT-PCR), primers were designed according to a stringent set of criteria using the Genoplante™ Specific Primers and Amplification Design Software (SPADS) (http://urgi.versailles.inra.fr/spads/). The primers were designed with the following parameters: melting temperatures (Tm) of 60 ± 2 ºC, primer lengths of 20-24 nucleotides, guanine-cytosine (GC) content of 45-55%, and PCR amplicon lengths of 100-150 base pairs. All primers used for sequencing, cloning purposes, RT-PCR, and qRT-PCR analysis are listed as supplemental data (Table 6 and Table 7).

Primers recommended in the publication of Lukowitz (Lukowitz et al. 2000) and further primers chosen by their position in the genome were used for mapping (Supplemental Data Table 5). Sequences and position on the chromosomes of known markers were obtained from the TAIR

Database (http://www.arabidopsis.org/index.jsp). New markers were designed using the Monsanto Arabidopsis Polymorphism and Ler Sequence Collections, which lists all known polymorphisms between the *Arabidopsis thaliana* ecotypes Columbia and Landsberg *erecta* (http://www.arabidopsis.org/browse/Cereon/index.jsp) and named after the respective BAC clones where they are located.

2.6 Growth conditions and culture methods

2.6.1 Bacteria and yeast growth conditions

The microbial cultures were grown under standard conditions as described (Bertrani 1951; Rose et al. 1990; Sambrook and Russel 2001). *E. coli* strains were grown overnight at 37 °C in liquid or on solid LB media containing the appropriate antibiotics (Table 1). *A. tumefaciens* was grown at 28 °C in liquid or on solid LB for 2-3 days if used for plasmid selection or plasmid propagation, or in liquid YEP if used for plant transformation. *S. cerevisiae* was grown at 30 °C in liquid or on solid YPD or YNB media containing the appropriate amino acids and glucose or galactose. Liquid cultures were grown while shaking with 200 rpm (*E. coli*), 160 rpm (*A. tumefaciens*) or 150 rpm (*S. cerevisiae*) at the respective temperatures. Selective components were added to the medium according the plasmid requirements.

2.6.2 Plant growth conditions

After stratification at 4 °C for 2-4 days to synchronize germination, plants were grown in controlled environment at 20-22 °C under long day conditions (16-hours light/ 8-hours dark) in the greenhouse or in light chambers or short day conditions (8-hours light/ 16-hours dark) in light chambers. In the green house light was provided by sunlight and/or fluorescent tubes. In growth chambers light was provided by fluorescent tubes (~100 µE/m^2).

For plant growth on soil, seeds were sown directly on soil or grown in vitro on selection plates containing the appropriate antibiotics (Table 1) and transferred to soil after 12 to 15 days. After sowing or potting, plants were kept under plastic covers for 2-3 days to prevent dehydration.

Plants on plates were grown on MS or Ats media under long day conditions in growth chambers. For *in vitro* experiments on plates, seeds were surface sterilized with 0,1 % (v/v) Triton in 70 % ethanol for 5 min, then washed three times with 70% ethanol and air dried on sterile whatman paper. For *in vitro* plant growth in liquid media, seeds were surface sterilized with a 1.2 % sodium hypochlorite

solution for 10 min and then washed three times with sterile water. After stratification at 4 °C for 2-4 days, seeds were transferred to 100 ml Erlenmeyer flask and grown while shaking with 100 rpm.

2.6.3 Plant transformation

Plasmids were transformed into *Arabidopsis* plants by the floral dip method (Clough and Bent 1998) or a simplified variant of this method. If the transformation of *Arabidopsis* plants was carried out by the floral dip method according to the protocol by Clough and Bent, a single colony of *Agrobacterium* bearing the desired binary vector was inoculated into 5 ml of LB medium containing selective antibiotics and grown as starting culture at 28 °C for two days. This culture was then transferred into 300 ml YEP selection media and grown for another 24h at 28 °C. Bacteria were centrifuged at 6,000 × g for 15 min at 4 °C and resuspended in 300 ml infiltration medium (50 g/L sucrose; 2.19 g/L MS salts; 50 µl/L Silwet 77). Inflorescences of approximately four week old plants were dipped into the *Agrobacterium* solution for 30 seconds, under gentle agitation. Dipped plants were then placed under a plastic cover for 24 hours to maintain high humidity and then transferred to the greenhouse. After 2-3 weeks seeds were harvested and dried. Transformants were selected using appropriate antibiotics or the herbicide BASTA (Bayer Crop Science, Monheim) (Table 1). For selection based on antibiotics, plants were grown *in vitro* on Ats or MS plates containing the appropriate antibiotic. The herbicide BASTA was sprayed on 10-20 day old seedlings growing on soil three times in a 3-day interval. Resistant seedlings were transferred to individual soil pots and grown under standard conditions as described in chapter 2.7.2.

If the simplified variant was used, 30 ml of YEP medium containing selective antibiotics were used as starting culture and grown for 24h at 28 °C. The starting culture was then transferred into 300 ml YEP and grown for another 24h at 28 °C. After adding 50 µl/L Silwet 77 to the culture, plant inflorescences were directly dipped into the YEP medium for 30 seconds.

35S:AtCKX1 transgenic plants were sprayed with a chemical CKX inhibitor (10 µM inhibitor; 0.01/ Silwet 77) (Zatloukal et al. 2008) to suppress the cytokinin deficiency syndrome and enhance flower production. Plants were sprayed in a 3-day interval until one week before transformation.

2.6.4 Bacteria transformation

For transformation of plasmid DNA to competent *E. coli* cells, chemical or electro-competent cells were used. Before transformation the competent cells were thawed on ice for 5 min.

1 µl plasmid DNA (approximately 50-200 ng) was added to tubes containing 50-100 µl thawed electro competent cells and mixed by swirling with pipette tip. DNA and cells were then transferred to a pre-

chilled electroporation cuvette and plasmid DNA was transformed into *E. coli* cells by electroporation with GenePulserII (Bio-Rad, München) with the following settings: 200 Ω, 1.8 kV, 2.5 to 5 ms. Immediately 1 ml SOC medium was added and the cells were incubated 30 to 60 minutes at 37 °C on a shaker with moderate shaking to allow for plasmid expression.

For heat shock transformation 1-2 µl plasmid DNA was added to tubes containing 100 µl thawed chemical competent cells, mixed by swirling with pipette tip and incubated on ice for 30 min. The transformation mixture was then incubated at 42 °C in a water bath for exactly 45 seconds and immediately transferred on ice. 400 µl of SOC medium was added and incubated for 30 to 60 minutes at 37 °C on a shaker.

Aliquots of the electroporation mixture or heat shock mixture were then plated on LB-agar plates supplemented with the appropriate antibiotics (Table 1) and incubate plates at 37 °C over night.

Transformation of *Agrobacterium tumefaciens* cells was done by electroporation as described for *E. coli* cells. Different to E*. coli* cells, *A. tumefaciens* cells were incubated at 28 °C for 2 h after electroporation and then at 28 °C for two days.

2.6.5 Yeast transformation

Yeast transformation was performed after Gietz and Schiestl (2007) with minor modifications. The yeast was grown in YPD medium at 30 °C over night. 1 ml of this culture was centrifuged for five seconds in a micro centrifuge and supernatant was decanted by inverting the tube and shaking it once, leaving cells in 50-100 µl of liquid. 2 µl of 10 mg/L of sheared carrier DNA (herring's sperm DNA) and 1 µg transforming plasmid DNA was added and mixed by vortexing. Then 0.5 ml freshly made PLATE solution (40% PEG 3350; 0.1 M LiAc; 10 mM Tris-HCl; pH 7.5; 1 mM EDTA) and 20 µl 1 M DTT was added and well mixed by vortexing. The transformation mixture was incubated at room temperature over night. After incubation, heat shock transformation was performed at 42 °C for 10 min. The transformed cell suspension was plated on YNB media lacking the appropriate amino acids and incubated at 30 °C for 3-4 days.

2.7 Nucleic acid methods

2.7.1 DNA extraction methods

2.7.1.1 DNA extraction from Arabidopsis

Genomic DNA was isolated from *Arabidopsis thaliana* using the CTAB method (Weigel and Glazebrook 2002) if DNA was used for PCR amplification and construct cloning.

A "quick prep" method was used if the genomic DNA was only used for standard PCR tests. Approximately 1 cm^2 of *Arabidopsis* leaf tissue was shredded in 400 µl extraction buffer (200 mM Tris/HCl pH 7.5; 250 mM NaCl; 25 mM EDTA) in a 1.5 ml plastic tube with a 1.5 mm metal ball for 2 min at 30 rpm using a Reetsch-Mill. 20 µl of 5% SDS was added, mixed and plant material centrifuged at full speed in a micro centrifuge for 5 min. 1 volume of isopropanol was added to the supernatant and centrifuged for 5 min. The pellet was washed with 70% ethanol, air dried and resuspended in 100 µl dH_2O or TE buffer (Weigel and Glazebrook 2002).

2.7.1.2 DNA extraction from bacteria

Purification of plasmid DNA from *E. coli* was carried out using alcaline lysis based on the manufacturer's guide „QIAGEN Plasmid Purification Handbook" by Qiagen (Hilden) followed by alcohol precipitation. A single bacterial colony was picked and grown overnight at 37 °C in LB media containing appropriate antibiotics. 1.5 ml of this culture were centrifuged down and the pellet was resuspended in 300 µl buffer P1 (50 mM Tris-HCl, pH 8.0; 10 mM EDTA; 100 µg/ml RNase A). 300 µl lysis buffer P2 (200 mM NaOH; 1 % SDS) was added and carefully mixed by inverting the tube 5-6 times. After incubation for 5 min 300 µl neutralization buffer P3 (3 M K-acetate, pH 5.5) was added, mixed by inverting and centrifuged at 16000 x *g* for 5 min. The supernatant was carefully transferred into a new 1.5 ml plastic tube, mixed with 1 volume isopropanol and centrifuged at 16000 x *g* for 10 min. DNA pellet was washed with 70% ethanol, air-dried and resuspended in 50-100 µl bidest H_2O.

Alternatively plasmid DNA was isolated using the „E.Z.N.A. Plasmid Miniprep Kit I" (Peqlab, Erlangen) or the "Invisorb Spin miniprep kit" (Invitek, Berlin) according to the manufacturer's instruction manual.

The plasmid DNA from *Agrobacterium* was isolated by alcaline lysis based on the manufacturer's guide „QIAGEN Plasmid Purification Handbook" by Qiagen (Hilden) followed by a phenol/chloroform purification step and alcohol precipitation. *Agrobacterium* was grown for 2-3 days at 28 °C in LB containing appropriate antibiotics. 3 ml of this culture was centrifuged down and resuspended in

500µl buffer (150 mM NaCl; 50 mM Tris-HCl, pH 8.0; 10 mM EDTA). The culture was centrifuged down again, the pellet was resuspended in buffer P1 (50 mM Tris-HCl, pH 8.0; 10 mM EDTA; 100 µg/ml RNase A) containing 20 mg/ml lysozyme (in 10 mM Tris-HCl, pH 8), and incubated at 37 °C for 15 min. 300 µl buffer P2 (200 mM NaOH; 1 % SDS) and 300 µl buffer P3 (3 M K-acetate, pH 5.5) were added and mixed by inverting the tube and suspension was centrifuged at 16000 x *g* for 5 min. 500 µl phenol/chloroform/isoamylalkohol (25:24:1) was added to 800 µl supernatant and centrifuged at 16000 x g for 5 min. 1 volume isopropanol was added to the supernatant, incubated on ice for 10 min and centrifuged at 16000 x *g* for 10 min. Pellet was washed with 70% ethanol, air-dried and resuspended in 20 µl bidest H_2O.

2.7.1.3 DNA extraction from yeast

Yeast was grown in YNB lacking the appropriate amino acids for 3 days. 3 ml of this culture was centrifuged at 16000 x *g* for 30 seconds, and pellet was resuspended in 200 µl buffer A (10 mM Tris-HCl pH 8; 1 mM EDTA pH 8; 100 mM $NaCl_2$; 1% SDS; 2% Triton X-100). 200 µl phenol:chloroform:isoamylalcohol (25:25:1) were added and yeast tissue was ground with 0,3 g glass beads (600 µm) in a Reetsch-Mill at 30 rpm for 1 min. After centrifugation at 16000 x *g* for 5 min, the upper phase was transferred into a fresh plastic tube and DNA was precipitated with 1 volume isopropanol and 2.5 volumes 3M Na-acetate (pH 5.2). After centrifugation at 16000 x *g* at 4 °C for 30 min, the pellet was washed with 70% ethanol and resuspended in 20 µl distilled water.

2.7.2 RNA extraction from *Arabidopsis* and purification of RNA

Total RNA from tobacco and *Arabidopsis* tissue was extracted according to Brenner (Brenner et al. 2005), with slight modifications.

8-day-old seedlings were used for the isolation of total RNA from *Arabidopsis* plants. Seedlings were grown in liquid 1/2 MS plus 0.25% sucrose. 100-200 mg of plant tissue was ground in liquid nitrogen and transferred to 2 ml plastic tubes. 1 ml TRIzol (38% Phenol; 800 mM guanidinium thiocyanate; 400 mM ammonium thiocyanate; 100 mM sodium acetate; 5% glycerol) was added immediately and vortexed for 30 seconds. After incubation at RT for 5 min, the tubes were centrifuged at 16000 × g at 4 °C for 5 min. 400 µL of chloroform-isoamylalcohol 24:1 was added to the supernatant and vigorously shaken until the mixture looked homogenous. After incubation at RT for 5 min, the mixture was centrifuged at 16000 × g at 4 °C for 15 min and the upper phase (ca. 700 µl) transferred to a fresh plastic tube. 1/2 volume of isopropanol and 1/2 volume of high salt solution (1.2 M sodium chloride; 800 mM sodium citrate) were added, mixed by inversion and incubated on ice for 30 min.

The precipitated RNA was centrifuged at 12000 x *g* at 4 °C for 15 min and the supernatant was removed with a pipette. The RNA was washed twice with 75% ethanol by centrifugation at 7500 × *g* at 4 °C for 5 min. The RNA pellet was dried at RT and dissolved in 40 µl (RT-PCR) or 100 µl (qRT-PCR) RNase-free water.

If RNA was used for reverse transcriptase (RT)-PCR, DNA was digested using DNAse I (Fermentas, St. Leon-Rot) following the "Protocol for Preparation of DNA-free RNA prior to RT-PCR" (Fermentas, St. Leon-Rot).

For quantitative real-time PCR (qRT-PCR), RNA was further purified using Qiagen RNeasy mini-columns including the on-column DNase digestion as described in the Qiagen RNeasy Mini Handbook (Qiagen, Hilden), with slight modifications. 350 µL buffer RLT (Qiagen, Hilden) plus 250 µL of ethanol was added to the RNA samples, mixed and transferred to an RNeasy mini column and incubated at RT for 1 min. The samples were centrifuged at 8000 × *g* at RT for 15 seconds and this step was repeated by applying the filtrate once again to the column. Then 350 µl buffer RW1 (Qiagen, Hilden) was added to the mini column and centrifuged at 8000 × *g* at RT for 15 seconds. Next on-column DNase digestion was performed using Qiagen RNase-Free DNase kit (Qiagen, Hilden, Germany). 70 µl buffer RDD (Qiagen, Hilden) were mixed with 10 µl DNAse, applied on the mini column and incubated at RT for 15 min. After DNase digestion the columns were washed with 350 µl buffer RW1 and then twice with 500 µL of wash buffer RPE (Qiagen, Hilden) by centrifugation at 8000 × *g* at RT for 15 seconds. The columns were dried by a 1 min centrifugation step at 16000 x *g*. RNA was then diluted with 35 µl RNase-free water into a fresh plastic tube by centrifugation at 8000 x *g* for 15 seconds. To increase RNA concentration, filtrate was again put on the same column and centrifuged once more.

Photometric measurement of the RNA was performed by 260/280/230 nm UV light absorption with a NanoDrop ND-1000 spectrophotometer (Peqlab, Erlangen) to calculate the amount and quality of RNA. The RNA was considered clean if the ratio of 260/280 > 2.00 and 260/230 > 2.150.

2.7.3 Agarose gel electrophoresis

For agarose gel electrophoresis 0.8% to 3.5% agarose gels were used depending on the expected DNA size. Samples were prepared by mixing with a suitable volume of 10x loading buffer (10x TAE with 30 % (v/v) glycerine; 0.25 % (w/v) bromphenole blue; 0.25 % (w/v) xylencyanol). To visualise DNA fragments, 0.2 µg/ml ethidium bromide were added to the agarose gel. As running buffer 1 x TAE buffer (40 mM Tris-HCl; 1 mM EDTA, pH 8,0) was used. The molecular weight marker

HyperLadderI™ (Bioline, Luckenwalde) was used for DNA size determinations. Visualization and pictures of gel were taken by using the SynGene Bioimaging system (Merck, Darmstadt).

2.7.4 Isolation of DNA fragments from agarose gel

10 to 20 µl of restriction enzyme digested or PCR amplified DNA fragments were separated by agarose gel electrophoresis (see chapter 2.7.3). The DNA was visualized using a UV-table (Bachofer, Reutlingen), the desired DNA bands of the size ranges from 100 bp to 10 kb were excised from the agarose gel and purified using the QIAEX II Gel Extraction Kit, according to the manufacturer's (Qiagen, Hilden) instruction manual.

2.7.5 Purification of PCR products

DNA fragments were purified with the QIAquick PCR Purification Kit according to the manufacturer's (Qiagen, Hilden, Germany) instruction manual.

2.7.6 Sequencing of DNA

DNA sequencing was done by the company Seqlab (Göttingen) or GATC Biotech (Konstanz).

2.7.7 Restriction digestion

All restriction enzymes were purchased from New England Biolabs (Frankfurt) and Fermentas (Leon-Rot) and used with the supplied buffers. A typical reaction mixture consisted of 10 units of the appropriate restriction enzymes, not exceeding 10% of the final reaction volume, 1 µl of the manufacturer recommended reaction buffer, 50-500 ng of DNA, and sterile water to a final volume of 10 µl. The reaction mixture was incubated at recommended temperatures for 1-3 hours.

2.7.8 Gateway™ recombination

The cloning of constructs in Gateway™ compatible vectors was done according to the manufacturer's (Invitrogen, Karlsruhe, Germany) protocol. The primers used for amplification of DNA fragments with attached att-sites are listed in Table 6 and the Gateway™ Entry- and Destination-Vectors which were used in this study are listed in Table 2.

2.7.9 Site-directed mutagenesis

Point mutations were introduced using QuikChange™ Site-Directed Mutagenesis Kit (Stratagene, Amsterdam, Netherlands) using mutagenic oligonucleotides listed in Table 6 (Supplemental Data).

2.7.10 Polymerase chain reactions (PCR)

2.7.10.1 Standard PCR

For standard PCR (analytic purposes and mapping) the heat resistant *Taq* polymerase was used. If the PCR product was used for cloning or sequencing, the polymerase Bio-X-Act-Short (Bioline, Luckenwalde) with *proofreading*-function (3´→5´ exonuclease) was used according to manufacturer's instructions. For site-directed mutagenesis a high-fidelity PCR enzyme (*Pfu Ultra*) (Stratagene, Amsterdam, Netherlands) was used to eliminate unwanted second-site errors. PCR was performed following manufacturer's (Stratagene, Amsterdam, Netherlands) instruction manual. The used primers are listed in Table 5 and Table 6.

For standard PCR following components and programs were used:

Standard PCR	dH_2O	12 µl
	Reaction buffer (10x)	2 µl
	$MgCl_2$ (50 mM)	0.8 µl
	dNTP's (20 mM)	0.8 µl
	5'-Primer (12.5 µM)	1 µl
	3'-Primer (12.5 µM)	1 µl
	Taq polymerase (1U)	0.5 µl
	DNA	1-2 µl

Standard PCR program	Initial denaturation	95 °C	2 min
	Denaturation	95 °C	15 sec
	Annealing*	55-62 °C	15 sec
	Elongation*	72 °C	1 min/1 kb
	Final elongation	72 °C	10 min
	Stop	16 °C	∞
	No. of cycles	30-38	

*The annealing temperature for the reactions depended on the melting temperature of the primers that were used.

2.7.10.2 Reverse transcriptase (RT)-PCR

cDNA synthesis was done using Superscript III Reverse Transcriptase (Invitrogen, Karlsruhe). 1 µl oligo dT (50 µM), 0.5 µl random primer (50 µM), 2 µl dNTPs (20 mM) and 10.5 µl DNAse-treated RNA were mixed and incubated at 65 °C for 5 min and then placed on ice. 4 µl 5x first strand buffer, 1 µl DTT (0.1 M) and 1 µl Superscript III Reverse Transcriptase were added and incubated at 25 °C for 5 min, followed by 50 °C for 60 min and 70 °C for 15 min. Concentration and quality of DNA was photometrical measured. Then standard PCR was performed with 400 ng DNA. Control reactions to check for the presence of mRNA were performed using the *Actin2* primer pair. The used primers are listed in Table 7.

2.7.10.3 Real time PCR or quantitative RT-PCR (qRT-PCR)

PCR reactions were performed in an Applied Biosystems 7500 Fast Real-Time PCR System (Applied Biosystems, Foster City, USA), using SYBR™ Green (Sigma) to monitor dsDNA synthesis and Immolase DNA Polymerase (Bioline) as hot start enzyme. Total RNA was extracted and purified as described (see chapter 2.8.2). cDNA synthesis was performed using oligo dT and random primer and Superscript III Reverse Transcriptase according to the manufacturer's (Invitrogen, Karlsruhe) protocol. 1 µl oligo dT (50 µM), 2 µl random primer (50 µM), 2 µl dNTPs (20 mM) and 8 µl RNA (1µg/µl) were mixed and incubated at 65 °C for 5 min and then placed on ice. 4 µl 5x first strand buffer, 1 µl DTT (0.1 M) and 1 µl Superscript III Reverse Transcriptase were added and incubated at 25 °C for 5 min, followed by 50 °C for 60 min and 70 °C for 15 min. The real time polymerase chain reactions were prepared in 20 µL volume containing 1 µL cDNA (300 ng), 0,12 µL of each primer (50 µM), 0.8 µL of $MgCl_2$ (2 mM), 2 µL 10x Immolase buffer, 0.4 µL dNTPs (5 mM each), 0.04 µL of ROX (1:1000 dilution from 2.5 mM stock) (Sigma, Munich), 0.20 µL SYBR Green I (1:10,000 dilution in DMSO) (Sigma, Munich), 0.04 µL Immolase polymerase (5 U/µL) (Bioline, Luckenwalde) and 14.28 µl distilled water. The following PCR program was used:

Initial denaturation	95 °C	15 min
Denaturation	94 °C	10 sec
Annealing*	55 °C	15 sec
Elongation*	72 °C	10 sec
Stop	16 °C	∞
No. of cycles	40	

Data were analyzed with the Applied Biosystems 7500 software V2.0.3 (Applied Biosystems). Two housekeeping genes (*Ubiquitin10* and *At3g25800*) were used as a control to normalize the varying amounts of cDNA between samples, and the relative expression was determined using the 2^{-DDCT}

method (Livak and Schmittgen 2001). Primer sequences for all genes analyzed are listed in Table 7 (Supplemental Data).

2.8 Establishment of transgenic lines

2.8.1 pAHK3:rock3

For the construction of the *pAHK3:rock3* transgene, the *AHK3* promoter and the *ROCK3* cDNA were combined with Multisite Gateway™ recombinational cloning. The AHK3 promoter was amplified and cloned by Andrea Stolz (Stolz et al. 2011) in the following way: A 2062 bp promoter region of *AHK3* was amplified by PCR from genomic DNA of *A. thaliana* Col-0 and the fragment was inserted into pDONR™P4-P1R entry vector (Invitrogen, Karlsruhe). The *AHK3* cDNA containing the open reading frame of the gene was PCR-amplified from *Arabidopsis thaliana* Col-0 and cloned into pDONR™222 entry vector (Invitrogen) by Klaas Wulfetange (Applied Genetics, FU Berlin). The *rock3* point mutation was introduced by PCR based mutagenesis with the „QuickChange Site-Directed Mutagenesis"-Kit (Stratagene, La Jolla, USA) to obtain the *rock3* allele. The mutation in the constructs was confirmed by DNA sequencing. The used mutagenic oligonucleotides are listed in Table 6 (Supplemental Data). To generate the binary destination vectors, the *AHK3* promoter and the *ROCK3* cDNA were then combined with Multisite Gateway™ recombinational cloning in the pK7m24GW,3 vector (Karimi et al. 2005). The construct was introduced into *Agrobacterium tumefaciens* strain GV3101 and *Arabidopsis thaliana* Col-0 plants and *35S:AtCKX1* plants (Werner et al. 2003) were transformed using the floral dip method (see chapter 2.6.3). Transgenic lines were selected using the antibiotic kanamycin.

2.8.2 pAHK2:rock2

The cloning of the construct *pAHK2:rock2* was done by Andrea Stolz (cloningof the promoter), Klaas Wulfetange (cloning of the *AHK2* gene) and Isabel Bartrina (all Applied Genetics, FU Berlin). A 2124 bp promoter region of *AHK2* was amplified by PCR from genomic DNA of *Arabidopsis thaliana* Col-0 and cloned with Gateway™ technology into the pDONR™P4-P1R entry vector (Invitrogen, Karlsruhe). After cloning the *AHK2* genomic sequence with Gateway™ technology into the pDONR™221 entry vector (Invitrogen, Karlsruhe) the *rock2* point mutation was introduced using the „QuickChange Site-Directed Mutagenesis"-Kit (Stratagene, La Jolla, USA) to get the *rock2* allele. The fragments were combined with Multisite Gateway™ recombinational cloning in the pK7m24GW,3 vector (Karimi et al. 2005). The construct was introduced into *Agrobacterium tumefaciens* strain

GV3101 and *A. thaliana* Col-0 plants and *35S:AtCKX1* plants (Werner et al. 2003) were transformed using the floral dip method (see chapter 2.6.3). Transgenic lines were selected using kanamycin.

2.8.3 pIPT3:rock4

To generate the promoter entry clone a 2008 bp promoter region of *IPT3* was amplified from genomic DNA of *A. thaliana* Col-0 with specific primers with GATEWAY™ tails (Supplemental Data Table 6), and cloned into the GATEWAY™ pDONR™P4-P1R entry vector (Invitrogen, Karlsruhe) through BP reaction. Absence of PCR induced mutations in the constructs was confirmed by DNA sequencing. As the *IPT3* gene has no introns, the *ROCK4* coding sequence was directly amplified from *rock4 CKX1ox* plants (Col-0 background) using specific primers with GATEWAY™ tails (Supplemental Data Table 6) and cloned into the pDONR™221 entry vector (Invitrogen, Karlsruhe). The existence of the *rock4* mutation and absence of PCR induced mutations was confirmed by DNA sequencing. To generate the binary destination vector *pIPT3:rock4*, the *IPT3* promoter and the *ROCK4* cDNA were combined with Multisite Gateway™ recombination cloning in the pK7m24GW,3 vector (Karimi et al. 2005). The construct was introduced into *Agrobacterium tumefaciens* strain GV3101 and *A. thaliana* Col-0 plants were transformed using the floral dip method (see chapter 2.6.3). Transgenic lines were selected using kanamycin.

2.9 Yeast complementation assay

The *rock2* and *rock3* point mutations were introduced into the previously described vectors *p423-TEF-AHK2* and *p423-TEF-AHK3* (Mähönen et al. 2006), respectively, with QuickChange Site-Directed Mutagenesis kits (Stratagene, La Jolla, USA) and subsequently called *TEF-ROCK2* and *TEF-ROCK3.* The vectors p*TEF-AHK4rock2* and p*TEF-AHK4rock3* were designed by introducing the conserved mutations *rock2* and *rock3* in *p423-TEF-CRE1* (Mähönen et al. 2006). The used mutagenic oligonucleotides are listed in Table 6 (Supplemental Data). After sequence confirmation of PCR induced mutations, plasmids were introduced into the yeast *S. cerevisiae* strain TM182 *(Δsln1*) (Maeda et al. 1994) by yeast transformation as described in chapter 2.7.5. For the complementation assay, yeast was cultured in appropriate YNB media containing leucine and 2% galactose until it reached stationary phase. These yeast transformants were centrifuged at 3000 rpm with a tabletop microcentrifuge for 5 min, washed three times with YNB media containing leucine and 2% glucose and subsequently diluted to OD600 = 0.1 and cultured with shaking in appropriate YNB media containing 2% galactose, 2% glucose with 1 µM *trans*-zeatin, or 2% glucose with 10 µM *trans*-zeatin, as indicated in Fig.7. Growth was monitored spectrophotometrically at 600 nm with an Uvikon 931 spectrophotometer (Kontron, Munich).

2.10 Live cell cytokinin binding assay

The plasmid pDONR201-AHK4 was obtained from Klaas Wulfetange (Applied Genetics, FU Berlin). Site-directed mutagenesis was carried out with the QuickChange II Site-Directed Mutagenesis kit (Stratagene, La Jolla, USA) using the respective primers (Supplemental Data Table 6) to introduce the conserved mutations *rock2* and *rock3* into the *AHK4* gene. The mutated fragments were sequenced and subsequently shuttled into the GATEWAY™ pDEST15 vector (Invitrogen, Karlsruhe) by LR reaction and transformed into the *E. coli* strain BL21DE3pLysS (Novagen, San Diego). As negative control, the plasmid pDEST15^{empty} (Klaas Wulfetange, Applied Genetics, FU Berlin) was used. For protein expression, bacteria were grown in M9 media at 37 °C until they reached stationary phase. After dilution to OD600 = 0.1, 1mM IPTG was added and bacteria were cultured with shaking at 22 °C for 4 hours. Labeled *trans*-[2-^{3}H]zeatin (^{3}H*tz*) was obtained from the Isotope Laboratory of the Institute of Experimental Botany (Prague,Czech Republic). The *in vivo* cytokinin binding assay was performed as published (Romanov et al. 2005). 2.5 µl ^{3}H*tz* with or without additional unlabeled 0.1 mM *t*Z were used for the binding assay. The radioactivity was determined in ACS-II scintillation cocktail (Amersham Biosciences, UK).

2.11 Histochemical analysis of GUS expression

Histochemical analysis of GUS expression was performed with 7-day-old seedlings. Seedlings were grown on Ats medium under standard long day conditions. For GUS staining, seedlings were incubated for 1 h in 90% acetone at -20 °C, rinsed with 50 mM sodium phosphate buffer (pH 7.0) and incubated over night, 90 min, or 20 min at 37 °C in staining solution (0.5 mg/ml X-Gluc (5-bromo-4-chloro-3-indolyl-β-D-glucuronide); 50 mM sodium phosphate buffer (pH 7,0); 10 mM potassium ferrocyanide; 10 mM potassium ferricyanide; 0,2% Triton X-100) in the dark. After staining, samples were washed with 50 mM sodium phosphate buffer (pH 7.0) and cleared in 70% ethanol. The GUS histochemical staining was visualized and recorded with a light stereomicroscope (Olympus SZX12, Olympus, Hamburg) equipped with an Olympus C-4040ZOOM photographic device.

2.12 Pollen vitality test

Double staining with propidium iodide and fluorescein diacetate (FDA) was carried out by a modified procedure of Huang (1986). A stock solution of 1 mg/ml FDA was made in acetone and diluted to 10 µg/ml with 7% sucrose (w/v). Propidium iodide was dissolved at 1 mg/ml in water and diluted to 10 µL/ml with 7% sucrose (w/v). Equal amounts of diluted propidium iodide and FDA were mixed and a drop was applied on a glass slide. For pollen staining, anthers from flowers stage 13 (Smyth et al.

1990) were dissected and swirled in the staining drop to release pollen grains. A coverslip was applied gently and pollen microscopic analysis was performed using an Axioskop 2 plus microscope (Zeiss, Jena). Images were photographed using an AxioCam ICc3 photographic device (Zeiss, Jena).

2.13 Analysis of plant phenotypes

2.13.1 Morphometric measurements

Plant height and rosette diameter was measured with a ruler. Plant height was measured after termination of flowering. Rosette diameter was calculated as a mean value between two measurements per rosette. Final rosette diameter was measured at the start of flowering.

For hypocotyl, silique and flower length, petal area, and stem diameter measurements digital pictures were taken with an Olympus C-4040ZOOM photographic device equipped on a light stereomicroscope (Olympus SZX12, Olympus, Hamburg) and areas and length were measured with the Scion Image program (Scion Corporation, Frederick, Maryland, USA).

Microscopy photographs were taken with an AxioCam ICc3 photographic device equipped on an Axioskop 2 plus microscope (Zeiss, Jena).

To measure the leaf area, the sixth leaves of 30 day old plants were dissected, digital pictures were taken and leaf area was measured using the Scion Image program (Scion Corporation, Frederick, Maryland, USA). For cell size analysis, leaf tissue was fixed in ethanol/acetic acid (6:1), rehydrated in an ethanol series and cleared with chloral hydrate/glycerine/H_2O (8:1:2; w/v/v) for 2-3 days. Leaves were mounted on microscope slides, and photographed. Three photos were taken per leaf, one at the tip area, one in the middle and one at the base of the leaf. Cell sizes were calculated from the number of cells per unit area of digital micrographs and the average epidermis cell sizes were calculated as a mean value between the three leaf areas. Leaf and cell areas were subsequently used to calculate cell numbers.

The area of petals stage 13 (Smyth et al. 1990) was measured from digital images of dissected organs. For cell size analysis, petals were cleared fixed with ethanol/acetic acid (6:1) and cleared with chloral hydrate/glycerine/H_2O (8:1:2; w/v/v). Petal cell size was measured on the abaxial side in the upper half of the blade. Average cell sizes were calculated from the number of cells per unit area of digital micrographs. Petal and cell areas were subsequently used to calculate cell numbers.

Stem thickness was measured from hand-sections. Hand-cut sections were prepared with a razor blade from the base of the inflorescence stems when the stem was approximately 15 cm in length.

Sections were stained with toluidine blue (0.02% [w/v] solution in water) for 2 min, rinsed with distilled water, mounted in 50% glycerol, and observed with a microscope.

For cell measurements, stem tissue samples were fixed in FAA (3,7% formaldehyde, 50% ethanol, 5% acetic acid, 0.1% Triton X-100). The fixed samples were washed twice for 30 min with PBS buffer and dehydrated through an ethanol series (50%, 70%, 85%, 100% ethanol). To clear the tissue, samples were incubated in 25% Histoclear/75% ethanol, 50% Histoclear/50% ethanol, 75% Histoclear/25% ethanol for 15 min each, and finally in 100% Histoclear for 2 x 30 min. One volume Paraplast was added and incubated at 55 °C over night. Paraplast was exchanged twice a day until no Histoclear smell was detectable any more. Sections of 10-15 µm were cut from the embedded stem sampled with a microtome (Leica, Nussloch), stained with 0.02% toluidine blue and viewed and photographed with an AxioCam ICc3 photographic device equipped on an Axioskop 2 plus microscope (Zeiss, Jena).

2.13.2 Determination of flowering time

For flowering time analysis seeds were stratified for three days at 4 °C and then sown on soil and grown in the greenhouse under long day conditions. Onset of flowering was defined as the plant age when the first fully developed flower was formed. Termination of flowering was defined when no more new flowers were formed. The number of rosette leaves was scored at the start of flowering.

2.13.3 Determination of yield parameters

The final number of siliques was determined after termination of flowering. For analysis of seed yield, plants were grown under standard long day conditions in the greenhouse. Plants were put into paper bags at the end of flowering and watered for an additional week. After plants were kept dry for additional three weeks, seed yield was measured by weighting harvested seeds using an analytic balance (LE244S; Sartorius, Göttingen). Seed size was measured using sieves with different sized pores (250, 300 and 355 μm^2). Harvested seeds were filtered through the sieves and the ratio of seeds that fell through the different sized pores was measured using an analytic balance (LE244S; Sartorius, Göttingen).

2.13.4 Analysis of embryogenesis

Seeds were removed from siliques at different time points after pollination as indicated. Seeds were fixed in ethanol/acetic acid (6:1) for 1 h, cleared with Hoyers solution (0,25 g/ml gum arabic; 3,3 g/ml chloral hydrate; 30% glycerine) for 1 h, mounted on microscope slides, and photographed with an AxioCam ICc3 photographic device equipped on an Axioskop 2 plus microscope (Zeiss, Jena).

2.13.5 Analysis of leaf senescence

For the analysis of dark-induced leaf senescence, seedlings were grown *in vitro* for 18 days. The sixth rosette leave was detached and floated on distilled water. In case of *rock2 CKX1ox* and *rock3 CKX1ox* (see Fig.2) seedlings were grown *in vitro* for 21 days and the fourth or fifth leaf was detached. After 7 days in the dark at room temperature chlorophyll was extracted over night with 1 ml 100% methanol per 25 mg plant tissue at room temperature in the dark. Light absorption was measured at 652, 664 and 750 nm with a spectrophotometer and chlorophyll content was calculted using the formula $[22{,}12 \times (OD_{652} - OD_{750}) + 2{,}71 \times (OD_{664} - OD_{750})]$ as described (Porra et al. 1989) and normalized to fresh weight. The chlorophyll content at the start of the experiments was taken as a reference and set 100%. The experiment was repeated twice and each replicate consisted of at least 10 leaves per genotype.

Natural occuring leaf senescence was analysed by measuring the photosynthetic efficiency of PS II (Fv/Fm) and the decrease of chlorophyll content. The maximum efficiency of PSII photochemistry (Fv/Fm ratio) of dark adapted plants was measured with FluorCam (Photon Systems Instruments, Brno, Czech Republic). The sixth leaf of plants that were grown in the greenhouse was measured every 2-3 days starting 16 days after emergence (DAE). Before measuring plants were kept dark for 20 min. Chlorophyll contents of individual leaves were measured using the Chlorophyll Meter SPAD-502 (Konika Minolta, Bremen), taking the mean value of three measurements (on the tip, the middle and the bottom part) of the sixth leaf.

2.13.6 Root growth measurements

For *in vitro* root measurements, *Arabidopsis* seeds were surface-sterilized and cold treated at 4 °C for 3 days in the dark. Seedlings were then grown on vertical plates on Ats medium with 1.5% agar in light cambers under standard long day conditions. The elongation of the primary root was measured between day 4 and 12 after germination from digital images using Scion Image beta 4.0.2 software (Scion Cooperation, Frederick, USA). The number of emerged lateral roots that had been grown through the root exodermis was counted 15 days after germination. A lateral root was counted if it was clearly visible under a stereomicroscope with 10 x magnification.

The hydroponic system was used as described previously (Tocquin et al. 2003). *Arabidopsis* seeds were placed on 0.7 ml microfuge tubes filled with quarter strength Hoagland medium and 0.8% agar. The conical ends of the tubes were cut off, what allowed the roots to grow through the tubes. The microfuge tubes were placed in blue pipette tip boxes (Eppendorf) filled with quarter strength Hoagland medium and *Arabidopsis* plants were cultured under standard long day conditions for 35

days. Only plants, which roots quickly grew through the microfuge tubes and looked green and healthy, were selected for root measurements. Root length was measured using a ruler.

2.13.7 Cytokinin sensitivity tests

For cytokinin sensitivity tests on whole seedlings, *Arabidopsis* seedlings were grown on MS medium containing 25 nM BA or 0.01% dimethyl sulfoxide (DMSO) as a negative control under standard long day conditions for 14 days, followed by visual expectation of the seedlings. The effect of cytokinin on root growth was tested on Ats medium containing 10 nM BA or 0.01% DMSO.

3 Results

3.1 Characterisation and map-based cloning of *rock2* and *rock3* mutants

The metabolic inactivation of the plant hormone cytokinin is mainly catalyzed by cytokinin oxidases/dehydrogenases (CKX). *35S:CKX1* expressing plants show a cytokinin deficiency syndrome, which mainly consists of a dwarfed shoot with a smaller apical meristem and an enhanced root system (Werner et al. 2003). Suppressor mutagenesis of *CKX1* overexpressing *Arabidopsis* plants (*CKX1ox*) led to the identification of the mutants *rock2 CKX1ox (#205)* and *rock3 CKX1ox* (#608) (Bartrina 2006). The *rock2* and *rock3* alleles were identified based on their ability to suppress the phenotypic consequences of cytokinin deficiency caused by the overexpression of the *CKX1* gene encoding a cytokinin oxidase/dehydrogenase (Bartrina 2006).

The goal of the first part of this thesis was to identify the gene causing the phenotypic changes in *rock3 CKX1ox Arabidopsis* plants using map-based cloning, unravel the function of the *rock2* and *rock3* genes, and to further investigate the phenotype of the *rock2* and *rock3* mutants in the cytokinin-deficient background as well as the wild-type background.

3.1.1 Phenotypic analysis of *rock2* and *rock3* in the *CKX1* overexpressing background

Consistent with former results shown in the doctoral thesis of Bartrina (2006), the phenotypic reversion of the cytokinin deficiency syndrome was already obvious early after germination. In the *CKX1* overexpressing background *rock2* and *rock3* developed longer petioles with larger cotyledons, which were even bigger than wild-type cotyledons (Fig. 1a). Later in development, *rock2 CKX1ox* and *rock3 CKX1ox* showed an increased expansion of rosette leaves as well as an increased rosette fresh weight compared to *CKX1ox* plants, but in this case the reversion was not complete (Fig. 1b and 1c). Cytokinin-deficient plants develop small shoots with a strongly reduced number of flowers compared to wild type (Werner et al. 2003). Here again the mutations *rock2* and *rock3* suppressed the cytokinin-deficient phenotypes to a great extend. *rock2 CKX1ox* and *rock3 CKX1ox* grew bigger shoots with more flowers compared to *CKX1ox* plants (Fig. 1d and 1e). In this case *rock2* suppressed the cytokinin deficient phenotype more strongly than *rock3*, developing a similar shoot height with an equivalent amount of siliques as wild-type *Arabidopsis* plants (Fig. 1d and 1e). *Rock3 CKX1ox* plants developed larger flowers (Fig. 1f) similar to *rock2 CKX1ox* plants (see Bartrina 2006). In *rock2 CKX1ox* and *rock3 CKX1ox* flowers, petal length and width and gynoecia were clearly larger when compared to wild type. Furthermore, *CKX1ox* plants formed thin inflorescence stems that bent downward,

whereas stems of *rock2 CKX1ox* and *rock3 CKX1ox* plants were thicker and did not bend down as easily (data not shown).

In order to find out if it is likely that the mutations *rock2* and *rock3* play a role in the cytokinin signalling and metabolism, or rather enhance plant growth independently of cytokinin and therefore complement the CDS, more specific phenotypical investigations were carried out. In the following parameters, which are good indicators for a changed cytokinin status of the *CKX1ox* plants were analysed.

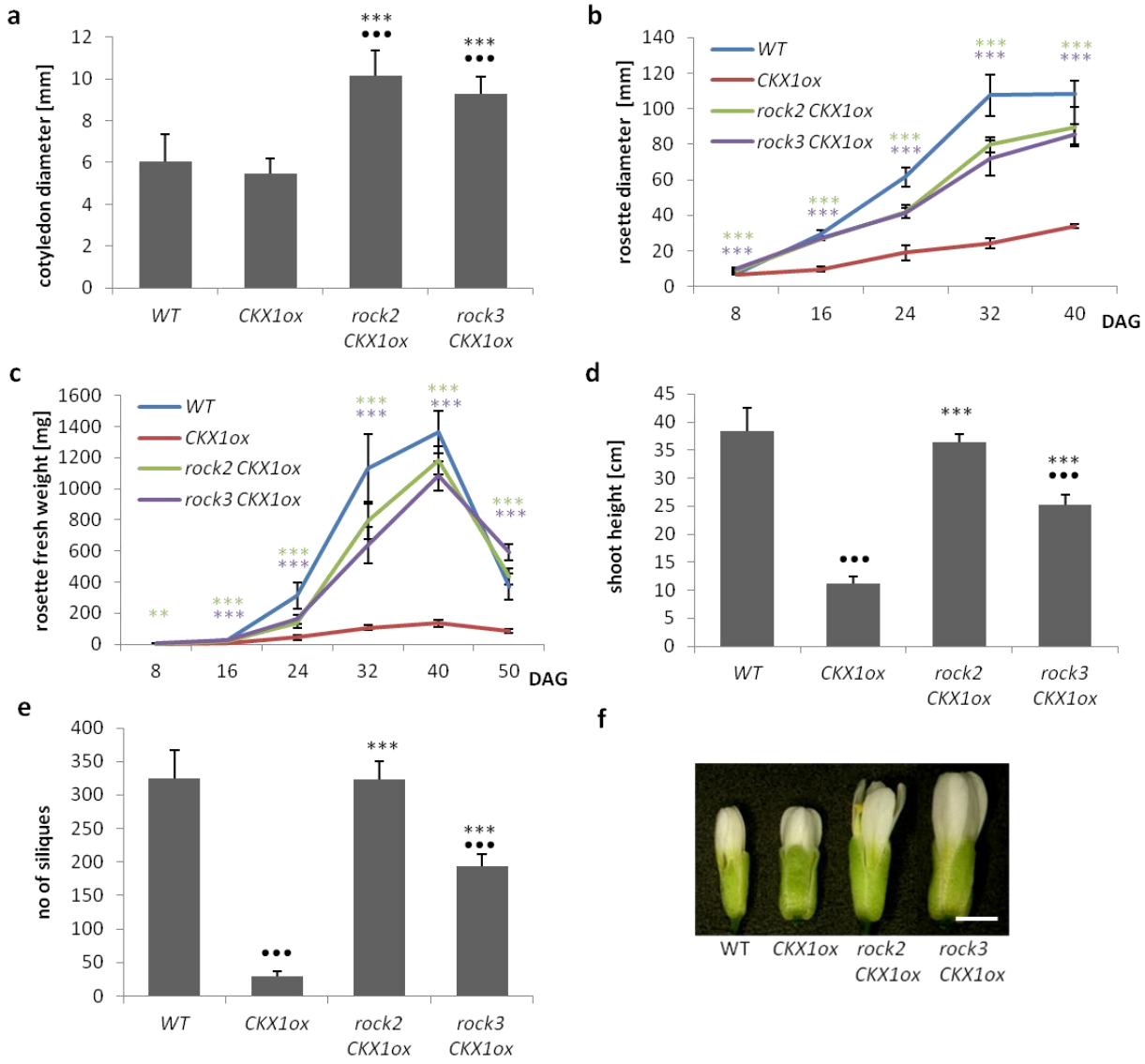

Fig. 1: Shoot phenotype of the suppressor mutants *rock2 CKX1ox* and *rock3 CKX1ox.*
(a) At seven days after germination, *rock2 CKX1ox* and *rock3 CKX1ox* seedlings show an increased cotyledon diameter compared to wild type and *CKX1ox* plants (n=5). **(b)** Comparison of rosette size between 8 and 40 days after germination (DAG) **(c)** and rosette fresh weight until end of flowering (n=5). **(d)** Shoot height at the end of flowering (n=5). **(e)** Number of siliques per plant (n=5). **(f)** Flowers stage 14 (Smyth et al. 1990). Scale bar: 1 mm. Error bars represent SE, ** = $p < 0{,}005$; *** = $p < 0{,}001$ compared to *CKX1ox* plants; ••• = $p < 0{,}001$ compared to wild type as calculated by pair wise student's t-test. Green asterisks: significance of the difference between *rock2 CKX1ox* and *CKX1ox;* purple asterisks: significance of the difference between *rock3 CKX1ox* and *CKX1ox.*

The influence of cytokinin on the chlorophyll content of leaves and their ability to retard leaf senescence was described soon after their discovery. Cytokinin delays senescence in detached leaves (Richmond and Lang 1957) and *in planta* (Gan and Amasino 1995; Mothes and Baudisch 1958) and it has been shown that modification of cytokinin biosynthesis and reception can significantly delay the senescence of plant organs (Kim et al. 2006; McCabe et al. 2001; Riefler et al. 2006).

Darkness is one of the most potent external stimuli that accelerate leaf senescence. It causes so-called dark-induced senescence, which mimics partially natural senescence, including chlorophyll degradation (Buchanan-Wollaston et al. 2005). Figure 2a and 2b show that the onset of leaf senescence in a dark-induced detatched leaf assay was clearly retarded in *rock2 CKX1ox* and *rock3 CKX1ox* mutant plants compared to wild-type and *CKX1ox* plants. After seven days in the dark the chlorophyll content was reduced by almost 80% in WT and and 90% in *CKX1ox* plants. *rock2 CKX1ox* showed slightly delayed leaf senescence, with the chlorophyll content being reduced by only 65%. The *rock3 CKX1ox* mutant delayed dark-induced leaf senescence even longer, and after seven days in the dark, the leaves were still green, with a chlorophyll content reduction of only 35%. Thus, in a cytokinin-deficient background *rock3* plays a more dominant role than *rock2* in delaying dark-induced leaf senescence.

Another feature of *CKX1* overexpressing plants is a delayed flowering time (Werner et al. 2003). Under long day conditions, *rock2* suppressed the delayed flowering phenotype completely, and flowered even a few days earlier than wild type (Fig. 2c). *rock3 CKX1ox* plants flowered slightly earlier than *CKX1ox* plants, but a few days later than wild type. Under short day conditions, *CKX1* overexpressing plants did not flower but either remained in the vegetative stage or eventually died. Here, *rock2* rescued the flowering phenotype of *CKX1ox* plants as *rock2 CKX1ox* plants flowered only slightly later than wild-type plants (Fig. 2d). The *rock3* mutation on the other hand did not suppress this phenotype. This indicates that *rock2* has a more important role in the regulation of flowering time compared to *rock3*.

It is also known that cytokinin induces photomorphogenesis. High concentrations of cytokinin induce some characteristics of light-grown plants in dark-grown wild-type seedlings, such as inhibition of hypocotyl elongation and development of leaves (Chory et al. 1994). Consistent with these results, triple cytokinin receptor mutants had longer hypocotyls than the wild type when grown in darkness (Riefler et al. 2006). To find out if the mutated genes participate in mediating this response, wild-type and mutant plants were grown in the dark and hypocotyl elongation was analysed after seven days. Cytokinin-deficient *CKX1ox* plants had slightly longer hypocotyls than wild type when grown in darkness whereas the *rock2* and *rock3* mutations caused an approximately 25% decrease in length

when compared to wild type, and almost a 50% decrease when compared to *CKX1ox* plants (Fig. 2e). Control seedlings grown in the light did not differ in length (data not shown).

Taken together, the mutations *rock2* and *rock3* trigger typical cytokinin related phenotypic changes in the *CKX1ox* background, clearly indicating a role in cytokinin signalling or metabolism.

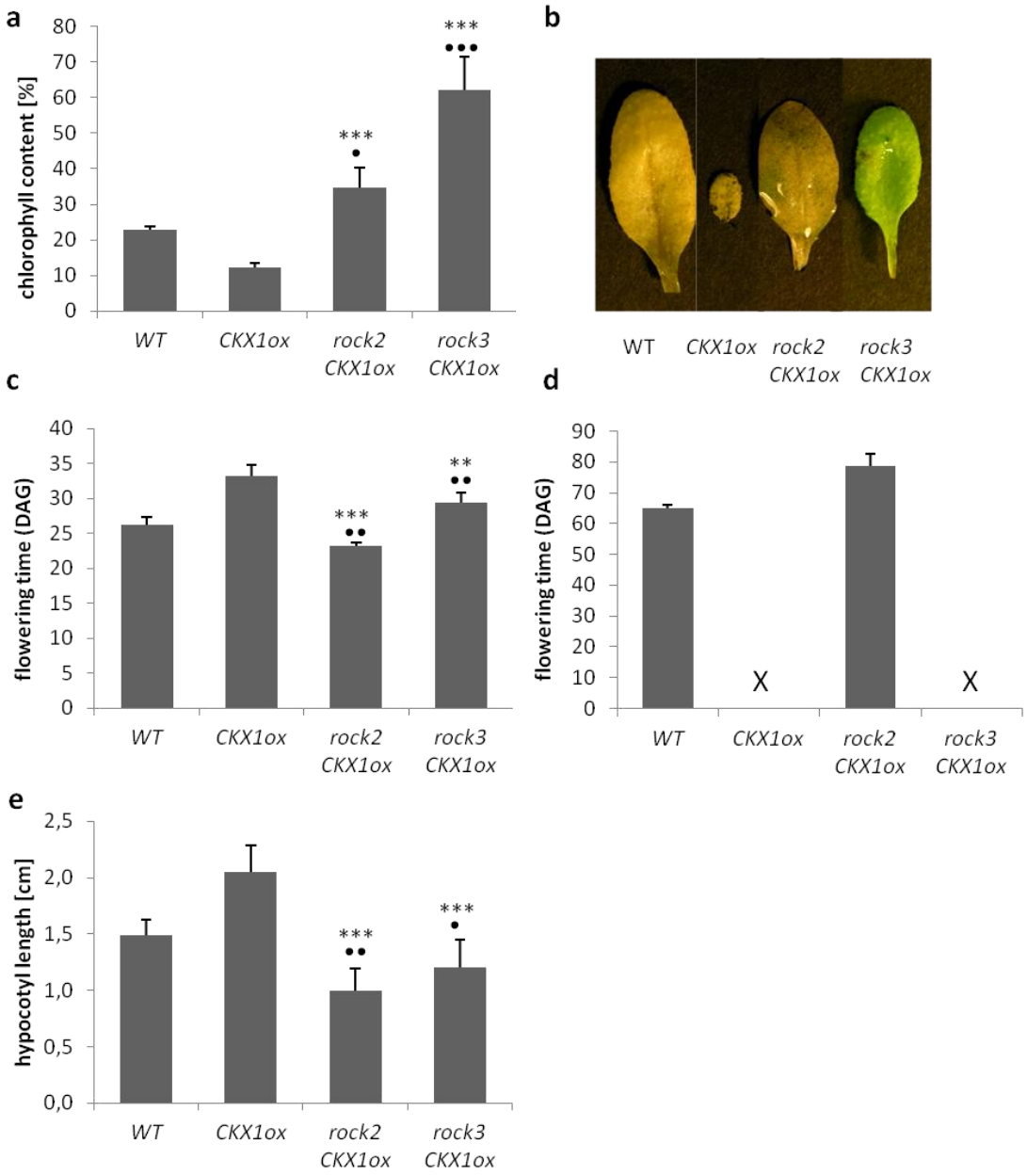

Fig. 2: The mutations *rock2* and *rock3* cause typical cytokinin-related phenotypic changes in the *CKX1ox* background.
(a) Dark-induced senescence in a detached leaf assay. The leaf chlorophyll content before the start of dark incubation was set at 100% for each genotype tested. Chlorophyll content was examined after 7 days in the dark (n = 15). **(b)** Leaves of different genotypes at the end of the chlorophyll retention assay described in (b). **(c)** Flowering time of wild-type and mutant plants grown in long day conditions or **(d)** short day conditions. Crosses illustrate that no transition to flowering occurred (n = 20). **(e)** Hypocotyl elongation after 10 days in the dark (n=10). Error bars represent SE. ** = $p < 0,005$, *** = $p < 0,001$ compared to *CKX1ox* plants; • = $p < 0,01$, •• = $p < 0,005$, ••• = $p < 0,001$ compared to wild type, as calculated by students t-test.

3.1.1.1 The mutants rock2 CKX1ox and rock3 CKX1ox show increased sensitivity towards exogenous cytokinin

So far, results indicate that *rock2 CKX1ox* and *rock3 CKX1ox* plants have a higher cytokinin status than *CKX1ox* plants, even though the transcript level of the *CKX1* transgene is not reduced in these plants (Bartrina 2006). Therefore it was suspected that the *rock2* and *rock3* mutants may show an increased sensitivity towards exogenous cytokinin. To test this experimentally, wild-type plants, *CKX1* overexpressing plants and the *rock* mutants were grown *in vitro* on medium containing 25 nM of the synthetic cytokinin benzyl adenine (BA) or on standard MS-medium (Fig. 3a). This experiment was previously performed by Bartrina (2006), but as the control plants did not grow as expected (a lot of seedlings were small and glossy), the experiment had to be repeated. On media containing 25 nM BA, wild-type seedlings were only slightly affected (Fig. 3a). 14 days after sowing wild-type seedlings were smaller than the control plants, but most leaves were still green. *CKX1ox* seedlings were less sensitive and grew on BA-containing media similarly as on medium without BA. In contrast, *rock2* and *rock3* seedlings, which were grown on media containing 25 nM BA had yellow leaves and stayed smaller than control plants on standard media. Interestingly, *rock* mutant seedlings showed an even increased sensitivity towards applied cytokinins compared to wild-type seedlings, which confirms the results achieved by Bartrina (2006).

Another often used parameter to test for a changed cytokinin status is root growth. In contrast to its promotional role in shoot organs, cytokinins are negative regulators of root meristem activity, root primordia initiation and lateral cell expansion (Heyl et al. 2008; Mason et al. 2005; Miyawaki et al. 2006; Riefler et al. 2006; Werner et al. 2003; Werner et al. 2001). Contrary to the retarded shoot development, the root formation and growth of *35S:CKX1* transgenic *Arabidopsis* plants is enhanced (Werner et al. 2003). Consistent with published results, the primary roots of *CKX1* overexpressing seedlings grown for 15 days under *in vitro* conditions were 60% longer than that of wild-type seedlings (Fig. 3b). Additionally, the formation of lateral roots was strongly enhanced (Fig. 3c). On average, the number of initiated lateral roots in *CKX1* overexpressing plants was 2.5 times greater than that of the wild type. Consistent with the results shown by Bartrina (2006), *rock2 CKX1ox* seedlings showed a complete reversion and *rock3 CKX1ox* seedlings a partial reversion of the primary root elongation phenotype (Fig. 3b). The same effect was observed regarding number of lateral root outgrowth (Fig. 3c). *rock2 CKX1ox* seedlings showed a complete reversion of the lateral root growth phenotype, whereas *rock3 CKX1ox* plants grew less lateral roots compared to *CKX1ox* seedlings but had longer primary roots with more lateral roots when compared to wild type or *rock2* seedlings (Fig. 3b and 3c). Thus, *rock2* seems to have a more important role in the regulation of primary root growth and lateral root outgrowth compared to *rock3*.

Inconsistent with results achieved by Bartrina (2006), but similar to seedling growth, root growth of *rock2 CKX1ox* and *rock3 CKX1ox* mutants was sensitive towards applied cytokinin (Fig. 3b and 3c). Wild-type seedlings that were grown on media containing 10 nM BA were not affected in their root growth, whereas *rock* mutants showed a strong inhibition of root growth. This is particularly obvious when looking at the formation of lateral roots. On media containing 10 nM BA, formation of lateral roots was reduced to 15% and 18% in *rock2 CKX1ox* and *rock3 CKX1ox* mutants, respectively. 15 days after germination, no lateral roots could be counted in 30% of the *rock2 CKX1ox* and 25% of the *rock3 CKX1ox* seedlings.

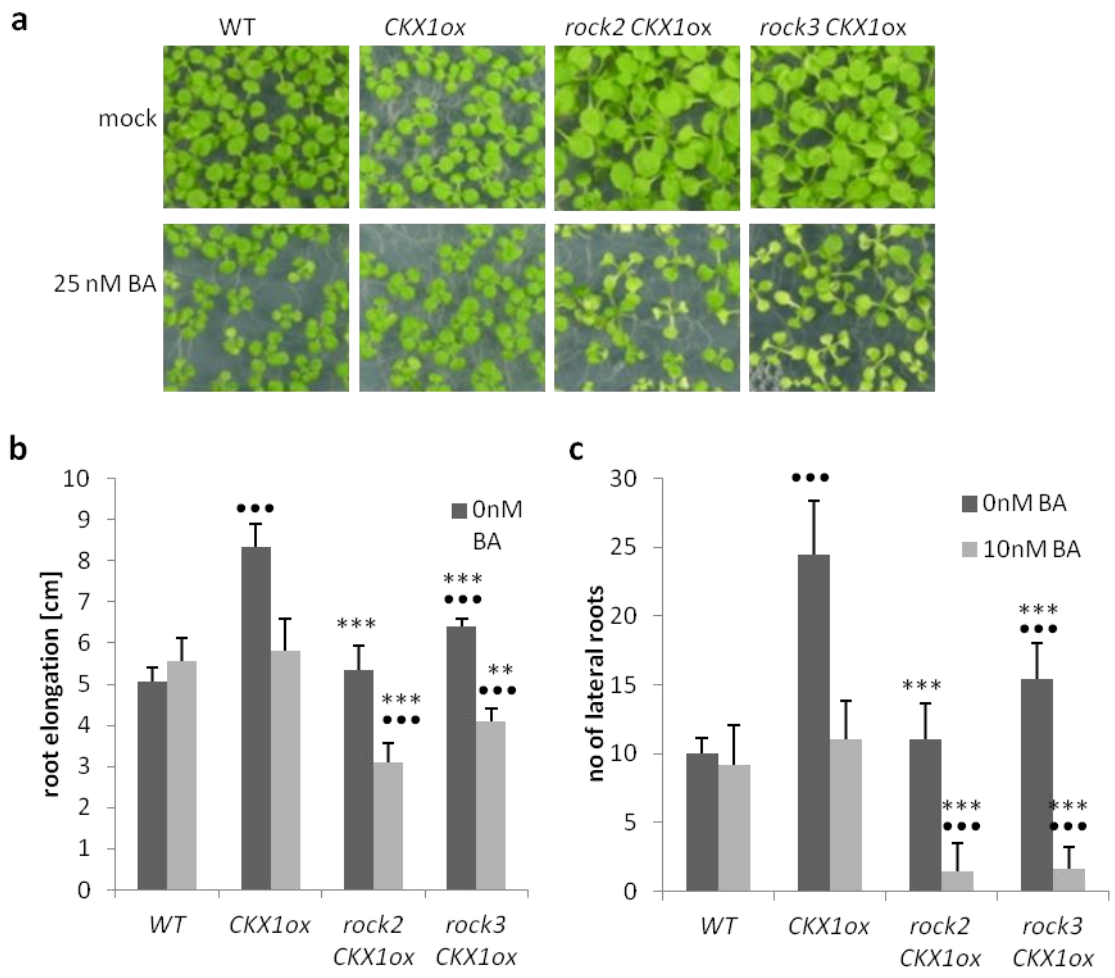

Fig. 3: *Rock2* and *rock3* show enhanced sensitivity towards exogenously applied cytokinin.
(a) Effects of applied BA on seedling growth: seedlings grown on standard MS-medium (mock) or MS-medium containing 25 nM synthetic cytokinin benzyl adenine (BA) for 14 days under standard conditions. The experiment was repeated twice with similar results. **(b-c)** Root elongation within eight days **(b)** and emergence of lateral roots within 15 days **(c)** of seedlings grown on standard Ats-medium (0 nM BA) or Ats-medium containing 10 nM BA. Error bars represent SE. ** = $p < 0{,}005$, *** = $p < 0{,}001$ compared to *CKX1ox* plants; ••• = $p < 0{,}001$ compared to wild type, as calculated by students t-test.

3.1.2 Map-based cloning of the dominant *rock2* and *rock3* mutant alleles

Map-based cloning is the process of identifying the genetic basis of a mutant phenotype by looking for linkage to markers, whose physical location in the genome is known. To identify the mutated genes responsible for the reversion of the cytokinin deficiency syndrome, a recombinant mapping population was generated by crossing *rock2 CKX1ox* and *rock3 CKX1ox* homozygotes in the Columbia 0 (Col) background with Landsberg *erecta* (L*er*) plants. The resulting F1-plants are heterozygote for all L*er*/Col-polymorphisms. During meiosis recombination occurs and previously linked DNA-polymorphisms get separated. The resulting F2 plants are genetic individuals and can then be used to analyse the linkage between the *rock2* or *rock3* mutant alleles and any DNA marker that distinguishes the ecotypes Col and L*er*. The recessive phenotypical characteristics will reappear in the F2 population, and the segregation of molecular markers in this population allows the identification of markers that are closely linked to the mutation of interest.

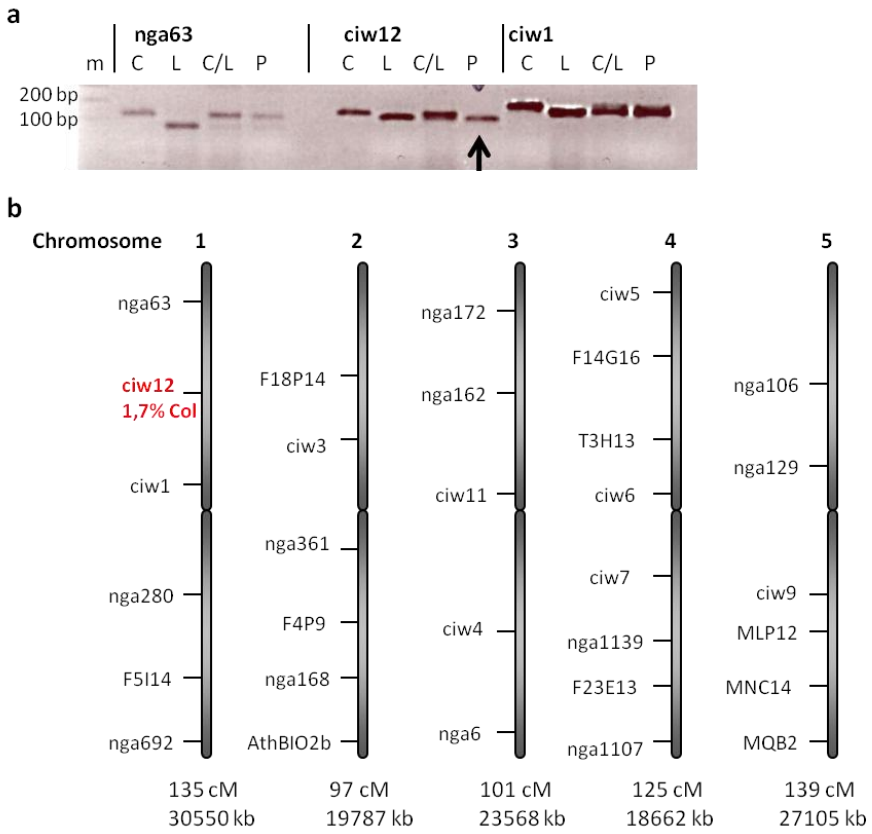

Fig. 4: Rough segregant analysis of the *rock3* locus using molecular markers.
(a) Example for a bulked segregant analysis of the SSLP markers nga63, ciw12 and ciw1. ciw12 is the only molecular marker that shows a clear bias toward the L*er*-specific band (arrow). At all other loci the ratio of Col to Ler amplification is approximately the same between the heterozygous control and the F2 mutants, indicating the mutation is unlinked to these loci. Genomic DNA of Col (C), L*er* (L), heterozygous Col x L*er* (C/L) plants, and a pool of 62 *CKX1ox* looking plants from the F2 mapping population (P) were used. m, 100 bp DNA-ladder. **(b)** Schematic *Arabidopsis* chromosomes with approximate location of the 31 molecular markers used for rough mapping. The length of each chromosome according to the recombinant inbred map (in centimorgans, cM) is listed below the chromosome. The marker ciw12 (red) is linked to the *rock3* mutation. 1.7% of the examined samples were genomically Col at this location.

For map-based cloning, homozygous plants have to be used. This would be a homozygous mutant in the case of a recessive mutation, or homozygous wild type (or in this case the mother plant *CKX1ox*) in the case of a dominant mutation. Segregation analysis showed that the mutations *rock2* and *rock3* are both dominant as the dominant characteristics appear in the F1 population (Bartrina 2006). Therefore, mapping was carried out with *CKX1ox* plants. The first step was to roughly map the *rock3* mutation to a chromosomal region. Bulked segregant analysis (Peters et al. 2003) was used to detect linkage between the *rock3* mutation and a DNA marker. In this method pools of DNA are examined rather than many individual samples. This substantially reduces the number of PCR reactions required to establish linkage.

In order to preselect plants that contain the *CKX1* transgene, the segregating F2 population was grown on media containing hygromycin B. In this case, seedlings containing the *rock3* mutation were easily distinguishable from *CKX1ox* seedlings by the cotyledon size (Fig. 1a). *CKX1ox* seedlings have smaller cotyledons and were used for mapping. *CKX1ox* DNA is homozygous L*er* at the *rock3* mutation and therefore mostly L*er* in the neighbourhood of the mutation, but essentially heterozygous for unlinked markers. DNA samples were prepared from leaf tissue and DNA samples of 62 *CKX1ox* looking plants were pooled. For a PCR, control DNA was isolated from homozygous Col and L*er* plants, as well as heterozygous Col/L*er* F1 plants from a cross between Col and L*er*. Samples were genotyped with a collection of 31 SSLP markers spaced evenly over the entire genome in intervals of approximately 20 centimorgan (cM) (http://arabidopsis.org/servlets/mapper). Figure 4b shows the result of a bulked segregant analysis. Only the molecular marker ciw12 shows a clear bias toward the L*er*-specific band in the *CKX1ox* pool, when compared to the heterozygous control (Fig. 4a). This indicates that the mutation maps to the upper arm of chromosome I. To verify this result, the marker ciw12 was also tested with individual samples. Two out of sixty samples were heterozygous for Col/L*er* at the ciw12 locus, which is a recombination frequency of 1.7%.

The next step was to identify robust, the mutation *rock3* flanking, PCR markers as the next flanking markers used for rough mapping were too distant. Additional markers were designed using polymorphisms described by the Cereon Arabidopsis Polymorphism database (http:// www.arabidopsis.org/Cereon). The two SSLP markers F3I6 and F1K23 (on BACs F3I6 and F1K23, respectively) on either side of the mutation were used as flanking markers in further work. The markers are approximately 1500 kb (approximately six cM) apart.

For fine-resolution mapping a larger F2 population was necessary. A total of 930 plants with the *CKX1ox* phenotype were selected from the F2 population derived from the *rock3 CKX1ox* line and their genomic DNA was analysed by PCR. A total of 132 recombinants were identified. Afterwards, molecular SSLP and CAPS markers at a high density were designed to narrow down the genetic

interval between the markers F3I6 and F1K23 on either side of the mutation (Supplemental Data Table 5). All 132 recombinants were genotyped with these markers to narrow down the region of interest.

The *rock3* locus was mapped to a roughly 130 kb interval between the markers T7N9 and F17L21b on chromosome 1, containing 33 annotated genes on the bacterial artificial chromosomes (BAC) T7N9 and F17L21 (http://www.arabidopsis.org) (Fig. 5b). In this interval the cytokinin receptor *AHK3* is annotated. A gain-of-function cytokinin receptor was thought to be a likely candidate to cause a reversion of the cytokinin deficiency phenotype. Therefore, genomic DNA from *rock3 CKX1* mutants was sequenced for the *AHK3* coding region and comparison with wild-type Col sequence identified a single base change from G to A. This results in an amino acid change from Thr to Ile at position 179 from translational start in the predicted extracellular domain of the cytokinin receptor. The mutation *rock2* was mapped by Isabel Bartrina (Applied genetics, FU Berlin). In an approximately 500 kb interval the cytokinin receptor gene *AHK2* annotated. Sequencing revealed a G to A mutation in the *AHK2* gene, which results in an amino acid change from Leu to Phe at position 552 (Fig. 5a).

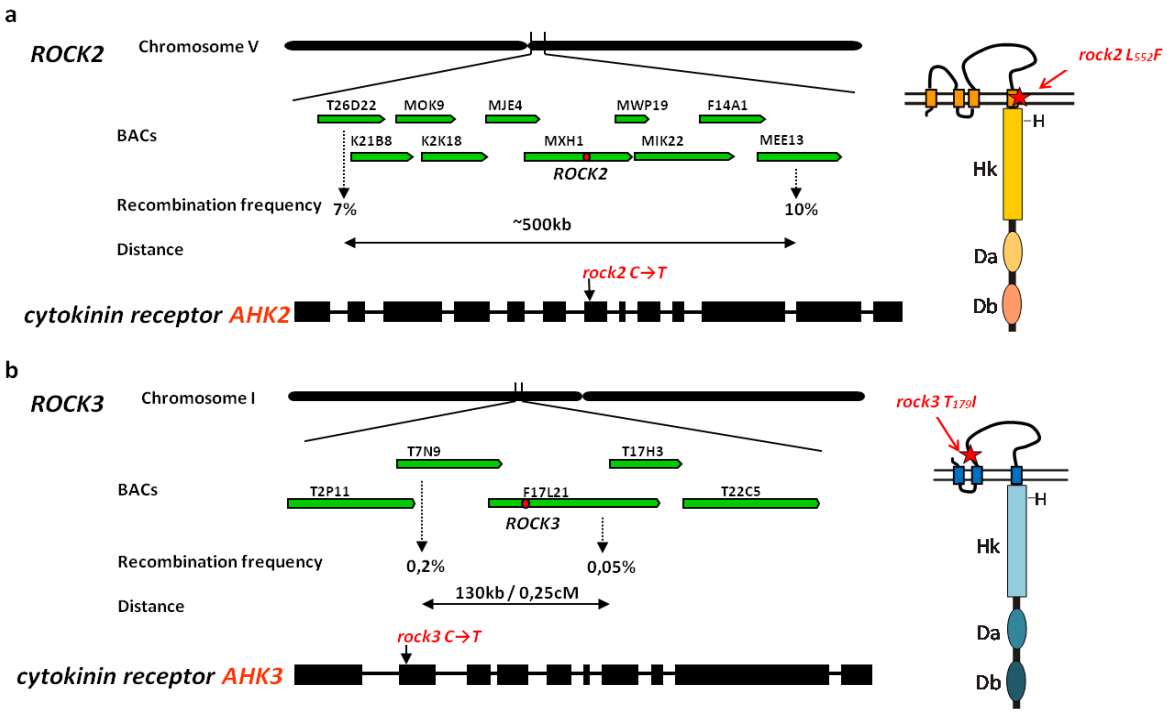

Fig. 5: Map-based cloning: *rock2* and *rock3* are mutant alleles of AHK2 and AHK3, two histidine kinase cytokinin receptors.
(a) Fine mapping of the *rock2* mutation identified markers on the bacterial artificial chromosomes (BAC) T26D22 and MEE13 (ca. 500 kb apart) as the closest flanking markers based on recombination events. The *rock2* mutation is marked as a red dot on BAC MXH1. Bottom and right side: structure of the *AHK2* gene and its protein product. The arrow and the asterisk indicate the position of the *rock2* mutation. Mapping and cloning was done by I. Bartrina (Applied Genetics, FU Berlin). **(b)** Fine mapping of *rock3*: closest flanking markers were identified on the BACs T7N9 and F17L21 (ca. 130 kb apart). The *rock3* mutation is marked as a red dot on BAC F17L21. The *rock3* mutation was identified as a missense mutation in the extracellular cytokinin binding CHASE domain of the *AHK3* histidine kinase cytokinin receptor (asterisk). H, histidine; Hk, histidine kinase domain; Da, receiver like domain; Db, receiver domain.

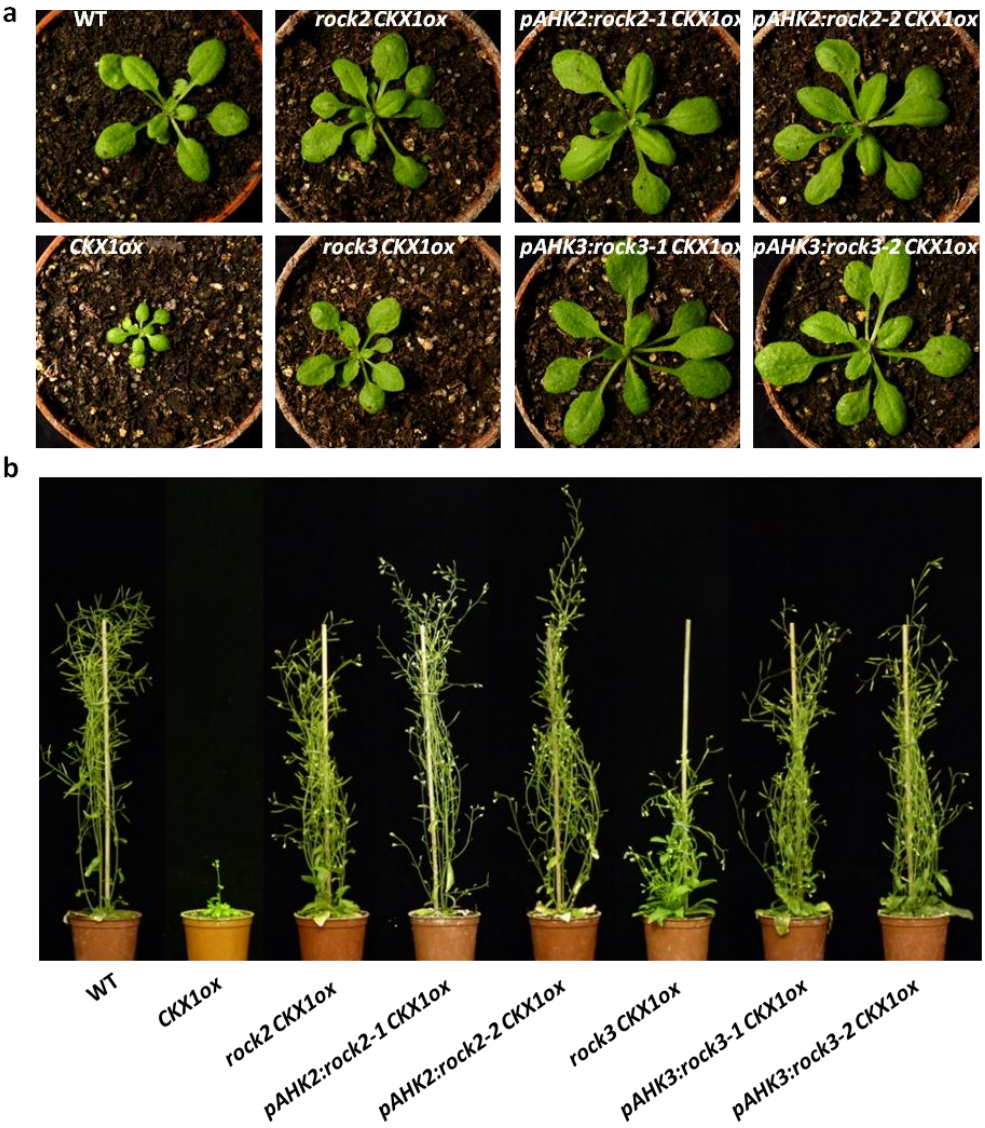

Fig. 6: Transgenic plants expressing *rock2* or *rock3* recapitulate the reversion of the cytokinin deficiency syndrome.
(a) Two independent transgenic *rock2* and *rock3* lines in the *CKX1ox* background in comparison to the original *rock2* and *rock3* lines, *CKX1ox* and wild type 18 DAG. **(b)** Comparison of shoot growth 42 DAG.

To prove that the identified mutated alleles of *AHK2* and AHK3 were indeed the cause of the reversion of the cytokinin deficiency phenotype, the reversion of the cytokinin deficiency phenotype was recapitulated in transgenic plants expressing the *rock2* and *rock3* genes in the *CKX1* overexpressing background, respectively (Fig. 6a and 6b). In order to achieve this, *Arabidopsis CKX1ox* plants were sprayed with the CKX1 inhibitor INCYDE to increase their growth (Zatloukal et al. 2008); then transformed with genes comprising ca. 2 kb of the 5' upstream regulatory regions of *AHK2* and *AHK3*, and the *rock2* and *rock3* coding sequences. These genes were named *pAHK2:rock2* and *pAHK3:rock3*, respectively. Two independent transgenic *rock2* lines (named *pAHK2:rock2 CKX1ox*) and three independent transgenic *rock3* lines (named *pAHK3:rock3 CKX1ox*) were identified. Compared to *CKX1ox* plants, all identified transgenic *pAHK2:rock2 CKX1ox* and

pAHK3:rock3 CKX1ox lines showed increased rosette and shoot growth similar to *rock2 CKX1ox* and *rock3 CKX1ox* plants. This confirms that the phenotypes were indeed derived from the mutations in the *AHK2* and *AHK3* genes. Thus, *rock2* and *rock3* encode two novel gain-of-function variants of the cytokinin receptors AHK2 and AHK3.

Interestingly, transgenic *rock2* and *rock3* lines grew even bigger than the original *rock2* and *rock3* lines derived from EMS mutagenesis, with transgenic *rock2* lines developing even longer shoots than wild-type plants, indicating an even more enhanced cytokinin status (Fig. 6a and 6b).

3.1.3 The mutations *rock2* and *rock3* cause constitutive activation of cytokinin receptors

The rock2 and *rock3* mutant alleles were identified as missense mutations in the *AHK2* and *AHK3* cytokinin receptor genes, which led to a reversion of the cytokinin deficiency phenotype of *CKX1* overexpressing plants. Obviously the mutations caused gain-of-function versions of the cytokinin receptors. It is possible that the mutations cause a higher binding affinity towards the remaining cytokinin, and can therefore compensate for the lower cytokinin concentrations. This is especially a possibility for *rock3,* as the mutation is in the cytokinin binding domain. Another possibility is a conformational change of the receptors causing constitutively active cytokinin receptors. Therefore, it was tested whether the mutations cause a higher binding affinity towards cytokinin, or constitutively active receptors.

Unfortunately, neither a live cell cytokinin binding assay (Romanov et al. 2005) nor a yeast complementation assay (Mähönen et al. 2006), which is used to test histidine kinase activity, were successful when either AHK2 or AHK3 was used. The measured binding activity of the AHK2 and AHK3 receptors was too low to see any significant and trustworthy differences in binding. Furthermore, cytokinin dependent yeast complementation was not successful when *AHK2* or *AHK3* were expressed because, inconsistent with published results (Mähönen et al. 2006), yeast grew normally without cytokinin (Supplemental Data Fig. 33). In *Arabidopsis,* it has been shown that the cytokinin signal is perceived by three members of the cytokinin receptor family: AHK2, AHK3 and AHK4 (Inoue et al. 2001; Suzuki et al. 2001; Yamada et al. 2001). These three cytokinin receptors show a high degree of sequence identity, and the mutated nucleotides in *rock2* and *rock3* are conserved in all three receptors (Fig. 7a). AHK2 shows 52% and AHK3 a 54% sequence similarity, when compared to the AHK4 protein (Inoue et al. 2001). Hereafter the *rock2* and *rock3* mutations were introduced into the *AHK4* gene (and named *AHK4rock2* and *AHK4rock3*), and the cytokinin binding assay and yeast complementation assay were performed with these proteins. The nature of the mutant proteins was compared with the wild-type protein.

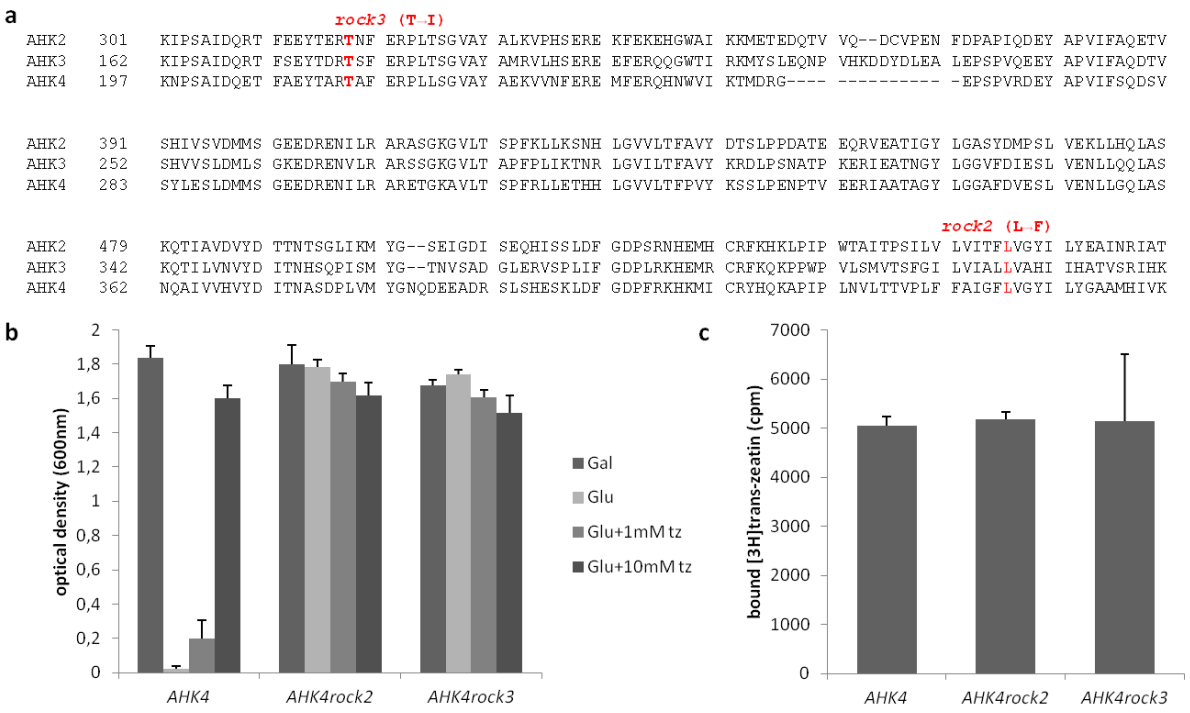

Fig. 7: The *rock2* and the *rock3* mutation cause constitutive activation of receptors.
(a) Sequence alignment between the three cytokinin receptors: AHK2, AHK3, and AHK4. The mutated nucleotides in *rock2* and *rock3* are conserved in all three receptors (red). **(b)** Growth of *Δsln1* yeast strains carrying *AHK4rock2* or *AHK4rock3* was independent of the presence of the cytokinin *trans-zeatin*. The control yeast carrying *AHK4* did not grow in the absence of cytokinin and grew slowly in media containing low *trans*-zeatin concentrations. In control media containing galactose (Gal) instead of glucose (Glu) yeast grow similar in all cases. The experiment was repeated twice with similar results. Error bars represent SE (n = 3). **(c)** Binding of [^{3}H]*trans*-zeatin to *AHK4*-expressing bacteria. The *rock* mutations do not change binding capacity. The experiment was repeated twice with similar results. Error bars represent SE (n = 5).

A live cell based assay (Romanov et al. 2005), using transgenic bacteria expressing the cytokinin receptor *AHK4,* its mutated versions *AHK4rock2,* and *AHK4rock3* were performed in order to test the binding capacity towards the tritium-labelled cytokinin *trans*-zeatin. It could be shown that E. *coli* expressing the cytokinin receptor *AHK4,* its mutated versions *AHK4rock2,* or *AHK4rock3* showed no differences in specific binding of trans-zeatin (Fig. 7c).

To test if the *rock* mutations cause constitutively active forms of AHK4; *AHK4* and its mutated versions *AHK4rock2* and *AHK4rock3* were expressed in a yeast strain deficient in the *SLN1* gene, which encodes an osmosensing histidine kinase (Maeda et al. 1994). The *Δsln1* mutant is lethal because a phosphorelay is blocked and the downstream response regulator SSK1 is always dephosphorylated, which over activates a downstream MAPK pathway. When AHK4 is expressed in *sln1* deficient yeast, cytokinin can activate the histidine kinase activity of the AHK4 protein to initiate the phosphorelay, suppressing the lethality of *Δsln1*. When no cytokinin is added to the media, the cytokinin receptor AHK4 is not active, and the yeast strain *Δsln1* is still lethal. However, when the mutated versions *AHK4rock2* or *AHK4rock3* were expressed, the lethality of the *Δsln1* mutant was

suppressed without adding cytokinin to the media (Fig. 7b). This shows that the activity of AHK4rock2 or AHK4rock3 is at least partially independent of cytokinin. Thus, mutated versions of the receptor AHK4 are constitutively active.

3.1.4 Impact of *rock2* and *rock3* mutations on *ARR5* expression

ARABIDOPSIS RESPONSE REGULATOR 5 (*ARR5*) is a response regulator gene of the two-component system that is transcriptionally upregulated by cytokinin (D'Agostino et al. 2000). The activity of the cytokinin reporter gene reflects the cytokinin status.

To investigate whether the constitutively active cytokinin receptors *rock2* and *rock3* are reflected by changes in the expression of a cytokinin response gene, promoter*ARR5:GUS* (*pARR5:GUS*) expression in the *rock2* and *rock3* mutants was analysed and compared to wild-type expression levels.

Figure 8 shows strongly increased GUS expression in various parts of *rock2* and *rock3* seedlings. At five days after germination increased GUS expression could be detected in the vascular tissue of cotyledons and leaves, in the shoot apex, vasculature of the whole root and in the root tip. Especially *rock2* mutants showed high GUS activity all over the root, whereas in *rock3* roots the GUS signal was weaker but still detectable. In wild-type seedlings *ARR5:GUS* activity was completely absent in the upper half of the root.

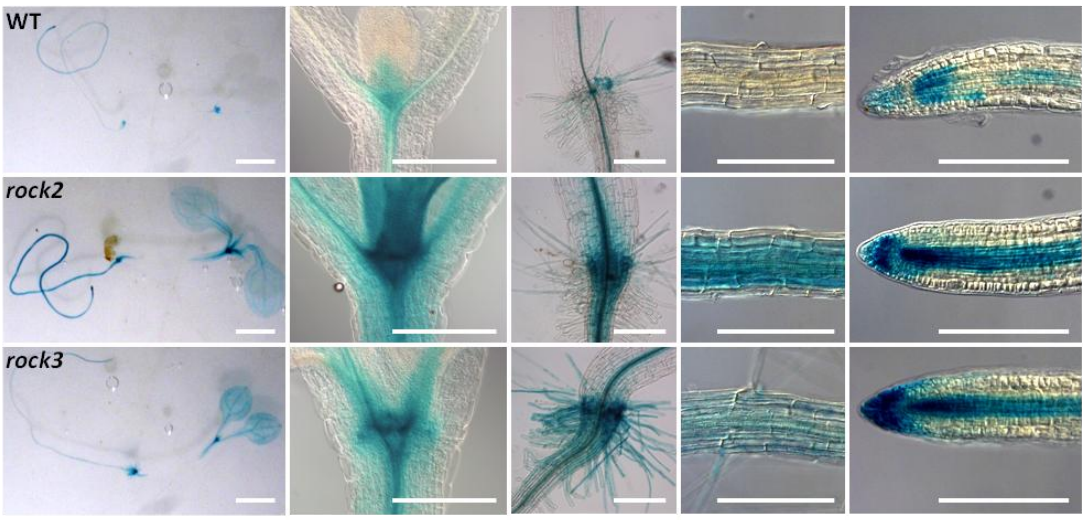

Fig. 8: Transcriptional activation of *ARR5* in *rock2* and *rock3* mutants as demonstrated by promoter-GUS fusions.
GUS staining of wild-type (WT), *rock2* and *rock3* seedlings, which were grown on Ats medium for 7 days in the light. Pictures show whole seedlings, shoot apices, the section between hypocotyl and root, the upper third of the root and the root tip (from left to right). Seedlings on photos were stained overnight (whole seedling), for 90 min (shoot apices), or for 20 min (section between hypocotyl and root, the upper third of the root and the root tip). Size bars: 1 mm (whole seedlings) and 100 µm (all other photos). Experiments were repeated twice with similar results.

The higher expression of the reporter gene in *rock2* and *rock3* mutants suggests that the enhanced cytokinin receptor activity is not compensated for by a reduced sensitivity of the signalling system. Moreover, the increase in *pARR5:GUS* expression is in accordance with the idea that enhanced signalling through the two-component system is involved in the phenotypic changes in the transgenic plants.

3.1.5 Phenotypic characterisation of *rock2* and *rock3* in the wild-type background

3.1.5.1 Transgenic pAHK2:rock2 and pAHK3:rock3 *lines show a more pronounced phenotype compared to* rock2 *and* rock3 *plants*

Suppressor mutagenesis of *35S:AtCKX1* overexpressing *Arabidopsis* plants led to the identification of two new dominant gain-of-function alleles of the cytokinin receptor genes, *AHK2* and *AHK3*. In the first part of this thesis, phenotypic changes in a cytokinin-deficient background have been described. In order to analyze the consequences of the *rock2* and *rock3* mutations in the wild-type background, the *rock2* and *rock3* suppressor mutants in *CKX1ox* backgrounds were crossed to wild-type Col plants. The F2 generation was screened for *rock2* and *rock3* plants in wild-type background (named then *rock2* and *rock3* mutants).

The reversion of the cytokinin-deficiency phenotype was recapitulated in transgenic plants expressing *pAHK2*:*rock2* and *pAHK3*:*rock3* in the *35S:CKX1* background. Interestingly, these transgenic lines showed an even stronger reversion of the CDS (Fig. 6). In order to find out if transgenic expression of *rock2* and *rock3* under their own promoter also cause stronger effects in WT background, *pAHK2*:*rock2* and *pAHK3*:*rock3* were also transformed into Col-0 plants (named *pAHK2*:*rock2* and *pAHK3*:*rock3* mutants). Ten independent transgenic *rock2* lines (named *pAHK2:rock2*) and five independent transgenic *rock3* lines (named *pAHK3:rock3*) were identified. The expression of *rock2* and *rock3* was verified by RT-PCR (Fig. 9b).

Figure 9a shows 50 days old *rock2* and *rock3*, as well as transgenic *pAHK2:rock2* and *pAHK3:rock3* plants compared to wild type. In particular, *rock2* and the transgenic *pAHK2:rock2* and *pAHK3:rock3* lines show an enhanced shoot growth compared to wild type. Similar to the *pAHK2:rock2* and *pAHK3*:*rock3* lines in the *35S:CKX1* background (see chapter 3.1.1), transgenic lines expressing *rock2* or *rock3* show an even more pronounced phenotype compared to non-transgenic *rock2* and *rock3* plants derived from EMS mutagenesis. To exclude that the stronger phenotypes are due to the extra *AHK2* or *AHK3* allele in the transgenic lines, *pAHK2:rock2* and *pAHK3*:*rock3* lines were crossed into an *ahk2* or *ahk3* knock-out background.

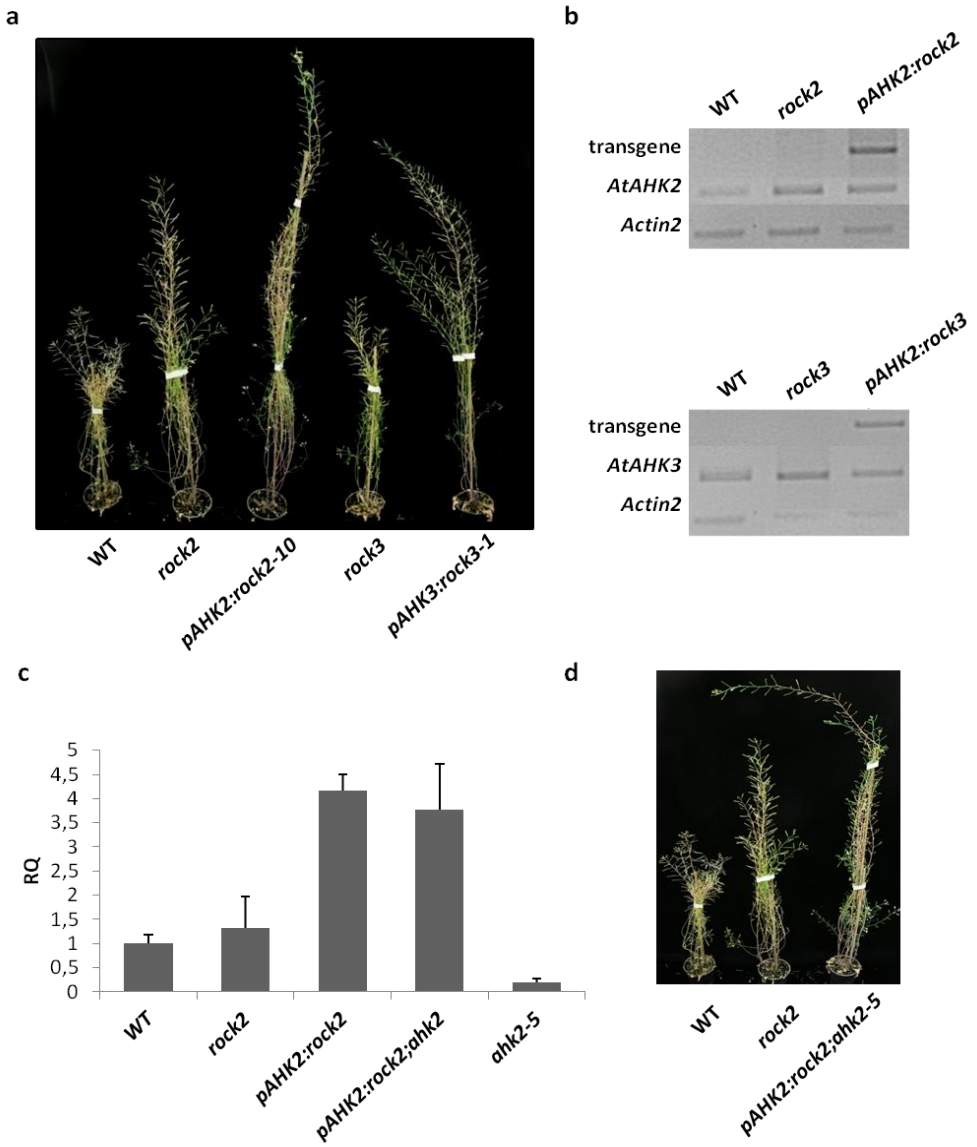

Fig. 9: In the wild-type background, transgenic *rock2* and *rock3* lines show a more pronounced phenotype compared to wild type.
(a) Shoot phenotype of *rock2*, *rock3*, and the transgenic lines *pAHK2:rock2-10* and *pAHK3:rock3-1* compared to wild type 50 days after germination. **(b)** Semiquantitative RT-PCR with RNA isolated from wild-type, *rock2* and *pAHK2:rock2-10* seedlings show *AHK2* transcripts in all three samples and the transcript of transgene *pAHK2:rock2-10* in transgenic plants (top). RT-PCR with RNA isolated from wild-type, *rock3* and *pAHK3:rock3-1* seedlings show *AHK3* transcripts in all three samples and the transcript of transgene *pAHK3:rock3-1* in transgenic plants (bottom). Actin was used as a loading control. **(c)** Transcript abundance of the *AHK2* gene determined by qRT-PCR in seedlings of wild type, the *ahk2-5* mutant, *rock2* and the transgenic *Arabidopsis* lines *pAHK2:rock2-10* and *pAHK2:rock2-10;ahk2-5* double mutant grown *in vitro* for 10 days. Transcript levels are given as relative values compared with the corresponding wild-type tissue. Relative expression levels were normalized using *AtUBC10* (At5g53300) and At3g25800 as an internal controls. The experiment was repeated with biological replicates with similar results. **(d)** Shoot phenotype of the *pAHK2:rock2-10;ahk2-5* double mutant compared to wild type and *rock2* plants 50 days after germination.

Figure 9d shows that transgenic *pAHK2:rock2;ahk2-5* lines still show the enhanced shoot phenotype, suggesting that the stronger effects are not due to an extra *AHK2* allele in the transgenic line. It is possible that negative regulatory elements are missing in the chosen promoters and the promoters

are therefore more active. To test this hypothesis, quantitative *real time* RT-PCRs were performed in order to compare the expression levels of the transgenic *AHK2* with wild-type *AHK2* expression levels (Fig. 9c). Transcript abundance of the *AHK2* gene was determined in wild type, the *ahk2-5* mutant, *rock2* and the transgenic *Arabidopsis* lines *pAHK2:rock2-10* and *pAHK2:rock2-10;ahk2-5* double mutant, grown *in vitro* for 10 days. The *pAHK2:rock2-10;ahk2-5* double mutant was chosen to measure exclusively the level of transgenic *AHK2*, whereas in the *pAHK2:rock2-10* line the transgenic and the levels of wild-type *AHK2* were measured. As expected, transcript abundance of *AHK2* was similar in wild-type and *rock2* seedlings, and in the negative control *ahk2-5* almost no *AHK2* transcript was measured. Interestingly, the transgenic lines *pAHK2:rock2-10* and *pAHK2:rock2-10;ahk2-5,* did indeed show strongly enhanced levels of *AHK2*, confirming the hypothesis that the chosen *AHK2* promoter is more active.

Subsequently, a detailed phenotypic analysis of *rock2, rock3* and the transgenic *rock2* and *rock3* lines was performed.

3.1.5.2 rock2 *and* rock3 *mutants show an enhance cotyledon and rosette leaf size*

In the wild-type background, the *rock2* and *rock3* mutations lead to plants featuring improved shoot growth characteristics. Examination of homozygous *rock2* and *rock3* as well as *pAHK2:rock2* and *pAHK3*:*rock3* plants revealed that *rock2* and *rock3* act as positive regulators of lateral shoot organ size during vegetative as well as reproductive development.

Figure 10 shows that *rock2* and *rock3* alleles significantly enhance vegetative growth. This effect can already be seen early after seed germination and is also evident from leaf size comparison at a later developmental stage (Fig. 10a and 10c). At four days after germination *rock2* and *rock3* seedlings show an increased cotyledon diameter (Fig. 10a). This phenotype is more prominent in transgenic *rock2* and *rock3* lines. The mutations *rock2* and *rock3* caused an increase of rosette leaf size compared to wild type throughout the plant life cycle (Fig. 10b). Analysis of the increase of fresh weight of rosettes throughout the plant life cycle showed that the increase in fresh weight is particularly evident at 32-40 DAG and the effect is strongest in *rock2* plants (Fig. 10c). After day 40, fresh weight decreases due to senescing leaves. This process is delayed in *rock3* plants due to a delayed senescence (see chapter 3.1.5.8).

Organ size can be influenced by cell number, cell expansion or both. In order to find out if the increased leaf size of *rock* mutants is due to either more cells or larger cells, microscopic analyses of leaf epidermis cells were performed. The *rock2* mutant showed a more pronounced phenotype and was therefore chosen for analysis. Leaf area, abaxial epidermal cell size and the number of epidermal cells per leaf of the sixth fully grown rosette leaves of wild-type and *rock2* plants were measured and

compared. Figure 11c shows that *rock2* leaves are significantly bigger than wild-type leaves even though they have slightly smaller epidermis cells (Fig. 11a). Calculations revealed that *rock2* rosette leaves have approx. 25% more epidermis cells per leaf compared to wild type (Fig. 11d). This clearly illustrates that the increase in leaf size of *rock2* plants is due to more cells rather than bigger cells. Thus, the *rock2*-dependent changes in organ size are due to increased numbers of normal sized cells.

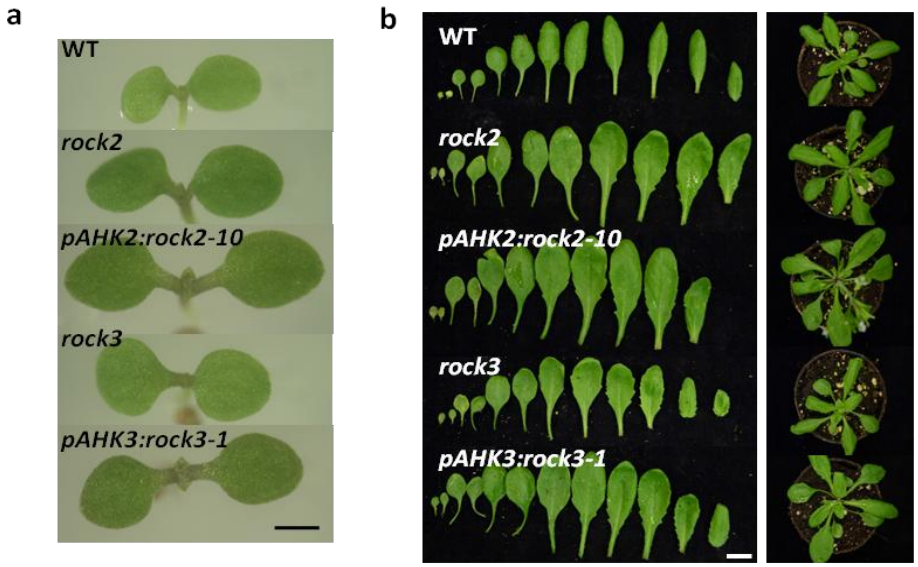

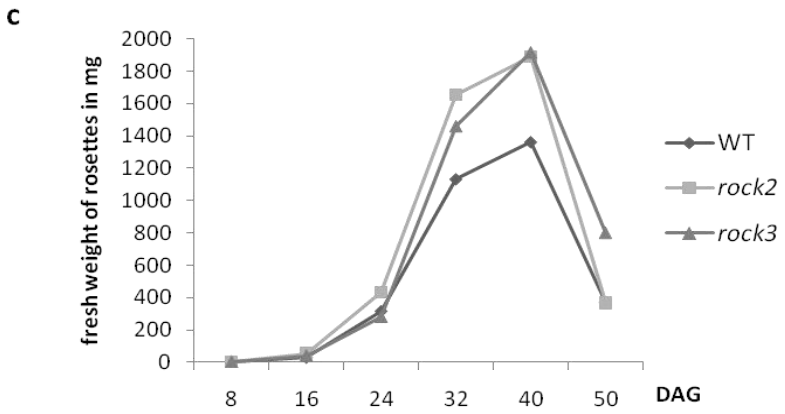

DAG	8	16	24	32	40	50
WT	2,24±0,30	27,8±5,6	315±67	1133±218	1363±136	368±84
rock2	3,98±0,65 **	54,4±9,1 ***	434±57 *	1654±192 **	1889±158 ***	368±156
rock3	3,00±0,16 **	40,7±4,3 **	282±21	1459±156 *	1915±93 ***	800±198 **

Fig. 10 The *rock2* and *rock3* alleles enhance cotyledon and leaf size.
(a) Cotyledon size of seedlings grown on Ats media for five days. Scale bar, 1mm. **(b)** Rosette leaves in the order of appearance, starting with cotyledon leaves (from left to right) at 24 days after germination. Scale bar, 1cm. **(c)** Increase of rosette fresh weight in milligram over the time (n=8). Table shows mean values and standard deviations. WT, wild type. * = $p < 0,01$; ** = $p < 0,005$; *** = $p < 0,001$ compared to wild type, as calculated by pair wise students t-test.

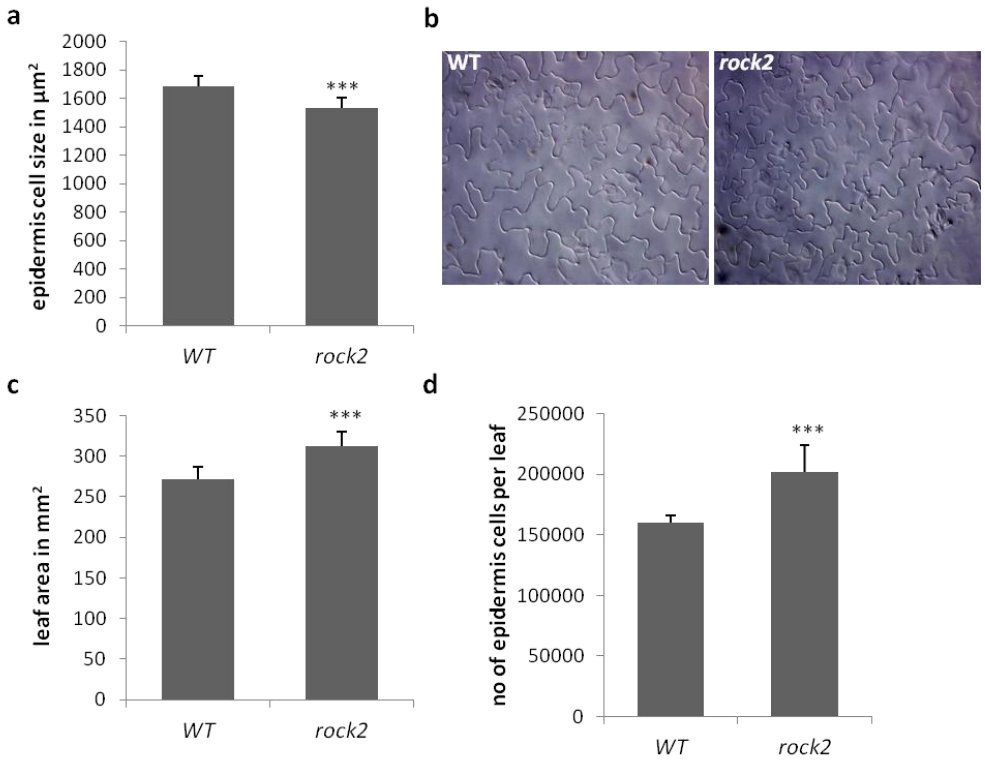

Fig. 11: In *rock2* plants the increased rosette leaf size is due to more epidermis cells per leaf.
(a) Average abaxial epidermis cell size of the sixth fully grown rosette leaves of wild type and *rock2* plants. (n = 5). **(b)** An example of epidermis cells as seen under the microscope. Similar sized epidermis cells of wild type and *rock2*. (n=5) **(c)** Leaf size of the sixth leaves used for cell measurements in (a). **(d)** Number of epidermis cells per leaves calculated from average epidermis cell size and leaf size. Error bars represent SE, ***= $p < 0{,}001$ compared to WT as calculated by pair wise students t-test.

3.1.5.3 The rock2 *and* rock3 *mutations enhance radial stem growth*

Stems of dicotyledonous plants thicken by cell proliferation and growth in the vascular cambium. Cytokinin has been shown to positively regulate primary and secondary vascular development and cell proliferation activity in the cambium (Hejatko et al. 2009; Matsumoto-Kitano et al. 2008; Nieminen et al. 2008).

Consistent with these results, comparison of *Arabidopsis* stems revealed enhanced radial expansion of *rock* inflorescence stems. The diameter of the primary inflorescence stems of wild-type and *rock* mutant plants were measured at the base of the stems when the stems were between 15 and 20 cm long. In particular in transgenic *rock2* and *rock3* lines expressing *pAHK2*:*rock2* or *pAHK3*:*rock3,* stem diameter had increased by more than 25% compared to wild-type stems (Fig. 12a and 12b). Transverse sections of the primary inflorescence stem showed that stem morphology was normal in all mutants, but the overall number of cells in transgenic stems had increased compared to wild-type stems; this can be seen in the transverse sections of *pAHK3:rock3* inflorescence stems (Fig. 12c), which suggests higher mitotic activity in the cambium.

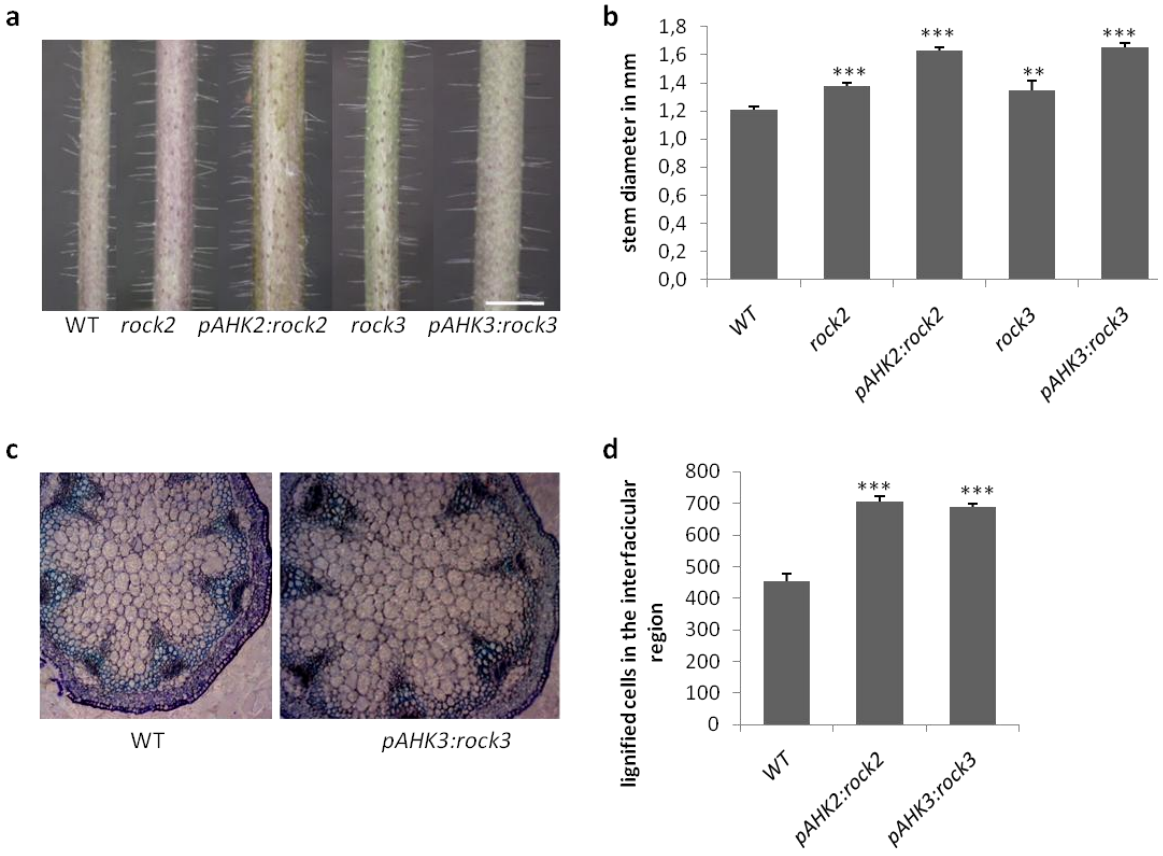

Fig. 12: Comparison of stem diameter between wild-type and *rock* mutants.
(a) Photos of *Arabidopsis* primary inflorescence stem three cm above the rosette. All stem were between 15 and 20 cm long. Scale bar: 2 mm. **(b)** Stem diameter at the base of primary inflorescence stems when the stems were about 15 to 20 cm long. Error bars represent SE (n=10). **(c)** Stem sections of wild type and *pAHK3*:*rock3* at the base of primary inflorescence stems when the stems were about 15 to cm long. Sections were stained with toluidine blue and photographed at the same magnification. **(d)** Number of lignified cells in the interfascicular region of sectioned and stained stems as seen in (c). (n=3). Error bars represent SE, ** = $p < 0,005$; ***= $p < 0,001$ compared to WT as calculated by pair wise students t-test.

During shoot development, the term “fascicular cambium” describes the part of the cambium cylinder formed within the vascular bundles of primary development, whereas “interfascicular cambium” develops in the regions between the vascular bundles (Esau 1965). The lignified cells in the interfascicular region can be interpreted as secondary xylem parenchyma and are easily countable after toluidine-blue staining of stem sections (Altamura et al. 2001; Matsumoto-Kitano et al. 2008). Transgenic lines expressing *pAHK2:rock2* or *pAHK3:rock3* show an increased number of lignified cells by up to 70% in the interfascicular region (Fig. 12d). These results indicate that fascicular and interfascicular cambial activity is enhanced when the cytokinin receptors AHK2 or AHK3 are constitutively active.

3.1.5.4 The rock2 *and* rock3 *mutations increase the size of floral organs*

Phenotypic analysis of *rock2* and *rock3* mutants showed that the expansion and final size of flower organs are also significantly enhanced when compared to wild-type flowers (Fig. 13a and 13b). Here again, the phenotype is more pronounced in the transgenic *rock* lines *pAHK2:rock2* and *pAHK3:rock3*.

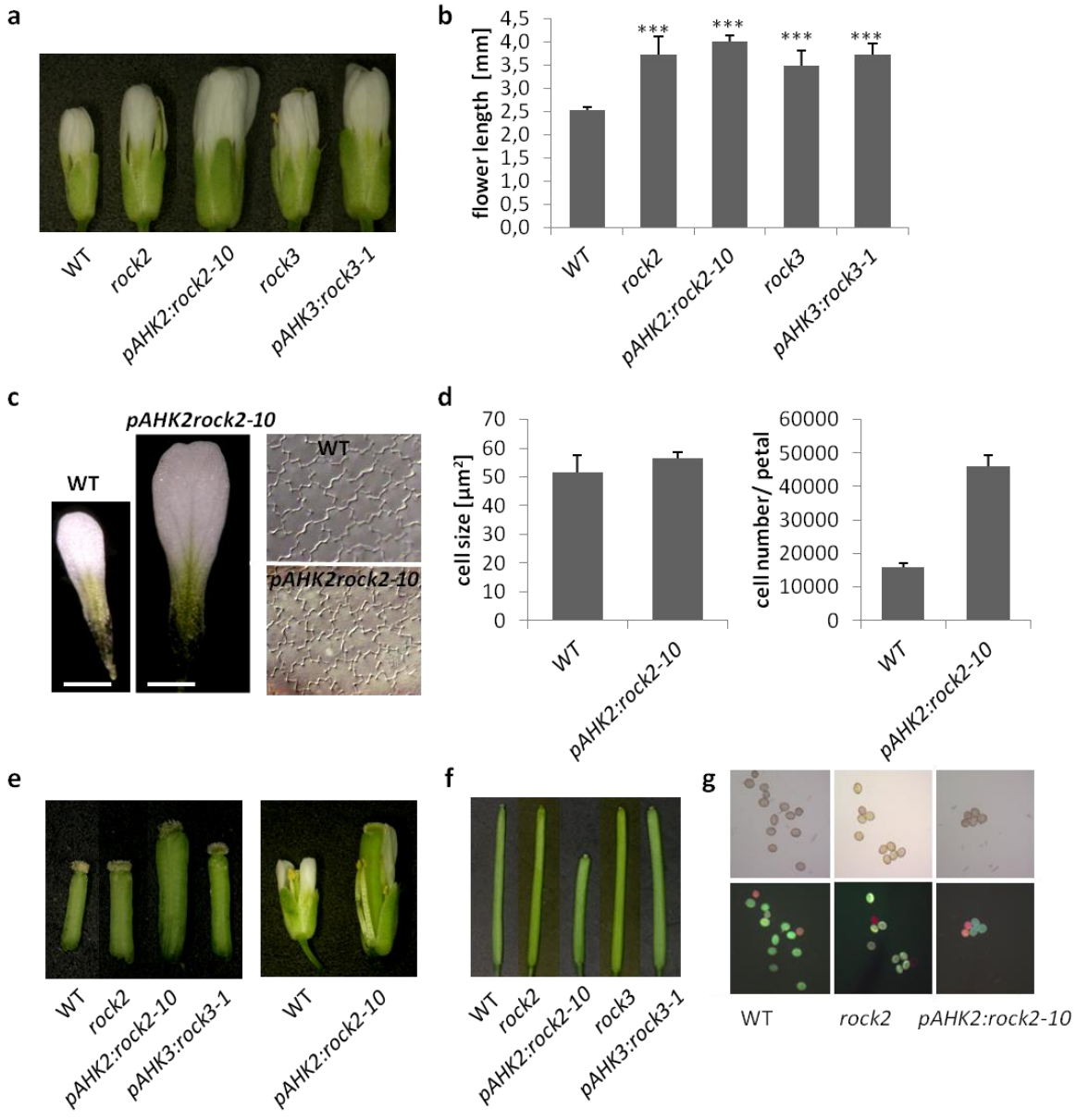

Fig. 13: Comparison of floral organs between wild-type and *rock* mutants.
(a) Flowers of mutant plants compared to wild-type flowers. **(b)** Flower length at stage 13 (Smyth et al. 1990). Error bars represent SE (n = 10), ***= p < 0,001 compared to wild type as calculated by pair wise students t-test. **(c)** Wild-type and *pAHK2:rock2* petals and abaxial petal epidermis. Scale bar, 1mm. **(d)** Average petal cell size of petals stage 13 and calculated cell size per petal. (n=5). **(e)** Gynoecia of wild type, *rock2* and *pAHK2:rock2* at stage 13. **(f)** Fully grown siliques of wild type and *rock* mutants. **(g)** Pollen viability test: Propidium iodide and fluorescein diacetate stained pollen grains from freshly open flowers of the wild-type and mutant plants. Viable pollen grains appear green under UV light, dead pollen grains red. Experiment was repeated twice with similar results.

Analysis of flowers in stage 13 (Smyth et al. 1990) revealed a significant increase in flower length in all analysed *rock* mutants compared to wild type (Fig. 13a and 13b). *Rock2* seems to have a slightly stronger effect on flower size than *rock3*, as *rock2* and *pAHK2:rock2* plants exhibit slightly bigger flowers. The phenotype was especially pronounced in *pAHK2:rock2* mutants, as they developed flowers that where 58% longer compared to wild-type flowers. Flower length of the *rock2*, *rock3* and *pAHK3:rock3* mutants were increased by 47%, 37% and 46% compared to wild-type flowers, respectively.

The increased flower size was mainly due to an increased petal size (Fig. 13c). To determine whether the increase in petal size was a result of an increased cell proliferation, cell expansion or both, abaxial petal epidermis cell size and number per surface area were analyzed in *rock2* flowers stage 13 (Smyth et al. 1990) and compared to wild-type petals. Microscopic analysis revealed that the petals of transgenic *rock2* plants contained almost three times more epidermis cells compared to wild-type petals, whereas cell size was not significantly altered (Fig. 13d); similar to rosette leaves (Fig. 11), an enhanced cell number rather than cell enlargement, resulted in bigger petals.

Additionally, the growth and final size of gynoecia was increased in *rock2* mutants and *pAHK2:rock2* and *pAHK3:rock3* transgenic plants (Fig. 13e). This phenotype was strongest in *pAHK2:rock2* mutants, causing reduced self-pollination of mutant flowers, with approximately 98% of the flowers not producing any seeds, while in the *rock2* mutant only 10% failed to produce seeds. At flower stage 13 (Smyth et al. 1990), when wild-type flowers open, the petal blades extend above the sepals, reflexed stigmatic papillae expand, the anthers dehisced, and the long stamens are level with the stigma. Especially in transgenic *pAHK2:rock2* flowers gynoecia were strongly enlarged whereas anthers were not. As a result, the gynoecia are longer than the stamens, causing the pollen to be shed on the side of the gynoecia rather than on the stigma, explaining the failure of pollination (Fig. 13e). In addition, *rock2* and especially *pAHK2:rock2* flowers seem to produce a smaller amount of pollen. Nevertheless, it is possible to pollinate wild-type flowers with this pollen, as it is possible to hand-pollinate *rock2* and *pAHK2:rock2* mutants. A pollen viability test showed that pollen of *rock2* and *pAHK2:rock2* plants were viable (Fig. 13g).

Figure 13f shows fully grown siliques of *rock* mutant plants compared to wild-type siliques. Siliques of *rock2*, *rock3* and the transgenic *rock3* line *pAHK3:rock3-1* were similar in length when compared to wild type but somewhat flattened. Siliques of *pAHK2:rock2* mutants were never completely filled and therefore shorter (Fig. 17), and filled with approximately one to 20 viable seeds, whereas wild-type siliques harboured up to 60 seeds (Fig. 16c).

3.1.5.5 The rock2 *and* rock3 *mutations positively regulate shoot growth*

The growth of *rock* mutants was also increased during reproductive development. *rock2*, *pAHK2:rock2* and *pAHK3:rock3* transgenic plants had a significantly increased shoot height compared to wild-type plants, which was most evident in transgenic *pAHK2:rock2* plants (Fig. 14a). Here shoot height had increased by up to 80%. An analysis of the increase in shoot height over the complete life cycle of plants showed that the increase in height got more evident over time, resulting in a greater increase in fresh weight of shoots at the end of the plant's life cycle (Fig. 14b and 14f). Fresh weight of shoots of the transgenic *pAHK2:rock2* and *pAHK3:rock3* lines increased by 53% and 35%, respectively. Fresh weight of *rock2* shoots was 21% greater compared to wild type and rock3 shoots had the smallest increase in fresh weight. The increased shoot biomass is not only due to longer stems and bigger leaves (Fig. 10), but also due to thicker stems caused by an enhanced number of larger cells in the radial dimension (Fig. 12).

Under long-day conditions, the *rock2* mutation promotes the onset of flowering as *rock2* and *pAHK2:rock2* plants flowered 2-3 days and up to a week earlier than wild type, respectively (Fig. 14c). Transgenic *pAHK3:rock3* plants flowered slightly but significantly earlier than wild type plants and *rock3* plants showed no flowering phenotype. Consistent with results described for *rock* mutants in the *CKX1* overexpressing background (chapter 3.1.1), the constitutively active AHK2 receptor caused by the *rock2* mutation seems to play a more prominent role in promoting flowering than the constitutively active AHK3 receptor.

The developmental timing of floral transition was affected similarly, as comparable results were obtained when taking rosette leaf number, rather than number of days to flower appearance, as measure of flowering time (Fig. 14d). *rock2* plants form one less and transgenic *pAHK2:rock2* plants form 2-3 less rosette leaves, compared to wild type. In the case of transgenic *pAHK3:rock3* plants, the changes in developmental timing of flowering were more pronounced when compared to number of days to flower appearance. Even though these plants flowered only one day earlier than wild-type plants, they have 1-2 less rosette leaves, indicating a prolonged plastochron (Fig. 14c and 14d).

Interestingly, *rock2* and transgenic *rock* mutant shoots did not only flower earlier and grew faster, the plants also showed a markedly increased life span. Seven-week-old wild-type control plants had stopped flowering, whereas *rock* mutants of the same age continued to flower at almost all inflorescences, with *pAHK2:rock2* plants showing the strongest phenotype. On average, transgenic *pAHK2:rock2* plants flowered two weeks longer than wild-type plants (Fig. 14e). Unlike the other *rock* mutants, *rock3* plants did not flower early, and its shoots grew slightly slower than wild-type shoots (Fig. 14b). However, *rock3* plants also flowered a few days longer, and therefore reached the same height as wild type at the end of their life cycle (Fig. 14b and 14e).

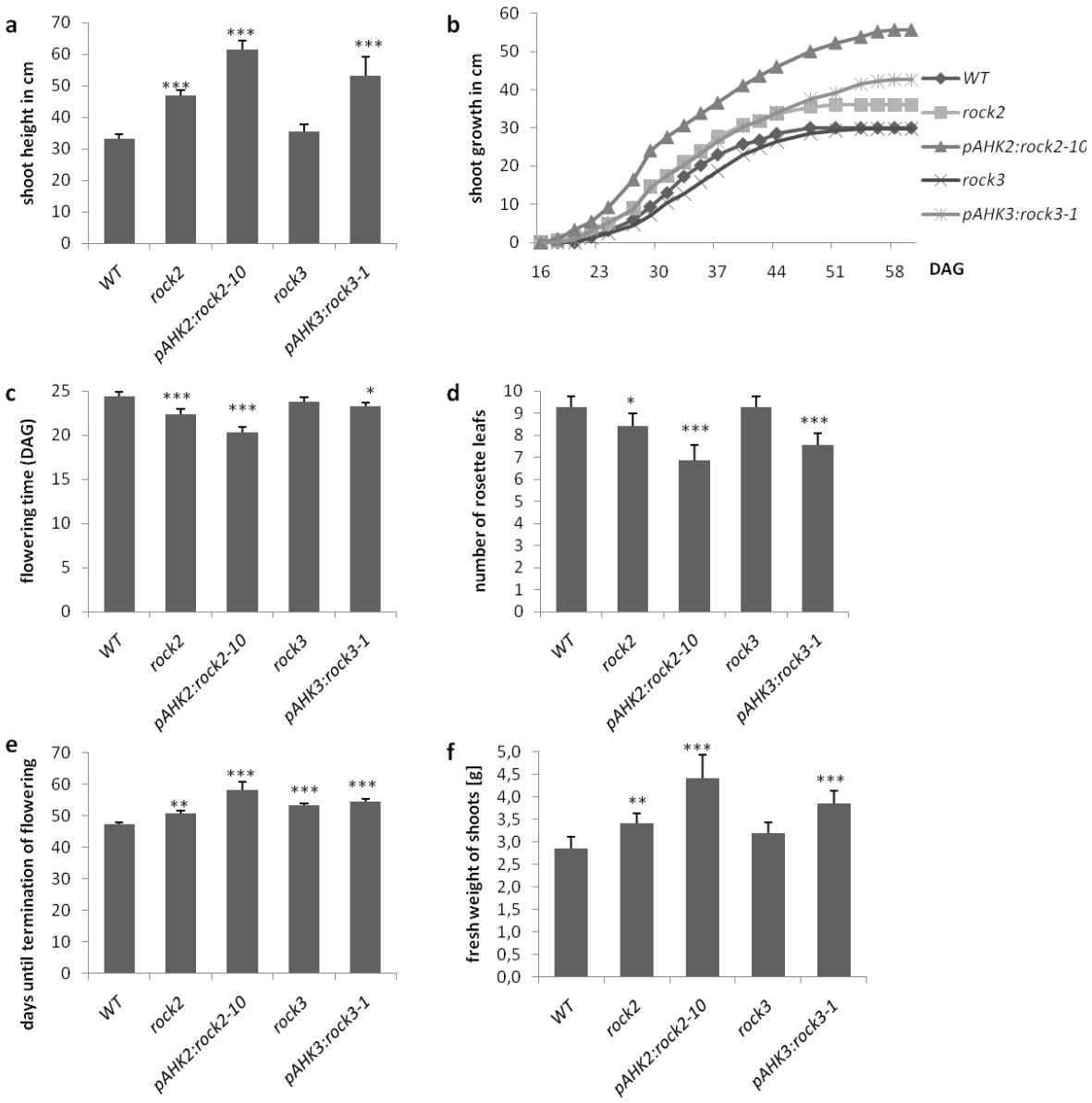

Fig. 14: *rock2* and *rock3* positively regulate flowering time and shoot growth.
(a) Shoot height of fully grown plants (n = 20). **(b)** Shoot growth between 16 and 58 days after germination (DAG) (n=10). **(c)** Flowering time of wild-type and mutant plants grown in long day conditions (n=10). **(d)** Number of rosette leaves at the start of flowering. **(e)** Compared to wild type, *rock* mutant shoots flower longer (n=10). **(f)** Fresh weight of shoots at the end of the plants life cycles (n=10). Experiments were repeated twice with similar results. Standard bars represent SE. * = $p < 0.01$; ** = $p < 0.005$; *** = $p < 0.001$ compared to wild type as calculated by student t-test.

In some extreme cases, which were mainly observed in winter, transgenic *pAHK2:rock2* plants flowered for more than 10 weeks and produced huge, long, thick and bushy shoots (Fig. 15a). Figure 15b was taken 90 days after germination. At this time lots of flowers were abnormally formed, grown together, and showed malformed tissue (right picture), while other flowers still looked normal (left picture).

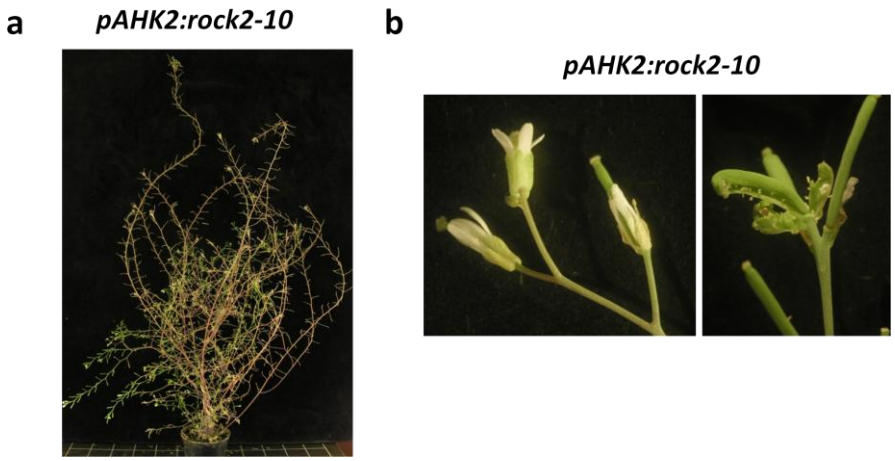

Fig. 15: Sometimes transgenic *pAHK2:rock2* plants grow and flower for more than 12 weeks.
(a) A transgenic *pAHK2:rock2* plant 90 days after germination. **(b)** Flowers of the same plant. Some branches still produce normal looking flowers (left) whereas other flowers are grown together with malformed tissue (right).

3.1.5.6 Transgenic expression of pAHK3:rock3 *increases seed yield*

As mentioned before, *rock* mutants flowered longer, and shoot height was increased (Fig. 14a). On the main stem, the distance between formed siliques (internode length) was not altered (Supplemental Data Fig. 34), raising the question: do these plants form more siliques per plant and as a result have an increased seed yield? Counting of all siliques per plant revealed that *rock2*, *pAHK2-rock2* and *pAHK3:rock3* plants did indeed form more siliques compared to wild-type plants (Fig. 16b). The transgenic *pAHK2-rock2* line showed the largest increase, generating more than twice as many siliques than the wild-type. Preliminary results indicate that the increased amount of siliques is due to a shorter floral plastochron, as *rock2*, *pAHK2-rock2* and *pAHK3:rock3* plants formed more flowers per time unit compared to wild type (Supplemental Data Fig. 35).

Seed yield was not increased in the *rock2* and *pAHK2-rock2* lines, which can be explained by the reduced fertility of these plants (Fig. 13 and Fig. 17). The *rock3* mutation on the other hand does not interfere with fertility. The siliques were usually completely filled and the size of siliques and number of seeds per silique were not altered in *pAHK3:rock3* transgenic plants compared to wild-type siliques (Fig. 13f and Fig. 16c). Measurements of seed size revealed no notable changes in seed size of *pAHK3:rock3* transgenic plants (Fig. 16d). Consequently, transgenic *rock3* plants produced more than 40% more seeds compared to wild-type plants. Similar results were found for a second transgenic *rock3* line (*pAHK3:rock3-5*), proving that seed yield is in fact positively influenced by the *rock3* mutation (Supplemental Data Fig. 36).

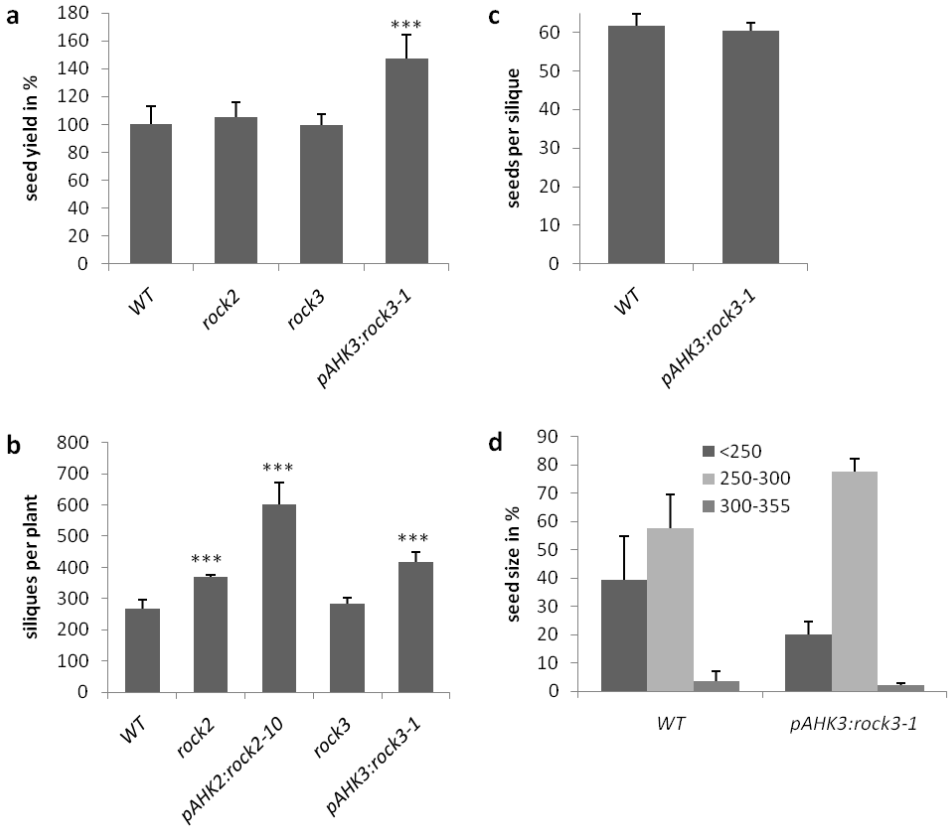

Fig. 16 Transgenic *rock3* plants produce more seeds than wild type.
(a) Transgenic *pAHK3:rock3* line has an up to 45% increase of seed yield compared to wild-type plants (n=20). **(b)** Number of siliques per plant, counted after formation of the last flower. Also unfilled siliques were counted (n=15). **(c)** Wild type and transgenic *rock3* plants produce the same number of seeds per silique (n=6). **(d)** Seed size of wild type and transgenic *rock3* plants. Seeds per plant were collected and filtered through sieves with different sized pores (250, 300 and 355 μm^2). Error bars represent SE, *** = $p < 0{,}001$ compared to WT as calculated by student t-test.

3.1.5.7 Transgenic expression of pAHK2:rock2 *causes reduced fertility*

As mentioned before (see chapter 3.1.5.4), transgenic expression of *pAHK2:rock2* reduces fertility. In transgenic *pAHK2:rock2* lines only a small amount of siliques produced a few seeds. Figure 17 shows typical siliques of hand-pollinated wild-type and homozygous *pAHK2:rock2-10* plants (left side). Wild-type fruits were evenly filled whereas *pAHK2:rock2* siliques were shorter, flattened and exhibited reduced fertility, with between one and twenty seeds developing per pollinated siliques, leaving a lot of empty spaces that should be occupied with seeds, indicating unfertilized ovules or early embryo abortion (Fig. 17, second from left). Typically seed distribution was biased toward the apical half of the carpel, but fertilization also occurred in the basal half.

Fig. 17: The *rock2* mutation in the *AHK2* gene causes reduced fertility.
Pictures show typically shaped and opened siliques of hand-pollinated wild-type and hand-pollinated homozygous *pAHK2:rock2* plants, and reciprocal crosses between wild-type and *pAHK2:rock2* plants, ten days after pollination (left to right).

To determine whether male or female gametophytes were affected, reciprocal crosses between wild type and the transgenic line *pAHK2:rock2-10* were performed. Reciprocal crosses with wild type also caused a reduced seed set. Wild-type gynoecia pollinated with *pAHK2:rock2* pollen showed no obvious abnormal phenotype except a reduced length. Opened siliques revealed empty spaces, which should be occupied by seeds over the whole length of the silique, indicating pollen-mediated defects or defects in early embryogenesis (Fig. 17, second from right). Transgenic *pAHK2:rock2* siliques which were pollinated with wild-type pollen were longer than siliques pollinated with transgenic pollen and produced more seeds. Nevertheless many empty spaces could be found mainly in the basal half of the silique but also in the apical half (Fig. 17, right picture), showing that reduced fertility was also due to defects in female reproductive tissues. Hence, the reduced fertility is neither female nor male specific.

Analysis of the progeny of heterozygous *pAHK2:rock2-10* plants revealed no normal 3:1 segregation pattern of the T-DNA insertion, but a segregation pattern of 0,26:1 (49 out of 241 plants were kanamycin-resistent), indicating that the majority of embryos which carried the *pAHK2:rock2* transgene died during early embryogenesis.

3.1.5.8 Expression of pAHK2:rock2 *impairs embryogenesis*

Transgenic *pAHK2:rock2* plants contained a large number of undeveloped ovules and very few normal seeds. To address the question of whether embryogenesis is disturbed in transgenic *rock2* plants, developing seeds per silique of the wild-type and *pAHK2:rock2* plants were inspected at various stages after manual pollination (Fig. 18a).

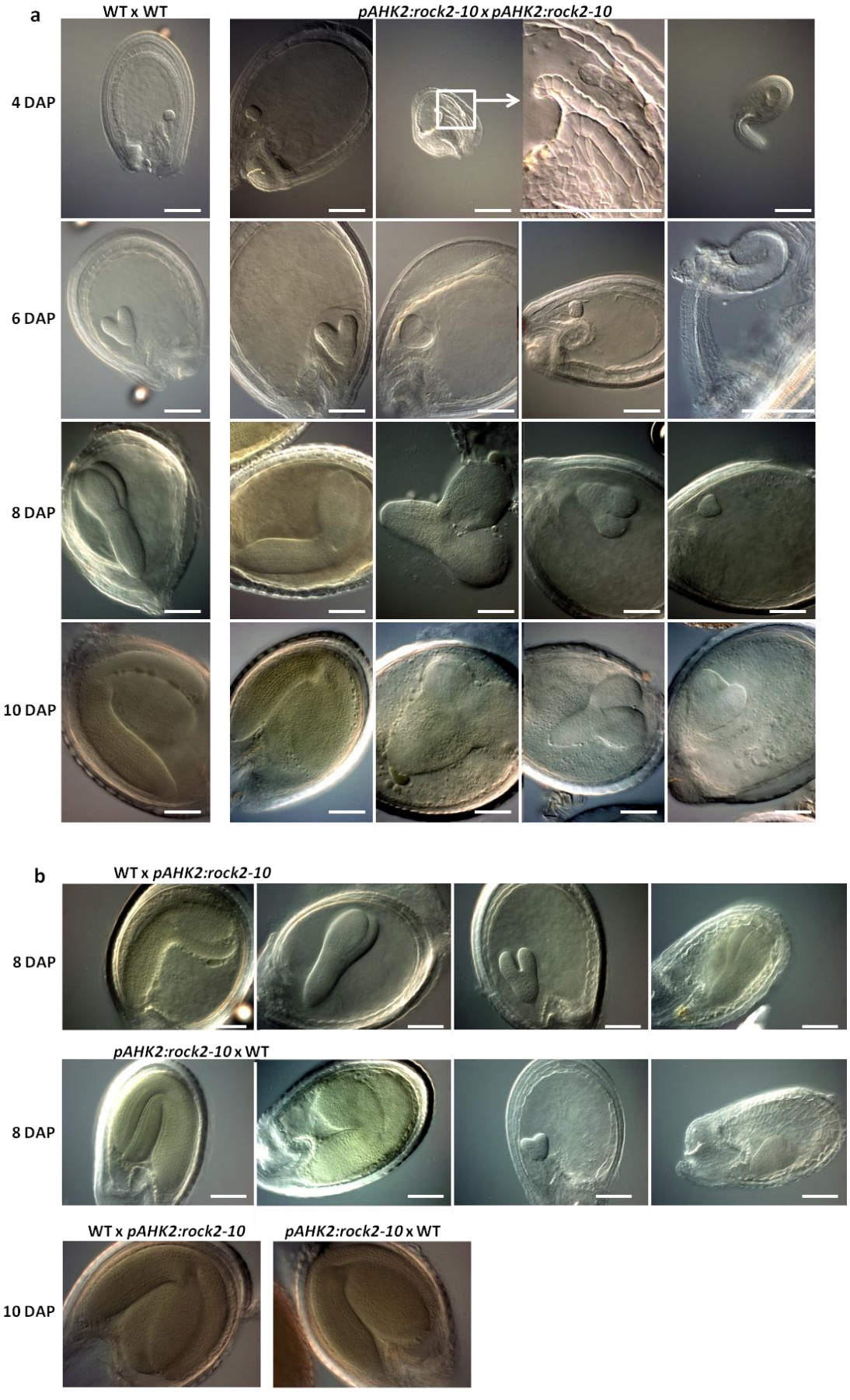

Fig. 18: Seed development in wild-type and transgenic *pAHK2:rock2* plants.

Fig. 18 continued.
(a) Cleared seeds of wild type (WT, left column) and homozygous *pAHK2:rock2* plants at different time points after manual pollination (DAP). Wild-type seeds grow synchronically and siliques contain seeds with embryos at similar developmental stages. In transgenic *pAHK2:rock2* plants seed development is unsynchronized. In all inspected siliques embryos at different developmental stages were found. **(b)** Developing seeds received from reciprocal crosses between WT and *pAHK2:rock2* plants at eight and ten DAP. Similar to homozygous *pAHK2:rock2* plants embryo development is unsynchronized but delayed embryos apparently died after eight DAP. Right photos show collapsing seeds. At ten DAP only similar sized, almost fully grown embryos were present. Scale bar, 50 µm.

At four days after pollination (DAP), wild-type seeds had reached the globular stage of embryogenesis. At the same time point, three different kinds of seeds could be found in *pAHK2:rock2* homozygous seeds. Roughly half of the *pAHK2:rock2* seeds developed similarly to wild-type seeds and contained globular staged embryos. The remaining seeds were very small and contained embryos of the two- to eight-cell stages, and seeds, which seemed to be unfertilised ovules (first row, right picture).

At six days after pollination, wild-type embryos had reached the heart to early torpedo stages. Here again, about half of the *pAHK2:rock2* seeds looked similar to wild-type seeds and contained heart stage embryos, but in other seeds, embryogenesis was delayed and contained embryos of the globular to early heart stages. Small unfertilised ovules could also be found with a low frequency six days after pollination (second row, right photo).

At eight days after pollination, wild-type seeds contained late torpedo-shaped embryos, while *pAHK2:rock2* seeds contained mostly embryos between early heart-stage (third row, right photo) and late torpedo stage (third row, second photo from the left) which appeared to develop normally, but also contained slightly malformed, thickened and swollen looking embryos at the heart and torpedo stage (third row, second and third photo from the right). Interestingly, seeds of delayed embryos were as big as other seeds.

At ten days after pollination, wild-type and the larger *pAHK2:rock2* embryos were almost full-sized, but a low percentage of *pAHK2:rock2* embryos were abnormally thickened and swollen looking of late heart and torpedo stage (fourth row, three photos on the right side).

In most cases, abortion of the abnormal looking and strongly delayed embryos occurred at some time point during embryo development, as later on, only a few normal sized seeds remained per silique, which in most cases germinated normally and produced normal looking seedlings in most cases. However, in some cases, the seedlings were malformed, with smaller and irregular shaped cotyledons (Fig. 19a). Later on these plants stayed smaller, their leaves would often curl, and the plants usually failed to produce any seeds.

In order to find out if defects in embryogenesis are female- or male-specific, reciprocal crosses with wild type were performed and embryo development was examined at different time points after manual pollination (Fig. 18). Reciprocal crosses revealed the defect in embryogenesis to be neither female nor male-specific, indicating defects in embryo development.

Wild-type flowers pollinated with *pAHK2:rock2* pollen, and *pAHK2:rock2* flowers pollinated with wild-type pollen, both showed defects in embryogenesis similar to homozygous *pAHK2:rock2* (Fig. 18b). In both cases, embryogenesis was unsynchronised, and many seeds showed delayed embryogenesis and embryo abortion. Figure 18b shows developing seeds eight and ten days after pollination. After eight days embryo size ranged from heart-shaped to almost full-sized embryos and in some cases embryos were malformed and thickened. Interestingly, shrunken collapsed seeds containing heart-shaped to torpedo-shaped embryos could be found eight days after pollination (first and second row, right picture), but not ten days after pollination. Ten days after pollination only a few seeds were left per silique (Fig. 17). Presumably, delayed and malformed embryos had been aborted, and only normal sized almost fully-grown embryos developed further and reached maturity. These embryos were usually able to generate normal looking plants.

Taken together, unfertilized ovules, delay of seed development, malformed embryos and embryo abortion was observed in pollinated *pAHK2:rock2-10* siliques and wild-type flowers pollinated with *pAHK2:rock2-10* pollen. Similar results were found in the independent *pAHK2:rock2* lines 7 and 9 (Supplemental Data Fig. 37), indicating an important role of AHK2 in embryo development.

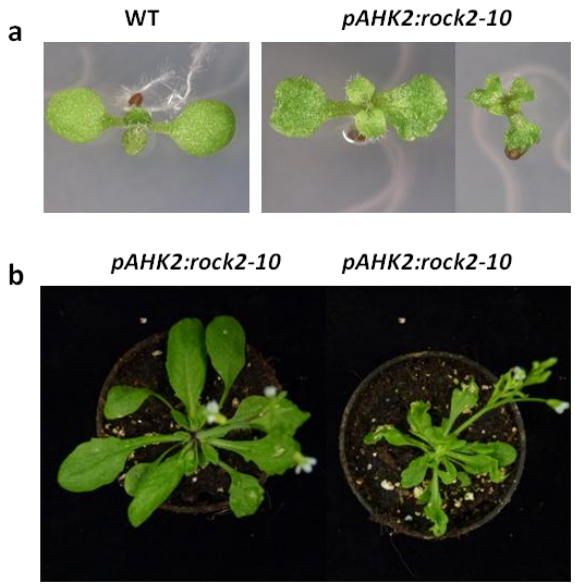

Fig. 19: A low percentage of transgenic *pAHK2:rock2* plants show irregularly shaped cotyledons and a disturbed plant growth.
(a) Wild–type and *pAHK2:rock2* seedlings grown on Ats-media for six days. In some cases *pAHK2:rock2* seedlings have malformed cotyledons to a different extent. **(b)** Homozygous transgenic *pAHK2:rock2* plants 30 days after germination. Most mutants look like wild-type (left) but malformed seedlings like those shown in (a) grew into dwarfed plants with curled rosette leaves (right side).

3.1.5.9 The rock2 and rock3 mutants exhibit delayed leaf senescence

Darkness is one of the most potent external stimuli that accelerate leaf senescence. lt is known that an enhanced cytokinin status delays leaf senescence, and AHK2 and AHK3 are required to mediate cytokinin-dependent chlorophyll retention in the dark (Kim et al. 2006; Riefler et al. 2006). In the *CKX1* overexpressing background, constitutively active versions of the cytokinin receptors AHK2 and AHK3 delayed dark-induced leaf senescence, with AHK3 playing a more dominant role than AHK2 (see chapter 3.1.1). To address the question of whether the same is true in wild-type background, a detached leaf assay was performed with *rock2* and *rock3*.

Figure 20a shows that dark-induced leaf senescence is clearly retarded in *rock3* mutant plants compared to wild type. After seven days in the dark, chlorophyll content was reduced by 90% in wild-type plants, whereas *rock3* leaves were still green with a remaining chlorophyll content of almost 60%. The constitutively active versions of the cytokinin receptor AHK2 does not seem to play an important role in delaying dark-induced leaf senescence as chlorophyll content was as low as in wild-type leaves.

Next, natural occuring leaf senescence in wild-type plants and the *rock2* and *rock3* mutants were compared. Visual examination of the sixth rosette leaves throughout their life spans showed that the onset of natural leaf senescence is clearly retarded in *rock3* mutant plants compared to wild type (Fig. 20b). The *rock3* mutant leaves maintained their green pigmentation and architectural integrity for a longer period than the wild-type leaves. This difference in timing of leaf senescence led to *rock3* leaves having roughly a seven day longer life span compared to wild-type leaves. The *rock2* allele only slightly delayed leaf senescence by up to two days (Fig. 20b).

These results were confirmed by measuring two physiological parameter of senescence at increasing leaf age, the photosynthetic efficiency of photosystem II (Fv/Fm) and the chlorophyll content (Fig. 20c and 20d). Photosynthetic efficiency of photosystem II started to decline in the sixth rosette leaf of wild-type plants around 17 days after leaf emergence (DAE) and 21 to 23 DAE in the mutant plants *rock2* and *rock3*, respectively (Fig. 20d). Once again, *rock2* plants showed an earlier onset of leaf senescence compared to *rock3*. Compared to wild type, the further decrease of photosythethic efficiency of photosystem II in the sixth rosette leaves occured at about three later in *rock2* leaves, and aroung seven days for *rock3* leaves (Fig. 20d). The decrease of chlorophyll content of the sixth rosette leaves measured by SPAD confirmed these results, with the chlorophyll content of *rock2* leaves decreasing two days later than that of wild-type leaves, and *rock3* leaves catabolised chlorophyll about seven days later than wild type (Fig. 20c).

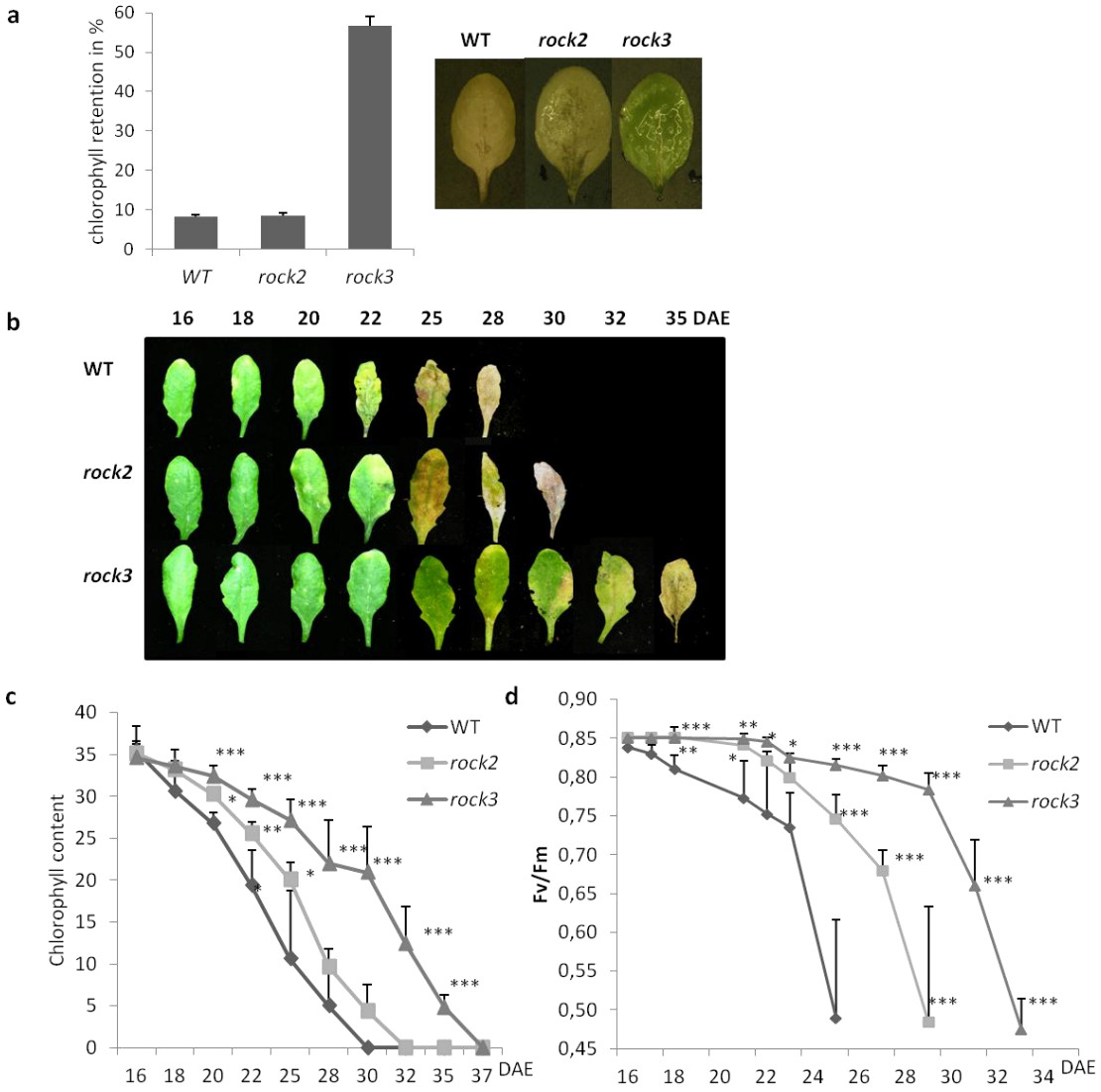

Fig. 20: The *rock3* mutant shows extended leaf longevity.
(a) Dark-induced senescence in a detached leaf assay. The leaf chlorophyll content before the start of dark incubation was set at 100% for each genotype tested. Chlorophyll content was examined after 7 days in the dark. Error bars represent SE (n = 10). Right side: leaves of wild type, *rock2* and *rock3* at the end of the chlorophyll retention assay described. Experiment was repeated twice with similar results. **(b)** Natural senescence of leaf 6 of *rock* mutants and wild type under long day conditions starting at 16 days after leaf emergence (DAE) when the leaf had just reached its full size. **(c)** Chlorophyll contents of individual sixth leaves measured with the Chlorophyll Meter SPAD from 16 to 37 DAE. **(d)** Reduction of photosynthetic efficiency of photosystem II of leaf 6 from 16 to 34 DAE. Standard bars represent SE. * = $p < 0.01$; ** = $p < 0.005$; *** = $p < 0.001$ compared to wild type as calculated by student t-test.

Consistent with published results (Kim et al. 2006), these results confirm that a gain-of-function mutation in the AHK3 cytokinin receptor significantly delays various senescence-associated symptoms in *Arabidopsis*. AHK2 on the other hand plays only a minor, but significant role in delaying leaf senescence.

Kim et al. (2006) published that another gain of function version of *AHK3* (*ore12*) delays various senescence-associated symptoms, indicating that ORE12 is a regulator of leaf longevity in

Arabidopsis. The mutation *ore12* seems to cause a weaker gain-of-function version of AHK3 than *rock3*, as *ore12* does not complement the cytokinin deficiency syndrome as strongly as *rock3* and also does not show most of its growth promoting aspects (Supplemental Data Fig. 38). In order to find out if the mutations *ore12* and *rock3* show different degrees in delaying leaf senescence, leaf senescence of wild-type plants, the *rock2* and *rock3* mutants, and *ore12* were compared. Visual examination of individual leaves throughout their life spans, as well as measuring the photosynthetic efficiency of photosystem II and the decrease in chlorophyll content, proved that *rock3* allele indeed having a greater effect in delaying senescence than *ore12* allele (Supplemental Data Fig. 39).

3.1.5.10 The root phenotype of rock2 *and* rock3 *mutants*

In contrast to their promotional role in shoot organs, cytokinins are negative regulators of root development (Heyl et al. 2008; Mason et al. 2005; Miyawaki et al. 2006; Riefler et al. 2006; Werner et al. 2003; Werner et al. 2001).

Root growth was inhibited in all tested *rock* seedlings grown under *in vitro* conditions (Fig. 21a and 21b). In general, the transgenic *rock* mutants *pAHK2:rock2* and *pAHK3:rock3* have a more pronounced phenotype. Surprisingly, this was not the case during early root growth. Primary root elongation within 8 days was reduced by 37% in the case of *rock2* and by 28% in *rock3*, but the transgenic *rock* lines *pAHK2:rock2-10* and *pAHK3:rock3-1* showed slightly milder root phenotypes, with a reduction in root elongation by 23% and 18%, respectively (Fig. 21a). The formation of lateral root outgrowth was strongly inhibited as well. On average, the numbers of outgrowing lateral roots in wild-type plants were around 1.8 to 2.4 times greater than that of the *rock* mutants, with *rock2* showing the strongest phenotype (Fig. 21b). Here once again, the phenotype of the transgenic *rock* lines *pAHK2:rock2-10* and *pAHK3:rock3-1* was slightly less pronounced when compared to *rock2* and *rock3*.

A hydroponic system was used to examine root growth over a longer time period. After 35 days, the root length of wild-type plants and the *rock* mutants were compared (Fig. 21c). In the *rock* mutants, root length was reduced by 27 to 45%. Here, the *pAHK2:rock2* plants showed the strongest phenotype.

The root systems were also examined at the end of the plants life cycles; by drying the flower pots after the end of the plants life cycle, and visually examining the amount of roots in the pots. When compared to wild type and the other *rock* mutants, the transgenic *pAHK2:rock2* plants had developed fewer roots (Fig. 21d). *Rock2* plants seemed to have also developed fewer roots than wild type, while between wild type, *rock3* mutants and *pAHK3:rock3-1* mutant no obvious differences could be seen.

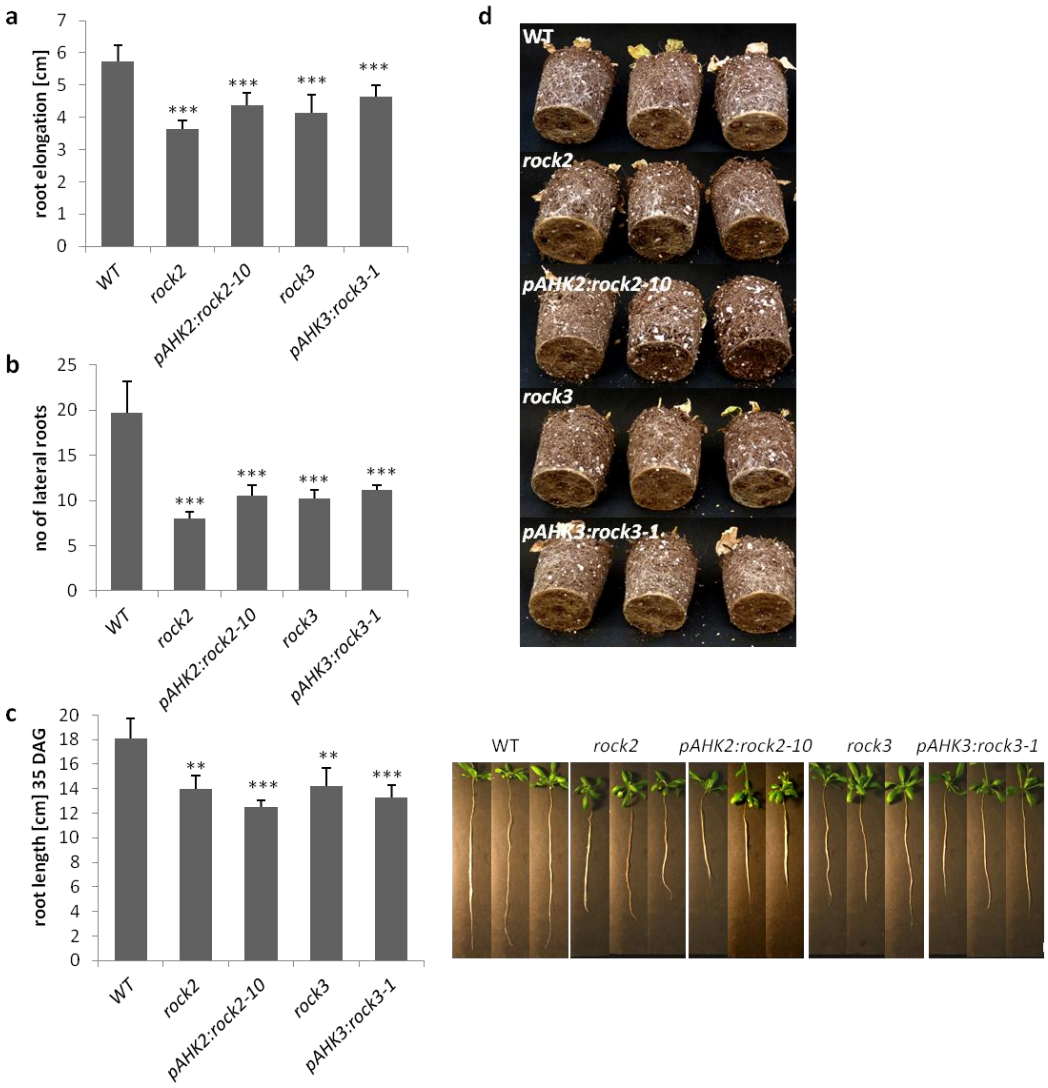

Fig. 21: The *rock2* and *rock3* mutants form a reduced root system.
(a) Elongation of primary roots of wild type and *rock* mutants grown on vertical plates on standard Ats medium within 8 days (n=20) **(b)** Number of lateral roots at 16 days after germination of wild type and *rock* mutants grown on vertical plates on standard Ats medium (n=20). **(c)** Reduced root system of *rock* plants grown in hydroponic cultures in long day conditions for 35 days and photos of these plants (n=10). **(d)** Visual inspection of the root system of plants grown on soil in pots at the end of their life cycle. Error bars represent SE. ** = $p < 0{,}005$; *** = $p < 0{,}001$ compared to the wild type, as calculated by students t-test.

3.2 *Rock4* is a gain-of-function variant of the cytokinin synthesis protein IPT3

Like *rock2* and *rock3,* the *rock4* mutant was also identified from a screen of plants derived from an EMS-mutagenized seed pool and showed a reversion of the cytokinin deficiency syndrome (Bartrina 2006). Segregation analysis of backcrossed mutants revealed that the *rock4* mutation is also dominant (Bartrina 2006).

3.2.1 Phenotypic analysis of *rock4* in the CKX1 overexpressing background

In contrast to the phenotypic reversion of the cytokinin deficiency syndrome caused by *rock2* and *rock3*, the phenotypic reversion of *rock4 CKX1ox* plants was only obvious much later in development (Fig. 1 and Fig. 22a). Consistent with published results (Bartrina 2006), no obvious difference in size could be found in *rock4 CKX1ox* seedlings compared to *CKX1ox* seedlings at seven days after germination, but later in development *rock4 CKX1ox* plants showed an increased expansion of rosette leaves when compared to *CKX1ox* plants and the reversion of the CDS became more and more obvious over time (Fig. 22). At the end of the life cycle *rock4 CKX1ox* rosette leaves were almost as big as wild-type leaves.

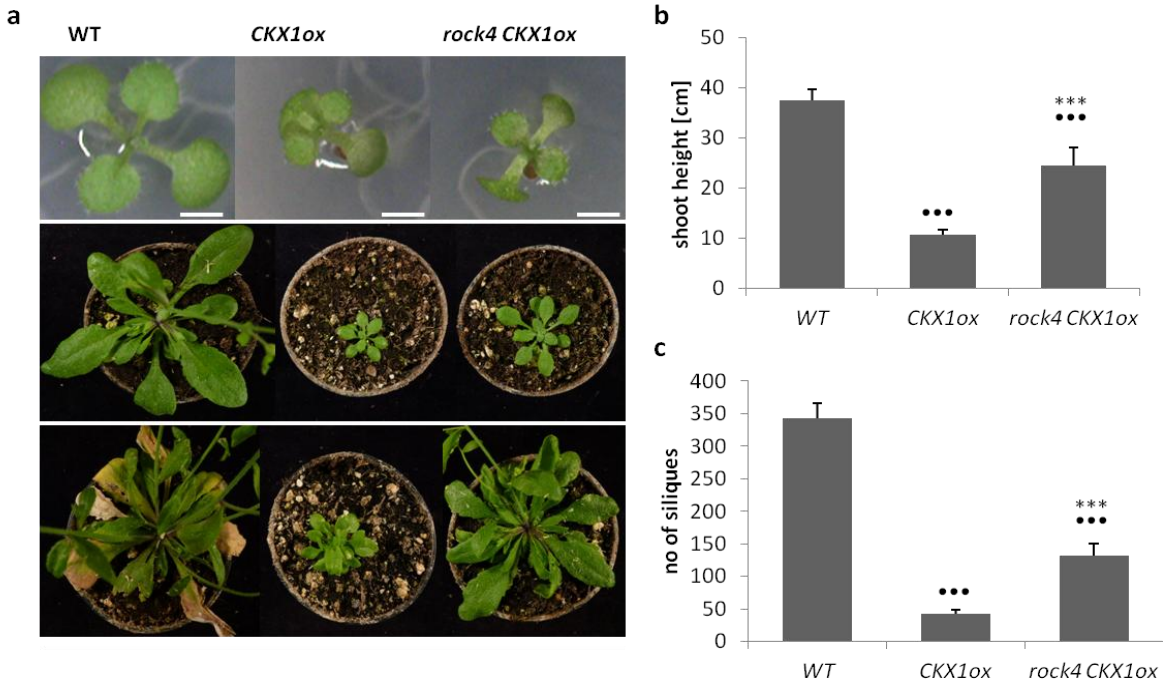

Fig. 22: Shoot phenotype of the suppressor mutant *rock4 CKX1ox.*
(a) At seven days after germination *rock4 CKX1ox* seedlings show no obvious reversion of the reduced shoot growth of *CKX1ox* plants (top), comparison of rosette size and morphology at 26 days after germination (middle) and 40 days after germination (bottom). Scale bars: 1 mm. **(b)** Shoot height at the end of flowering (n=8). **(c)** Number of siliques per plant (n=10). Error bars represent SE, *** = $p < 0{,}001$ compared to *CKX1ox* plants; ••• = $p < 0{,}001$ compared to wild type as calculated by pair wise student's t-test.

In comparison with wild type plants, cytokinin deficient plants developed smaller shoots with a greatly reduced number of flowers. *rock4 CKX1ox* grew bigger shoots with more flowers compared to *CKX1ox* plants but the degree of reversion for different phenotypic effects was not complete Fig. 22b and 22c). Furthermore *CKX1ox* plants formed thin inflorescence stems that bent downward whereas stems of *rock4 CKX1ox* plants were thicker and did not bend down as easily (data not shown).

To address the question of whether it is likely that *rock4* plays a role in the cytokinin signalling, is a developmental factor controlling the intrinsic organ size (e.g. *BIG BROTHER*-like proteins), or a component of a metabolic pathway, which may compensate for the loss of cytokinin, more precise phenotypical investigations were carried out.

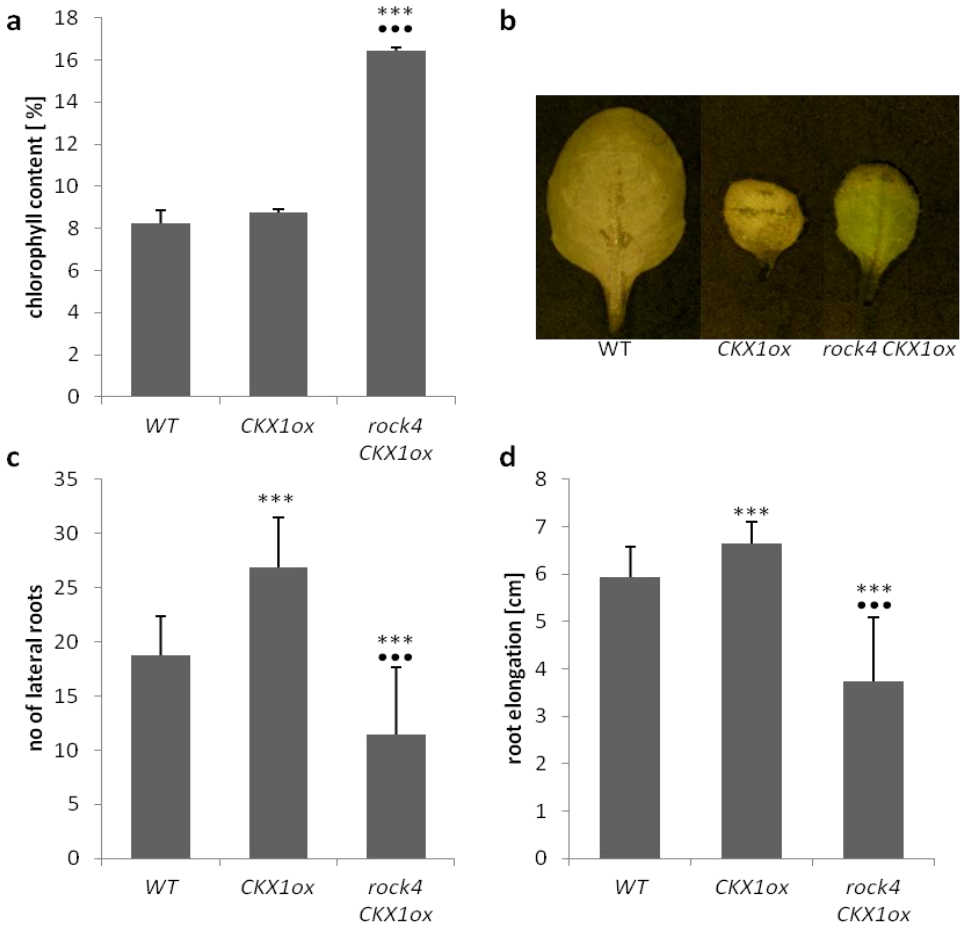

Fig. 23: The *rock4* allele delays senescence and reduces root formation indicating an enhanced cytokinin status.
(a) Dark-induced senescence in a detached leaf assay. The leaf chlorophyll content before the start of dark incubation was set at 100% for each genotype tested. Chlorophyll content was examined after 7 days in the dark (n = 3). **(b)** Leaves of different genotypes at the end of the chlorophyll retention assay described in (a). **(c)** Primary root elongation within eight days and **(d)** emergence of lateral roots within 15 days of wild-type, *CKX1ox* and *rock3 CKX1ox* seedlings grown on vertical plates on standard Ats medium. Error bars represent SE. *** = p < 0,001 compared to *CKX1ox* plants; ••• = p < 0,001 compared to wild type, as calculated by students t-test.

In the following, parameters which are good indicators for a changed cytokinin status of the *CKX1ox* plants were analysed. As mentioned before, an enhanced cytokinin status delays leaf senescence (Kim et al. 2006; Richmond and Lang 1957; Riefler et al. 2006). As darkness is one of the most potent external stimuli that accelerate leaf senescence (Buchanan-Wollaston et al. 2005), a dark-induced chlorophyll retention assay was carried out and chlorophyll degradation of *rock4 CKX1ox* plants was compared to wild-type and *CKX1ox* plants. Figures 23a and 23b show that in a dark-induced detached leaf assay the onset of leaf senescence is clearly retarded in *rock4 CKX1ox* mutant plants compared to wild type and *CKX1ox* plants. After seven days in the dark, the chlorophyll content was reduced to 8% in wild-type and *CKX1ox* plants. *rock4 CKX1ox* leaves were still green and contained 17% of their initial chlorophyll content, suggesting a role for *rock4* in leaf longevity.

Another parameter which indicates a changed cytokinin status is an altered root growth, because contrary to the retarded shoot development, the root formation and growth of *35S:CKX1* transgenic *Arabidopsis* plants is enhanced (Werner et al. 2003). Consistent with published results (Werner et al. 2003), the formation of lateral roots was strongly enhanced in *CKX1* over-expressing seedlings grown for 15 days under *in vitro* conditions compared to wild type (Fig. 23c). On average, the number of initiated lateral roots of *CKX1* overexpressing plants was 50% greater than that of the wild type. Primary root elongation of *CKX1ox* plants was only slightly enhanced in this experiment, which is probably due to experimental conditions. In the *CKX1* overexpressing background, the *rock4* mutation caused a reduction of root growth and lateral root formation when compared to *CKX1ox* and wild-type plants (Fig. 23c and 23d). The number of initiated lateral roots was reduced by 34% compared to wild type and 54% compared to *CKX1ox* (Fig. 23c) and primary root elongation was reduced by 38% and 44%, respectively (Fig. 23d). Thus, *rock4* seems to play an important role in regulation of root growth.

3.2.2 Map-based cloning of the dominant *rock4* mutation

Rock4 is another dominant mutation which leads to a partial reversion of the cytokinin deficiency syndrome similar to *rock2* and *rock3*. In order to discover if *rock4* is another gain-of-function allele of a cytokinin receptor, genomic DNA was isolated from *rock4 CKX1ox* tissue and coding regions of the three known cytokinin receptors *AHK2*, *AHK3* and *AHK4* were sequenced and compared with wild-type Columbia-0 (Col) sequence. No single base changes were found in any of the *AHK* receptor sequences, suggesting a mutation in another cytokinin-related protein.

In order to identify the mutated gene responsible for the reversion of the cytokinin deficiency syndrome, map-based cloning was carried out, as described in more detail for *rock2* and *rock3* in chapter 3.1.2. First, a recombinant mapping population was generated by crossing homozygote *rock4*

CKX1ox plants in the Col background with wild-type L*er* (Landsberg *erecta*) plants. The dominant phenotypical characteristics reappeared in the F1 population, confirming that the *rock4* mutation is dominant. Therefore mapping was carried out with homozygous *CKX1ox* plants. In order to preselect plants that contained the *CKX1* transgene, the segregating F2 population was grown on media containing Hygromycin B.

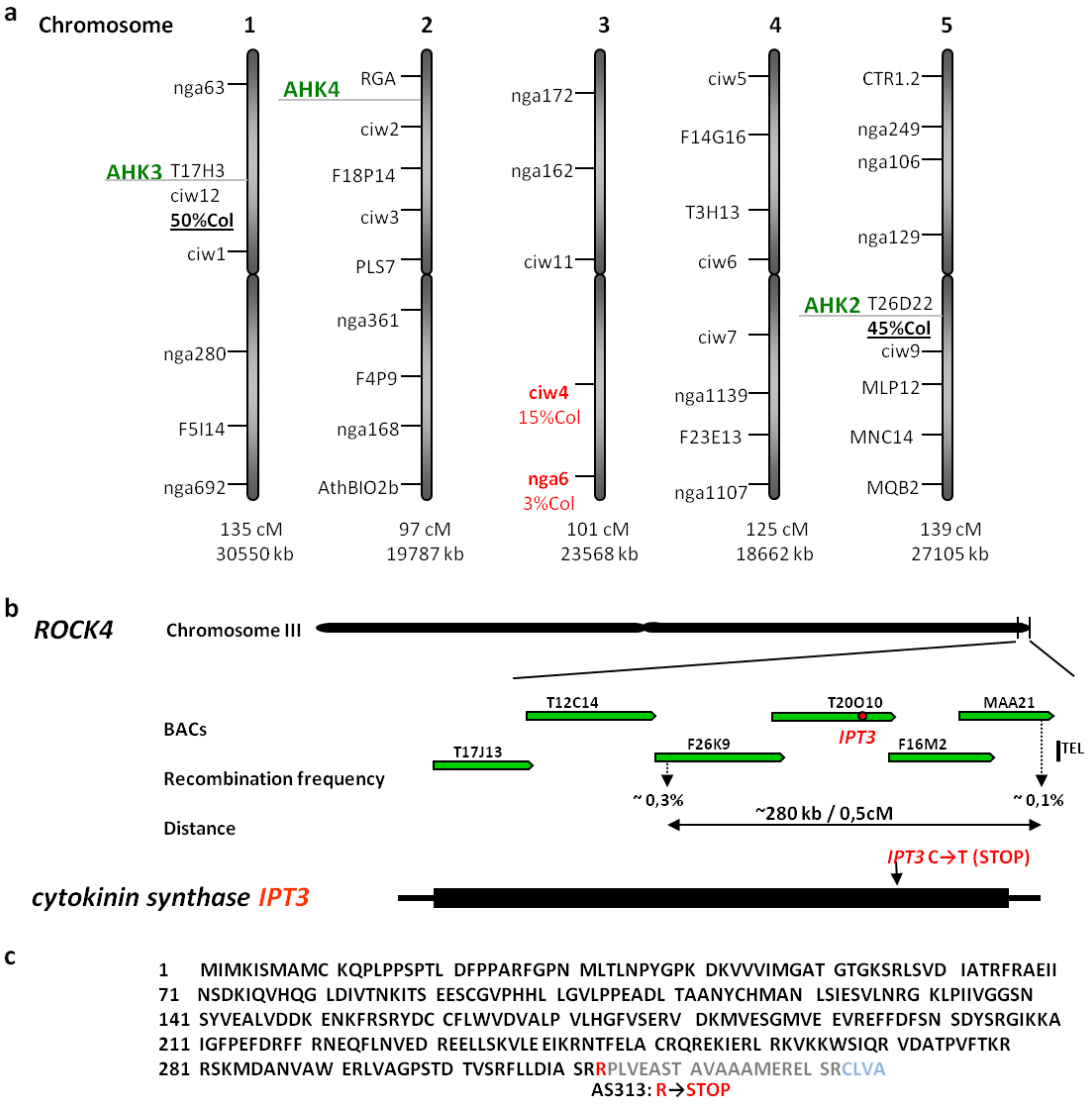

Fig. 24: The *rock4* mutation causes a truncated version of IPT3.
(a) Rough segregant analysis of the *rock4* locus using molecular markers: Schematic *Arabidopsis* chromosomes with approximate location of the 38 molecular markers used for rough mapping and location of the genes *AHK2*, *AHK3* and *AHK4*. Genomic DNA of Col, L*er*, heterozygous Col x L*er* plants, and a pool of 60 *CKX1ox* looking plants from the mapping population were used for rough mapping. The markers ciw4 and nga6 (red) are linked to the *rock4* mutation. 15% and 3% of the examined samples were genomically Col at this location, respectively. **(b)** Fine mapping of the *rock4* mutation identified markers on the bacterial artificial chromosomes (BAC) F26K9 and MAA21 (289 kb or 0.5 cM apart) as the closest flanking markers based on recombination events. The *rock4* mutation is marked as a red dot on BAC T20O10. Sequence analysis identified *rock4* as a mutation in the cytokinin synthase gene *IPT3*. **(c)** Based on the cDNA sequence, it was predicted that the *rock4* mutant protein has a premature stop codon at amino acid position 313. The truncated version of IPT3 results in the loss of a predicted farnelysation site (blue).

Segregation of molecular markers in a pooled F2 population of 60 *CKX1ox* x L*er* plants allowed the identification of markers that were closely linked to the mutation of interest. Samples were genotyped with a collection of 38 SSLP markers spaced evenly over the entire genome in intervals of approximately 20 centimorgan (cM) (Fig. 24a). *CKX1ox* DNA was homozygous L*er* at the *rock4* mutation and therefore mostly L*er* in the neighbourhood of the mutation, but essentially heterozygous for unlinked markers. Bulked analysis suggested that the *rock4* mutation roughly maps to a chromosomal region at the bottom end of the lower arm of chromosome 3 close to the marker nga6 (Fig. 24a). To verify the results of the bulked segregant analysis, the markers nga6 and ciw4 were also tested with individual samples. Four and 18 out of sixty samples were heterozygous for Col/L*er* at the nga6 and the ciw4 locus, respectively, which equals to a recombination frequency of 3% and 15%, respectively (Fig. 24a).

In addition, markers close to the cytokinin receptor genes *AHK2*, *AHK3* and *AHK4* were tested to confirm that *rock4* is not an additional gain-of-function cytokinin receptor. In all cases, the markers were unlinked and *CKX1ox* DNA was clearly heterozygous for Col/L*er*.

The next step was to identify robust, the mutation *rock4* flanking, PCR markers. The SSLP marker F2A19 and the CAPS marker MAA21 on either side of the mutation were used as flanking markers for further work. A CAPS marker was used because no SSLP marker could be found at the far end of chromosome 3. The markers are approximately 520 kb apart from each other.

A total of 970 plants with the *CKX1ox* phenotype were selected from the F2 population, which were derived from the *rock4 CKX1ox* line, and their genomic DNA was analysed with PCR markers. A total of 26 recombinants were identified with the markers F2A19 and MAA21. Following this, molecular markers were designed at a high density to narrow down the genetic interval between the markers F2A19 and MAA21 on either side of the mutation (Supplemental Data Table 5) and all 26 recombinants were genotyped with these markers to narrow down the position of the region of interest.

The *rock4* locus was mapped to a roughly 289-kb interval between the markers nga112 on BAC F26K9 and MAA21 (on BAC MAA21) on chromosome 3 containing 83 annotated genes on BAC F26K9, T20O10, F16M2 and MAA21 (http://www.arabidopsis.org) (Fig. 24b). In this interval the candidate gene *IPT3* annotates, which codes for a cytokinin synthesis protein. The genomic DNA of *rock4 CKX1* mutants was sequenced for the *IPT3* coding region and compared with the wild-type Col sequence, leading to the identification of a single base change from C to T at amino nucleotide position 939 from translation start of IPT3, which results in a premature stop codon (Fig. 24c). These changes result in the loss of the predicted farnelysation site of the protein (Galichet et al. 2008).

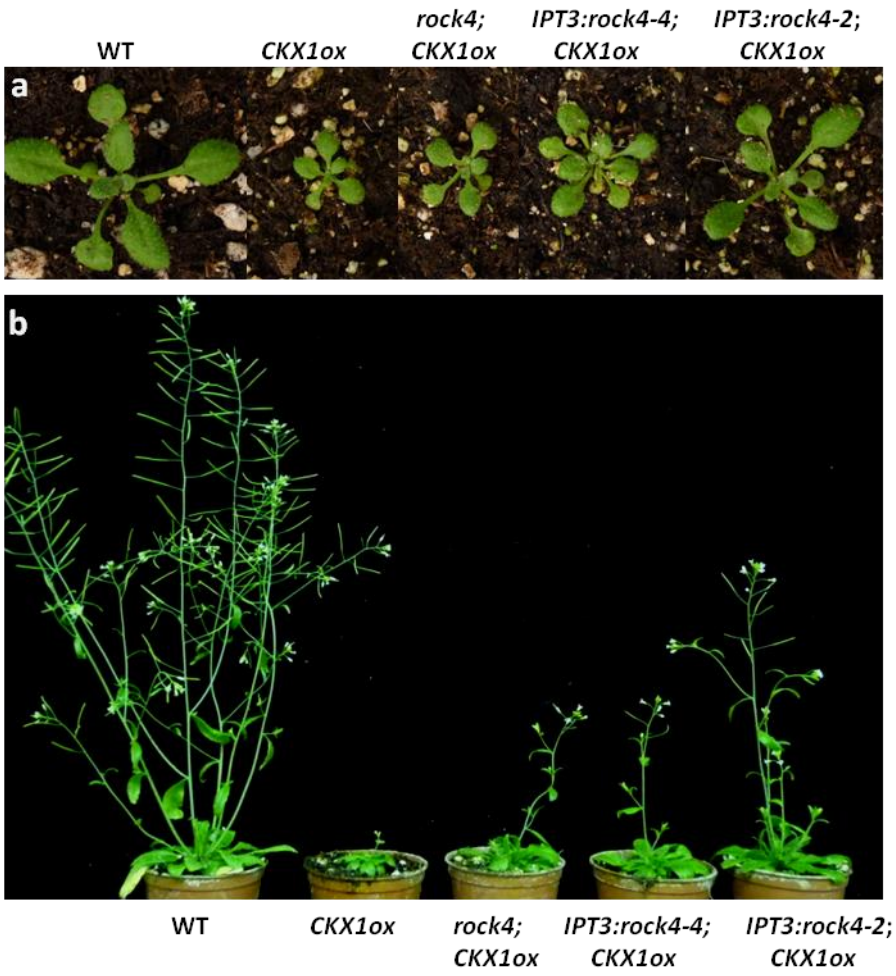

Fig. 25: Transgenic plants expressing *rock4* recapitulate the reversion of the CDS.
(a) Two independent transgenic *rock4* lines in the *CKX1ox* background in comparison to the original *rock4 CKX1ox* line, *CKX1ox* and wild type at 16 days after germination (DAG). **(b)** Comparison of shoot growth 36 DAG.

Taken together, map-based cloning led to the identification of *rock4* as a missense mutation in the cytokinin synthesis gene *IPT3,* which causes a truncated version of the IPT3 protein. As *rock4* causes a reversion of the cytokinin deficiency syndrome, the premature stop codon in the *IPT3* cDNA sequence seems to cause a gain-of-function version of the IPT3 protein.

In order to verify that the dominant *rock4* mutation is in fact responsible for the suppression of the CDS, the reversion of the CDS was recapitulated in transgenic plants expressing *rock4* under its own promoter in the *CKX1* overexpressing background. Therefore, a construct comprising 2 kb of the 5' upstream regulatory region of *IPT3*, and the *rock4* coding sequences (named *pIPT3:rock4)* was cloned and introduced into wild-type plants, as transformation into *CKX1ox* plants failed. Seven independent transgenic lines were identified. The transgene was then crossed into *CKX1ox* plants. Compared to *CKX1ox* plants, all independent transgenic *rock4* lines (named *IPT3:rock4 CKX1ox*) showed increased rosette and shoot growth similar to *rock4 CKX1ox* plants (Fig. 25a and 25b). The line *IPT3:rock4-2*

CKX1ox seemed to have a more enhanced cytokinin status compared to *rock4 CKX1ox* plants, as the degree of reversion of the cytokinin deficient shoot phenotype was more pronounced in this line. This confirms that the phenotypes are indeed derived from the mutation in the *IPT3* gene.

3.2.3 Phenotypic characterization of *rock4* in the wild-type background

In order to analyze the consequences of the *rock4* mutation in wild-type background, the *rock4 CKX1ox* mutant was crossed with Col-0 wild-type plants. The F1 progeny of these crosses still showed the revertant phenotype, confirming that the *rock4* allele is dominant. The F2 generation was screened for homozygous *rock4* plants in wild-type background (named then *rock4* mutant).

Figure 26 shows that the truncated version of the IPT3 protein caused by the *rock4* mutation did not cause strong phenotypic changes in the wild-type background. The overall appearance of *rock4* plants was similar to wild-type plants. A detailed phenotypic analysis of the *rock4* mutants was performed to reveal phenotypic changes. Since the *rock4* mutant is another gain-of-function cytokinin mutant, its effect on vegetative growth and development were also compared to the phenotypic changes that were caused by the *rock2* and *rock3* mutants.

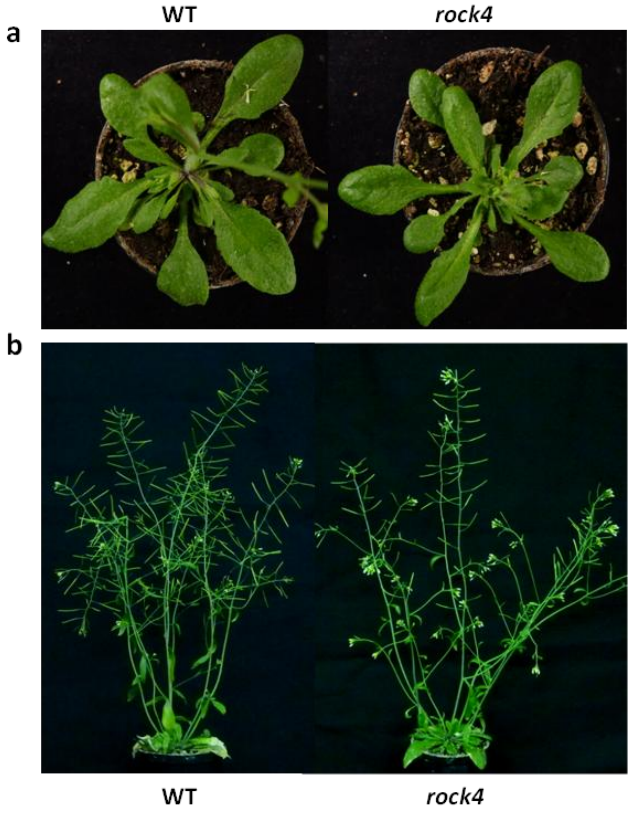

Fig. 26: The *rock4* allele does not cause a strong shoot phenotype in the wild-type background.
(a) Comparison of rosettes at 26 days after germination and **(b)** shoots at 40 days after germination.

3.2.3.1 rock4 *mutants showed an increased thickening of stems*

The dominant gain-of-function cytokinin receptor variants *rock2* and *rock3* increased organ growth throughout the plants life cycle (see chapter 3.1.5). As *rock4* is another dominant mutant with an enhanced cytokinin status, organ size was also inspected in this mutant. Interestingly, in *rock4* plants the effects on shoot growth were more restricted to specific organs compared to the *rock2* and *rock3* mutants.

Contrary to *rock2* and *rock3*, the *rock4* mutation had no obvious effects on cotyledon and leaf expansion, and flower size was also unchanged compared to wild-type flowers (Fig. 27b and 27c). However, *rock4* mutants showed an increased thickening of stems similar to *rock2* and *rock3* mutants (Fig. 12 and Fig. 27a). When the stems were about 20 to 25 cm in length, the diameters of the primary inflorescence stem of wild-type and *rock4* mutant plants were measured below the first node from the base. The diameter of *rock4* mutant stems, showed a significant 25% increase when compared to wild-type stems (Fig. 27a). Transverse sections of the primary inflorescence stem showed that stem morphology was normal in *rock4* mutants but there were extra cells of many types, suggesting higher mitotic activity in the cambium.

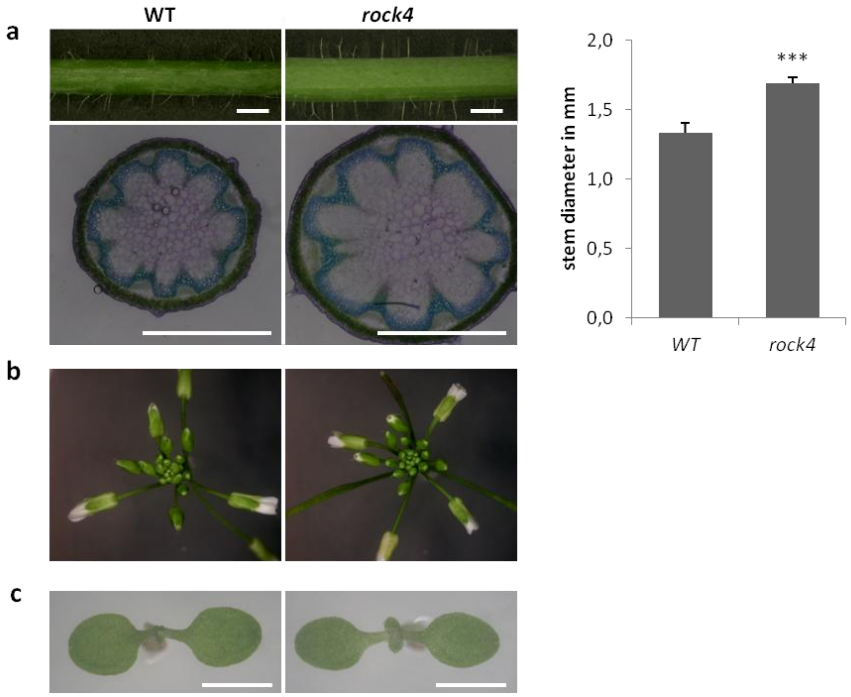

Fig. 27: The *rock4* mutation enhances radial stem growth but has no obvious growth effects on organs like cotyledons and flowers.
(a) Photos of *Arabidopsis* primary inflorescence stem (top) and stem sections of wild type and *rock4* below the first node of primary inflorescence stems, when stems were between 20 and 25 cm in length. Sections were stained with toluidine-blue and photographed at the same magnification. Right side: Stem diameter below the first node of the primary inflorescence stems when the stems were 20 to 25 cm in length. **(b)** Comparison of wild-type and *rock4* flowers. **(c)** Comparison of wild-type and *rock4* cotyledons five days after germination. Error bars represent SE (n=10). *** = $p < 0{,}001$ compared to wild-type plants, as calculated by students t-test. Scale bars: 1 mm.

3.2.3.2 *rock4* plants flower longer than wild type

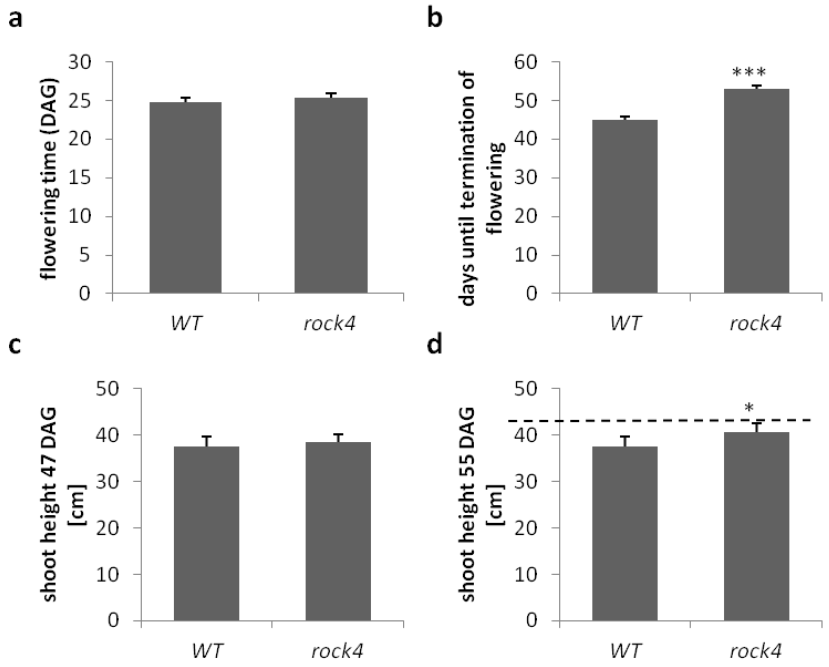

Fig. 28: *rock4* plants flower for a longer period of time and therefore grow longer shoots.
(a) Flowering time of wild type and *rock4* mutant plants grown in long day conditions (n=20). **(b)** Compared to wild type, *rock* mutant shoots flower longer (n=20). **(c)** The rate of shoot elongation is not changed in *rock4* plants compared to wild type (n=20). **(d)** *rock4* plants flower longer and are therefore a few centimetres taller at the end of their life cycle (n=20). Error bars represent SE. * = p<0,01; *** = p<0,001 compared to the wild type, as calculated by students t-test.

A higher cytokinin status is known to affect the onset of flowering (D'Aloia et al. 2011; He and Loh 2002), but in contrast to *rock2* and transgenic *rock3 Arabidopsis* plants, *rock4* plants showed no early flowering phenotype under long day conditions and no enhanced rate of shoot elongation (Fig. 14 and Fig. 28a and 28c). On average, wild-type *Arabidopsis* plants had finished flowering at 47 days after germination. At this time wild-type and *rock4* plants were the same height (Fig. 28c). However, similar to *rock2* and *rock3* plants (Fig. 14e), *rock4* plants flowered about a week longer than wild-type plants, and s a result, shoots were a few centimetres higher at the end of their life cycle (Fig. 28b and 28d), suggesting a function of cytokinin in the duration of inflorescence growth.

3.2.3.3 *The* rock4 *mutant exhibits delayed leaf senescence*

In the *CKX1* overexpressing background, the truncated version of the cytokinin synthesis protein IPT3 delayed dark-induced leaf senescence (chapter 3.2.1). To address the question of whether the same is true in wild-type background, a detached leaf assay was performed with *rock4* in the wild-type background. Figure 29 shows that the onset of leaf senescence was clearly retarded in *rock4* plants in a dark-induced detached leaf assay.

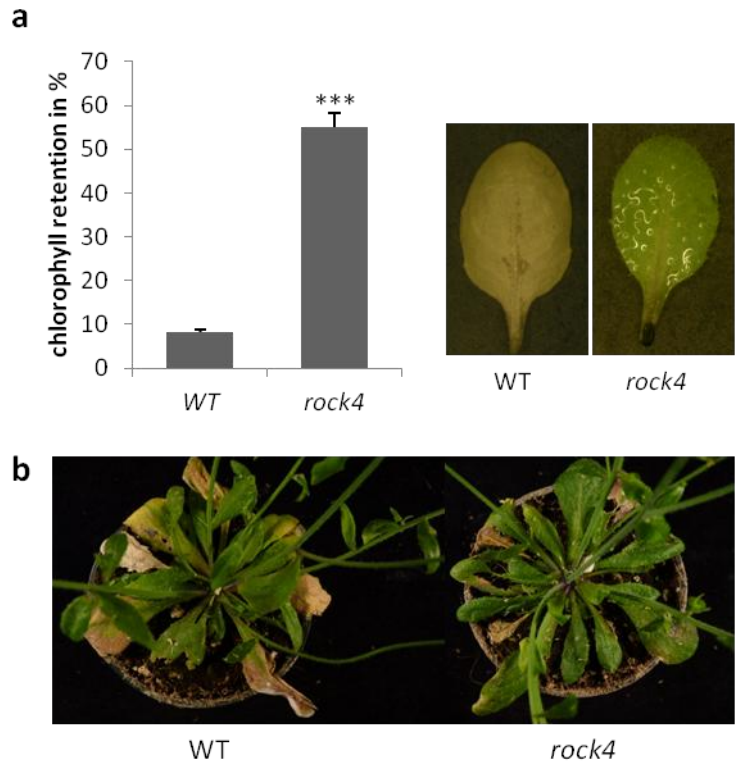

Fig. 29: The *rock4* allele delays leaf senescence.
(a) Dark-induced senescence in a detached leaf assay. The leaf chlorophyll content before the start of dark incubation was set at 100% for each genotype tested. Chlorophyll content was examined after seven days in the dark. Right side: Leaves of wild type (WT) and *rock4* at the end of the chlorophyll retention assay (n = 3). **(b)** Visual inspection of rosettes grown in long day conditions at 40 days after germination. Error bars represent SE. *** = p<0,001 compared to the wild type, as calculated by students t-test.

In a chlorophyll retention assay of detached leaves, the *rock4* mutation led to a delayed senescence of leaves similar to the *rock3* mutant (Fig. 20a and Fig. 29a). After seven days in the dark the chlorophyll content had reduced by approximately 90% in wild-type plants, whereas *rock4* leaves were still green and contained almost 60% of their initial chlorophyll content.

Visual inspection of leaves grown in long day conditions indicated that *rock4* also delays natural leaf senescence (Fig. 29b). At 40 days after germination, wild-type rosette leaves were almost completely yellow and dried out, whereas the oldest *rock4* rosette leafs were still green.

3.2.3.4 The rock4 *mutants exhibit reduced fertility and an impaired embryo development*

Investigations during the reproductive state of *rock4* plants revealed that *rock4* mutants developed slightly shorter siliques than wild-type plants, indicating reduced fertility. The overall shape of the siliques was not altered. Besides *rock4* plants, three independent transgenic *pIPT3:rock4* lines were also used for the analysis of seed development. Transgenic *rock4* lines showed various degrees of shortened siliques with the *pIPT3:rock4-2* line showing the strongest phenotype with siliques 50%

shorter than wild-type siliques. Siliques of the line *pIPT3:rock4-6* were approximately 20% shorter than wild-type siliques and comparable to *rock4* siliques (Fig. 30a). Interestingly, unlike *rock2* flowers (Fig. 13), *rock4* flowers were indistinguishable from wild-type flowers and had no obvious problems with pollination (Fig. 27b).

Opening of the siliques 10 days after pollination revealed disturbed seed development in all examined *rock4* lines. Wild-type siliques were evenly filled with large green seeds whereas *rock4* siliques exhibited large green seeds, shrivelled yellow seeds, and empty spaces that should be occupied by seeds, indicating unfertilized ovules and early embryo abortion. Seed development seemed to be even more disturbed in the transgenic lines *pIPT3:rock4-2* and *pIPT3:rock4-4*, which had an even more severely shortened silique phenotype than *rock4*. Beside normal looking green seeds, approximately 50% of their seeds were yellowish, shrivelled and brown, and siliques exhibited a lot of empty spaces (Fig. 30b). Disturbed seeds were distributed evenly over the silique with no clear bias towards either the apical or basal part of the silique.

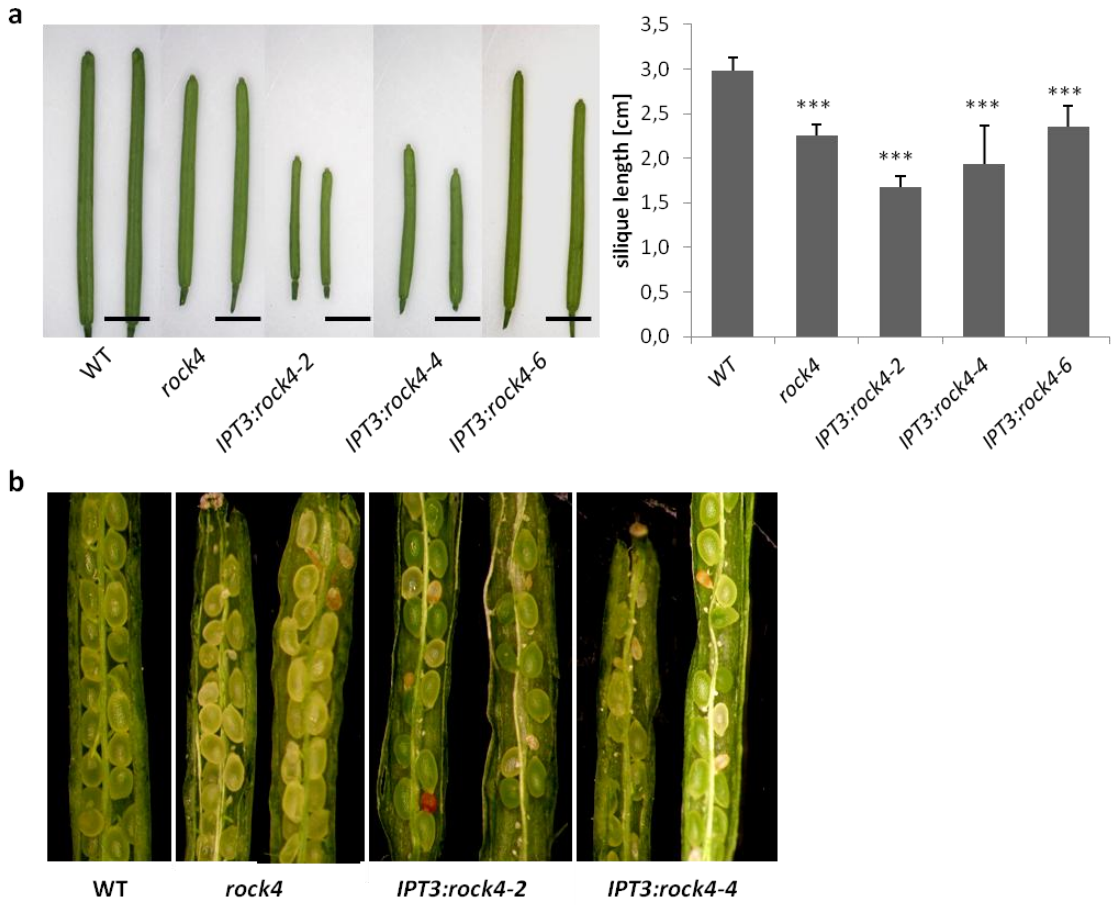

Fig. 30: The *rock4* mutation in the *IPT3* gene results in reduced fertility.
(a) Photos of typical fully grown siliques of wild type, *rock4* and transgenic *pIPT3:rock4* mutant lines and mean length of these siliques (n=10). Error bars represent SE. *** = p<0,001 compared to the wild type, as calculated by students t-test. Scale bar: 0.5 mm. **(b)** Pictures show opened siliques of wild type, *rock4* and transgenic *pIPT3:rock4* mutant lines at 10 days after germination. Wild-type fruits are evenly filled with green seeds whereas in *rock4* and *pIPT3:rock4* siliques empty spaces and shrivelled brown seeds can be seen.

Interestingly, analysis of the progeny of heterozygous *pIPT3:rock4* plants showed a normal 3:1 segregation pattern of the T-DNA insertion, indicating that wild-type embryos aborted with the same frequency as transgenic embryos.

To address the question of whether embryogenesis is disturbed in *rock4* plants, developing seeds of wild-type, *rock4* and *pIPT3:rock4* siliques were cleared and inspected at various stages (Fig. 31). All inspected wild-type siliques contained similar sized seeds per silique and embryogenesis was highly synchronised. *rock4* and transgenic *pIPT3:rock4* mutant plants showed similar defects as described for the *rock2* mutant lines (see chapter 3.1.5.8), such as unfertilized ovules, embryos developing in an asynchronous manner and seed abortion occurring at different time points.

Figure 31a shows cleared *rock4* seeds of the eighth silique from the top of the inflorescence, which equals 6-7 days after pollination. Most embryos had reached the heart stage like the wild type, but some seeds still contained embryos in the globular stage (right side), even though seed size was the same. Approximately two days later, in the 10th siliques, embryo development ranged from early heart to late torpedo stages in *rock4* siliques (Fig. 31b). At this time point some seeds were shrunken and embryos aborted (right side). In some cases globular to heart shaped embryos could still be found in collapsed seeds (second from the right).

Figure 31c shows wild-type and *rock4* seeds of the 11th silique from the top of the inflorescence. *Rock4 e*mbryo developmental stages ranged from torpedo stage to almost full-sized embryos. A few days later in development, in silique number 14, only fully sized embryos, similar to wild-type embryos, were found in *rock4* plants (Fig. 31d). Obviously all slowly developing embryos aborted at some earlier time point.

The transgenic *rock4* line *pIPT3:rock4-2* showed even stronger defects in silique and seed development than *rock4* (Fig. 31). For this reason, embryo development was also inspected in this line. Figures 31e and 31f show cleared seeds of the 11th and 14th silique, respectively. As expected, embryo development was even more severely disturbed in this line compared to *rock4*. In silique number 11, the biggest *pIPT:rock4* embryos were almost full-sized and normal looking, but several seeds contained embryos which were strongly delayed in development, ranging from globular to late torpedo stage embryos. All the seeds were approximately the same size. Shrunken and collapsed seeds were also found. Figure 31e (left side) shows a collapsing seed which contains an embryo at globular stage.

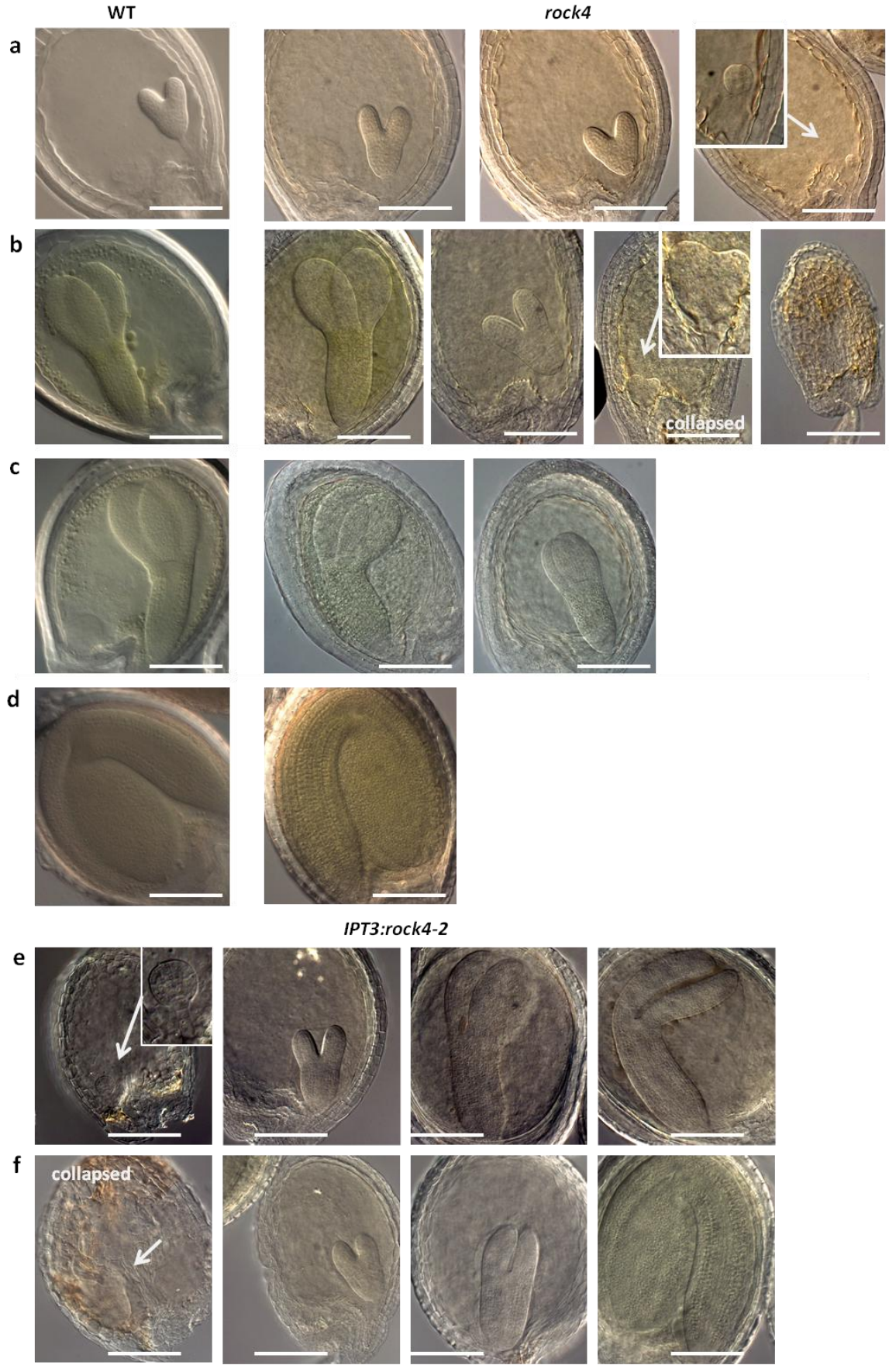

Fig. 31: The *rock4* allele causes unsynchronised embryo development and seed abortion.

Fig. 31. continued.
(a-d) Photos show developing wild-type (WT) and *rock4* seeds at different time points after pollination. **(a)** Cleared WT and *rock4* seeds from the eighth silique from the top of the inflorescence. Developmental stages of *rock4* embryos reach from early globular to heart stage. **(b)** Seeds from 10th silique. *Rock4* siliques contain embryos from early heart to late torpedo stage. The two photos on the right side show collapsed and shrivelled seeds. In one seed sack a heart shaped embryo can still be seen. **(c)** Seeds from 11th silique. *Rock4* siliques contain embryos from torpedo to late torpedo stage. **(d)** Only embryos of one size were found in silique number 14. **(e-f)** Photos show developing seeds of transgenic *pIPT3:rock4-2* plants. **(e)** Seeds from 11th silique contain embryos from globular to late torpedo stage. **(f)** In silique number 14 embryo development stages range from heart stage to fully grown embryos. Arrow marks a heart shaped embryo in a collapsing seed. Scale bars: 100µm.

Different to the results found for *rock4* seed development, not all the seeds containing slowly developing embryos had aborted earlier than silique 14. At this point *pIPT3:rock4* siliques still contained embryos of different developmental stages ranging from early heart to fully grown embryos (Fig. 31f), even though abortion of the strongly delayed embryos must have occurred eventually, as later on, only few normal sized seeds remain per silique which germinate normally and produce normal looking seedlings.

Taken together, unfertilized ovules, delayed seed development, and embryonic lethality could be observed in *rock4* and *pIPT3:rock4* siliques. This is consistent with the results found for *rock2* mutants (chapter 3.1.5.8), further supporting the assumption that cytokinin plays a role in seed and embryo development.

3.2.3.5 The root phenotype of rock4 plants

In the *CKX1* overexpressing background, the *rock4* mutation caused a strongly reduced root formation, indicating an enhanced cytokinin status in the roots as well (chapter 3.2.1). To address the question of whether the same is true in wild-type background, a root growth assay was performed with *rock4* in the wild-type background, and primary root growth and lateral root formation were inspected in *rock4* mutants and compared to wild-type roots. The negative role of CK on the lateral root formation was previously documented (Li et al. 2006; Riefler et al. 2006; Werner et al. 2003). As expected, the *rock4* mutation inhibited root growth and the formation of lateral roots. *rock4* seedlings grown for 16 days under in vitro conditions developed 40% shorter primary roots and the average number of initiated lateral roots in wild-type plants was two to three times greater than that of the *rock4* plants (Fig. 32). This shows that cytokinin produced by the truncated version of IPT3 also functions in roots.

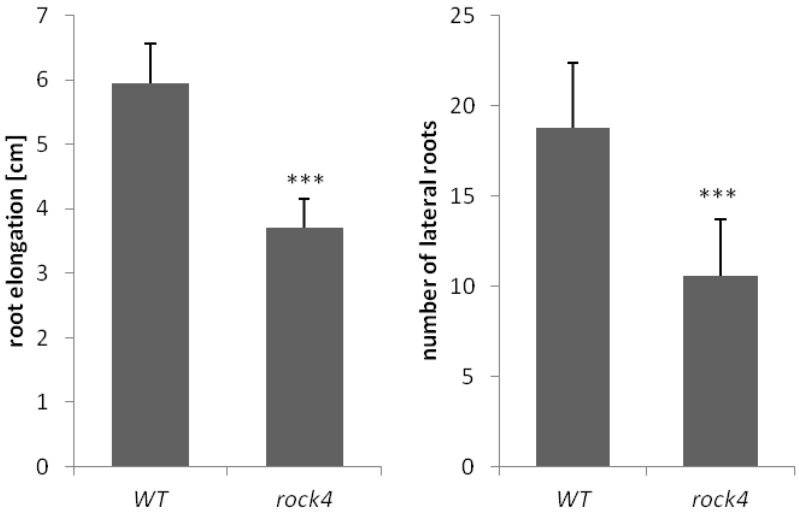

Fig. 32: The *rock4* mutant forms a reduced root system.
Primary root elongation within eight days and emergence of lateral roots within 15 days of wild-type and *rock4* seedlings grown on vertical plates on standard Ats medium (n=20). Error bars represent SE. *** = p<0,001 compared to the wild type, as calculated by students t-test.

4 Discussion

4.1 The *rock2* and *rock3* mutations cause the formation of constitutively active cytokinin receptors

The *rock2* and *rock3* mutant alleles were identified as missense mutations in the *AHK2* and *AHK3* cytokinin receptor genes. Because the point mutations led to a reversion of the cytokinin deficiency phenotype of *CKX1* overexpressing plants, it was concluded that the mutations *rock2* and *rock3* cause gain-of-function variants of the cytokinin receptors AHK2 and AHK3, respectively. There are several possibilities that could cause an increased cytokinin output signal. It is possible that the mutations cause a higher binding affinity towards the remaining cytokinin and can therefore compensate for the lower cytokinin concentrations. This is especially a possibility for *rock3,* as the mutation is in the predicted cytokinin binding domain (Anantharaman and Aravind 2001). Another possibility is a conformational change of the receptors causing constitutively active cytokinin receptors. Different tests were carried out to distinguish these possibilities.

As described in Inoue et al. (2001), an *in vitro* kinase assay was used to test if the kinase activity of the new receptor variants is basically independent of cytokinin binding and therefore proving that the receptors are constitutively active. The test is based on the lethality of the yeast strain *Δsln1* in the absence of an active histidine kinase. Suppression of the lethality of *Δsln1* represents histidine kinase activity of the introduced gene product. Mähönen et al. (2006) published that the *Δsln1* yeast strain, carrying either *AHK2* or *AHK3,* grew in the absence of cytokinins, but growth was faster in the presence of cytokinin. Unfortunately, these results could not be repeated, as the *Δsln1* yeast strain carrying either the *AHK2* or *AHK3* gene, showed no differences in growth in media with or without cytokinins (Supplemental Data Fig. 33). Hence, the receptors AHK2 and AHK3 exhibited kinase activity in the absence of cytokinins when expressed in the yeast strain *Δsln1*, which made this test unsuitable to test for constitutive activity of receptors, at least in the case of AHK2 and AHK3. As expected, there was no further increase in growth in the yeast carrying either *rock2* or *rock3,* when compared to the yeast carrying *AHK2* or *AHK3*, neither in media with cytokinin nor in media without cytokinin (Supplemental Data Fig. 33). The different results compared to the results published by Mähönen et al. (2006) could be explained by slightly different growth conditions, even though the experiments were carried out as described in Mähönen et al. (2006).

The three cytokinin receptors, AHK2, AHK3, and AHK4, show a high degree of sequence identity (Heyl et al. 2007; Inoue et al. 2001; Spichal et al. 2004), and the amino acids mutated in *rock2* and *rock3* are conserved in all three receptors (Fig. 7). The mutations *rock2* and *rock3* were introduced into

AHK4 and then an *in vitro* kinase assay was carried out with these constructs instead. When no cytokinin is added to the media, the cytokinin receptor AHK4 is not active, and the yeast strain *Δsln1* is lethal (Mähönen et al. 2006). However, expression of either *AHK4rock2* or *AHK4rock3* suppressed the lethality of *Δsln1* in the absence of cytokinin, suggesting that the *rock2* and *rock3* point mutations cause constitutively active versions of the AHK4 cytokinin receptor (Fig. 7).

A live cell-based assay, using transgenic bacteria expressing the cytokinin receptor AHK4 or its mutated versions AHK4rock2 or AHK4rock3 was used to test the binding affinity towards the tritium-labelled cytokinin *trans*-zeatin. It could be shown that *E. coli* expressing the cytokinin receptor AHK4 or its mutated versions AHK4rock2 or AHK4rock3, showed no differences in specific binding of *trans*-zeatin, further supporting the assumption that the gain-of-function variants of the cytokinin receptors are caused by constitutive receptor activity rather than increased cytokinin binding affinities (Fig. 7).

Receptor activity is most likely caused by conformational changes due to ligand binding, which would result in the propagation of the cytokinin signal across the membrane and consequently modulate the cytoplasmic His-kinase activity. The *rock2* and *rock3* mutations might cause a conformational change comparable to that caused by cytokinin binding, and therefore render the receptor constitutively active, independent of cytokinin. This hypothesis is supported by work of Miwa et al. (2007). They could show, by introducing the *wol* mutation (Mähönen et al. 2000) into a constitutively active AHK4 receptor, that in the presence of a constitutive mutation, the cytokinin-binding capacity of the receptor plays no role in signal transduction.

From the fact that the *rock2* and *rock3* mutations do not change binding affinities but rather turn the AHK4 receptor constitutively active, one might infer that the same is true for the AHK2 and AHK3 receptors. This hypothesis is further supported by the work of Miwa et al. (2007), who identified a set of AHK4 mutants with constitutive cytokinin independent His-kinase activity in an *E. coli* and a yeast assay. Similar to the *rock2* and *rock3* point mutations, the amino acid substitutions that rendered AHK4 constitutively active are conserved in the three known cytokinin receptors (AHK2, AHK3 and AHK4), and it could be shown that the analogous amino acid substitutions rendered the homologous AHK2 and AHK3 mutants constitutively active as well. However, it should be mentioned that in this case, all tested amino acid substitutions were located within the second membrane-spanning segment, or within the region around the phosphorylated histidine site (Miwa 2007), whereas the *rock3* mutation is located in the CHASE domain. Besides, functional specificity was shown for the AHK3 CHASE domain (Stolz et al. 2011). AHK3 developed a relatively lower affinity to iP in comparison with *t*Z, whereas AHK2 and AHK4 bind iP and *t*Z with similar affinity (Romanov et al. 2006; Stolz et al. 2011). Furthermore, AHK4 could not functionally replace AHK3 in a promoter swap

experiment, possibly because of a specific function of the AHK3 extracytosolic CHASE domain (Stolz et al. 2011). Therefore, conclusions which were arrived at with AHK4 should be only carefully reassigned to AHK3.

So far research on the cytokinin receptor CHASE domain concentrated mainly on amino acid residues that participate in the interaction with cytokinins, and substitution of these residues typically resulted in a loss of hormone-binding capacity and therefore receptor inactivation (Heyl et al. 2007). Recently, the CHASE domain of the AHK4 receptor was successfully expressed and crystallised by Hothorn et al. (2011). This allowed determining the structure of the ligand-binding CHASE domain in complex with cytokinins. According to the data obtained, the N-terminus of the CHASE domain folds into a long α-helix followed by two Per-ARNT-Sim (PAS) domains connected by helical linkers. For cytokinin recognition, AHK4 uses the membrane-distal PAS domain, which is in accordance with mutagenesis and binding studies published by Heyl et al. (2007). The cytokinin-binding site is formed by the β-sheets of the PAS domain and is lined by small hydrophobic amino acid residues. Substitutions of these residues with bulkier amino acids most likely restricts the size of the binding pocket and blocks cytokinin binding, thus inactivating the receptor (Heyl et al. 2007; Hothorn et al. 2011).

The presence of a signal alters the molecular affinity of one part of a protein or domain for another through a change in structure and dynamics. In receptors with PAS domains, signals originate within the conserved core and generate structural and dynamic changes predominantly within the β-sheet, from which they propagate via amphipathic α-helical and/or coiled-coil linkers to the effector domains (Möglich et al. 2009). In general, transmembrane domains play a key role in transmitting the signal from the sensor to the kinase domain (Chervitz and Falke 1996; Ottemann et al. 1999). It would be interesting to find out what impact the *rock2* and *rock3* gain-of-function mutations have on the structures of the CHASE domain and the transmembrane domain, respectively, to shed light into the mechanism which turns the receptor constitutively active.

4.2 The mutations *rock2* and *rock3* cause pleiotropic phenotypes

The constitutively active versions of the cytokinin receptors AHK2 and AHK3 caused pleiotropic phenotypes. In the following chapters, the phenotypes of the *rock2*, *rock3* mutants in the *CKX1ox* and wild-type background will be discussed in the context of known mutants and pathways. The phenotypes that are caused by the *rock4* mutation will be discussed afterwards in chapter 4.4. For an overview, the phenotypes of *rock2*, *rock3,* and *rock4* mutants that are described and discussed in this thesis are listed in Table 1.

Table 4: Summary of the phenotypes caused by the mutations *rock2*, *rock3,* and *rock4*.

Phenotypes	**changes compared to the wild type**		
	rock2	***rock3***	***rock4***
cotyledon size	increased	increased	unchanged
rosette leaf size	increased	increased	unchanged
stem diameter	increased	increased	increased
flower size	increased	increased	unchanged
gynoecia size	increased	increased	unchanged
seed size	unchanged	unchanged	unchanged
shoot height	increased	increased for transgenic lines	slightly increased
number of siliques per plant	increased	increased for transgenic lines	not checked
silique length	reduced	unchanged	reduced
number of seeds per silique	reduced	unchanged	reduced
embryo development	disturbed	unchanged	disturbed
seed yield	reduced	increased for transgenic lines	reduced
number of rosette leafs	reduced	reduced for transgenic lines	unchanged
flowering time	earlier	slightly earlier	unchanged
flower plastochron	shorter	shorter in transgenic lines	not checked
length of life cycle	prolonged	prolonged	prolonged
duration of flowering	prolonged	prolonged	prolonged
senescence	slightly delayed	delayed	delayed
primary root length	reduced	reduced	reduced
lateral bud outgrowth	reduced	reduced	reduced

4.2.1 Phenotypes in the *CKX1ox*-background

Cytokinin deficiency results in the diminished activity of the vegetative and floral shoot apical meristems and enhances activity of the root meristems, which causes stunted shoots with less flowers, reduced apical dominance, small rosette leaves, and an enhanced root system (Galuszka et al. 2004; Werner et al. 2003; Werner et al. 2001). Phenotypic characterization of the *rock2* and *rock3* mutants in a *CKX1* overexpressing background revealed that the gain-of-function versions of AHK2 and AHK3 can compensate for the reduced cytokinin levels to a great extent Fig. 1 1 and Fig. 2), which is an indication for the functional importance of the different cytokinin receptors at specific developmental processes. It should be considered however, that gain-of-function mutations

sometimes lead to false-positive phenotypes, because of which changes in phenotypes should be interpreted carefully and are no direct prove for a role of the mutated gene in the respective processes.

In the cases of rosette diameter, fresh weight and shoot height (Fig. 1), the suppression of the cytokinin-deficient phenotype was not complete compared to the wild type. Presumably, the other non-mutated cytokinin receptors also play important roles in these developmental processes and therefore a constitutively active version of either AHK2 or AHK3 is not enough to completely overcome the effects caused by decreased cytokinin levels in *Arabidopsis* plants.

Interestingly, in some cases, the *rock2* and *rock3* mutations caused specific cytokinin related gain-of-function phenotypes already in the *CKX1* overexpressing background; for example, *rock2 CKX1ox* and *rock3 CKX1ox* mutants developed bigger flowers, grew shorter hypocotyls in the dark and delayed senescence in a detached leaf assay even when compared to wild-type plants (Fig. 1 and Fig. 2). The strong gain-of-function phenotypes indicate an important function for the cytokinin receptors AHK2 and AHK3 in the respective organs and developmental programmes. Other phenotypical characterizations hinted at the different levels of contribution, AHK2 and AHK3 have in specific parts of plant development. *Rock2* seems to have a more important role in the regulation of shoot height, which includes the production of more siliques and the onset of flowering (Fig. 1 and Fig. 2). *Rock3* on the other hand seems to play a far more important role in the delay of senescence (Fig. 2). In the case of AHK3, its important role in delaying leaf senescence was already described by Kim et al. (2006). Consistent with these results, *rock3* mutants play a more dominant role in delaying leaf senescence compared to *rock2* plants. Nevertheless, as *rock2* plants showed slightly delayed leaf senescence as well, it seems that AHK2 has a minor role in delaying leaf senescence. These results are consistent with the results achieved by Riefler et al. (2006), who revealed, next to the major role of AHK3, a role of AHK2 in mediating cytokinin-dependent chlorophyll retention in leaves, using single, double, and triple cytokinin receptor mutants.

Interestingly, the characterization of *rock2 CKX1ox* and *rock3 CKX1ox* mutants also revealed a so far unknown function of the cytokinin receptors AHK2 and AHK3 in cotyledon expansion, as *rock2 CKX1ox* and *rock3 CKX1ox* seedlings had remarkably bigger cotyledons (Fig. 1 and Bartrina et al. 2006).

All of these phenotypes also occurred in the wild-type background and were further investigated.

4.2.2 Phenotypes of *rock2* and *rock3* mutants in the wild-type background

The phenotypic characterizations of the *rock2* and *rock3* mutants were expected to yield information about the processes which are regulated by the cytokinin receptors AHK2 and AHK3, as well as giving an insight into the effects caused by an enhanced cytokinin status. It should be noted that the function of cytokinins was mainly studied on plants with a reduced cytokinin status, which was achieved by constitutive overexpression of *CKX* genes (Matsumoto-Kitano et al. 2008; Werner et al. 2008; Werner et al. 2003; Yang et al. 2003), reduction of cytokinin biosynthesis (Kuroha et al. 2009; Miyawaki et al. 2006), a disrupted downstream cytokinin signalling pathway (Argyros et al. 2008; Heyl et al. 2008; Ishida et al. 2008; Mason et al. 2005), or loss-of-function mutation of cytokinin receptor genes (Higuchi et al. 2004; Nishimura et al. 2004; Riefler et al. 2006). Nevertheless, studies on plants with an enhanced cytokinin status led to additional insights into the functions of the cytokinin hormone as well; for example, studies on a gain-of-function version of AHK3 revealed the importance of the cytokinin receptor in delaying leaf senescence (Kim et al. 2006) and expression of *IPT* genes under the control of the senescence-induced *pSAG12*-promoter or the stress-induced *pSARK*-promoter delayed plant senescence in tobacco, maize, rice, lettuce, and tomatoes (Gan and Amasino 1995; Ma and Liu 2009; McCabe et al. 2001; Peleg et al. 2011; Rivero et al. 2007; Robson et al. 2004). Bartrina et al. (2011) could show that CKX enzymes play a role in regulating inflorescence and floral meristem size, as the mutation of the *CKX3* gene in combination with other *CKX* genes, leads to the formation of a larger reproductive meristem. Furthermore, mutations in a type-A response regulator cause an enlarged meristem in maize (Giulini et al. 2004) and gain-of-function type-B ARR mutants exhibit hyperactive meristems causing ectopic shoot formation and unusual proliferation of tissues (Imamura et al. 2003; Sakai et al. 2001; Tajima et al. 2004).

4.2.2.1 The rock2 *and* rock3 *mutants exhibit enlarged organs*

An interesting phenotype of the *rock2* and *rock3* mutants was an enlargement of lateral organs. Cotyledons, rosette leaves, flower petals, gynoecia, and inflorescence stems were enlarged relative to wild-type organs (Fig. 10, Fig. 12 and Fig. 13). These results indicate a role for cytokinin in regulating shoot organ size during vegetative as well as reproductive development.

It has been known for a long time that cytokinin plays a major role in regulating meristem function (Mok and Mok 2001; Werner and Schmülling 2009). Studies on plants with lowered cytokinin status have shown that cytokinin positively regulates the size and proliferative activity of the shoot apical meristem (Higuchi et al. 2004; Miyawaki et al. 2004; Nishimura et al. 2004; Werner et al. 2003). *ahk2 ahk3 ahk4* triple mutants show a dramatic reduction in meristem size, as well as impaired leaf development (Higuchi et al. 2004; Nishimura et al. 2004; Riefler et al. 2006). Similar defects were

observed in *Arabidopsis* quadruple and quintuple *ipt* mutants and triple *log* mutants (Kuroha et al. 2009; Miyawaki et al. 2006). A drastic reduction of endogenous cytokinins in shoot meristems results in a strong decrease in meristem size and organ primordia formation, giving direct evidence for the requirement of cytokinin for proliferative shoot apical meristem activity (Werner et al. 2003; Werner et al. 2001). Furthermore, overexpression of a constitutively active type-A ARR ($ARR7^{D85E}$) causes meristem arrest, suggesting that type-A ARRs negatively regulate meristem function by phospho-dependent interactions (Leibfried et al. 2005). By contrast, increased cytokinin production either in the *altered meristem program1* (*amp1*) mutant or by *IPT* overexpression is associated with the formation of larger vegetative meristems (Chaudhury et al. 1993; Rupp et al. 1999). Similarly, mutation in *ABERRANT PHYLLOTAXY1* (*ABPH1*), encoding a type-A ARR in maize, leads to a significantly larger shoot apical meristem size (Giulini et al. 2004).

Rosette leaves

The increase in sizes of the lateral organs in *rock2* and *rock3* mutants indicates an increased activity of the shoot apical meristem. The growth and final size of shoot organs are determined by the extent of cell proliferation during early organ development and the subsequent cell expansion phase, during which cells expand to appropriate sizes (Anastasiou and Lenhard 2007; Donnelly et al. 1999; Mizukami 2001). In the current model, cytokinin retards cellular differentiation of meristematic cells in the shoot, resulting in an increased organ cell number (Bartrina et al. 2011; Holst et al. 2011).

Consistent with these results, analysis of the epidermis cell number and the cell area of mature rosette leaves of *rock2* plants, revealed that changes in organ size are due to an increase in the numbers of normal sized cells (Fig. 11); demonstrating that an increased cytokinin status results in an increase in cell division. The fact that organs of the *rock* mutants grow even larger than those of wild-type plants, indicates that cytokinins are not only required for growth, but that their level in wild type is a limiting factor in organ size.

Inflorescence meristem activity

In addition to the primary SAM, cytokinin levels also regulate the size of the inflorescence meristems, as indicated by smaller inflorescences with less flowers in plants with a lowered cytokinin status (Holst et al. 2011; Nishimura et al. 2004; Riefler et al. 2006; Werner et al. 2003). Furthermore, increased cytokinin levels in *Arabidopsis ckx3 ckx5* double mutants lead to larger inflorescence meristems due to an increased number of cells, and an increased number of flowers (Bartrina et al. 2011).

Consistent with these results, the increased cytokinin status of *rock2* and *rock3* plants results in enhanced inflorescence growth and development of an increased number of flowers, indicating increased activity of the inflorescence meristems (Fig. 14 and Fig. 16). Inflorescences of *rock2*,

pAHK2:rock2 and *pAHK3:rock3* transgenic plants grew faster compared to the wild type, resulting in a significant increase in shoot height. Furthermore, the formation of floral buds was enhanced, resulting in significantly more siliques per plant. In *Arabidopsis ckx3 ckx5* double mutants, increased flower formation was due to an enlarged inflorescence meristem, producing more flower primordia than the wild type (Bartrina et al. 2011). It can be speculated that the same is true for *rock2* and *rock3* mutants, as these mutants also show a shorter flower plastochron (Supplemental data Fig. 35). However, the size of the inflorescence meristems was not further investigated.

Interestingly, in the case of *rock3*, only the transgenic *pAHK3:rock3* mutants showed increased shoot growth and produced more flowers, whereas the *rock3* mutant, originated from the EMS mutagenesis, grew similar to wild type (Fig. 14). It is possible that the AHK3 cytokinin receptor plays no major role in regulating inflorescence growth and floral primordia initiation if expressed at wild-type levels, as is expected with the *rock3* mutant. Therefore, even the constitutively active *rock3* version of the AHK3 receptor may not cause a strong phenotype. The *AHK3* promoter, used in transgenic *pAHK3:rock3* mutants, is expected to be more active than the wild-type *AHK3* promoter, which might cause a stronger phenotype. It is also possible that the expression patterns are changed in the transgenic lines, causing AHK3 to function in cells where it is usually not expressed.

It would be interesting to investigate the *AHK2* and *AHK3* expression pattern in the inflorescence meristem. Cytokinin receptor availability and concentration in specific domains hints at the relevance of the receptors in these domains, and might show overlaps with known regulators for meristem size and activity, like WUS, CLV1, CLV3 or STM. Unfortunately, RNA localisation by *in situ* hybridization of AHK2 or AHK3 transcripts failed.

Gordon et al. (2009) could show that the expression of the cytokinin receptor gene *AHK4* and the meristem regulator gene *WUS* overlapped in the shoot apical and floral meristems, and that expression of *WUS* requires a locally increased cytokinin perception capability in the WUS domain. In addition, an enlarged WUS domain was induced by increased cytokinin concentrations in the *ckx3 ckx5* double mutant (Bartrina et al., 2011). Interestingly, while AHK2 and AHK4 play a major role in regulating *WUS* expression, AHK3 does not (Gordon et al. 2009). For *AHK2,* it can be speculated that it is also expressed in the WUS domain similar to *AHK4* and that the constitutively active *rock2* version of the AHK2 receptor mimics for high cytokinin concentrations in the WUS domain, resulting in an increase in *WUS* expression, and therefore an increase in meristem activity and probably also meristem size.

AHK3 does not seem to act via WUS (Gordon et al. 2009). Nevertheless, a role for AHK3 in regulating shoot growth is apparent from mutant analysis. The shoot phenotypes of single, double and triple receptor mutants of *Arabidopsis* indicate that each of the receptors has a function in maintaining

normal shoot growth. Either AHK2 or AHK3 alone are sufficient to maintain normal shoot development but *ahk2 ahk3* double mutants showed reduced shoot growth with smaller leaves and a reduced number of progeny, indicating a joint and partly redundant a role for AHK2 and AHK3 in the regulation of the activity of the inflorescence meristems (Higuchi et al. 2004; Nishimura et al. 2004; Riefler et al. 2006).

Apart from the WUS/CLV circuit, other factors are important for meristem function. For example, STM, which is required to maintain meristem cells in the undifferentiated state and for cell division in the peripheral zone (Endrizzi et al. 1996; Long et al. 1996). An enhanced cytokinin status caused by a constitutively active AHK2 or AHK3 cytokinin receptor may enhance *STM* expression and thus increase meristem activity.

Furthermore, the inflorescence meristems stayed in an active state for a longer time, as the length of the reproductive phase of the *rock2* and *rock3* mutants was significantly increased compared to the wild type, indicating that cytokinin plays a role in the endurance of the activity of the inflorescence meristems (Fig. 14). However, it is unclear if this effect is direct or indirect, as cytokinin receptors regulate multiple aspects of plant growth and development, which makes it hard to discriminate the direct and indirect effects that mutations might have on late phenotypic traits. For example it is possible that the prolonged activity of the inflorescence meristems is a consequence of either a retarded leaf senescence or an increase in shoot sink strength (Gan and Amasino 1995; Werner et al. 2008), rather than from any direct effects of the cytokinin receptors AHK2 or AHK3 on inflorescence meristem activity. Gan and Amasino (1995) could show that the expression of a cytokinin biosynthesis *IPT* gene under the control of the senescence induced *SAG12* promoter, results in the suppression of leaf senescence in tobacco, and transgenic plants continued to grow and produce flowers for a longer time period than wild-type control plants, resulting in an increased dry weight and seed yield. These studies indicate that a prolonged photosynthetic lifespan of leaves is likely to delay the termination of reproductive inflorescences, and therefore increase the length of the reproductive phase. It should be noted however, that no such effects were described for other cytokinin mutants delaying senescence in *Arabidopsis* or tobacco plants (Kim et al. 2006; Ma and Liu 2009; Rivero et al. 2007).

In the case of *rock2*, the prolonged reproductive phase may also be caused by a reduced fertility. *Arabidopsis* inflorescence meristems undergo proliferative arrest after a predictable number of fruit has been produced (Bleecker and Patterson 1997). Examination of sterile mutants and the removal of their bolts have shown that, when the plants do not produce seeds, they produce more bolts and flowers, supposedly caused by their repeated attempts to produce seeds (Bleecker and Patterson 1997; Hensel et al. 1994). Sterile and even reduced-fertility plants did not undergo proliferative

arrest, but inflorescence meristems continued to proliferate and produce flowers, although not indefinitely (Hensel et al., 1994). Inflorescences of sterile plants did not arrest with a terminal cluster of arrested buds as seen in wild type, but terminated in fully developed structures, e.g. unfused carpel-like structures at the apex of each branch (Hensel et al., 1994). Interestingly, similar terminal structures were also occasionally observed in transgenic *pAHK2:rock2* plants (Fig. 19).

So far, only a few genes are known to play a role in regulating reproductive inflorescence meristem arrest. Melzer et al. (2008) showed that the proteins FLOWERING LOCUS T (FT), *SUPPRESSOR OF OVEREXPRESSION OF CO1* (*SOC1*) and FRUITFULL (FUL) not only control flowering time, but also affect determinacy of all meristems. The modulation of the activities of these genes had a clear effect on indeterminacy of meristems and longevity of the plants. For example, combination of the *ft* and *ful* mutations led to an exaggerated indeterminacy of the apical meristem, with plants reaching a height of up to 1 m (Melzer et al. 2008). As cytokinin is known to function in meristems and control flowering genes like TWIN SISTER OF FT (*TSF)* and *SOC1* (Bonhomme et al. 2000; D'Aloia et al. 2011), it might well be that cytokinin receptors also have a direct role in the proliferative arrest of inflorescences at the end of a plant's life cycle, maybe together with FT, SOC1 or FUL.

Radial stem growth and cambium activity

Cytokinin has been shown to positively regulate primary and secondary vascular development and cell proliferation activity in the cambium (Hejatko et al. 2009; Matsumoto-Kitano et al. 2008; Nieminen et al. 2008). Stems of *ahk2*, *ahk3* and *ahk2 ahk3* mutants had a reduced number of cell layers in the procambium, smaller vascular bundles, and the interfascicular cambium was not formed in the *ahk2 ahk3* mutant indicating impairment at the onset of secondary growth (Hejátko et al. 2009). Consistently, Nieminen et al. (2008) could show that reduction of the cytokinin content in the cambium of poplar and birch trees reduced cambial activity. Similarly, mutation of multiple *IPT* genes in *Arabidopsis* caused a complete loss of cambium and reduced thickening of the root and stem (Matsumoto-Kitano et al. 2008). Consistent with these results, comparison of *Arabidopsis* stems revealed an enhanced radial expansion of *rock2* and *rock3* inflorescence stems compared to wild-type stems (Fig. 12).

Transverse sections of the primary inflorescence stem showed that stem morphology was normal in all mutants, but the overall number of cells in transgenic stems was increased compared to wild-type stems, which suggest higher mitotic activity in the cambium (Fig. 12). Transgenic lines expressing *pAHK2:rock2* or *pAHK3:rock3* showed an increased number of lignified cells by up to 70% in the interfascicular region. These results indicate that fascicular and interfascicular cambial activity is enhanced when the cytokinin receptors AHK2 or AHK3 are constitutively active. This difference is

most likely due to increased cambial activity, which is known to be affected by cytokinin (Matsumoto-Kitano et al. 2008; Nieminen et al. 2008).

Experiments with *ipt loss-of-function* mutants (Matsumoto-Kitano et al. 2008) strongly suggest that the phenotype is caused by an enhanced activity in the cambial zone, but it is also known that cytokinin regulates the size of the reproductive shoot apical meristem (Bartrina et al. 2011). It is still unclear, if the enhanced stem thickness in *rock2* and *rock3* mutants results from enhanced cell division in the cambial zone, or from a more larger shoot apical meristem or both. Scanning electron micrographs of inflorescence meristems would reveal if the *rock2* and *rock3* mutations lead to a larger inflorescence meristem, but this experiment still has to be done.

Flower size

When compared with wild-type flowers, flowers of the *rock2* and *rock3* mutants were significantly larger (Fig. 13). The increase in petal surface of the *rock2* and *rock3* flowers was due to a larger cell number. Additionally, growth and final size of gynoecia was enhanced. This effect was strongest in transgenic *pAHK2:rock2* mutants and the least pronounced in *rock3* mutants, indicating that AHK2 has a greater role in the regulation of gynoecia expansion.

The phenotype of *rock2* and *rock3* mutant flowers is comparable to mutants lacking cytokinin degrading enzymes (Bartrina et al. 2011). Here it could be shown that a possibly enhanced cytokinin status in the WUS domain of floral meristems, caused by the mutation of the *CKX3* gene in combination with other *CKX* genes, leads to an enlargement of the *WUS* expression domain and therefore, the formation of larger floral meristems (Bartrina et al. 2011). The enlargement of the *WUS* expression domain in the inflorescent meristem of *ckx* mutants suggests that a similar relationship exists between *WUS* and cytokinin in both the vegetative and the reproductive meristems (Bartrina et al. 2011). However, the cytokinin receptors mediating this activity are not yet known. Phenotypic analysis of the *rock2* and *rock3* gain-of-function cytokinin receptor mutants indicates a major role for AHK2 in the cytokinin signalling events controlling the size of the WUS domain and thus, floral meristem size. However, floral meristem size and size of the WUS expression domain have yet to be analyzed. AHK3 seems to have a minor role in regulating flower size. As there seems to exist a similar relationship between *WUS* and cytokinin in the vegetative and the reproductive meristems (Bartrina et al. 2011), the potential role of AHK3 in regulating flower size might be independent of WUS. It would be interesting to detect the specific expression domains of the cytokinin receptors in flowers and flower meristems, which might indicate the specific function of the receptors; unfortunately *in situ* hybridizations of developing flowers failed.

Bossinger and Smyth (1996) could show that floral organs arise from a defined number of meristematic cells. This may also be relevant for regulating gynoecia size, as enhanced cytokinin

activity in the floral meristem caused by the *rock2* and *rock3* mutations may affect the population of cells that are recruited into the gynoecium primordium and thus determine the final gynoecium size. Additionally, a function of cytokinin in regulating ovule formation by the placenta was described by Bartrina et al. (2011). *ckx3 ckx5* mutant gynoecia contained almost twice as many ovules as wild-type gynoecia, indicating an enhanced activity of the mutant placenta tissue, and leading to a higher density of seeds within the carpels. The same is probably true for *rock2* mutants, as preliminary data revealed an increased number of ovules in young gynoecia (data not shown); however, most seeds abort during embryo development and only a few seeds remain per silique at the end of embryo development (Fig. 17). Nevertheless, it may be speculated, that the cytokinin receptor AHK2 is involved in regulating the activity of meristematic cells in the placenta and thus influences ovule primordia formation.

In contrast, the cytokinin receptor AHK3 receptor does not seem to effect ovule formation, as *rock3* gynoecia form as many seeds per silique as wild-type (Fig. 16).

4.2.2.2 Mainly the rock2 *mutants show an early flowering phenotype*

The *rock2* mutants flowered significantly earlier than wild-type *Arabidopsis* plants. Earlier flowering was developmentally regulated, as less leaves had formed at the onset of flowering. In the case of *rock3*, only the transgenic lines *pAHK3:rock3* flowered slightly earlier than the wild type, whereas *rock3* flowered at the same time as wild type (Fig. 14). This is in agreement with the results shown for the *rock2* and *rock3* mutants in the *CKX1* overexpressing background (Fig. 2). Under long day conditions, *rock2* suppressed the delayed flowering phenotype of *CKX1ox* plants completely and flowered even a few days earlier than wild type, whereas *rock3 CKX1ox* plants flowered only slightly earlier than *CKX1ox* plants and still a few days later than wild type. Furthermore, only *rock2* plants rescued the flowering phenotype of *CKX1ox* plants under short day conditions. These results indicate a more pronounced role of AHK2 in the regulation of flowering under long and short day conditions.

The early flowering phenotype of the *rock2* and *rock3* mutants is in agreement with previous studies, which suggest cytokinins stimulate the transition from vegetative growth to flowering in *Arabidopsis.* In plants with a lowered cytokinin content, flowering was retarded (Werner et al. 2003), whereas an increase in the levels of cytokinin, either by application of cytokinin or simultaneous mutation of several *CKX* genes, caused early flowering; at least under short day conditions (Bartrina 2006; D'Aloia et al. 2011). In addition, high endogenous levels of cytokinins either in the *amp1* mutant or after various chemical treatments was found to correlate with early flowering in *Arabidopsis* (Chaudhury et al. 1993; He and Loh 2002). Cytokinin content increases in the SAM, leaves, and phloem sap in

response to one single long day in *Arabidopsis* and in *Sinapis alba* (Corbesier et al. 2003; Lejeune et al. 1994), suggesting that cytokinins might be involved in flowering as systemic signals.

Interestingly, the rate of leaf formation and flowering time was not altered in *ahk* single and double mutants (Riefler et al., 2006), indicating either redundancy or no function in the transition to flowering. Only the *ahk2 ahk3 ahk4* triple mutant showed retarded flower induction, but because of an overall strong reduction of shoot development, it is hard to discriminate the direct and indirect effects that the mutations in the cytokinin receptors have on flowering.

Recently, cytokinins could be integrated into the current knowledge of genetically defined molecular pathways to flowering. D'Aloia et al. (2011) could show that treatment of the synthetic cytokinin BAP to roots promotes flowering in short days, and that this occurs independently of FT, through transcriptional activation of TSF in leaves, which then moves to the meristem and induces the activation of *SOC1* transcription. Based on this knowledge, it would be interesting to find out, if critical flowering-time genes like *TSF*, *FT,* and *SOC1* are upregulated in *rock2* and *rock3* plants. Activation of *SOC1* is currently viewed as the earliest critical event caused in the SAM by photoperiodic floral induction (Giakountis and Coupland 2008; Jang et al. 2009; Lee and Lee 2010).

Interestingly, cytokinins in the SAM also seem to have a function in the control of flowering time, as the export of cytokinins out of the leaves increased, and enrichment of active cytokinins in the SAM was observed upon photoperiodic induction of flowering by a long day in *Arabidopsis* and *Sinapis* plants. This enrichment of cytokinins correlates well with the early events of floral transition (Corbesier et al. 2003; Jacqmard et al. 2002). Furthermore, exogenous cytokinin applied on the shoot apex of *Sinapis* plants induced the *SaSOC1* gene (Bonhomme et al. 2000), and it cannot be excluded that root-produced cytokinin upregulates *SOC1* in the SAM also independently of TSF (D'Aloia et al. 2011).

In *Sinapis,* the initial activation of *SaSOC1* by cytokinin occurred in the organizing centre of the SAM (Bernier 2011). The cytokinin receptor AHK4 was found to be expressed highly in the same area of the SAM, where it is involved in the maintenance of the SAM via positive feedback loops with the meristem regulator WUSCHEL (WUS) (Gordon et al. 2009; Leibfried et al. 2005). The expression domains of the cytokinin receptors AHK2 and AHK3 within the SAM are still unknown, but interestingly, cytokinin-induced upregulation of *WUS* transcript in the SAM is mediated primarily through AHK2 and AHK4 dependent pathways and does not require the AHK3 receptor (Gordon et al. 2009). It is quite possible that the initial activation of *SOC1* in the SAM at floral transition is linked to the cytokinin/WUS circuit. This could be a reason why the *rock2* mutation, which causes a constitutively active AHK2 receptor, causes a stronger flowering phenotype than the *rock3* mutation in the AHK3 receptor. The constitutively active AHK2 receptor might mimic high cytokinin levels in

the organizing centre of the SAM, which might result in an increased *WUS* and *SOC1* expression. As AHK3 does not seem to have a function in the cytokinin/WUS circuit, the *rock3* mutation might not have an effect on *SOC1* expression, at least not in the SAM.

Another possibility for a more pronounced role of AHK2 in the regulation of flowering is its different ligand affinity compared to AHK3. AHK2 shows a higher affinity for iP and *t*Z, whereas AHK3 mainly senses *t*Z-type cytokinins (Romanov et al. 2006; Romanov et al. 2005; Spichal et al. 2004; Stolz et al. 2011). It was found that only isopentenyl adenosines induce flowering (He and Loh 2002), and the level of iP-type cytokinins increase in leaf tissue and leaf exudate after induction of flowering by one long day (Corbesier et al. 2003; Lejeune et al. 1994). Additionally, only iP was increased in SAM tissues after floral induction, while the level of zeatin remained unchanged (Jacqmard et al. 2002). Maybe, rather a constitutively active AHK2 receptor than a constitutively active AHK3 receptor, mimics for increased iP levels in the leaves and/or in the shoot apical meristem, what leads to earlier flowering compared to wild-type plants.

4.2.2.3 The rock2 *mutation causes impaired embryo development*

The *rock2* mutation, but not the *rock3* mutation, caused reduced fertility in *Arabidopsis* plants (Fig. 17). Examination of embryo development revealed retarded embryogenesis, partially malformed embryos and embryo abortion, indicating a role for AHK2, but not AHK3, in the regulation of embryo growth and development (Fig. 18).

So far, not much is known about the role of cytokinin and the cytokinin receptors in embryo development. Nevertheless, a role for cytokinin signalling in embryogenesis was shown by Müller and Sheen (2008). During embryo development, cytokinin signalling components were first detected in the hypophysis, the founder cell of the root meristem at the early (16-cell) globular stage of the embryo (Müller and Sheen 2008; Su et al. 2011). Upon asymmetric cell division of the hypophysis, the resulting basal cell lineage down-regulated cytokinin output, while the apical cell maintained activity. Later during embryogenesis, by the heart stage, a second cytokinin signalling output appeared near the shoot stem-cell primordium.

Furthermore, it could be shown that auxin induced cytokinin response regulators ARR7 and ARR15 are involved in specifying root stem cells (Müller and Sheen, 2008). The *arr7 arr15* double mutants were reported to cause female gamethophytic lethality (Leibfried et al. 2005), but experiments with ethanol-inducible double loss-of-function *arr7 arr15* embryos showed ectopic cytokinin signalling in the basal cell lineage of the embryos after *ARR7* transgene induction, causing irregular cell shapes and numbers, distorted morphology of the embryo root stem-cell system and eventually embryo development arrest (Müller and Sheen, 2008).

Using *in situ* hybridizations, Mähönen et al. (2000) detected the expression domains of the cytokinin receptor gene *AHK4* during embryo development, and revealed the role of AHK4 in embryonic root development. *AHK4* is expressed in the innermost four cells of the embryo at the globular stage. These four progenitor cells of the procambium develop subsequently into the vascular tissue (Mähönen et al. 2000). During the heart, torpedo, and nearly mature stages of embryogenesis, expression was detected in the procambium of the cotyledon shoulders, prospective hypocotyl, and embryonic root, leading to primary root defects in the *wooden leg* (*wol*) mutant (Mähönen et al. 2000). The precise expression domains of the cytokinin receptor genes *AHK2* and *AHK3* during embryo development are still unknown. However, with regard to the embryo defects caused by the expression of the constitutively active version of the AHK2 receptor ROCK2, a role for AHK2 in the regulation of embryo development seems apparent. A constitutively active AHK3 receptor did not cause noticeable embryonic defects, revealing no role or at least no major role for AHK3 in embryo development.

Cytokinins are promoters of cell division in shoot organs and are generally considered to play a role in regulating the balance of cell division in meristems and the recruitment of cells to form lateral organs. Surprisingly, during early embryo development, at the stage at which a high rate of cell division is required, the *rock2* mutant embryos exhibited retarded development, suggesting that the mutant embryos were unable to undergo rapid cell division (Fig. 18). Besides that, the morphology of the *rock2* embryos appeared to be normal up to the heart stage of embryogenesis. After reaching late heart stage, mutant embryos were often swollen looking with thickened cotyledons and stem and a thick short root, suggesting defects in the regulation of cell division in root and shoot.

Supposedly, a constitutively active AHK2 receptor mimics an increased cytokinin level in the AHK2 expression domain of the developing embryo. During early embryo development this causes reduced cell division rates and can later on lead to a distorted shape of the embryo and eventually embryo abortion. As cytokinin usually supports cell division, at least in the apical part of the plant, the observed retarded embryo development was surprising. However, smaller embryos correlate with the finding that embryos with reduced cytokinin content or signalling were bigger compared to wild-type embryos (Heyl et al. 2008; Hutchison et al. 2006; Miyawaki et al. 2006; Riefler et al. 2006; Werner et al. 2003). It is not yet clear whether cytokinin plays a direct role in the regulation of seed size or if other factors, such as a reduced seed set, are involved in producing enlarged embryos. It is therefore possible that AHK2 mediates inhibition of cell division during early embryo development, but retarded embryo development might also be due to secondary effects like disturbed embryo-endosperm communication, or a less optimal nutrient translocation to the developing embryo. In *Arabidopsis* the endosperm has an important role in the control of embryo growth and seed size (Kondou et al. 2008; Olsen 2004). However, in contrast to the embryo, abnormal endosperm

development was not observed and mutant seed size was comparable to wild-type seed size at all stages, suggesting normal endosperm growth.

Misshaped embryos were observed after embryos had reached heart stage, the stage where the first signalling output was detected at the shoot apex using the artificial cytokinin receptor *TCS::LUC* (Müller and Sheen, 2008). It is possible that the AHK2 receptor is only active at the shoot stem-cell primordium from heart stage on, leading to increased cell division and subsequently thicker misshaped embryos. It would be interesting to identify the expression domains of the cytokinin receptors AHK2 and AHK3 in the developing embryo using RNA *in situ* hybridization, as well as investigate the role of the receptors in the context of known pathways, and factors that play a role during embryo development, like auxin or ARR7 and ARR15 (Müller and Sheen, 2008). Furthermore, it would be interesting to test if the cytokinin output is indeed increased, for example, by detecting expression levels of cytokinin response regulators or by using the artificial cytokinin reporter *TCS::LUC* (Müller and Sheen, 2008).

4.2.2.4 The rock2 *and* rock3 *mutations inhibit root growth*

Root growth is ensured by the activity of meristematic cells and elongation of maturing cells. While auxin increases the size of the cell-division zone by promoting cell division (Blilou et al. 2005; Dello Ioio et al. 2007), cytokinin acts as a negative regulator of root meristem size by controlling the rate of meristematic cell differentiation at the root transition zone (Dello Ioio et al. 2007; Kuderová et al. 2008; Moubayidin et al. 2010; Werner et al. 2003), and represses lateral root development by disrupting the organization and development of lateral root primordia (Laplaze et al. 2007; Werner et al. 2003; Werner et al. 2001).

Lowering endogenous cytokinin levels by overexpressing cytokinin degrading CKX enzymes, disruption of cytokinin synthesis genes, or reducing cytokinin responsiveness, leads to an increase in apical root meristem size (Dello Ioio et al. 2007; Werner et al. 2003) and plants with a reduced cytokinin content or cytokinin signalling display a greater number of lateral roots (Hutchison et al. 2006; Mason et al. 2005; Riefler et al. 2006; Tokunaga et al. 2012; Werner et al. 2003). Conversely, exogenously applied cytokinins, or overexpression of the bacterial cytokinin biosynthesis *IPT* gene, were shown to induce a decrease in root meristem size and thus reduces primary root growth (Dello Ioio et al. 2007; Dello Ioio et al. 2012; Kuderová et al. 2008), and were shown to repress lateral root initiation and development in *Arabidopsis* (Kuderová et al. 2008; Laplaze et al. 2007; Li et al. 2006). Consistent with these results, the *rock2* and *rock3* mutants, which comprise constitutively active versions of the cytokinin receptors AHK2 and AHK3, respectively, display short roots and the number of emerged lateral roots was decreased (Fig. 21).

It was shown that cytokinins act specifically at the root transition zone, as only the reduction of endogenous cytokinin levels at the transition zone affected root meristem size (Dello Ioio et al. 2007). Interestingly, cytokinin receptor mutant analysis revealed that control of root meristem size was mediated solely by cytokinin perception of AHK3 in the vascular tissue at the root transition zone, while AHK2 and AHK4 had no significant effect on root growth or meristem size (Dello Ioio et al. 2007; Dello Ioio et al. 2008). Nevertheless, *rock2* mutants show a clear reduction in primary root growth similar to *rock3* mutants (Fig. 21). Consistent with these results, the primary roots of the *ahk2-5 ahk3-7* double mutant were longer than in the wild type, whereas the single mutants did not show significant changes in primary root length (Riefler et al. 2006). Moreover, *ahk2–2 ahk3–3* double mutants were less sensitive to cytokinin in a root elongation assay than either single mutant (Higuchi et al. 2004), indicating also a role for AHK2 and AHK3 in the control of primary root growth. Furthermore, expression of the primary response cytokinin target *ARR5* was strongly upregulated in roots, including in the roots tips of *rock2* and *rock3* plants compared to wild type (Fig. 8). This revealed an enhancement of cytokinin signalling in roots, including the root apical meristem area.

Taken together, loss-of-function and gain-of-function mutant analysis indicate that AHK2 has a yet unknown function in the control of primary root growth, supposedly independently of the known AHK3/ARR1,ARR12 pathways which act via SHY2 on the downregulation of *PIN* genes and thus auxin transport (Dello Ioio et al. 2007; Dello Ioio et al. 2008; Moubayidin et al. 2010).

4.3 Transgenic *rock2* and *rock3* lines show a more pronounced phenotype

Interestingly, the transgenic *pAHK2:rock2* and *pAHK3:rock3* lines showed more pronounced phenotypes in almost all aspects compared to the mutants *rock2* and *rock3*. For *pAHK2:rock2* it could be shown that this is due to an increased expression of the transgene compared to wild-type *AHK2* expression (Fig. 9). It had not been tested if the location of expression had changed as well, but this is unlikely, as the phenotypic differences are merely stronger and do not occur in different tissues or different parts of the plants. The increased expression of the transgene is most probably due to an incomplete *AHK2* promoter. The chosen *AHK2* promoter contains 2124 bp upstream of the *AHK2* transcriptional start and was shown to be sufficient in complementation assays (Stolz et al. 2011). Nevertheless the promoter might lack negative regulatory elements either in a distal 5' promoter region or 3' of the gene. For example, it could be shown for *FT*, that *FT* activation requires not only proximal but also distal promoter regions that, together with LIKE HETEROCHROMATIN PROTEIN1 (LHP1) mediated chromatin status, orchestrate the interplay between activating and repressing inputs to FT regulation (Adrian et al. 2010). *CLV3* is another example for a gene that requires 3' regulatory elements for correct expression (Brand et al. 2002).

Interestingly, the chosen promoters for *AHK2* and *AHK3* have no effect on the overall growth and appearance of *Arabidopsis* plants when used for the expression of the non-mutated versions of *AHK2* and *AHK3*, respectively (Stolz et al. 2011). This shows that it is most likely not an increased expression of *AHK2* or *AHK3* that cause a cytokinin gain-of-function phenotype, but rather the expression of a constitutively active version of *AHK2* or *AHK3* being the crucial factor. In the future, transgenic expression of *pAHK2:rock2* and *pAHK3:rock3* could be used for promoter studies to find out more about regulatory elements of the *AHK2* and *AHK3* promoters.

4.4 The *rock4* mutation causes a gain-of-function variant of IPT3

Rock4 CKX1ox plants showed a reversion of the cytokinin-deficient shoot and root phenotype (Fig. 22 and Fig. 23). Surprisingly, a mutated form of the *IPT3* gene was found to be the cause for the reversion of the cytokinin deficiency syndrome. EMS mutagenesis caused a single base change from C to T at amino acid position 313 from the translation start of IPT3, resulting in a truncated version of the IPT3 protein (Fig. 24). As *rock4* caused a reversion of the cytokinin deficiency syndrome, the premature stop codon in the *IPT3* cDNA sequence causes a gain-of-function version of the protein. This was unexpected because IPT3 is a substrate of the protein farnesyl transferase (Galichet et al. 2008), and the truncated version lacks the predicted farnelysation motif CLVA of the IPT3 protein. Galichet et al. (2008) proposed that the cysteine residue of the CLVA motif at the C-terminal end of IPT3 is essential for IPT3 function. In *Arabidopsis* IPT3 overexpressing plants, as well as in yeast and *E. coli* cells expressing AtIPT3$_{C333S}$, it was shown that mutation of the farnesyl acceptor cysteine-333 of IPT3 abolishes cytokinin production, suggesting that cysteine-333 has an essential role in IPT3 catalytic activity, although the attachment of a farnesyl group to Cys-333 did not inhibit enzyme activity. These findings contradict with the finding that the truncated *rock4* version of the IPT3 protein, which lacks the last 23 amino acids and therefore also the CLVA motif, results in a gain-of-function version of the protein. If the cysteine-333 residue was in fact essential for IPT3 function, the ROCK4 protein would fail to produce cytokinin, and not show gain-of-function phenotypes.

Galichet et al. (2008) could further show that AtIPT3 is effectively farnesylated *in vivo* and that farnesylation regulates IPT3 subcellular localization, which affects cytokinin biosynthesis. Despite the presence of a chloroplast transit peptide at the N-terminal end of the protein (Kasahara et al. 2004), the farnesylated form of IPT3 was shown to localize in the nucleus and cytoplasm, where it participates in the biosynthesis of isopentenyl-type cytokinins. The lack of protein farnesylation in *era1-1* mutants directed the non-farnesylated form of AtIPT3 to the plastids, where it participates in the biosynthesis of zeatin-type cytokinins. Since the *rock4* version of IPT3 lacks the predicted farnelysation motif CLVA of the IPT3 protein, the protein most likely does not get farnesylated.

Therefore, it may be speculated that the protein locates to the plastids, where it promotes *trans*-zeatin production in *Arabidopsis*. Further experiments would be necessary in order to verify this hypothesis. IPT3 subcellular localization studies could be performed with GFP-tagged IPT3 and *rock4* proteins. Here it would be important to clone GFP behind the first 55 amino acids of IPT3, which function as a chloroplast peptide (Kasahara et al. 2004). A fusion of GFP at the C-terminus of IPT3 would block farnesylation of the protein by masking the functional CLVA box. Furthermore, the measurement and comparison of the cytokinin content and metabolic profile in wild-type and *rock4 Arabidopsis* plants will have to be carried out in the future. Assuming that the non-farnesylated *rock4* version of the IPT3 protein mainly produces zeatin-type cytokinins, the question arises: Are these types of cytokinin sufficient to overcome the cytokinin deficiency syndrome, and thus reflect the differences in the biological roles of iP and *t*Z? To test this hypothesis, the endogenous cytokinin composition of wild-type, CKX1 overexpressing, and *rock4 CKX1ox Arabidopsis* plants will have to be determined and compared.

Recent publications support the idea of the importance of *t*Z in regulating shoot growth. Matsumoto-Kitano et al. (2008) showed that the mutation of multiple *IPT* genes in *Arabidopsis* caused a complete loss of cambium and reduced thickening of the roots and stem. When grafted onto wild-type root stock, mutant shoots were completely restored. Interestingly, only *t*Z-type cytokinins in the shoot were restored to wild-type levels while iP-type cytokinins in the shoot remained unchanged. Furthermore, Bartrina et al. (2011) could show that *trans*-zeatin-type cytokinins are the predominant form of the hormone in the inflorescence, and upregulation of *trans*-zeatin-type cytokinins increases inflorescence meristem activity.

It is also possible, that the gain-of-function version of the IPT3 protein is caused by an increased expression or stability of the protein. However, *rock4* expression levels and protein stability have not yet been tested.

4.4.1 Phenotypes caused by the *rock4* mutation

Compared to phenotypes caused by an overexpression of *IPT* genes (Sakamoto et al. 2006; Sun et al. 2003; Zubko et al. 2002), the *rock4* mutation results in relatively mild but characteristic cytokinin gain-of-function phenotypes. *rock4* plants develop a reduced root system, but show an improved shoot growth, which is typical for cytokinin gain-of-function mutants. Interestingly, when compared to the gain-of-function receptor mutants, *rock2* and *rock3,* the effect of the *rock4* mutation on shoot development is more restricted to specific organs, even though *IPT3* is expressed throughout the plant's vasculature (Miyawaki et al. 2004). For example, the *rock4* mutation had no obvious effect on cotyledon and rosette leaf growth, and flower size also remained unchanged in *rock4* mutants

compared to the wild type (Fig. 26 and Fig. 27). However, *rock4* mutants did show an increased thickening of stems, similar to *rock2* and *rock3* mutants, and also delayed senescence (Fig. 27and Fig. 29).

4.4.1.1 The rock4 mutants exhibit an enhanced stem diameter

Transverse sections of the primary inflorescence stem showed that stem morphology was normal in *rock4* mutants, but stems were thicker and there were extra cells of different types, which suggested a higher and or prolonged mitotic activity (Fig. 27). These results are consistent with published results, demonstrating that cytokinin synthesis contributes to the development of the vascular cambium and radial plant growth. Matsumoto-Kitano et al. (2008) showed that the quadruple *Arabidopsis* mutant *atipt1,3,5,7*, which has strongly decreased levels of cytokinins, was unable to form cambium and showed reduced thickening of the root and stem. The *atipt3* single mutant exhibited decreased root thickening but no recognizable morphological changes in the stem. However, these results were based solely on *ipt loss-of-function* mutants with a reduced cytokinin content. The gain-of-function IPT3 mutant *rock4* however, shows the effects of an enhanced cytokinin status, further supporting that the hormone positively regulates radial plant growth.

In *Arabidopsis*, inflorescence stem thickness depends both on the size of the shoot apical meristem and on the secondary thickening growth; the latter of which involves cell division in the cambial zone and cell enlargement. Experiments with *ipt loss-of-function* mutants (Matsumoto-Kitano et al., 2008) strongly suggest that the phenotype is caused by an enhanced activity in the cambial zone, but it is also known that cytokinin regulates the size of the reproductive shoot apical meristem (Bartrina et al. 2011). It is unclear if the enhanced stem thickness in *rock4* mutants results from enhanced cell division in the cambial zone, or from a larger shoot apical meristem or both. Scanning electron micrographs of inflorescence meristems would reveal if the *rock4* mutation leads to a more active inflorescence meristem, but this experiment still has to be carried out.

It is surprising, that compared with the gain-of-function receptor mutants *rock2* and *rock3*, the only recognizable phenotype of *rock4* mutants concerning shoot organ size, was the increased radial expansion of the inflorescence stem. Even though *IPT3* is expressed in vasculature throughout the plant, neither cotyledons nor rosette leaves nor flower petals were enlarged (Miyawaki et al. 2004; Takei et al. 2004b), revealing that cambium activity responds most sensitively to cytokinins produced by the non-farnesylated version of the IPT3 protein, which is presumably *t*Z. Other organs are either less sensitive, or are regulated by other types of cytokinin, e.g. iP-type cytokinins.

4.4.1.2 The rock4 *mutation causes impaired embryo development*

Investigations during the reproductive state of *rock4* plants revealed that *rock4* mutants develop slightly shorter siliques than wild-type plants, indicating reduced fertility (Fig. 30). Unlike *rock2*, *rock4* flowers were indistinguishable from wild-type flowers and had no obvious problems with pollination. Microscopic analysis of developing embryos revealed embryo phenotypes, which were very similar to the embryo phenotypes observed in transgenic *rock2* plants (see chapter 3.1.5.8). The embryos developed in an asynchronous manner, and seed abortion occurred at different time points. Unfertilized ovules, delayed seed development, and embryonic lethality could be observed in *rock4* and *pIPT3:rock4* siliques (Fig. 31). This is consistent with the results found for *rock2* mutants, further supporting the assumption that cytokinin functions in seed and embryo development, with potential regulatory roles for IPT3 and AHK2.

4.4.1.3 The rock4 *mutant exhibits delayed leaf senescence*

An increased expression of cytokinin biosynthesis genes during the senescence phase can significantly delay the senescence of plant organs (Gan and Amasino 1995). Consistent with these results, the *rock4* mutation prolonged leaf longevity, indicating an enhanced cytokinin status during senescence and supporting a function of IPT3 as a regulator of leaf longevity (Fig. 29). Here again, it can be speculated that *t*Z-type cytokinins play a major role in delaying leaf senescence, assuming that the truncated version of IPT mainly produces *t*Z-type cytokinins. A major role for *trans*-zeatin-type cytokinins in delaying leaf senescence is supported by the fact that AHK3, the cytokinin receptor that predominately regulates the onset of leaf senescence (Kim et al. 2006), binds *trans*-zeatin-type cytokinins with a higher affinity compared to iP-type cytokinins (Romanov et al. 2006; Stolz et al. 2011).

4.4.1.4 The rock4 *allele inhibits root growth*

Compared to the rather mild phenotypes in the shoot, the *rock4* mutation caused a strong reduction in root growth and lateral root formation, similar to the phenotype seen in the gain-of-function receptor mutants *rock2* and *rock3* (Fig. 21 and Fig. 32). Already in the *CKX1ox* background, *rock4 CKX1* mutants developed shorter roots with less lateral roots than wild type, indicating that *Arabidopsis* roots react very sensitively to cytokinins produced by the non-farnesylated version of IPT3. As the cytokinin content in the roots has not yet been measured, it can only be speculated if a special type of cytokinin (e.g. *trans*-zeatin) is responsible for this effect, or if cytokinin production in

general counteracts the increased cytokinin degradation. It is also possible that the cellular location of cytokinin production is of importance.

Based on the assumption that *rock4* mainly produces *t*Z-type cytokinins, one would conclude that *t*Z-type cytokinins are particularly important for the reversion of the root phenotype of cytokinin deficient plants. This is not in agreement with previous experiments published by Matsumoto-Kitano et al. (2008). When a wild-type shoot was grafted onto an *atipt1,3,5,7* root, both the root and shoot grew normally. iP-type cytokinins in the root were restored to wild-type levels, but levels of *t*Z-type cytokinins were only partially restored. These results might suggeste that *t*Z-type cytokinins are of less importance than iP-type cytokinins for normal root growth.

4.5 Cytokinin-mediated crop design

The continuous increase in the human population and our increasing demand not only for food, but also for renewable plant resources and other plant-based biotechnological applications will require a more efficient production of plant biomass and high-yield food crops under environmentally limiting conditions. It is expected that traditional breeding combined with improved agronomical practices will not be able to keep up with an ever increasing global demand. Biotechnological innovations are expected to further improve plant productivity and/or growth characteristics in an effort to meet the worlds needs (Borlaug 2007).

Cytokinins are key regulators in plant growth and development and play positive regulatory roles in many aspects of plant growth and development. They stimulate the formation and activity of shoot meristems and have an probably essential function in the quantitative control of organ growth, in regulating yield, retarding leaf senescence, and play a role in seed germination and stress responses (Bartrina et al. 2011; Mok and Mok 2001; Werner and Schmülling 2009). Therefore, the regulation of the cytokinin status has become an interesting strategy for improving plant growth characteristics and crop productivity. Expression of *IPT* genes, which drive cytokinin synthesis, under the control of the senescence-induced *pSAG12* promoter, was shown to delay senescence in tobacco, maize, rice, lettuce, and tomato (Gan and Amasino 1995; McCabe et al. 2001; Robson et al. 2004). In a similar approach, it was shown that in tobacco, rice and peanuts, the expression of an *IPT* gene under the stress-induced *pSARK*-promoter delayed stress-induced plant senescence, which resulted in an improvement in both drought tolerance and yield (Ma and Liu 2009; Peleg et al. 2011; Rivero et al. 2007). An alternative method for increasing cytokinin concentrations in crop plants has been applied in rice and barley. Mutant plants with a reduced expression of cytokinin-degrading CKX enzymes developed an increased number of inflorescences, resulting in an increased grain yield (Ashikari et al.

2005; Zalewski et al. 2010). Taken together, these findings demonstrate that an enhanced cytokinin status is of potential interest for agricultural breeding purposes.

This work presents two new gain-of-function cytokinin receptor versions (*rock2* and *rock3*), and a gain-of-function IPT3-variant (*rock4*), whose transgenic expression in *Arabidopsis* resulted in plants with an enhanced cytokinin status and promising growth characteristics, which are summarised in Table 4. It was found, when compared to wild type *Arabidopsis* plants, that the AHK2 and AHK3 gain-of-function variants have a significant effect on shoot growth, the number of siliques per main stem, stem thickness, flower size, and senescence, and the *rock4*-mutation causes thicker inflorescence stems and delays senescence. Thus, transgenic expression of *rock2*, *rock3* and *rock4* may be promising tools in enhancing growth characteristics of crop plants, such as an increase in plants biomass and seed yield and delaying senescence.

5 Summary

Suppressor mutagenesis of *CKX1* overexpressing *Arabidopsis* plants (*CKX1ox*) led to the identification of the dominant mutants *rock2 CKX1ox, rock3 CKX1ox* and *rock4 CKX1ox* (Bartrina 2006), which showed a partial reversion of the cytokinin-deficient phenotype. Using map-based cloning, the *rock3* mutant allele was identified as missense mutation in the *AHK3* cytokinin receptor gene, and the *rock4* mutant allele was identified as a missense mutation in the cytokinin synthesis gene *IPT3*. It could be shown in a yeast experiment that the *rock2* and *rock3* mutations cause the formation of constitutively active cytokinin receptors.

Phenotypic analysis of the *rock2, rock3,* and *rock4* mutants in the *CKX1* overexpressing background revealed that the mutations caused a partial to full reversion of the cytokinin deficiency syndrome in matters of rosette diameter, shoot height, number of siliques, and root growth, and caused delayed leaf senescence in a dark-induced senescence assay. In addition, *rock2 CKX1ox* and *rock CKX1ox* plants showed an increased cotyledon diameter and an earlier onset of flowering.

In order to analyze the consequences of the *rock2, rock3,* and *rock4* mutations in wild-type background, the *35S:CKX1* transgene was outcrossed. Additionally, transgenic lines expressing *rock2, rock3,* and *rock4* under control of their own promoters were generated in wild-type *Arabidopsis* plants. The expression of *rock2* and *rock3* in the transgenic lines was verified by RT-PCR. In most cases, transgenic *pAHK2*:*rock2* and *pAHK3*:*rock3* lines showed more prominent phenotypes compared to *rock2* and *rock3* mutant plants, indicating a higher cytokinin status in the transgenic lines. For *pAHK2*:*rock2* plants it could be shown that the stronger effects are not due to an extra *AHK2* allele in the transgenic lines, but an increased expression level of the transgene compared to wild-type *AHK2* expression levels.

The *rock2* and *rock3* mutations caused an enhancement of vegetative and reproductive growth of wild-type plants throughout the plant's life cycle. Mutants exhibited bigger cotyledons, an increased rosette leaf size, thicker stems and bigger flowers. Microscopic analysis revealed that the increased growth is mainly due to the formation of more cells rather than bigger cells. In addition, the *rock3* mutants exhibited the strongest effect in delaying senescence, while the *rock2* allele had a greater effect on the onset of flowering. Similar to *rock2* and *rock3,* the *rock4* mutant also showed enhanced thickening of stems, a reduced root system, and delayed senescence. Contrary to the *rock2* and *rock3* mutations, the *rock4* mutation did not cause an enhanced cotyledon expansion or an increase in leaf and flower size.

Interestingly, *rock2, rock3,* and *rock4* mutant shoots grew and flowered for a longer period of time. Additionally, *rock2* and *rock3* plants produced more flowers per time unit, which led to a strongly increased number of siliques per plant. This resulted in an increased seed yield per plant, at least in case of *pAHK3:rock3* transgenic plants. The size of siliques, number of seeds per silique and seed size were not altered in *pAHK3:rock3* transgenic plants.

Detailed microscopic analysis of developing embryos revealed that expression of the *rock2* or *rock4* alleles resulted in a disturbed embryo development and seed abortion. Embryo development was retarded and unsynchronized compared to wild type, and in the case of *pAHK2*:*rock2,* embryos were often malformed at developmental stages later than the heart stage. However, a low percentage of mutant embryos developed normally and grew into typical looking *pAHK2:rock2* or *rock4* plants.

Taken together, the *rock2, rock3,* and *rock4* mutations are interesting tools to research the effects of an enhanced cytokinin status during plant development and gave new insight into cytokinin regulated processes. In addition, the characterisation of the gain-of-function cytokinin mutants *rock2, rock3,* and *rock4* revealed that an enhanced cytokinin status causes several effects on plant development, which are of potential interest for agricultural breeding purposes, for example an enhanced organ growth and delayed senescence.

6 Zusammenfassung

Eine Suppressormutagenese von *CKX1*-überexprimierenden *Arabidopsis* Pflanzen (*CKX1ox*) führte zur Identifikation der dominanten Mutanten *rock2 CKX1ox, rock3 CKX1ox* und *rock4 CKX1ox* (Bartrina 2006), welche eine Reversion des cytokinindefizienten Phänotyps zeigten. Die Kartierung der Mutationen ergab, dass es sich bei *rock2* und *rock3* um Missense-Mutationen in den Cytokinin-Rezeptorengenen *AHK2* und *AHK3* handelt, und bei *rock4* um eine Missense-Mutation im Cytokinin-Synthesegen *IPT3*. Es konnte mit einem Test in Hefe gezeigt werden, dass die *rock2*- und *rock3*-Mutationen zu konstitutiv aktiven Cytokinin-Rezeptoren führen.

Eine phänotypische Analyse der *rock2*-, *rock3*- und *rock4*-Mutanten in *CKX1*-überexprimierenden Pflanzen zeigte, dass die Mutationen bei Rosettendiameter, Sprosshöhe, Anzahl der Schoten und Wurzelwachstum eine partielle bis komplette Reversion des Cytokinindefizienzsyndroms bewirkten und die Blattseneszenz in einem Dunkelheit-induzierten Seneszenztest verzögerten. Außerdem zeigten *rock2 CKX1ox*- und *rock3 CKX1ox*-Pflanzen einen vergrößerten Kotyledonen-Durchmesser und einen früheren Blühzeitpunkt.

Um die Auswirkung der *rock2-, rock3*- und *rock4*-Mutationen im Wildtyphintergrund zu untersuchen, wurde das *35S:CKX1*-Transgen ausgekreuzt. Außerdem wurden transgene *Arabidopsis* Pflanzen hergestellt, die die *rock2-, rock3*- und *rock4*-Gene unter den jeweiligen eigenen Promotoren exprimieren. Die Expression der Transgene *rock2* und *rock3* wurde mit Hilfe von RT-PCRs nachgewiesen. In den meisten Fällen zeigten die transgenen *pAHK2*:*rock2*- und *pAHK3*:*rock3*-Pflanzen stärker veränderte Phänotypen im Vergleich zu *rock2* und *rock3* Pflanzen, was für einen höheren Cytokininstatus in den transgenen Linien spricht. Im Fall von *pAHK2*:*rock2* konnte gezeigt werden, dass die stärkeren Effekte nicht durch ein weiteres *AHK2*-Allel, sondern durch eine verstärkte Expression des Transgens, verglichen mit dem wildtypischen *AHK2*-Expressionlevel, ausgelöst wurden.

Verglichen mit Wildtyppflanzen bewirken die *rock2*- und *rock3*-Mutationen verstärktes vegetatives und reproduktives Wachstum während des gesamten pflanzlichen Lebenszyklus. So bildeten die Mutanten größere Kotyledonen, Rosettenblätter und Blüten und dickere Stängel. Mikroskopische Analysen zeigten, dass die Vergrößerung der Organe im Vergleich zum Wildtyp durch die Bildung von mehr Zellen bewirkt wird. Des Weiteren zeigten vor allem *rock3*-Mutanten eine verzögerte Seneszenz, während das *rock2*-Allele eine stärkere Auswirkung auf den Blühzeitpunkt von *Arabidopsis*-Pflanzen hatte. Die *rock4*-Mutantion bewirkte, ebenso wie die *rock2*- und *rock3*-Mutantionen, dickere Stängel, ein reduziertes Wurzelsystem und verzögerte Seneszenz, aber kein gesteigertes Kotyledonen-Wachstum oder eine Vergrößerung von Rosettenblättern oder Blüten.

Interessanterweise zeigten *rock2-, rock3*- und *rock4*-Pflanzen eine spätere Termination der Blüte verglichen mit dem Wildtyp. Außerdem produzierten *rock2*- und *rock3*-Pflanzen mehr Blüten pro Zeiteinheit, was zu einer stark erhöhten Schotenanzahl und somit zu einem gesteigerten Samenertrag führte. Zumindest war dies bei transgenen *pAHK3:rock3*-Pflanzen der Fall, da in diesen Pflanzen die Größe der Schoten, die Anzahl der Samen pro Schote und die Samengröße im Vergleich zum Wildtyp nicht verändert war.

Mikroskopische Untersuchungen von sich entwickelnden Embryonen machten deutlich, dass die Expression der *rock2*- und *rock4*-Allele zu einer gestörtem Embryo-Entwicklung und einem Abort der Samen führen kann. Die embryonale Entwicklung war verlangsamt und asynchron verglichen mit dem Wildtyp, und im Fall von *pAHK2*:*rock2* waren die Embryos nach Erreichen des Herz-Stadiums außerdem oft missgebildet. Allerdings entwickelte sich ein geringer Prozentsatz der mutanten Embryos normal und adulte Pflanzen zeigten später die für *pAHK2*:*rock2* und *rock4* typischen Ausprägungen.

Zusammengefasst konnte gezeigt werden, dass *rock2-, rock3*- und *rock4*-Allele interessante Werkzeuge zur Erforschung von Effekten in der pflanzlichen Entwicklung, ausgelöst durch einen erhöhten Cytokininstatus, darstellen, und neues Licht in Cytokinin-regulierte Prozesse bringen können. Außerdem offenbarte die Charakterisierung der *gain-of-function* Cytokinin-Mutanten *rock2*, *rock3* und *rock4*, dass ein erhöhter Cytokininstatus verschiedene Effekte in der pflanzlichen Entwicklung bewirkt, wie zum Beispiel größere Organe und eine verspätete Seneszenz, die von potentiellem Interesse für die Pflanzenzüchtung sind.

7 References

Adrian J, Farrona S, Reimer JJ, Albani MC, Coupland G, Turck F (2010) cis-Regulatory Elements and Chromatin State Coordinately Control Temporal and Spatial Expression of FLOWERING LOCUS T in Arabidopsis. The Plant Cell Online 22: 1425-1440

Altamura MM, Possenti M, Matteucci A, Baima S, Ruberti I, Morelli G (2001) Development of the vascular system in the inflorescence stem of Arabidopsis. New Phytologist 151: 381-389

Anantharaman V, Aravind L (2001) The CHASE domain: a predicted ligand-binding module in plant cytokinin receptors and other eukaryotic and bacterial receptors. Trends Biochem Sci 26: 579 - 582

Anastasiou E, Lenhard M (2007) Growing up to one's standard. Current Opinion in Plant Biology 10: 63-69

Argueso CT, Ferreira FJ, Kieber JJ (2009) Environmental perception avenues: the interaction of cytokinin and environmental response pathways. Plant, Cell & Environment 32: 1147-1160

Argyros RD, Mathews DE, Chiang Y-H, Palmer CM, Thibault DM, Etheridge N, Argyros DA, Mason MG, Kieber JJ, Schaller GE (2008) Type B Response Regulators of Arabidopsis Play Key Roles in Cytokinin Signaling and Plant Development. Plant Cell 20: 2102-2116

Ashikari M, Sakakibara H, Lin S, Yamamoto T, Takashi T, Nishimura A, Angeles ER, Qian Q, Kitano H, Matsuoka M (2005) Cytokinin Oxidase Regulates Rice Grain Production. Science 309: 741-745

Bartrina I (2006) Molekulare Charakterisierung von *ckx* Insertionsmutanten und Suppressormutanten des Cytokinindefizienzsyndroms in *Arabidopsis thaliana*. Dissertation. Freie Universität Berlin.

Bartrina I, Otto E, Strnad M, Werner T, Schmülling T (2011) Cytokinin Regulates the Activity of Reproductive Meristems, Flower Organ Size, Ovule Formation, and Thus Seed Yield in Arabidopsis thaliana. The Plant Cell Online 23: 69-80

Benková E, Michniewicz M, Sauer M, Teichmann T, Seifertová D, Jürgens G, Friml J (2003) Local, Efflux-Dependent Auxin Gradients as a Common Module for Plant Organ Formation. Cell 115: 591-602

Bernier G (2011) My favourite flowering image: the role of cytokinin as a flowering signal. Journal of Experimental Botany 62: 1-5

Bertrani G (1951) Studies on lysogenesis I.: The mode of phage liberation by lysogenic *Escherichia coli*. Journal of Bacteriology 62: 293-300

Beveridge CA, Murfet IC, Kerhoas L, Sotta B, Miginiac E, Rameau C (1997) The shoot controls zeatin riboside export from pea roots. Evidence from the branching mutant rms4. The Plant Journal 11: 339-345

Bilyeu KD, Cole JL, Laskey JG, Riekhof WR, Esparza TJ, Kramer MD, Morris RO (2001) Molecular and Biochemical Characterization of a Cytokinin Oxidase from Maize. Plant Physiol. 125: 378-386

Bleecker AB, Patterson SE (1997) Last exit: senescence, abscission, and meristem arrest in Arabidopsis. The Plant Cell Online 9: 1169-1179

Blilou I, Xu J, Wildwater M, Willemsen V, Paponov I, Friml J, Heidstra R, Aida M, Palme K, Scheres B (2005) The PIN auxin efflux facilitator network controls growth and patterning in Arabidopsis roots. Nature 433: 39-44

Bonhomme F, Kurz B, Melzer S, Bernier G, Jacqmard A (2000) Cytokinin and gibberellin activate SaMADS A, a gene apparently involved in regulation of the floral transition in Sinapis alba. The Plant Journal 24: 103-111

Borlaug N (2007) Feeding a Hungry World. Science 318: 359

Bossinger G, Smyth DR (1996) Initiation patterns of flower and floral organ development in Arabidopsis thaliana. Development 122: 1093-1102

Brand U, Fletcher JC, Hobe M, Meyerowitz EM, Simon R (2000) Dependence of Stem Cell Fate in Arabidopsis on a Feedback Loop Regulated by CLV3 Activity. Science 289: 617-619

Brand U, Grünewald M, Hobe M, Simon R (2002) Regulation of CLV3 Expression by Two Homeobox Genes in Arabidopsis. Plant Physiology 129: 565-575

Brenner WG, Romanov GA, Kollmer I, Burkle L, Schmulling T (2005) Immediate-early and delayed cytokinin response genes of Arabidopsis thaliana identified by genome-wide expression profiling reveal novel cytokinin-sensitive processes and suggest cytokinin action through transcriptional cascades. The Plant Journal 44: 314-333

Brzobohaty B, Moore I, Kristoffersen P, Bako L, Campos N, Schell J, Palme K (1993) Release of active cytokinin by a beta-glucosidase localized to the maize root meristem. Science 262: 1051-1054

Buchanan-Wollaston V, Page T, Harrison E, Breeze E, Lim PO, Nam HG, Lin J-F, Wu S-H, Swidzinski J, Ishizaki K, Leaver CJ (2005) Comparative transcriptome analysis reveals significant differences in gene expression and signalling pathways between developmental and dark/starvation-induced senescence in Arabidopsis. The Plant Journal 42: 567-585

Buechel S, Leibfried A, To JPC, Zhao Z, Andersen SU, Kieber JJ, Lohmann JU (2010) Role of A-type ARABIDOPSIS RESPONSE REGULATORS in meristem maintenance and regeneration. European Journal of Cell Biology 89: 279-284

Bürkle L, Cedzich A, Döpke C, Stransky H, Okumoto S, Gillissen B, Kühn C, Frommer WB (2003) Transport of cytokinins mediated by purine transporters of the PUP family expressed in phloem, hydathodes, and pollen of Arabidopsis. The Plant Journal 34: 13-26

Caesar K, Thamm AMK, Witthöft J, Elgass K, Huppenberger P, Grefen C, Horak J, Harter K (2011) Evidence for the localization of the Arabidopsis cytokinin receptors AHK3 and AHK4 in the endoplasmic reticulum. Journal of Experimental Botany 62: 5571-5580

Calvin NM, Hanawalt PC (1988) High-efficiency transformation of bacterial cells by electroporation. J Bacteriol. 170: 2796-2801

Carabelli M, Possenti M, Sessa G, Ciolfi A, Sassi M, Morelli G, Ruberti I (2007) Canopy shade causes a rapid and transient arrest in leaf development through auxin-induced cytokinin oxidase activity. Genes & Development 21: 1863-1868

Cedzich A, Stransky H, Schulz B, Frommer WB (2008) Characterization of Cytokinin and Adenine Transport in Arabidopsis Cell Cultures. Plant Physiol. 148: 1857-1867

Chaudhury AM, Letham S, Craig S, Dennis ES (1993) amp1 - a mutant with high cytokinin levels and altered embryonic pattern, faster vegetative growth, constitutive photomorphogenesis and precocious flowering. The Plant Journal 4: 907-916

Chen C-M, Kristopeit SM (1981) Metabolism of Cytokinin: Deribosylation of Cytokinin Ribonucleoside by Adenosine Nucleosidase from Wheat Germ Cells. Plant Physiol. 68: 1020-1023

Chervitz SA, Falke JJ (1996) Molecular mechanism of transmembrane signaling by the aspartate receptor: a model. Proceedings of the National Academy of Sciences 93: 2545-2550

Chory J, Reinecke D, Sim S, Washburn T, Brenner M (1994) A Role for Cytokinins in De-Etiolation in Arabidopsis (det Mutants Have an Altered Response to Cytokinins). Plant Physiol. 104: 339-347

Clough SJ, Bent AF (1998) Floral dip: a simplified method forAgrobacterium-mediated transformation ofArabidopsis thaliana. The Plant Journal 16: 735-743

Corbesier L, Prinsen E, Jacqmard A, Lejeune P, Van Onckelen H, Périlleux C, Bernier G (2003) Cytokinin levels in leaves, leaf exudate and shoot apical meristem of Arabidopsis thaliana during floral transition. Journal of Experimental Botany 54: 2511-2517

D'Agostino IB, Deruere J, Kieber JJ (2000) Characterization of the Response of the Arabidopsis Response Regulator Gene Family to Cytokinin. Plant Physiol. 124: 1706-1717

D'Aloia M, Bonhomme D, Bouché F, Tamseddak K, Ormenese S, Torti S, Coupland G, Périlleux C (2011) Cytokinin promotes flowering of Arabidopsis via transcriptional activation of the FT paralogue TSF. The Plant Journal 65: 972-979

Davanloo P, Rosenberg AH, Dunn JJ, Studier FW (1984) Cloning and expression of the gene for bacteriophage T7 RNA polymerase. Proceedings of the National Academy of Sciences of the United States of America 81: 2035-2039

Dello Ioio R, Linhares FS, Scacchi E, Casamitjana-Martinez E, Heidstra R, Costantino P, Sabatini S (2007) Cytokinins Determine Arabidopsis Root-Meristem Size by Controlling Cell Differentiation. Current Biology 17: 678-682

Dello Ioio R, Nakamura K, Moubayidin L, Perilli S, Taniguchi M, Morita MT, Aoyama T, Costantino P, Sabatini S (2008) A Genetic Framework for the Control of Cell Division and Differentiation in the Root Meristem. Science 322: 1380-1384

Dello Ioio R, Galinha C, Fletcher Alexander G, Grigg Stephen P, Molnar A, Willemsen V, Scheres B, Sabatini S, Baulcombe D, Maini Philip K, Tsiantis M (2012) A PHABULOSA/Cytokinin Feedback Loop Controls Root Growth in Arabidopsis. Current Biology 22: 1699-1704

Donnelly PM, Bonetta D, Tsukaya H, Dengler RE, Dengler NG (1999) Cell Cycling and Cell Enlargement in Developing Leaves of Arabidopsis. Developmental Biology 215: 407-419

Endrizzi K, Moussian B, Haecker A, Levin JZ, Laux T (1996) The SHOOT MERISTEMLESS gene is required for maintenance of undifferentiated cells in Arabidopsis shoot and floral meristems and acts at a different regulatory level than the meristem genes WUSCHEL and ZWILLE. The Plant Journal 10: 967-979

Esau K (1965) Fixation images of sieve element plastids in beta*. PNAS 54: 429-437

Estelle MA, Somerville C (1987) Auxin-resistant mutants of *Arabidopsis thaliana* with an altered morphology. Molecular and General Genetics MGG 206: 200-206

Fukaki H, Tasaka M (2009) Hormone interactions during lateral root formation. Plant Molecular Biology 69: 437-449

Galichet A, Hoyerova K, Kaminek M, Gruissem W (2008) Farnesylation Directs AtIPT3 Subcellular Localization and Modulates Cytokinin Biosynthesis in Arabidopsis. Plant Physiol. 146: 1155-1164

Galuszka P, Frébortová J, Werner T, Yamada M, Strnad M, Schmülling T, Frébort I (2004) Cytokinin oxidase/dehydrogenase genes in barley and wheat. European Journal of Biochemistry 271: 3990-4002

Galuszka P, Popelková H, Werner T, Frébortová J, Pospíšilová H, Mik V, Köllmer I, Schmülling T, Frébort I (2007) Biochemical Characterization of Cytokinin Oxidases/Dehydrogenases from *Arabidopsis thaliana* Expressed in *Nicotiana tabacum*. Journal of Plant Growth Regulation 26: 255-267

Gan S, Amasino RM (1995) Inhibition of Leaf Senescence by Autoregulated Production of Cytokinin. Science 270: 1986-1988

Giakountis A, Coupland G (2008) Phloem transport of flowering signals. Current Opinion in Plant Biology 11: 687-694

Gietz RD, Schiestl RH (2007) Quick and easy yeast transformation using the LiAc/SS carrier DNA/PEG method. Nat. Protocols 2: 35-37

Gillissen B, Burkle L, Andre B, Kuhn C, Rentsch D, Brandl B, Frommer WB (2000) A New Family of High-Affinity Transporters for Adenine, Cytosine, and Purine Derivatives in Arabidopsis. Plant Cell 12: 291-300

Giulini A, Wang J, Jackson D (2004) Control of phyllotaxy by the cytokinin-inducible response regulator homologue ABPHYL1. Nature 430: 1031-1034

Golovko A, Sitbon F, Tillberg E, Nicander B (2002) Identification of a tRNA isopentenyltransferase gene from Arabidopsis thaliana. Plant Molecular Biology. Springer Netherlands, pp 161-169

Gordon SP, Chickarmane VS, Ohno C, Meyerowitz EM (2009) Multiple feedback loops through cytokinin signaling control stem cell number within the Arabidopsis shoot meristem. Proceedings of the National Academy of Sciences 106: 16529-16534

Grant SG, Jessee J, Bloom FR, Hanahan D (1990) Differential plasmid rescue from transgenic mouse DNAs into Escherichia coli methylation-restriction mutants. Proceedings of the National Academy of Sciences of the United States of America 87: 4645-4649

Hall TA (1999) BioEdit: a user-friendly biological sequence alignment editor and analysis program for Windows 95/98/NT. Nucleic Acids Symposium Series: 95-98

Hanahan D (1983) Studies on transformation of Escherichia coli with plasmids. Journal of Molecular Biology 166: 557-580

He YW, Loh CS (2002) Induction of early bolting in Arabidopsis thaliana by triacontanol, cerium and lanthanum is correlated with increased endogenous concentration of isopentenyl adenosine (iPAdos). Journal of Experimental Botany 53: 505-512

Hejatko J, Ryu H, Kim G-T, Dobesova R, Choi S, Choi SM, Soucek P, Horak J, Pekarova B, Palme K, Brzobohaty B, Hwang I (2009) The Histidine Kinases CYTOKININ-INDEPENDENT1 and ARABIDOPSIS HISTIDINE KINASE2 and 3 Regulate Vascular Tissue Development in Arabidopsis Shoots. Plant Cell 21: 2008-2021

Hensel LL, Nelson MA, Richmond TA, Bleecker AB (1994) The Fate of Inflorescence Meristems Is Controlled by Developing Fruits in Arabidopsis. Plant Physiology 106: 863-876

Heyl A, Ramireddy E, Brenner WG, Riefler M, Allemeersch J, Schmulling T (2008) The Transcriptional Repressor ARR1-SRDX Suppresses Pleiotropic Cytokinin Activities in Arabidopsis. Plant Physiol. 147: 1380-1395

Heyl A, Wulfetange K, Pils B, Nielsen N, Romanov G, Schmulling T (2007) Evolutionary proteomics identifies amino acids essential for ligand-binding of the cytokinin receptor CHASE domain. BMC Evolutionary Biology 7: 62

Higuchi M, Pischke M, Mahonen A, Miyawaki K, Hashimoto Y, Seki M, Kobayashi M, Shinozaki K, Kato T, Tabata S (2004) In planta functions of the Arabidopsis cytokinin receptor family. Proc Natl Acad Sci USA 101: 8821 - 8826

Hirose N, Makita N, Yamaya T, Sakakibara H (2005) Functional Characterization and Expression Analysis of a Gene, OsENT2, Encoding an Equilibrative Nucleoside Transporter in Rice Suggest a Function in Cytokinin Transport. Plant Physiol. 138: 196-206

Hirose N, Takei K, Kuroha T, Kamada-Nobusada T, Hayashi H, Sakakibara H (2008) Regulation of cytokinin biosynthesis, compartmentalization and translocation. Journal of Experimental Botany 59: 75-83

Holst K, Schmülling T, Werner T (2011) Enhanced cytokinin degradation in leaf primordia of transgenic Arabidopsis plants reduces leaf size and shoot organ primordia formation. Journal of Plant Physiology 168: 1328-1334

Hothorn M, Dabi T, Chory J (2011) Structural basis for cytokinin recognition by Arabidopsis thaliana histidine kinase 4. Nat Chem Biol 7: 766-768

Houba-Hérin N, Pethe C, D'Alayer J, Laloue M (1999) Cytokinin oxidase from Zea mays: purification, cDNA cloning and expression in moss protoplasts. The Plant Journal 17: 615-626

Huala E, Dickerman AW, Garcia-Hernandez M, Weems D, Reiser L, LaFond F, Hanley D, Kiphart D, Zhuang M, Huang W, Mueller LA, Bhattacharyya D, Bhaya D, Sobral BW, Beavis W, Meinke DW, Town CD, Somerville C, Rhee SY (2001) The Arabidopsis Information Resource (TAIR): a comprehensive database and web-based information retrieval, analysis, and visualization system for a model plant. Nucleic Acids Research 29: 102-105

Huang C-N, Cornejo, M.J., Bush, D.S., and Jones R.L. (1986) Estimating viability of plant protoplasts using double and single staining. Protoplasma 135: 80-87

Hutchison CE, Li J, Argueso C, Gonzalez M, Lee E, Lewis MW, Maxwell BB, Perdue TD, Schaller GE, Alonso JM, Ecker JR, Kieber JJ (2006) The Arabidopsis Histidine Phosphotransfer Proteins Are Redundant Positive Regulators of Cytokinin Signaling. Plant Cell 18: 3073-3087

Hwang I, Sheen J (2001) Two-component circuitry in Arabidopsis cytokinin signal transduction. Nature 413: 383 - 389

Imamura A, Kiba T, Tajima Y, Yamashino T, Mizuno T (2003) In Vivo and In Vitro Characterization of the ARR11 Response Regulator Implicated in the His-to-Asp Phosphorelay Signal Transduction in Arabidopsis thaliana. Plant and Cell Physiology 44: 122-131

Inoue T, Higuchi M, Hashimoto Y, Seki M, Kobayashi M, Kato T, Tabata S, Shinozaki K, Kakimoto T (2001) Identification of CRE1 as a cytokinin receptor from Arabidopsis. Nature 409: 1060 - 1063

Ioio RD, Nakamura K, Moubayidin L, Perilli S, Taniguchi M, Morita MT, Aoyama T, Costantino P, Sabatini S (2008) A Genetic Framework for the Control of Cell Division and Differentiation in the Root Meristem. Science 322: 1380-1384

Ishida K, Yamashino T, Yokoyama A, Mizuno T (2008) Three Type-B Response Regulators, ARR1, ARR10 and ARR12, Play Essential but Redundant Roles in Cytokinin Signal Transduction Throughout the Life Cycle of Arabidopsis thaliana. Plant and Cell Physiology 49: 47-57

Jacqmard A, Detry N, Dewitte W, Van Onckelen H, Bernier G (2002) In situ localisation of cytokinins in the shoot apical meristem of Sinapis alba at floral transition. Planta 214: 970-973

Jang S, Torti S, Coupland G (2009) Genetic and spatial interactions between FT, TSF and SVP during the early stages of floral induction in Arabidopsis. The Plant Journal 60: 614-625

Jasinski S, Piazza P, Craft J, Hay A, Woolley L, Rieu I, Phillips A, Hedden P, Tsiantis M (2005) KNOX Action in Arabidopsis Is Mediated by Coordinate Regulation of Cytokinin and Gibberellin Activities. Current Biology 15: 1560-1565

Kakimoto T (1996) CKI1, a Histidine Kinase Homolog Implicated in Cytokinin Signal Transduction. Science 274: 982-985

Kakimoto T (2001) Identification of Plant Cytokinin Biosynthetic Enzymes as Dimethylallyl Diphosphate:ATP/ADP Isopentenyltransferases. Plant and Cell Physiology 42: 677-685

Kakimoto T (2003) Biosynthesis of cytokinins. Journal of Plant Research 116: 233-239

Kamada-Nobusada T, Sakakibara H (2009) Molecular basis for cytokinin biosynthesis. Phytochemistry 70: 444-449

Karimi M, De Meyer B, Hilson P (2005) Modular cloning in plant cells. Trends in Plant Science 10: 103-105

Karimi M, Inzé D, Depicker A (2002) GATEWAY(TM) vectors for Agrobacterium-mediated plant transformation. Trends in Plant Science 7: 193-195

Kasahara H, Takei K, Ueda N, Hishiyama S, Yamaya T, Kamiya Y, Yamaguchi S, Sakakibara H (2004) Distinct Isoprenoid Origins of cis- and trans-Zeatin Biosyntheses in Arabidopsis. Journal of Biological Chemistry 279: 14049-14054

Kiba T, Naitou T, Koizumi N, Yamashino T, Sakakibara H, Mizuno T (2005) Combinatorial Microarray Analysis Revealing Arabidopsis Genes Implicated in Cytokinin Responses through the His→Asp Phosphorelay Circuitry. Plant and Cell Physiology 46: 339-355

Kiba T, Yamada H, Mizuno T (2002) Characterization of the ARR15 and ARR16 Response Regulators with Special Reference to the Cytokinin Signaling Pathway Mediated by the AHK4 Histidine Kinase in Roots of Arabidopsis thaliana. Plant and Cell Physiology 43: 1059-1066

Kieber JJ, Schaller GE (2010) The Perception of Cytokinin: A Story 50 Years in the Making. Plant Physiology 154: 487-492

Kim H, Ryu H, Hong S, Woo H, Lim P, Lee I, Sheen J, Nam H, Hwang I (2006) Cytokinin-mediated control of leaf longevity by AHK3 through phosphorylation of ARR2 in Arabidopsis. Proc Natl Acad Sci USA 103: 814 - 819

Köllmer I (2009) Funktionelle Charakterisierung von *CKX7* und cytokininregulierten Transkriptionsfaktorgenen in *Arabidopsis thaliana*. Dissertation. Freie Universität Berlin.

Koncz C, Schell J (1986) The promoter of T L-DNA gene 5 controls the tissue-specific expression of chimaeric genes carried by a novel type of Agrobacterium binary vector. Molecular and General Genetics MGG 204: 383-396

Kondou Y, Nakazawa M, Kawashima M, Ichikawa T, Yoshizumi T, Suzuki K, Ishikawa A, Koshi T, Matsui R, Muto S, Matsui M (2008) RETARDED GROWTH OF EMBRYO1, a New Basic Helix-Loop-Helix Protein, Expresses in Endosperm to Control Embryo Growth. Plant Physiology 147: 1924-1935

Kramer U, Cotter-Howells JD, Charnock JM, Baker AJM, Smith JAC (1996) Free histidine as a metal chelator in plants that accumulate nickel. Nature 379: 635-638

Kuderová A, Urbánková I, Válková M, Malbeck J, Brzobohatý B, Némethová D, Hejátko J (2008) Effects of Conditional IPT-Dependent Cytokinin Overproduction on Root Architecture of Arabidopsis Seedlings. Plant and Cell Physiology 49: 570-582

Kurakawa T, Ueda N, Maekawa M, Kobayashi K, Kojima M, Nagato Y, Sakakibara H, Kyozuka J (2007) Direct control of shoot meristem activity by a cytokinin-activating enzyme. Nature 445: 652-655

Kuroha T, Tokunaga H, Kojima M, Ueda N, Ishida T, Nagawa S, Fukuda H, Sugimoto K, Sakakibara H (2009) Functional Analyses of LONELY GUY Cytokinin-Activating Enzymes Reveal the Importance of the Direct Activation Pathway in Arabidopsis. Plant Cell 21: 3152-3169

Laplaze L, Benkova E, Casimiro I, Maes L, Vanneste S, Swarup R, Weijers D, Calvo V, Parizot B, Herrera-Rodriguez MB, Offringa R, Graham N, Doumas P, Friml J, Bogusz D, Beeckman T, Bennett M (2007) Cytokinins Act Directly on Lateral Root Founder Cells to Inhibit Root Initiation. Plant Cell 19: 3889-3900

Lee J, Lee I (2010) Regulation and function of SOC1, a flowering pathway integrator. Journal of Experimental Botany 61: 2247-2254

Leibfried A, To JPC, Busch W, Stehling S, Kehle A, Demar M, Kieber JJ, Lohmann JU (2005) WUSCHEL controls meristem function by direct regulation of cytokinin-inducible response regulators. Nature 438: 1172-1175

Lejeune P, Bernier G, Requier MC, Kinet JM (1994) Cytokinins in phloem and xylem saps of Sinapis alba during floral induction. Physiologia Plantarum 90: 522-528

Lenhard M, Jürgens G, Laux T (2002) The WUSCHEL and SHOOTMERISTEMLESS genes fulfil complementary roles in Arabidopsis shoot meristem regulation. Development 129: 3195-3206

Letham DS (1963) Zeatin, a factor inducing cell division isolated from *zea mays*. Life sciences 8: 569-573

Letham DS, Palni LMS (1983) The Biosynthesis and Metabolism of Cytokinins. Annual Review of Plant Physiology 34: 163-197

Li X, Mo X, Shou H, Wu P (2006) Cytokinin-Mediated Cell Cycling Arrest of Pericycle Founder Cells in Lateral Root Initiation of Arabidopsis. Plant and Cell Physiology 47: 1112-1123

Livak KJ, Schmittgen TD (2001) Analysis of Relative Gene Expression Data Using Real-Time Quantitative PCR and the 2-[Delta][Delta]CT Method. Methods 25: 402-408

Long JA, Moan EI, Medford JI, Barton MK (1996) A member of the KNOTTED class of homeodomain proteins encoded by the STM gene of Arabidopsis. Nature 379: 66-69

Lukowitz W, Gillmor CS, Scheible W-R (2000) Positional Cloning in Arabidopsis. Why It Feels Good to Have a Genome Initiative Working for You. Plant Physiol. 123: 795-806

Ma Q-H, Liu Y-C (2009) Expression of isopentenyl transferase gene (ipt) in leaf and stem delayed leaf senescence without affecting root growth. Plant Cell Reports 28: 1759-1765

Maeda T, Takekawa M, Saito H (1995) Activation of yeast PBS2 MAPKK by MAPKKKs or by binding of an SH3-containing osmosensor. Science 269: 554-558

Maeda T, Wurgler-Murphy SM, Saito H (1994) A two-component system that regulates an osmosensing MAP kinase cascade in yeast. Nature 369: 242-245

Mähönen A, Bonke M, Kauppinen L, Riikonen M, Benfey P, Helariutta Y (2000) A novel two-component hybrid molecule regulates vascular morphogenesis of the Arabidopsis root. Genes Dev 14: 2938 - 2943

Mähönen AP, Higuchi M, Törmäkangas K, Miyawaki K, Pischke MS, Sussman MR, Helariutta Y, Kakimoto T (2006) Cytokinins Regulate a Bidirectional Phosphorelay Network in Arabidopsis. Current Biology 16: 1116-1122

Mason MG, Li J, Mathews DE, Kieber JJ, Schaller GE (2004) Type-B Response Regulators Display Overlapping Expression Patterns in Arabidopsis. Plant Physiol. 135: 927-937

Mason MG, Mathews DE, Argyros DA, Maxwell BB, Kieber JJ, Alonso JM, Ecker JR, Schaller GE (2005) Multiple Type-B Response Regulators Mediate Cytokinin Signal Transduction in Arabidopsis. Plant Cell 17: 3007-3018

Matsumoto-Kitano M, Kusumoto T, Tarkowski P, Kinoshita-Tsujimura K, Václavíková K, Miyawaki K, Kakimoto T (2008) Cytokinins are central regulators of cambial activity. Proceedings of the National Academy of Sciences 105: 20027-20031

McCabe MS, Garratt LC, Schepers F, Jordi WJRM, Stoopen GM, Davelaar E, van Rhijn JHA, Power JB, Davey MR (2001) Effects of PSAG12-IPT Gene Expression on Development and Senescence in Transgenic Lettuce. Plant Physiol. 127: 505-516

Melzer S, Lens F, Gennen J, Vanneste S, Rohde A, Beeckman T (2008) Flowering-time genes modulate meristem determinacy and growth form in Arabidopsis thaliana. Nat Genet 40: 1489-1492

Miller CO, Skoog F, Okumura FS, Von Saltza MH, Strong FM (1956) Isolation, Structure and Synthesis of Kinetin, a Substance Promoting Cell Division1,2. Journal of the American Chemical Society 78: 1375-1380

Miller CO, Skoog F, Von Saltza MH, Strong FM (1955) Kinetin, a cell division factor from deoxyribonucleic acid1. Journal of the American Chemical Society 77: 1392-1392

Miwa K, Ishikawa K, Terada K, Yamada H, Suzuki T, Yamashino T, Mizuno T (2007) Identification of Amino Acid Substitutions that Render the Arabidopsis Cytokinin Receptor Histidine Kinase AHK4 Constitutively Active. Plant and Cell Physiology 48: 1809-1814

Miyawaki K, Matsumoto-Kitano M, Kakimoto T (2004) Expression of cytokinin biosynthetic isopentenyltransferase genes in Arabidopsis: tissue specificity and regulation by auxin, cytokinin, and nitrate. The Plant Journal 37: 128-138

Miyawaki K, Tarkowski P, Matsumoto-Kitano M, Kato T, Sato S, Tarkowska D, Tabata S, Sandberg G, Kakimoto T (2006) Roles of Arabidopsis ATP/ADP isopentenyltransferases and tRNA isopentenyltransferases in cytokinin biosynthesis. PNAS 103: 16598-16603

Mizukami Y (2001) A matter of size: developmental control of organ size in plants. Current Opinion in Plant Biology 4: 533-539

Möglich A, Ayers RA, Moffat K (2009) Structure and Signaling Mechanism of Per-ARNT-Sim Domains. Structure (London, England : 1993) 17: 1282-1294

Mok D, Mok M (2001) Cytokinin metabolism and action. Annu Rev Plant Physiol Mol Biol 52: 89 - 118

Morris RO, Bilyeu KD, Laskey JG, Cheikh NN (1999) Isolation of a Gene Encoding a Glycosylated Cytokinin Oxidase from Maize. Biochemical and Biophysical Research Communications 255: 328-333

Mothes K, Baudisch W (1958) Untersuchungen über die Reversibilität der Ausbleichung grüner Blätter. Flora 146: 521-531

Moubayidin L, Di Mambro R, Sabatini S (2009) Cytokinin-auxin crosstalk. Trends in Plant Science 14: 557-562

Moubayidin L, Perilli S, Dello Ioio R, Di Mambro R, Costantino P, Sabatini S (2010) The Rate of Cell Differentiation Controls the Arabidopsis Root Meristem Growth Phase. Current Biology 20: 1138-1143

Müller B, Sheen J (2008) Cytokinin and auxin interaction in root stem-cell specification during early embryogenesis. Nature 453: 1094-1097

Mumberg D, Müller R, Funk M (1995) Yeast vectors for the controlled expression of heterologous proteins in different genetic backgrounds. Gene 156: 119-122

Murashige T, Skoog F (1962) A revised medium for rapid growth and bio assays with tobacco tissue cultures. Physiologia Plantarum 15: 473-497

Nieminen K, Immanen J, Laxell M, Kauppinen L, Tarkowski P, Dolezal K, Tähtiharju S, Elo A, Decourteix M, Ljung K, Bhalerao R, Keinonen K, Albert VA, Helariutta Y (2008) Cytokinin signaling regulates cambial development in poplar. Proceedings of the National Academy of Sciences 105: 20032-20037

Nishimura C, Ohashi Y, Sato S, Kato T, Tabata S, Ueguchi C (2004) Histidine Kinase Homologs That Act as Cytokinin Receptors Possess Overlapping Functions in the Regulation of Shoot and Root Growth in Arabidopsis. Plant Cell 16: 1365-1377

Nordström A, Tarkowski P, Tarkowska D, Norbaek R, Åstot C, Dolezal K, Sandberg G (2004) Auxin regulation of cytokinin biosynthesis in Arabidopsis thaliana: A factor of potential importance for auxin–cytokinin-regulated development. Proceedings of the National Academy of Sciences of the United States of America 101: 8039-8044

Olsen O-A (2004) Nuclear Endosperm Development in Cereals and Arabidopsis thaliana. The Plant Cell Online 16: S214-S227

Ottemann KM, Xiao W, Shin Y-K, Koshland Jr. DE (1999) A Piston Model for Transmembrane Signaling of the Aspartate Receptor. Science 285: 1751-1754

Peleg Z, Reguera M, Tumimbang E, Walia H, Blumwald E (2011) Cytokinin-mediated source/sink modifications improve drought tolerance and increase grain yield in rice under water-stress. Plant Biotechnology Journal 9: 747-758

Peters JL, Cnudde F, Gerats T (2003) Forward genetics and map-based cloning approaches. Trends in Plant Science 8: 484-491

Porra RJ, Thompson WA, Kriedemann PE (1989) Determination of accurate extinction coefficients and simultaneous equations for assaying chlorophylls a and b extracted with four different solvents: verification of the concentration of chlorophyll standards by atomic absorption spectroscopy. Biochimica et Biophysica Acta (BBA) - Bioenergetics 975: 384-394

Punwani JA, Hutchison CE, Schaller GE, Kieber JJ (2010) The subcellular distribution of the Arabidopsis histidine phosphotransfer proteins is independent of cytokinin signaling. The Plant Journal 62: 473-482

Raleigh EA, Murray NE, Revel H, Blumenthal RM, Westaway D, Reith AD, Rigby PWJ, Elhai J, Hanahan D (1988) McrA and McrB restriction phenotypes of some E.coli strains and implications for gene cloning. Nucleic Acids Research 16: 1563-1575

Rashotte AM, Carson SDB, To JPC, Kieber JJ (2003) Expression Profiling of Cytokinin Action in Arabidopsis. Plant Physiol. 132: 1998-2011

Rashotte AM, Mason MG, Hutchison CE, Ferreira FJ, Schaller GE, Kieber JJ (2006) A subset of Arabidopsis AP2 transcription factors mediates cytokinin responses in concert with a two-component pathway. Proceedings of the National Academy of Sciences 103: 11081-11085

Richmond AE, Lang A (1957) Effect of Kinetin on Protein Content and Survival of Detached Xanthium Leave. Science 125: 650-651

Riefler M, Novak O, Strnad M, Schmulling T (2006) Arabidopsis cytokinin receptor mutants reveal functions in shoot growth, leaf senescence, seed size, germination, root development and cytokinin metabolism. Plant Cell 18: 40 - 54

Rivero RM, Kojima M, Gepstein A, Sakakibara H, Mittler R, Gepstein S, Blumwald E (2007) Delayed leaf senescence induces extreme drought tolerance in a flowering plant. Proceedings of the National Academy of Sciences 104: 19631-19636

Robson PRH, Donnison IS, Wang K, Frame B, Pegg SE, Thomas A, Thomas H (2004) Leaf senescence is delayed in maize expressing the Agrobacterium IPT gene under the control of a novel maize senescence-enhanced promoter. Plant Biotechnology Journal 2: 101-112

Romanov GA, Lomin SN, Schmulling T (2006) Biochemical characteristics and ligand-binding properties of Arabidopsis cytokinin receptor AHK3 compared to CRE1/AHK4 as revealed by a direct binding assay. J. Exp. Bot. 57: 4051-4058

Romanov GA, Spíchal L, Lomin SN, Strnad M, Schmülling T (2005) A live cell hormone-binding assay on transgenic bacteria expressing a eukaryotic receptor protein. Analytical Biochemistry 347: 129-134

Rose MD, Winston F, Hieter P (1990) Methods in yeast genetics: A laboratory course manual (Cold Spring Harbor). Cold Spring Harbor Laboratory Press, New York.

Rozen S, Skaletsky H (2000) Primer3 on the WWW for general users and for biologist programmers. Methods Mol Biol. 132

Rupp HM, Frank M, Werner T, Strnad M, Schmülling T (1999) Increased steady state mRNA levels of the STM and KNAT1 homeobox genes in cytokinin overproducing Arabidopsis thaliana indicate a role for cytokinins in the shoot apical meristem. The Plant Journal 18: 557-563

Sakai H, Honma T, Aoyama T, Sato S, Kato T, Tabata S, Oka A (2001) ARR1, a Transcription Factor for Genes Immediately Responsive to Cytokinins. Science 294: 1519-1521

Sakakibara H (2006) CYTOKININS: Activity, Biosynthesis, and Translocation. Annual Review of Plant Biology 57: 431-449

Sakamoto T, Sakakibara H, Kojima M, Yamamoto Y, Nagasaki H, Inukai Y, Sato Y, Matsuoka M (2006) Ectopic Expression of KNOTTED1-Like Homeobox Protein Induces Expression of Cytokinin Biosynthesis Genes in Rice. Plant Physiology 142: 54-62

Sambrook J, Russel D (2001) Molecular cloning: A laboratory manual. Cold Spring Harbor Laboratory Press, New York.

Savidge R (2001) Intrinsic Regulation of Cambial Growth. Journal of Plant Growth Regulation 20: 52-77

Schmülling T, Werner T, Riefler M, Krupková E, Bartrina y Manns I (2003) Structure and function of cytokinin oxidase/dehydrogenase genes of maize, rice, *Arabidopsis* and other species. Journal of Plant Research 116: 241-252

Schoof H, Lenhard M, Haecker A, Mayer KFX, Jürgens G, Laux T (2000) The Stem Cell Population of Arabidopsis Shoot Meristems Is Maintained by a Regulatory Loop between the CLAVATA and WUSCHEL Genes. Cell 100: 635-644

Shani E, Yanai O, Ori N (2006) The role of hormones in shoot apical meristem function. Current Opinion in Plant Biology 9: 484-489

Smyth DR, Bowman JL, Meyerowitz EM (1990) Early Flower Development in Arabidopsis. Plant Cell 2: 755-767

Spichal L, Rakova N, Riefler M, Mizuno T, Romanov G, Strnad M, Schmulling T (2004) Two cytokinin receptors of Arabidopsis thaliana, CRE1/AHK4 and AHK3, differ in their ligand specificity in a bacterial assay. Plant Cell Physiol 45: 1299 - 1305

Stolz A, Riefler M, Lomin SN, Achazi K, Romanov GA, Schmülling T (2011) The specificity of cytokinin signalling in Arabidopsis thaliana is mediated by differing ligand affinities and expression profiles of the receptors. The Plant Journal 67: 157-168

Studier FW, Moffatt BA (1986) Use of bacteriophage T7 RNA polymerase to direct selective high-level expression of cloned genes. Journal of Molecular Biology 189: 113-130

Su Y-H, Liu Y-B, Zhang X-S (2011) Auxin–Cytokinin Interaction Regulates Meristem Development. Molecular Plant 4: 616-625

Sun J, Hirose N, Wang X, Wen P, Xue L, Sakakibara H, Zuo J (2005) Arabidopsis SOI33/AtENT8 Gene Encodes a Putative Equilibrative Nucleoside Transporter That Is Involved in Cytokinin Transport In Planta. Journal of Integrative Plant Biology 47: 588-603

Sun J, Niu Q-W, Tarkowski P, Zheng B, Tarkowska D, Sandberg G, Chua N-H, Zuo J (2003) The Arabidopsis AtIPT8/PGA22 Gene Encodes an Isopentenyl Transferase That Is Involved in De Novo Cytokinin Biosynthesis. Plant Physiology 131: 167-176

Suzuki T, Ishikawa K, Yamashino T, Mizuno T (2002) An Arabidopsis Histidine-Containing Phosphotransfer (HPt) Factor Implicated in Phosphorelay Signal Transduction: Overexpression of AHP2 in Plants Results in Hypersensitiveness to Cytokinin. Plant and Cell Physiology 43: 123-129

Suzuki T, Miwa K, Ishikawa K, Yamada H, Aiba H, Mizuno T (2001) The Arabidopsis sensor His-kinase, AHK4, can respond to cytokinins. Plant Cell Physiol 42: 107 - 113

Sweere U, Eichenberg K, Lohrmann J, Mira-Rodado V, Baurle I, Kudla J, Nagy F, Schafer E, Harter K (2001) Interaction of the Response Regulator ARR4 with Phytochrome B in Modulating Red Light Signaling. Science 294: 1108-1111

Tajima Y, Imamura A, Kiba T, Amano Y, Yamashino T, Mizuno T (2004) Comparative Studies on the Type-B Response Regulators Revealing their Distinctive Properties in the His-to-Asp Phosphorelay Signal Transduction of Arabidopsis thaliana. Plant and Cell Physiology 45: 28-39

Takei K, Sakakibara H, Taniguchi M, Sugiyama T (2001) Nitrogen-Dependent Accumulation of Cytokinins in Root and theTranslocation to Leaf: Implication of Cytokinin Species that Induces GeneExpression of Maize ResponseRegulator. Plant and Cell Physiology 42: 85-93

Takei K, Takahashi T, Sugiyama T, Yamaya T, Sakakibara H (2002) Multiple routes communicating nitrogen availability from roots to shoots: a signal transduction pathway mediated by cytokinin. Journal of Experimental Botany 53: 971-977

Takei K, Ueda N, Aoki K, Kuromori T, Hirayama T, Shinozaki K, Yamaya T, Sakakibara H (2004a) AtIPT3 is a Key Determinant of Nitrate-Dependent Cytokinin Biosynthesis in Arabidopsis. Plant and Cell Physiology 45: 1053-1062

Takei K, Yamaya T, Sakakibara H (2004b) Arabidopsis CYP735A1 and CYP735A2 Encode Cytokinin Hydroxylases That Catalyze the Biosynthesis of trans-Zeatin. Journal of Biological Chemistry 279: 41866-41872

Taniguchi M, Kiba T, Sakakibara H, Ueguchi C, Mizuno T, Sugiyama T (1998) Expression of Arabidopsis response regulator homologs is induced by cytokinins and nitrate. FEBS Letters 429: 259-262

Tocquin P, Corbesier L, Havelange A, Pieltain A, Kurtem E, Bernier G, Perilleux C (2003) A novel high efficiency, low maintenance, hydroponic system for synchronous growth and flowering of Arabidopsis thaliana. BMC Plant Biology 3: 2

Tokunaga H, Kojima M, Kuroha T, Ishida T, Sugimoto K, Kiba T, Sakakibara H (2012) Arabidopsis lonely guy (LOG) multiple mutants reveal a central role of the LOG-dependent pathway in cytokinin activation. The Plant Journal 69: 355-365

Weigel D, Glazebrook J (2002) Arabidopsis: A laboratory manual. Cold Spring Harbor Laboratory Press, New York.

Werner T, Holst K, Pörs Y, Guivarc'h A, Mustroph A, Chriqui D, Grimm B, Schmülling T (2008) Cytokinin deficiency causes distinct changes of sink and source parameters in tobacco shoots and roots. Journal of Experimental Botany 59: 2659-2672

Werner T, Köllmer I, Bartrina I, Holst K, Schmülling T (2006) New Insights into the Biology of Cytokinin Degradation. Plant biol (Stuttg) 8: 371,381

Werner T, Motyka V, Laucou V, Smets R, Van Onckelen H, Schmulling T (2003) Cytokinin-Deficient Transgenic Arabidopsis Plants Show Multiple Developmental Alterations Indicating Opposite Functions of Cytokinins in the Regulation of Shoot and Root Meristem Activity. Plant Cell 15: 2532-2550

Werner T, Motyka V, Strnad M, Schmulling T (2001) Regulation of plant growth by cytokinin. PNAS 98: 10487-10492

Werner T, Schmülling T (2009) Cytokinin action in plant development. Current Opinion in Plant Biology 12: 527-538

Wulfetange K, Lomin SN, Romanov GA, Stolz A, Heyl A, Schmülling T (2011) The Cytokinin Receptors of Arabidopsis Are Located Mainly to the Endoplasmic Reticulum. Plant Physiology 156: 1808-1818

Yamada H, Koizumi N, Nakamichi N, Kiba T, Yamashino T, Mizuno T (2004) Rapid Response of Arabidopsis T87 Cultured Cells to Cytokinin through His-to-Asp Phosphorelay Signal Transduction. Bioscience, Biotechnology, and Biochemistry 68: 1966-1976

Yamada H, Suzuki T, Terada K, Takei K, Ishikawa K, Miwa K, Yamashino T, Mizuno T (2001) The Arabidopsis AHK4 histidine kinase is a cytokinin-binding receptor that transduces cytokinin signals across the membrane. Plant Cell Physiol 42: 1017 - 1023

Yanai O, Shani E, Dolezal K, Tarkowski P, Sablowski R, Sandberg G, Samach A, Ori N (2005) Arabidopsis KNOXI Proteins Activate Cytokinin Biosynthesis. Current Biology 15: 1566-1571

Yang S, Yu H, Xu Y, Goh CJ (2003) Investigation of cytokinin-deficient phenotypes in Arabidopsis by ectopic expression of orchid DSCKX1. FEBS Letters 555: 291-296

Yonekura-Sakakibara K, Kojima M, Yamaya T, Sakakibara H (2004) Molecular characterization of cytokinin-responsive histidine kinases in maize. Differential ligand preferences and response to cis-zeatin. Plant Physiol 134: 1654 - 1661

Zalewski W, Galuszka P, Gasparis S, Orczyk W, Nadolska-Orczyk A (2010) Silencing of the HvCKX1 gene decreases the cytokinin oxidase/dehydrogenase level in barley and leads to higher plant productivity. Journal of Experimental Botany 61: 1839-1851

Zatloukal M, Gemrotová M, Dolezal K, Havlícek L, Spíchal L, Strnad M (2008) Novel potent inhibitors of A. thaliana cytokinin oxidase/dehydrogenase. Bioorganic & Medicinal Chemistry 16: 9268-9275

Zhao Z, Andersen SU, Ljung K, Dolezal K, Miotk A, Schultheiss SJ, Lohmann JU (2010) Hormonal control of the shoot stem-cell niche. Nature 465: 1089-1092

Zubko E, Adams CJ, Macháèková I, Malbeck J, Scollan C, Meyer P (2002) Activation tagging identifies a gene from Petunia hybrida responsible for the production of active cytokinins in plants. The Plant Journal 29: 797-808

8 Supplemental Data

Table 5: Oligonucleotides used for mapping.
*restriction enzymes used for CAPS markers.

primer name	chromosome	5' to 3' sequence	fragment length (bp) Col/L*er,* restriction enzyme*
Primer used for rough mapping of *rock3* and *rock4*			
ciw12-F ciw12-R	1	AGGTTTTATTGCTTTTCACA CTTTCAAAAGCACATCACA	128/115
T17H3-F T17H3-R	1	GCTGAAGACCTTGGAAAACG CCAAGAAAACTAGAAGAGCAAGC	398/342
nga63-F nga63-R	1	GCCTAAACCAAGGCACAGAAG TCATCAGTATTCGACCCAAG	111/89
ciw1-F ciw1-R	1	ACATTTTCTCAATCCTTACTC GAGAGCTTCTTTATTTGTGAT	159/135
nga280-F nga280-R	1	CCTGATCTCACGGACAATAGTG GGCTCCATAAAAAGTGCACC	105/85
F5I14-F F5I14-R	1	CTGCCTGAAATTGTCGAAAC GGCATCACAGTTCTGATTCC	195/>195
nga692-F nga692-R	1	AGCGTTTAGCTCAACCCTAGG TTTAGAGAGAGAGAGCGCGG	119/115
F18P14-F F18P14-R	2	ATTCCCGCAATTTATTTTGTTC GTTTGATGGCAGATTTGTTTTC	123/144
nga168-F nga168-R	2	GAGGACATGTATAGGAGCCTCG TCGTCTACTGCACTGCCG	151/135
RGA-F RGA-R	2	TTCGATTCAGTTCGGTTTAG GTTTAAGCAAGCGAGTATGC	140+128/268 RSAI
ciw2-F ciw2-R	2	CCCAAAAGTTAATTATACTGT CCGGGTTAATAATAAATGT	105/90
PLS7-F PLS7-R	2	GATGAATCTTCTCGTCCAAAAT GACAAACTAAACAACATCCTTCTT	109/>109
ciw3-F ciw3-R	2	GGAAACTCAATGAAATCCACTT GTGAACTTGTTGTGAGCTTTGA	230/220
nga361-F nga361-R	2	ACATATCAATATATTAAAGTAGC AAAGAGATGAGAATTTGGAC	114/120
F4P9-F F4P9-R	2	TGGTCCATACCCATTTCATAAC ATGAATTTTCATTCTACTGTTTTG	299/262
AthBIO2b-F AthBIO2b-R	2	TGACCTCCTCTTCCATGGAG TTAACAGAAACCCAAAGCTTTC	140/209
nga172-F nga172-R	3	AGCTGCTTCCTTATAGCGTCC CCATCCGAATGCCATTGTTC	162/136
nga6-F nga6-R	3	ATGGAGAAGCTTACACTGATC TGGATTTCTTCCTCTCTTCAC	143/123
nga162-F nga162-R	3	CATGCAATTTGCATCTGAGG CTCTGTCACTCTTTTCCTCTGG	107/89
ciw11-F ciw11-R	3	GTTTTTTCTAATCCCCGAGTTGAG GAAGAAATTCCTAAAGCATTC	179/230
ciw4-F ciw4-R	3	GTTCATTAAACTTGCGTGTGT TACGGTCAGATTGAGTGATTC	190/215
ciw5-F ciw5-R	4	GGTTAAAAATTAGGGTTACGA AGATTTACGTGGAAGCAAT	164/144
F14G16-F F14G16-R	4	ACAAACCGATCAGCATTCAAG GCCTTTGTCACGGATTCAAC	250/198

Table 4: Oligonucleotides used for mapping continued.

Primer name	Chromosome	5' to 3' Sequence	fragment length (bp) Col/L*er*, restriction enzyme*
T3H13-F T3H13-R	4	TTTGGTGGGTCAAGAGTCAAG GCAAAAGTCATTACGGACAATAC	275/229
ciw6-F ciw6-R	4	CTCGTAGTGCACTTTCATCA CACATGGTTAGGGAAACAATA	162/148
ciw7-F ciw7-R	4	AATTTGGAGATTAGCTGGAAT CCATGTTGATGATAAGCACAA	130/123
nga1139-F nga1139-R	4	TTTTTCCTTGTGTTGCATTCC TAGCCGGATGAGTTGGTACC	114/118
F23E13-F F23E13-R	4	TGACCGTTGAAAGTGTTGTTG GCCCGAGAAGCCTGATAG	264/246
nga1107-F nga1107-R	4	CGACGAATCGACAGAATTAGG GCGAAAAAACAAAAAAATCCA	150/140
nga129-F nga129-R	5	CACACTGAAGATGGTCTTGAGG TCAGGAGGAACTAAAGTGAGGG	177/179
ciw9-F ciw9-R	5	CAGACGTATCAAATGACAAATG GACTACTGCTCAAACTATTCGG	165/145
nga106-F nga106-R	5	TGCCCCATTTTGTTCTTCTC GTTATGGAGTTTCTAGGGCACG	157/123
CTR1.2-F CTR1.2-R	5	CCACTTGTTTCTCTCTCTAG TATCAACAGAAACGCACCGAG	159/143
nga249-F nga249-R	5	GGATCCCTAACTGTAAAATCCC TACCGTCAATTTCATCGCC	125/115
MLP12-F MLP12-R	5	GTCCCCAAAACCAATCATAAG TCCGAGTGAGAAGAGAGTTTG	319/293
MNC14-F MNC14-R	5	GTACCGGATCTGTGTTGTGAAG GTGCTCAAGGAAATGGGATAG	168/187
MQB2-F MQB2-R	5	CTTTGATAGTAACCTTTTTCAAACCA TGCCATTTATTTGGTCAACAC	252/231
T26D22-F T26D22-R	5	CCAACCCTAATTGTTACTGACGA TGATACTTTTGCCATCACTTTCAT	367/315
Primer used for fine mapping of *rock3*			
F3I6-F F3I6-R	1	CCTTGAAGATCAAGTAATTGAGAAAA TGGATAATTCAAGTAAAATTTGTTATG	287/263
F1K23-F F1K23-R	1	CCCTAGGCTCTGACCCTCTT TTCCAAAATGCAAAGAACGA	225/262
T7N9-F T7N9-R	1	GAAGCTGCGAGAAGAACCTG AAAAACAAAATCCCTCGTGGT	153/168
F17L21-F F17L21-R	1	GGAAAGCGAGTGTGGAAGAG CCAATTATGGTTTCAGAGAAGC	364+117/481 TasI
F17L21b-F F17L21b-R	1	TCTTGATTTCCCCCGGTTAT TGAGACTTGAAATTAAGGGCAAA	59+44+134+165/59+44+299 HinfI
F17L21c-F F17L21c-R	1	CATCGATGCTCACCACTGTC TCATGTGAAGGATGAGAAGCA	194+134+98/232+194 MaeI or BfaI
T17H3-F T17H3-R	1	GCTGAAGACCTTGGAAAACG CCAAGAAAACTAGAAGAGCAAGC	398/342
F13K9-F F13K9-R	1	GGTAGATGCCAATGGAGGAA TTCACATGTTTCAGGCGAAC	188/161
Primer used for fine mapping of *rock4*			
nga112-F nga112-R	3	CTCTCCACCTCCTCCAGTACC TAATCACGTGTATGCAGCTGC	197/189
MAA21-F MAA21-R	3	GTCAGATCTGCGACCTGCTA GATCTGCCATACTGGTTTTTGC	63+227/290 HinfI

Table 4: Oligonucleotides used for mapping continued.

Primer name	Chromosome	5' to 3' Sequence	fragment length (bp) Col/L*er*, restriction enzyme*
T20O10-F T20O10-R	3	TTGCACGATCATGCGTTTAC CATGTCGTATCAACGTGATTAGTG	205/180
F2A19-F F2A19-R	3	TTGGCATCAGTGGAGGTGTA ACCGATCTCAAAACATATTATCATC	252/219
F15G16-F F15G16-R	3	CACAGCATCAAAACCCATCA AAGAACCCTCAAGGAAGAAGAAA	249/230
F21F14-F F21F14-R	3	CCAATCGGATTTCTGACCAT TCAGTCAAAACTTAACACAACTCTTG	66+198/264 HinfI
nga6-F nga6-R	3	ATGGAGAAGCTTACACTGATC TGGATTTCTTCCTCTCTTCAC	143/123
F16M2-F F16M2-R	3	CACCGCCTAAGACAAAGAGC CTGGCTCATGTGCCTTTACA	121+81+78/202+78 SacI

Table 6: Oligonucleotides used for sequencing and cloning purposes

Primer name	Sequence	Purpose
AHK3-1-F	GCGAATTTTCGTACTCCCCT	Sequencing of *AHK3*
AHK3-1-R	GAGCAAAGATGACTGGAGCG	Sequencing of *AHK3*
AHK3-2-F	ACCCAGTTCACAAGGATGAC	Sequencing of *AHK3*
AHK3-2-R	GTTGGGACTTGCTAGAGAAGAG	Sequencing of *AHK3*
AHK3-3-F	GGAAAGCTTGAACTTGAGGAGG	Sequencing of *AHK3*
AHK3-3-R	GATTGCCTTTATCCCACTCTC	Sequencing of *AHK3*
AHK3-4-F	CGTAAACCTCAGAGTGGCAG	Sequencing of *AHK3*
AHK3-4-R	CCTCTCATGTTGATGTGGTGG	Sequencing of *AHK3*
AHK3-608-F AHK3-608-R	ttttgctgattgttgcttacag Cctatcaagaggaattgagtgaga	*ROCK3* marker (genomic DNA) ApoI cuts *ROCK3*: 136bp+459bp
ROCK3-QC-veri-F AHK3-1-R	GTTGGCTCTGTCGGTGATCT GAGCAAAGATGACTGGAGCG	*ROCK3* marker (full length cDNA) ApoI cuts *ROCK3*: 229bp+206bp
Rock3-chase-verif-F AHK3-1-R	tgggtcttggtctctatttgg GAGCAAAGATGACTGGAGCG	Marker for *ROCK3*-CHASE ApoI cuts *ROCK3*: 229bp+206bp
QCII-608-F QCII-608-R	GAGTACACTGATAGAATTTCCTTTGAGAGGCC GGCCTCTCAAAGGAAATTCTATCAGTGTACTC	site directed mutagenesis *AHK3→ROCK3*
TEF-ROCK3-QC-F TEF-ROCK3-QC-R	CCTCAGAGTGGCAGCGGGAGCTCTG CAGAGCTCCCGCTGCCACTCTGAGG	site directed mutagenesis correction of point mutation
CYC-ROCK3-QC-F CYC-ROCK3-QC-R	GAGGGTGCTCCATTCAGAGAGGGAAGAG CTCTTCCCTCTCTGAATGGAGCACCCTC	site directed mutagenesis correction of point mutation
QC-R3inA4-F QC-R3inA4-R	GGAGTACACGGCAAGAATAGCATTTGAGAGACC GGTCTCTCAAATGCTATTCTTGCCGTGTACTCC	site directed mutagenesis Rock3-mutation in AHK4
QC-R2inA4-F QC-R2inA4-R	CTTTGCGATTGGTTTCTTTGTGGGTTATATACTG CAGTATATAACCCACAAAGAAACCAATCGCAAAG	site directed mutagenesis Rock2-mutation in AHK4
QC-A4-F	TCATGCTTTGGCTATTCTCG	Sequencing of *rock* mutations in *AHK4*
DpnI-R3-A4-F DpnI-R3-A4-R	ACATTTGCGGAGTACACGGCAAGAT AACAGGAGCATACTCATCCCTAA	dCAPS marker to verify *rock3* mutation in *AHK4*; MboI cuts WT sequence: 24bp+153bp
StyI-R2-A4-F StyI-R2-A4-R	CTGTGCCATTGTTCTTTGCGATTGGTTCCTT CCATTCATTGGTGTCCTGAT	dCAPS marker to verify *rock2* mutation in *AHK4*; Sty1 cuts WT sequence: 30bp+160bp
rock4-F rock4-R	CACTAGACACCGCGACAACT AGGGATCAAGAAAGCAATCG	ROCK4-marker (genomic + cDNA) Hyp991 cuts WT: 73bp+318bp

Table 5: Oligonucleotides used for sequencing and cloning purposes continued.

QC-rock4-F QC-rock4-R	GACATTGCCAGCCGATGACCGCTCGTGGAAG CTTCCACGAGCGGTCATCGGCTGGCAATGTC	site directed mutagenesis *IPT3→ROCK4*
IPT3-prom-F IPT3-prom-R	CTTCGTATCTATCATGAACACT GATGAAACGCTTTGCAATATA	Amplification of the *IPT3* promotor
IPT3-F IPT3-R	ATGATCATGAAGATATCTATGG TCACGCCACTAGACACCGCGAC	Amplification of the *IPT3* DNA
attB4-IPT3-prom-F attB1R-IPT3-prom-R	GGGGACAACTTTGTATAGAAAAGTTGGACTTCGT ATCTATCATGAACACT GGGGACTGCTTTTTTGTACAAACTTGTGATGAAAC GCTTTGCAATATA	Amplification of the *IPT3* promotor with attached att-sites for cloning into pDONRP4P1R
attB1-IPT3-F attB2-IPT3-R	GGGGACAAGTTTGTACAAAAAAGCAGGCTCCATG ATCATGAAGATATCTATGG GGGGACCACTTTGTACAAGAAAGCTGGGTGTCAC GCCACTAGACACCGCGAC	Amplification of *IPT3* DNA with attached att-sites for cloning into pDONR201
pIPT3-seq-R	actgtgcatgctcctacacg	Sequencing of *IPT3*
pIPT3-seq-F	caattttgcctctccgtttc	Sequencing of *IPT3*

Table 7: Primers used for RT-PCR and qRT-PCR analysis

Primer name	**Sequence**	**Purpose**
ACTIN2-F ACTIN2-R	TACAACGAGCTTCGTGTTGC GATTGATCCTCCGATCCAGA	RT-PCR, amplification of housekeeping gene *ACTIN*
AHK2-RT-F AHK2-UTR-R	CTGAGCGCAGTGAGATGAAG caagatgcataggagacacgag	RT-PCR, amplification of *AHK2*
AHK2-RT-F T35S-R	CTGAGCGCAGTGAGATGAAG gctcaacacatgagcgaaac	RT-PCR, transgene-specific amplification of *AHK2*
AHK3-RT-F AHK3-UTR-R	GGGGATTGGGTATTGGAATC caagatgcataggagacacgag	RT-PCR, amplification of *AHK3*
AHK3-RT-F T35S-R	GGGGATTGGGTATTGGAATC gctcaacacatgagcgaaac	RT-PCR, transgene-specific amplification of *AHK3*
AtUBC10-F AtUBC10-R	CCATGGGCTAAATGGAAA TTCATTTGGTCCTGTCTTCAG	qRT-PCR analysis, amplification of housekeeping gene *UBC10*
At3g25800-F At3g25800-R	CCATTAGATCTTGTCTCTCTGCT GACAAAACCCGTACCGAG	qRT-PCR analysis, amplification of housekeeping gene *At3g25800*
RT-gAHK2-F RT-gAHK2-R	CTCTACACAGCGGTAGCAAG GTCTTAAGCTGAAAGAGACCTGT	qRT-PCR analysis, amplification *AHK2*
RT-tAHK2-F RT-tAHK2-R	GCATGAAATGTGGAATGG TAGATTTGTAGAGAGAGACTGGTGA	qRT-PCR analysis, amplification transgenic *AHK2* transcript
RT-g+tAHK3-F RT-gAHK3-R	TGGAATGGATGGGTATGTAT TACTACTTCAAGATGCATAGGAGAC	qRT-PCR analysis, amplification *AHK3*
RT-g+tAHK3-F RT-tAHK3-R	TGGAATGGATGGGTATGTAT GATTTGTAGAGAGAGACTGGTGATT	qRT-PCR analysis, amplification transgenic *AHK3* transcript

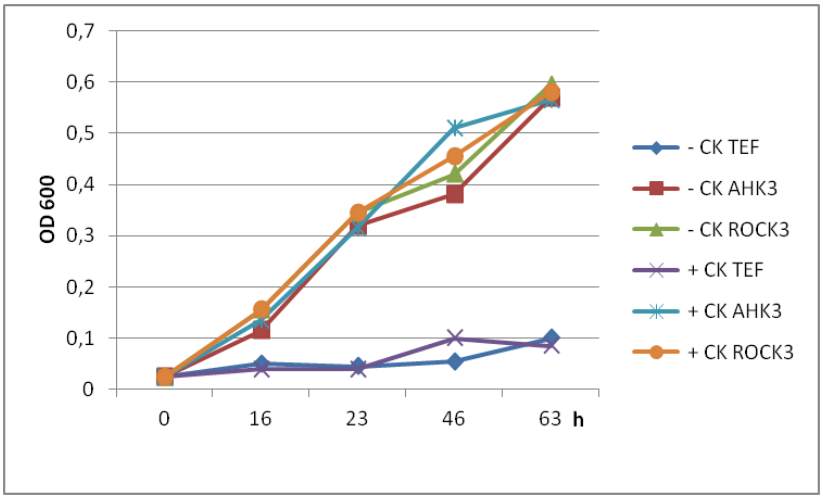

Fig. 33: Yeast complementation assay with *Δsln1* yeast expressing *AHK3* or *ROCK3*.
Growth of *Δsln1* yeast strains carrying the empty vector (TEF), *AHK3,* or *ROCK3* in the absence (- CK) and the presence of the cytokinin *trans*-zeatin (+ CK). The experiment was repeated twice with similar results.

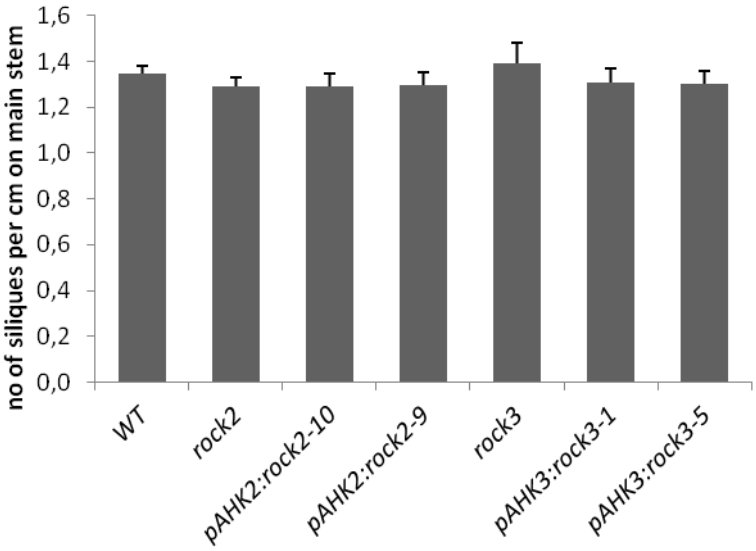

Fig. 34: The distance between siliques was not altered in *rock2* and *rock3* mutants.
Number of siliques per cm on the main stem of fully grown *Arabidopsis* plants.

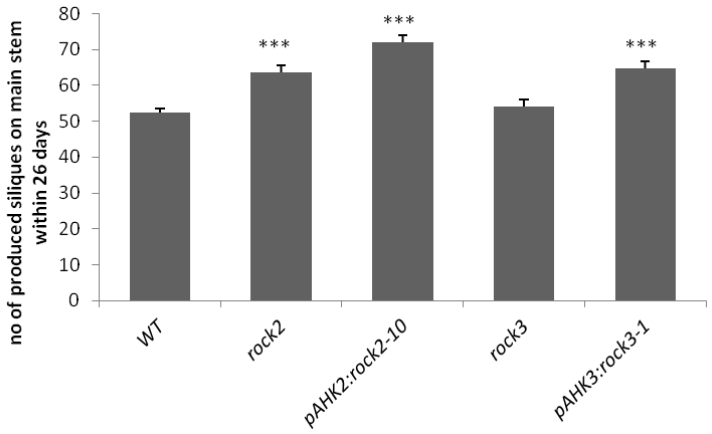

Fig. 35: The mutants *rock2*, *pAHK2:rock2* and *pAHK3:rock3* exhibit a shorter floral plastochron than wild type.
Number of produced siliques within 26 days on the main stems of *rock2* and *rock3* lines compared to the wild type. Error bars represent SE (n=5). *** = $p < 0.001$, as calculated by students t-test.

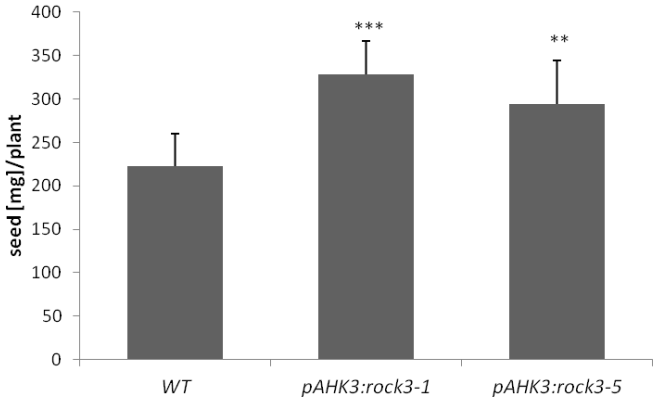

Fig. 36: Transgenic *rock3* plants produce more seeds than wild type.
Two independent *pAHK3:rock3* lines show an increased production of seeds compared to the wild type. The experiment was repeated twice with similar results. Error bars represent SE (n=10). ** = $p < 0{,}005$; *** = $p < 0{,}001$, as calculated by students t-test.

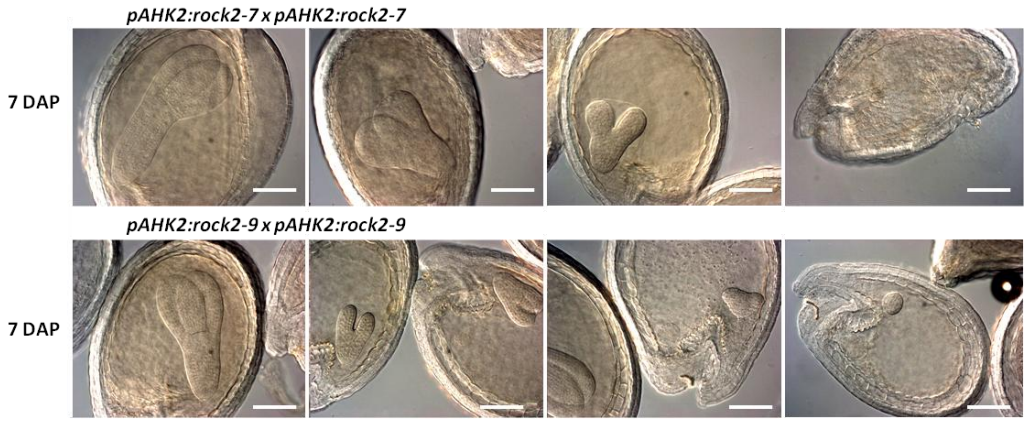

Fig. 37: Seed development of transgenic *pAHK2:rock2* lines.
Cleared seeds of two independent homozygous *pAHK2:rock2* lines at different time points after manual pollination (DAP). In all inspected siliques embryos at different developmental stages were found. Scale bar, 50 µm.

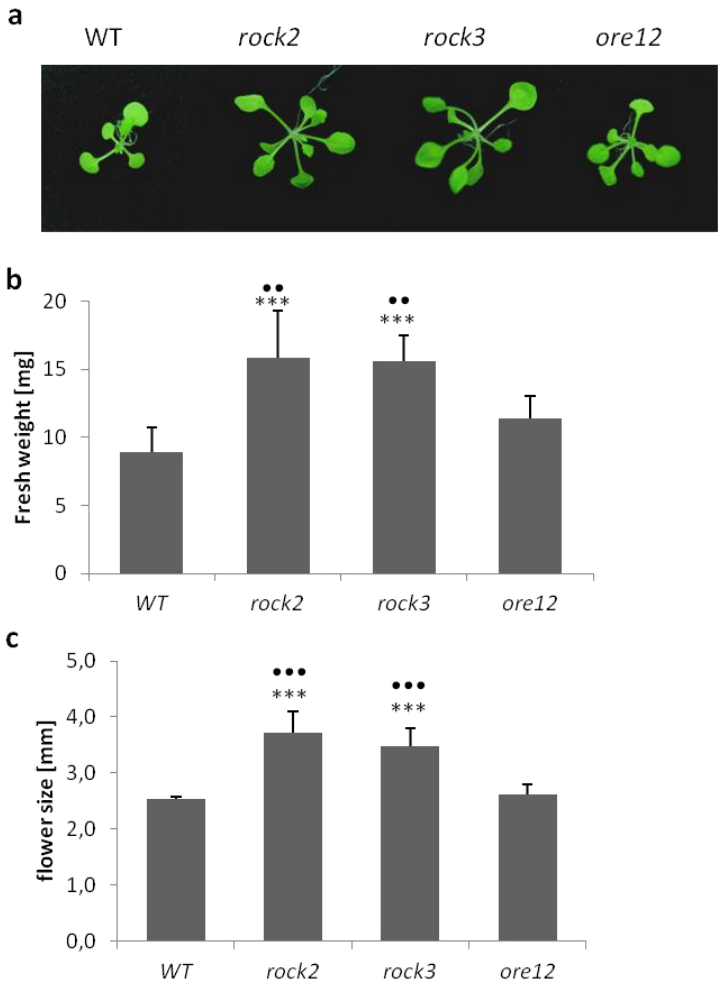

Fig. 38: Vegetative growth and flower size of *rock2*, *rock3* and *ore12* mutants in comparison to wild type.
(**a**) Photo of seedlings 19 days after germination (DAG). Plants were grown under long-day conditions. (**b**) Comparison of fresh weight 18 DAG (n=10). (**c**) Flower length at stage 13 (Smyth et al. 1990) (n=10). Error bars represent SE; *** = $p < 0{,}001$ compared to wild-type plants; •• = $p < 0{,}005$;••• = $p < 0{,}001$ compared to *ore12* plants, as calculated by pairwise student's t-test.

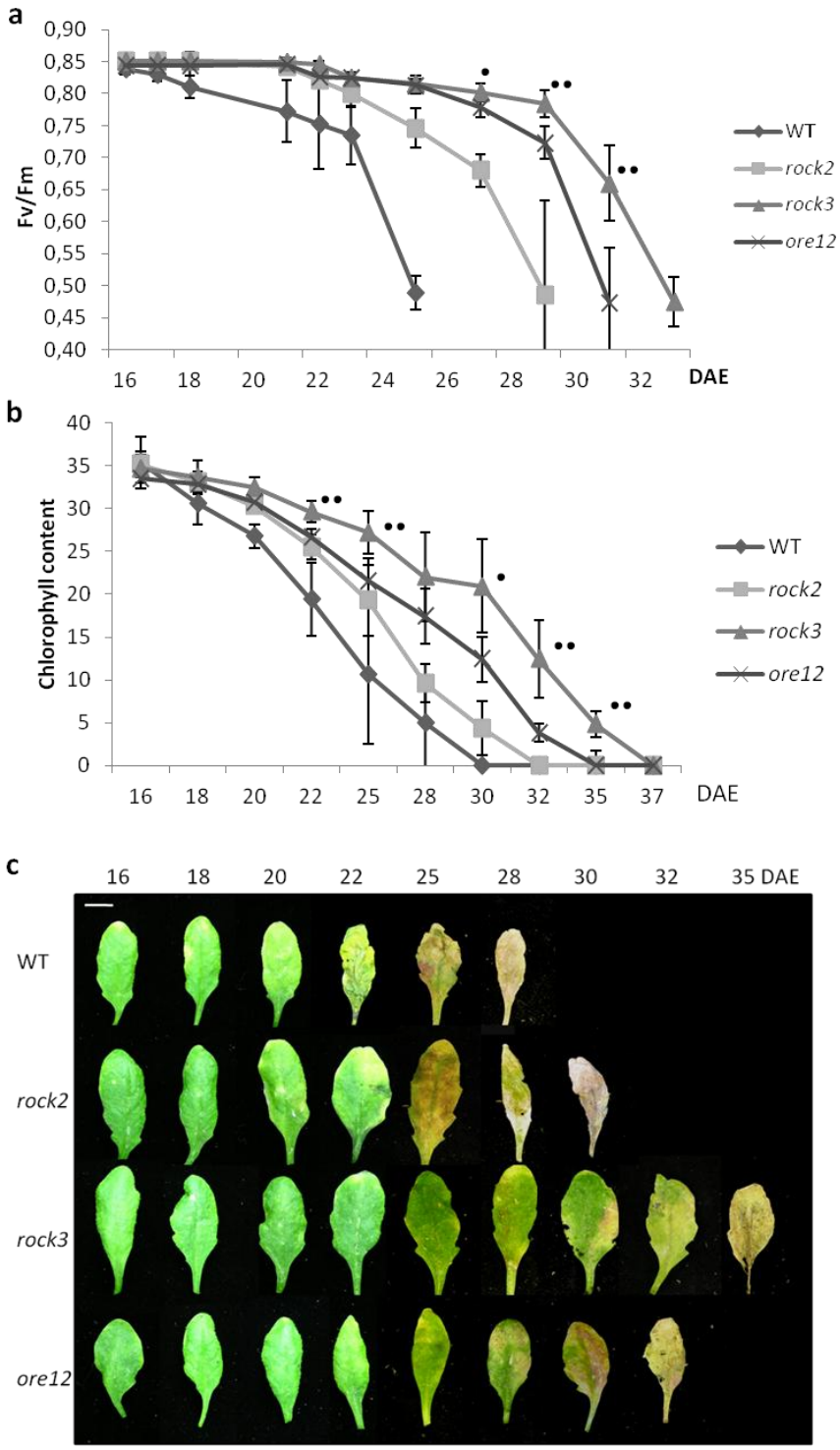

Fig. 39: Natural senescence of leaf 6 of *rock2, rock3* and *ore12* mutant plants under long day conditions.

(**a**) Reduction of photosynthetic efficiency of PS II from 16 to 35 DAE (*days after emergence*). (**b**) Reduction of the chlorophyll content 16 to 35 DAE. (**c**) Comparison of leaves from plants shown in (a) and (b). n=10; •=p<0,01; ••=p<0,005, compared to ore12, as calculated by pairwise students t-test.

9 Acknowledgement

Ich möchte mich herzlich bei allen bedanken, die mich in den letzten Jahren unterstützt haben und mit deren Hilfe ich diese Doktorarbeit anfertigen konnte. Ein besonderes Dankeschön geht an…

Prof. Thomas Schmülling für die Möglichkeit in seinem Institut diese Promotionsarbeit anfertigen zu können. Ich bedanke mich für die konstruktiven Gespräche und Denkanstöße und die vielen hilfreichen Anmerkungen für meine schriftliche Arbeit.

Prof. Tomáš Werner für die Betreuung meiner Arbeit. Seine Diskussionsbereitschaft wie auch Anregungen und Tipps und Tricks im Labor haben diese Arbeit bereichert.

Labor 107 für die vielen offenen Ohren, uneingeschränkte Hilfsbereitschaft und die entspannte Arbeitsatmosphäre im Labor. Es hat mir Spaß gemacht mit euch zu arbeiten!

die gesamte Angewandte Genetik für die Hilfsbereitschaft, das tolle Arbeitsklima und die vielen lustigen Momente während und nach der Arbeit.

Prof Wolfgang Schuster für seinen unermüdlichen Einsatz bei der Aufrechterhaltung des Computersystems.

Frau Schöne für ihren Einsatz bei der Bereitstellung von benötigtem Material und für ihre fröhliche Art.

das gesamte Gärtnerteam für die gute Pflege meiner Pflanzen und jeder Menge Hilfe.

meine Mädels, **Jessika Adrian und Steffi Werner**, für ihre Unterstützung in allen Lebenslagen, denn „Echte Fründe ston zesamme…".

Ein besonderes Dankeschön geht an **meine Eltern, meine Schwester und Steen**. Ich danke euch von Herzen für eure Liebe, Hilfe und Förderung, ohne die ich nicht hier wäre.